# Design, Synthesis, and Structure-Activity Relationship Investigation of Selective Sphingosine Kinase Inhibitors

Hao Li

Dissertation submitted to the faculty of the Virginia Polytechnic Institute and State University in partial fulfillment of the requirements for the degree of

**Doctor of Philosophy**

**In**

**Chemistry**

Webster L. Santos, chair

David G. Kingston

Paul R. Carlier

Andrew N. Lowell

(December 3, 2018)

Blacksburg, VA

Keywords: Sphingosine-1-phosphate, sphingosine kinase inhibitors, structure-activity relationships, tail-group modification, head-group modification

# Design, Synthesis, and Structure-Activity Relationship Investigation of Selective Sphingosine Kinase Inhibitors

Hao Li

## ABSTRACT

Sphingosine kinase 1 (SphK1) is the key enzyme catalyzing the formation of sphingosine-1-phosphate (S1P), which is an important signaling molecule that regulates multiple biological process including inflammatory responses. Elevated SphK1 activity as well as upregulated S1P levels is linked to various diseases such as cancer, fibrosis and sickle cell disease. Therefore, there is a growing interest in studying SphK1 as a potential target for these diseases. Through high-throughput screening, various SphK1 inhibitors have been discovered, among which PF-543 is the most potent and selective inhibitor reported to date ($K_i$=3.6 nM, >100 fold selectivity for SphK1). Previous research indicated that SphK1 inhibitor PF-543 is effective in reducing S1P levels and slowing down the development of sickle cell disease *in vivo.* However, the lack of *in vivo* stability of PF-543 still makes it necessary to develop inhibitors with an improved pharmacokinetic profile. In this study, PF-543 was employed as the lead compound, and the influence of different tails groups and head groups on binding affinity and *in vivo* stability were investigated. In brief, (*R*)-prolinol-based derivatives with various tail groups including alkyl, alkoxy and biphenyl groups were synthesized. Their inhibition potency was tested in a broken-cell assay, and hit compounds were further evaluated in a yeast cell assay to determine $EC_{50}$ values. The U937 cell line and mice model were utilized for hit compounds to quantify S1P reduction *in vitro* and *in vivo*. Our preliminary

results indicated compound **2.14d** was the best hit discovered, with 88% SphK1 inhibition at 1 μM. In addition, compound **2.14d** with a $K_i$ of 0.68 μM and an $EC_{50}$ of 0.15 μM, reduced the S1P of U937 cells by 90% at 1 μM. Its analog with a shorter tail group, **2.14a**, reduced plasma S1P levels by 20% in mice (10 mg/kg, 3 h). Further modification of the head group of **2.14d** produced compound **3.14c** bearing a secondary benzylamine head group, with an $EC_{50}$ value of 0.39 μM and less *in vivo* activity (14% plasma S1P reduction at 10 mg/kg, 6 h).

# Design, Synthesis, and Structure-Activity Relationship Investigation of Selective Sphingosine Kinase Inhibitors

Hao Li

## GENERAL AUDIENCE ABSTRACT

Sphingosine-1-phosphate (S1P) is a molecule related to various diseases, such as cancers and inflammatory diseases. Elevated levels of S1P promote the development of these diseases, thus making it necessary to reduce the production of S1P in patients. Since S1P is generated in human body by an enzyme called sphingosine kinase (SphK), inhibiting the activity of SphK can be beneficial for reducing S1P levels. Developing inhibitors for SphK is also a promising strategy for curing such diseases. A very potent inhibitor has been reported, but it could be metabolized quickly into other inactive metabolites in human, which renders it ineffective. To develop better drug candidates, a series of compounds with similar structure has been synthesized and tested for their potency and metabolic stability. Based on analysis of the relationship between the compound structures and activities, several compounds with less potency and different metabolic stability has been prepared and their efficacy in reducing S1P levels has been tested.

# Acknowledgements

I would like to thank my advisor Dr. Webster Santos sincerely for admitting me into this highly-motivated and productive research group and letting me work on the interesting sphingosine kinase project. When I was stuck on my first project after entering the group, Dr. Santos transferred me to this project that taught me valuable lessons about medicinal chemistry. His high standard for research prompted me to learn from my exemplary peers and improve myself. And his inspiring ideas for drug design always guided me to somewhere I could achieve useful compounds. Moreover, as the principal investigator, his education is not only limited to scientific research. He would always use his own experience to teach us the characteristics that would help us to succeed in our lives after graduate school.

I would also like to thank my committee members for joining my committee and helping me through my graduate study and research. Dr. David Kingston, Dr. Paul Carlier and Dr. Jatinder Josan taught insightful courses and helped me learn in-depth about medicinal natural products, advanced organic chemistry, and organic synthesis. Their critical comments have expanded my knowledge about medicinal chemistry. I also would like to sincerely thank Dr. Andrew Lowell for agreeing to join my committee and participate in my defense.

I also want to thank our collaborators for running biological assays and doing molecular docking studies. Dr. Kevin Lynch and Dr. Yugesh Kharel at the University of Virginia worked on all the biological evaluations for us. They also provided valuable suggestions for my drug design. Dr. David Bevan and Dr. Anne Brown in the

Biochemistry Department of Virginia Tech performed molecular modeling studies for our compounds.

Thanks to all other students of our group as well. Neeraj Patwardhan, Wenyu Zhang and Jessica Wynn helped me when I first enter the group and worked on the peptide project. Srinath Pashikanti, Emily Morris, Molly Congdon and Elizabeth Childress set good examples for me after I started to work on the sphingosine kinase project. Other students including Xi Guo, Amanda Nelson, Cheryl Peck, Russell Snead, Ashley Peralta, Yumin Dai and all lovely younger students helped me a lot in both my research and life. I would like to especially thank Russell Snead for helping me through all these years as my peer and Yumin Dai for staying very close to support me both in research and life.

I also wanted to thank my family for their endless support. My parents supported my study abroad since I planned to do so and my wife Gehui Liu stayed with me for years to make me a better person. Without them, life in Blacksburg would be much harder. Thank you!

# Table of Contents

## List of Figures

## List of Schemes

## List of Tables

## List of abbreviations

Aβ: amyloid-β peptide

ABC Transporters: ATP-binding cassette transporters

AC: adenylyl cyclase

AD: Alzheimer's disease

Alb: albumin

ALI: acute lung injury

AMD: age-related macular degeneration

ApoM: apolipoprotein M

BACE1: β-site APP cleaving enzyme-1

BCRP: breast cancer resistance protein

C1P: ceramide-1-phosphate

Cer: ceramide

CIB1: calcium and integrin-binding protein 1

CNS: central nervous system

EC: endothelial cell

EGF: epidermal growth factor

EGFR: epidermal growth factor receptor

ER: endothelial reticulum

ERK: extracellular signal-regulated kinases

GPCR: G-protein-coupled Receptors

GTPase: guanosine triphosphatase

HDAC: histone deacetylases

HDL: high-density lipoprotein

HIF-1α: hypoxia-inducible factor 1α

IL-6: interleukin-6

JAK: Janus kinase

LPS: lipopolysaccharide

mAb: monoclonal antibody

MAPK: mitogen-activated protein kinase

MPR1: multiple drug resistance protein 1

MS: multiple sclerosis

NF-κB: nuclear factor κ B

PA: phosphatidic acid

PAR1: protease-activated receptor 1

PDGFR: platelet-derived growth factor receptor

PHB2: prohibitin 2

Pi3K: phosphatidylinositol 3-kinase

PKB: protein kinase B

PKC: protein kinase C

PLC: phopspholipase C

PP2A: protein phosphatase 2A

RA: rheumatoid arthritis

RING domain: really interesting new gene domain

ROCK: Rho-associated kinase

RRMS: relapsing-remitting multiple sclerosis

S1P: sphingosine-1-phosphate

S1PL: sphingosine-1-phosphate lyase

S1PP: sphingosine-1-phosphate phosphatase

SCD: sickle cell disease

siRNA: small interfering RNA

SM: sphingomyelin

SMase: sphingomyelinase

Sph: sphingosine

SphK: sphingosine kinase

Spns2: spinster homolog 2

STAT3: signal transducer and activator of transcription 3

TNF: tumor necrosis factor

TNFR: tumor necrosis factor receptors

TRAF2: TNF receptor-associated factor 2

$T_{reg}$ cells: regulatory T cells

VEGF: vascular endothelial growth factor

VEGFR: vascular endothelial growth factor receptor

VSMC: vascular smooth muscle cell

# Chapter 1 Sphingosine-1-phosphate Signaling and Sphingosine Kinase 1 as Promising Therapeutic Target

## 1.1. Introduction

Sphingolipids are not only a component of the cell lipidome contributing to maintaining membrane integrity, but also important signaling molecules modulating a myriad of biological processes.[1] Sphingosine-1-phosphate (S1P) has been extensively studied due to its involvement of controlling cell fate including proliferation, migration and development.[2] S1P is synthesized by sphingosine kinase (SphK) and can activate intracellular targets or be transported out and agonize five S1P receptors ($S1PR_{1-5}$) to activate various signaling cascades, which is described as "inside-out signaling".[3] Up-regulation of S1P has been observed in various diseases including cancers, inflammatory diseases, and sickle cell disease (SCD).[4] To regulate this inside-out signaling pathway, different attractive strategies have been investigated such as developing selective SphK inhibitors and $S1PR_{1-5}$ antagonists.[5-6] The efficacy of modulating S1P signaling is a druggable pathway because of the FDA approval of **FTY720** (Figure 1.10), a selective $S1PR_1$ agonist, for treatment of relapsing-remitting multiple sclerosis (RRMS).[6] This chapter will focus on the sphingolipid rheostat, S1P inside-out signaling, implication of S1P in diseases, and development of potential therapeutics to modulate S1P-mediated pathogenesis.

## 1.2. Sphingolipid Metabolism

Sphingolipids, containing a backbone of sphingoid bases (eighteen carbon amino-alcohol, Figure 1.1), are critical for maintaining membrane structure and transmitting cellular signals.[2] Ceramide (Cer), as an abundant component of eukaryotic cell membrane, plays a central role in sphingolipid metabolic pathways (Figure 1.2). *De novo* synthesis of Cer occurs at the cytosolic leaflet of the endothelial reticulum (ER) and is

catalyzed by a set of enzymes with serine and palmitoyl-CoA as the substrates. Due to the low solubility of Cer in aqueous environment, relocation of Cer to cell membrane is accomplished through a vesicular transport mechanism.[7]

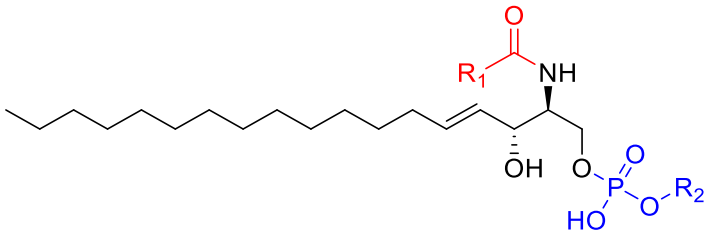


**Figure 1.1.** General structure of sphingolipids

In addition, Cer can also be transported through protein ceramide transfer protein (CERT) to Golgi apparatus for further modification. The primary alcohol of Cer can be modified with phosphate, phosphoethanolamine, galactosyl, or glucosyl to generate the corresponding ceramide-1-phosphate (C1P), sphingomyelin, galactoceramide or glucosylceramide, all of which are components found in cell membranes that can be reversibly converted to Cer.[7] Sphingomyelin, as the most abundant sphingolipid (~85%) in humans, is also an important component (10-20%) of cytomembrane. Acting as a bank of sphingolipids, sphingomyelin is essential for eukaryotic cell viability due to its function in membrane biology.

The final catabolism pathway of Cer includes: 1) deacylation of Cer by ceramidase to form sphingosine (Sph); 1) phosphorylation of Sph by sphingosine kinase (SphK) to form sphingosine-1-phosphate (S1P); 3) and break down of S1P by S1P lyase (S1PL) to hexadecenal and phosphoethanolamine. The first two steps can also be reversibly catalyzed by ceramide synthase and S1P phosphatase (S1PP), respectively.[3]

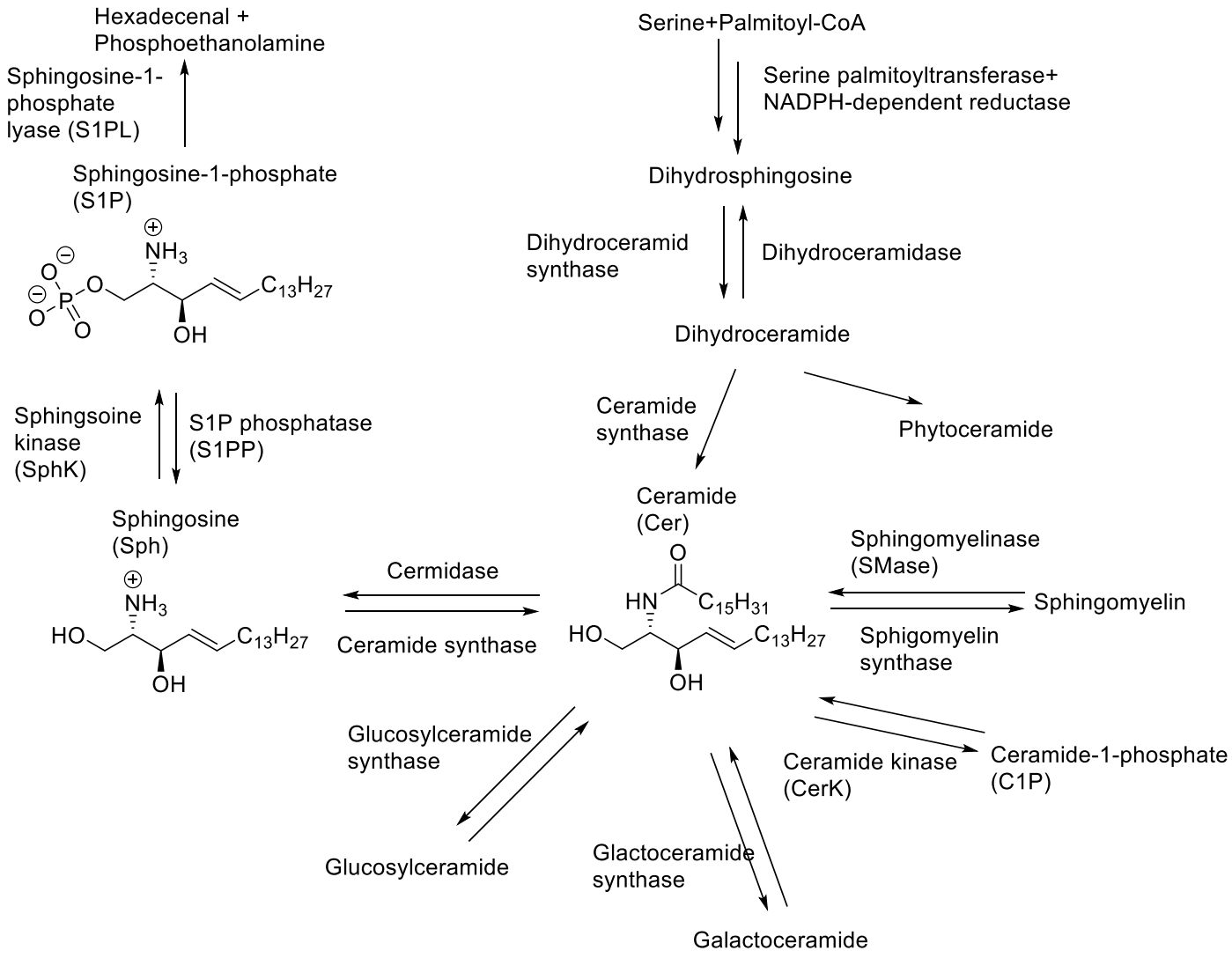


**Figure 1.2.** Metabolic pathways of sphingolipids, including structures of Cer, Sph and S1P

### 1.3. Sphingolipid rheostat

The sphingolipid rheostat is defined as the balance between the proapoptotic sphingolipids (Cer and Sph) and prosurvival S1P. It has been proposed that this balance rather than the absolute amount of individual sphingolipid is determining the fate of cells (Figure 1.3).[3] Numerous evidence in diseases, such as cancer, have shown that decreased Cer levels and upregulated S1P levels are inhibiting programmed cell death while

promoting metastasis and drug resistance.[8] However, this Cer/S1P balance is reversed upon treatment and programmed cell death of pathogenic cells is increased.[9]

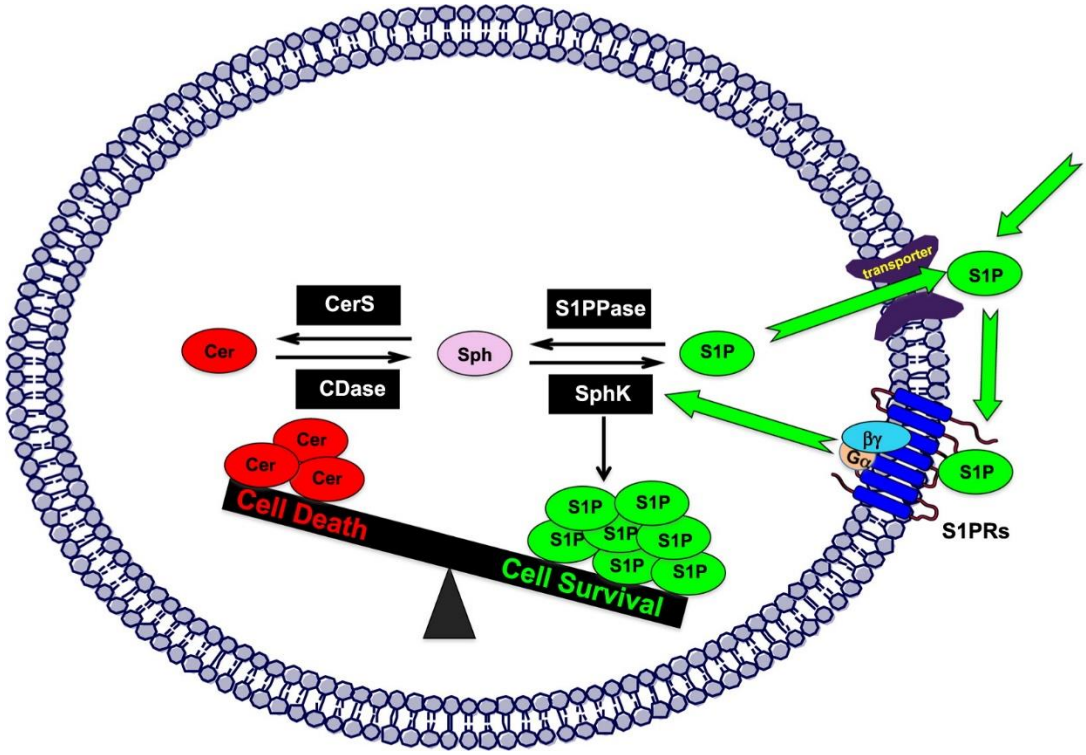


**Figure 1.3.** Sphingolipid rheostat that controls fate of cells. [Reprinted with permission from Newton, J.; Lima, S.; Maceyka, M.; Spiegel, S., Revisiting the sphingolipid rheostat: evolving concepts in cancer therapy. *Experimental cell research* **2015,** *333* (2), 195-200.]

Cer levels can be affected by a number of extracellular agents such as tumor necrosis factor α (TNFα), Fas ligand, ionizing radiation and chemotherapeutic agents.[10-11] Cer upregulation is closely correlated to activation of sphingomyelinase (SMase) and *de novo* synthetic enzymes of Cer as well as deregulation of its degrading enzyme glucosylceramide synthase (GCS).[12] Intracellular Cer, as a second messenger, binds to several targets implicated in apoptosis such as kinase suppressor of Ras, c-Raf, cathepsin D, and protein kinase C-ζ, and facilitate their pro-apoptotic functions.[8] Cer is also

essential for radiation-induced apoptosis of cancer cells, indicating its potential role in cancer therapy.[11, 13]

Stimuli inducing Cer production are also effective to elicit Sph generation during apoptosis.[14] Mechanisms of Sph-induced apoptosis include activation of mitogen-activated protein kinase (MAPK), caspases-dependent cleavage, and mitochondrion-dependent activation of caspases.

On the contrary, S1P acts as a counterbalance to Cer/Sph with its pro-survival effect. In response to pro-apoptotic stimuli, Sph levels are also increased, possibly due to the counteraction of SphK to clear out excess pro-apoptotic sphingolipids to maintain the sphingolipid rheostat.[14] SphK can be activated by ERK1/2 to increase S1P levels, whereas S1PP and S1PL convert S1P to Sph and degrade S1P, respectively. S1P is implicated in various pro-survival pathways.

### 1.4. Sphingosine-1-phostate Signaling Pathway

Signaling of S1P is regulated at different stages: 1) generation of S1P from Sph, which have two isoenzymes: SphK1 and SphK2;[15] 2) interaction of S1P with intracellular targets, such as TRAF2;[16] 3) export of S1P through transporters, such as ABCC1;[17] 4) interaction of S1P with S1P receptors ($S1P_{1-5}$) and triggering of downstream signaling processes.[18]

#### 1.4.1. Sphingosine Kinase

Sphingosine kinase (SphK) has two isoenzymes, SphK1 and SphK2, catalyzing the phosphorylation of sphingosine to generate sphingosine-1-phosphate (S1P). Spiegel first reported the molecular cloning and fuctional characterization of mouse SphK1 (mSphK1) and human SphK2 (hSphK2),[19-20] and Takacs reported hSphK1 (Figure 1.4).[15,

[21] The sequence of hSphK1a has 384 amino acids and a mass of 42.5 kDa, while hSphK2a has 618 amino acids and a mass of 65.2 kDa. SphK1 sequence aligns within SphK2 and share 47% and 43% sequence identity for its N-terminal domain and C-terminal domain respectively. However, the overall sequence similarity between SphK1 and SphK2 is much higher, about 80%.[2] They both contain five highly conserved domains (C1-C5), but SphK2 possesses additional four transmembrane domains and a proline-rich domain.

SphK1 and SphK2 have some functional redundancy, as they catalyze the same reaction. There is evidence that $SphK1^{-/-}$ knockout mice and $SphK2^{-/-}$ mice are both viable. However, knockdown of both SphK1 and SphK2 leads to embryonic death of mice, indicating that SphK is essential for mice survival.[22]

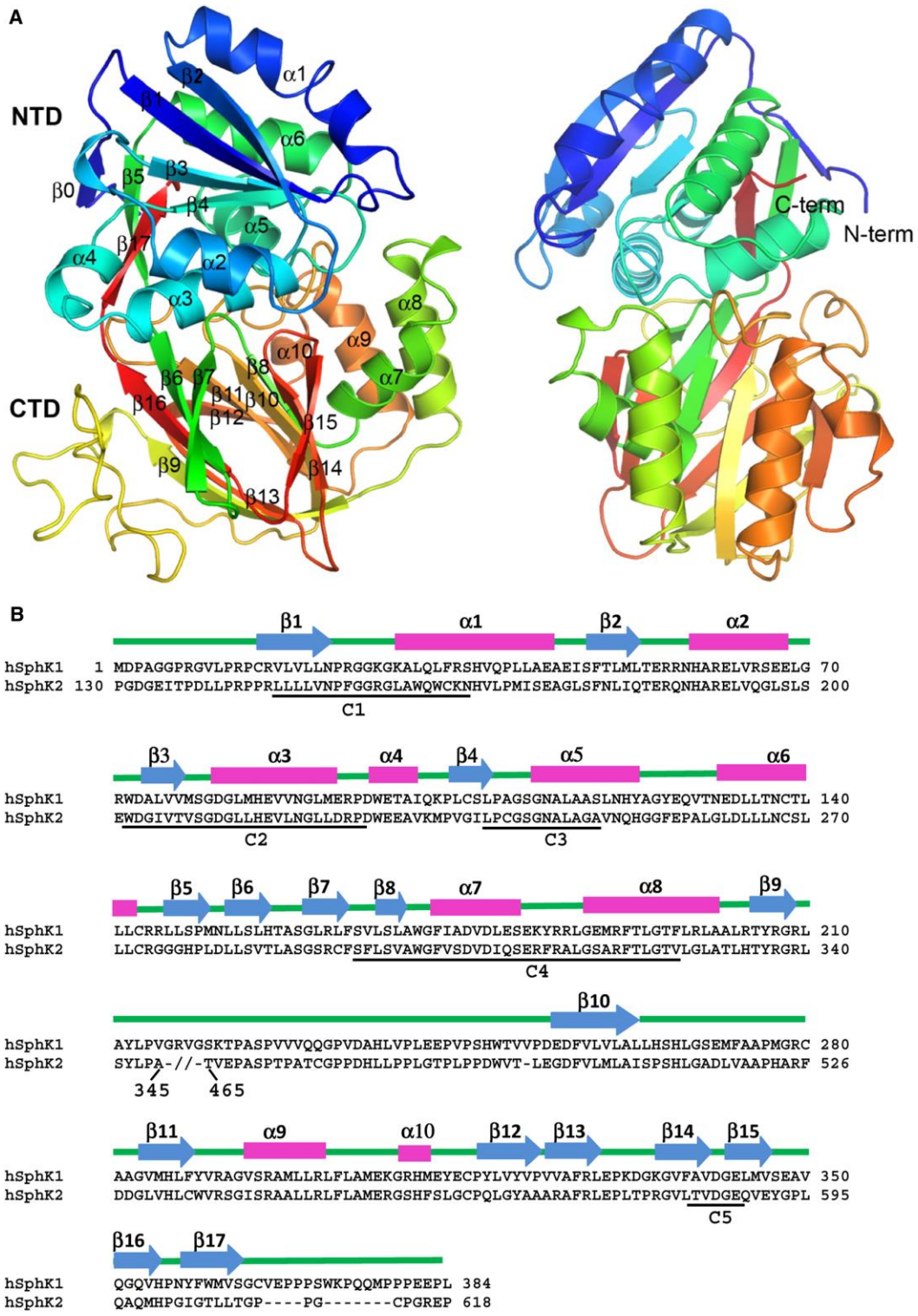


**Figure 1.4.** Crystal structural of SphK1 [Reprinted with permission from Wang, Z.; Min, X.; Xiao, S. H.; Johnstone, S.; Romanow, W.; Meininger, D.; Xu, H.; Liu, J.; Dai, J.; An, S.; Thibault, S.; Walker, N., Molecular basis of sphingosine kinase 1 substrate recognition and catalysis. *Structure* **2013,** *21* (5), 798-809.]

#### 1.4.1.1. Sphingosine Kinase 1

SphK1 mainly exists in the cytoplasm and can translocate to the cytoplasmic membrane. The crystal structure of SphK1 binding with substrate Sph has been reported.[23] In the lipid substrate binding pocket, Sph polar head groups form hydrogen bonds with Asp81, Ser 168 and Asp178 residues of SphK1,[23] while the lipid tail group forms a "J-shaped" structure and interacts with hydrophobic residues, such as Phe303, Leu302, Met272 and His311.[23] Certain agonists, such as TNF-α, can activate corresponding receptors and signaling cascades to activate ERK1/2. ERK1/2 phosphorylates Ser225 residue of SphK1, resulting in a 14-fold activation of SphK1.[24] The mechanism for SphK1 activation is still ellusive, but it has been suggested that phospho-Ser225 might relocate to displace Asp235 and potentially elicit structural transition on helices-α3/4, and ultimately cause conformational relaxation.[25] Ser225 phosphorylation is also essential for SphK1 translocation to the cytomembrane, which is promoted by four types of driving forces: 1) positively charged residues (Lys27, Lys29, Arg186) electrostatically interacting with negatively charged cytomembrane inner surface; 2) hydrogen bond-forming residues (Thr54 and Asn89) interacting with cytomembrane component phosphatidic acid (PA); 3) hydrophobic residues (Leu194, Phe197, Leu198) capable of inserting into the phospholipid bilayer and engaging in hydrophobic interactions; and 4) protein-protein interaction between SphK1 hydrophobic residues (Phe197, Leu198) with calcium and integrin-binding protein 1 (CIB1) myristoyl-binding pocket, causing migration of SphK1 with CIB1 and hydrophobic interaction between CIB1 myristoyl group and cytomembrane lipid tails.[26-29] Ser225

phosphorylation-associated SphK1 activation can also be reversed by dephosphorylation via catalysis of protein phosphatase 2A (PP2A).[30]

SphK1 has high specificity for Sph and contributes to most S1P production, which affects the sphingolipid rheostat and determines cell fate. The function of SphK1 is also affected by the translocation. Within the cytoplasm, S1P generated by SphK1 can easily target intracellular targets and induce corresponding signaling cascades. Upon translocation, due to increased SphK1 activity and availability of substrate Sph from the cytoplasmic membrane, production of S1P is greatly accelerated and S1P can be easily exported into the extracellular matrix. SphK1 translocation is essential for oncogenic signaling and promotes survival and proliferation.[31-32]

SphK1 has also been reported to be exported into the extracellular matrix. Specifically, vascular endothelial cells exported SphK1a isoform, which significantly contributed to vascular S1P levels.[33]

**1.4.1.2. Sphingosine Kinase 2**

Sph2 mainly exists in the nucleus due to its nuclear localization signal (NLS).[34] The structure of SphK2 is less well-studied. S1P produced by nuclear SphK2 inhibits intracellular target and affects gene expression.[35] Like SphK1, SphK2 can also be activated by ERK1/2-mediated phosphorylation. However, due its lack of corresponding Ser225 residue, SphK2 activation is accomplished through phosphorylation at other residues.[36] Signaling events associated with SphK2 usually cause inhibition of DNA synthesis and lead to apoptosis.[34] Translocation of SphK2 to ER, in response to serum deprivation, promotes pro-apoptotic signaling through recycling of Sph to Cer.[37]

Compared to SphK1, SphK2 has less substrate specificity and phosphorylates a broader scope of lipids or lipid-like molecules. Phosphorylation of FTY-720 by SphK2 produces phospho-FTY-720, which is an approved drug and acts as a potent S1PR agonist.[38]

### 1.4.2. S1P phosphatase and lyase

S1P level is also regulated by the presence of S1P phosphatase (SPPase) and lyase (S1PL), which catalyze the dephosphorylation and degradation of S1P, respectively. Knockdown of SPPase1 by si-RNA increased S1P levels in cells by 2-fold and induced resistance to TNF-α and chemotherapy.[39] Inhibition of S1PL also increased S1P levels in tissue and dysregulate lymphocyte trafficking.[40]

### 1.4.3. Intracellular Targets

Intracellular targets of S1P are affected by SphK subtypes, partly due to different distribution of SphK1 and SphK2. SphK1 binds with the amino-terminal RING domain of TNF receptor-associated factor 2 (TRAF2) and its product S1P is the missing cofactor for TRAF2 E3 ligase activity, regulating downstream NF-κB signaling for inflammatory and antiapoptotic processes.[16, 41]

S1P produced in the nucleus by SphK2 readily inhibits histone deacetylase 1/2 (HDAC1/2), since SphK2 is associated with multiprotein co-repressor complexes that include HDAC1/2. Moreover, SphK2 was also found to be overexpressed and related closely to the promoter of specific genes encoding functional proteins, such as cyclin-dependent kinase inhibitor p21 and transcriptional regulator c-fos.[35] S1P produced by mitochondrial SphK2 binds with prohibitin 2 (PHB2) and this interaction is critical for cytochrome-c oxidase assembly. Depletion of this interaction led to mitochondrial

respiration dysfunction.[42] In mouse neurons, S1P is also a modulator of β-site APP cleaving enzyme-1 (BACE1), the key enzyme for generating amyloid-β peptide (Aβ) that is involved in Alzheimer's disease (AD) pathogenesis. S1P is essential for BACE1 to maintain catalytic activity for Aβ generation, while Aβ fibrils (downstream product of BACE1) activate SphK2 reciprocally, indicating crucial role of SphK2 in AD development.[43]

### 1.4.4. Sphingosine-1-phosphate Transporters

ATP-binding Cassette (ABC) transporters for S1P are cell-type dependent. ABCA1 and ABCC1 (also known as multiple drug resistance protein 1, MPR1) play a critical role in transporting S1P for astrocytes and mast cells respectively.[44-45] Moreover, S1P transportation by ABCC1 is crucial for sphingosine-1-phosphate receptor 3 ($S1PR_3$) signaling for dexamethasone-induced cytoprotection in human fibroblasts and sphingosine-1-phosphate receptor 2 ($S1PR_2$) signaling for cell survival and proliferation in rat uterine leiomyoma cells.[17, 46] ABCG2 (also known as breast cancer resistance protein, BCRP) was found to be the major contributor of estradiol-induced S1P export in human breast cancer cells, although its interaction with ABCC1 is unknown.[47]

Spns2 transporter was reported to export both S1P and FTY720-phosphate.[48-49] However, Spns2 only functioned in vascular endothelial cells but not in erythrocytes and platelets.[50] Spns2 deficiency resulted in blocked lymphocyte egress from lymph nodes and humoral impaired immune response,[51-53] which is due to not only reduced plasma S1P levels but also elevated lymph and tissue S1P levels by an unknown mechanism.[54] In addition, Spns2-knockdown-enhanced cell migration in non-small cell lung cancer, indicates its potential in cancer therapeutics development.[55]

MFSD2B is a novel S1P transporter found in erythrocytes and platelets, with a critical role of regulating plasma S1P levels and maintaining morphology of erythrocytes.[56-57]

### 1.4.5. Sphingosine-1-phosphate Gradient in Blood and Tissues

S1P levels are normally low in lymphoid tissues and high in blood and lymph, and this gradient is essential for lymphocyte egress (Figure 1.5). Cellular sources of high S1P levels include erythrocytes, platelets and lymphatic endothelial cells, in which SphK activity is elevated and there're no expression of S1PP and S1PL. And it has been hypothesized that high activity of S1PL in tissue is also contributing to S1P gradient.

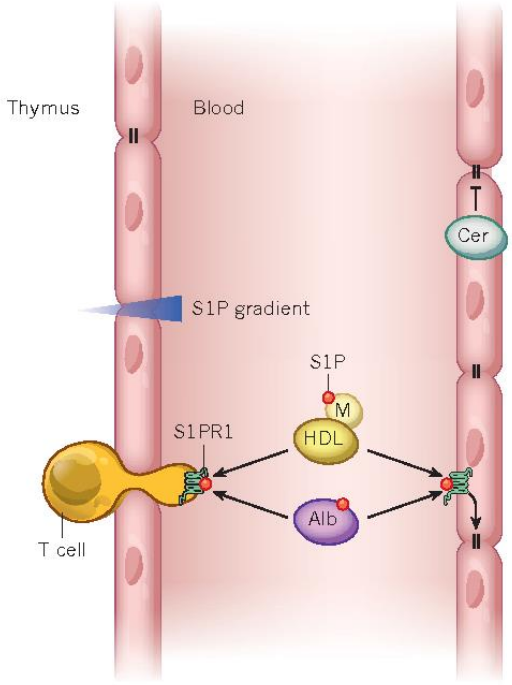


**Figure 1.5.** T cell egress induced by S1P gradient (S1P concentration high in blood and low in tissue) [Reprinted with permission from Maceyka, M.; Spiegel, S., Sphingolipid metabolites in inflammatory disease. *Nature* **2014,** *510* (7503), 58.]

Due to the hydrophobicity of S1P, free S1P levels are vey low (< 5%) in plasma and it is prone to be degraded quickly by blood phosphatase. Instead, the majority of S1P

is distributed through HDL (~65%) and the rest through Alb (~30%). Apolipoprotein M (ApoM), a minor component of HDL (~5%), plays a critical role in not only HDL metabolism but also S1P transport and distribution due to its high affinity for S1P. Overexpression of ApoM stimulated the generation of larger nascent preβ HDL initiated by lipid efflux by ABCA1, resulting in formation of ApoM/S1P enriched HDL.[58-59] $ApoM^+$ HDL-bound S1P, but not Alb-bound S1P, is responsible for $S1PR_1$ agonizing and internalization in ECs, causing increased endothelial adherence and reduced vascular inflammation.[60-61] ApoM/S1P-$S1PR_1$ signaling also inhibits lymphopoiesis and reduces neuroinflammation, indicating the potential of S1P chaperones as a novel therapeutic target.[62]

### 1.4.6. Sphingosine-1-phosphate receptors ($S1PR_{1-5}$)

Five G-protein-couple receptors (GPCR), also known as Sphingosine-1-phosphate receptors ($S1PR_{1-5}$), are expressed on plasma membrane (Figure 1.6). $G_{i/o}$ is associated with all $S1PR_{1-5}$ and is also the sole G-protein coupled with $S1PR_1$. While $G_{12/13}$ couples with $S1PR_{2-5}$, $G_q$ is only found to couple with $S1PR_{2-3}$. G-proteins coupled with $S1PR_{1-5}$ regulate a plethora of downstream signaling pathways.

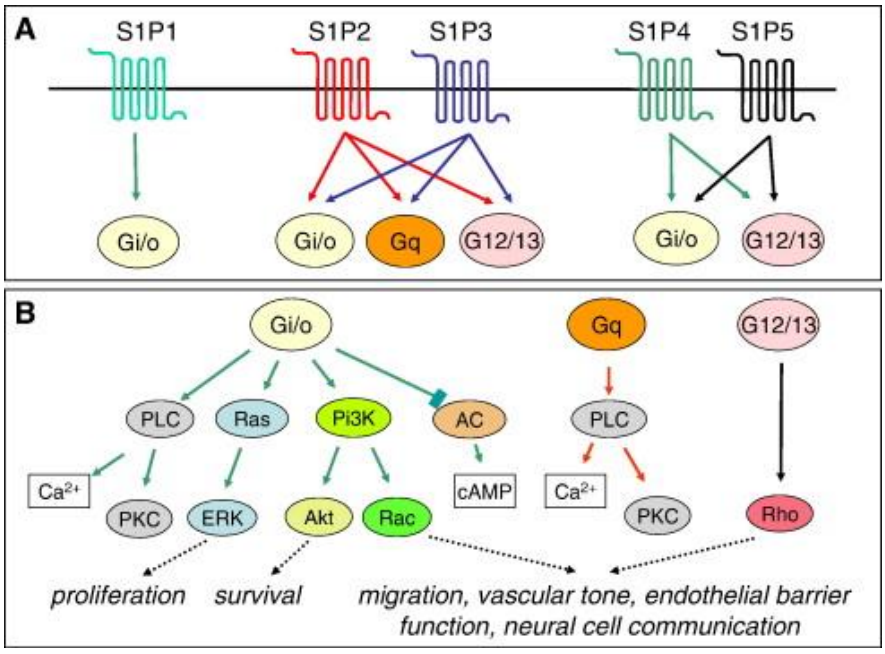


**Figure 1.6.** G-proteins coupled with S1P receptors (A); their downstream signaling and cellular function (B). [Reprinted from Brinkmann, V., Sphingosine 1-phosphate receptors in health and disease: mechanistic insights from gene deletion studies and reverse pharmacology. *Pharmacology & Therapeutics* **2007,** *115* (1), 84-105.]

$G_{i/o}$ is associated with activation of small guanosine triphosphatase (GTPase) Ras, phosphatidylinositol 3-kinase (Pi3K) and protein kinase C (PKC). Activation of Ras initiates Ras-ERK signaling cascade which promotes cell proliferation. Activation of Pi3K has been shown to have dual effects: 1) activating protein kinase B (PKB/Akt) to promotes survival and growth; 2) interacting with GTPase Rac signaling through Pi3K-

Rac axis, which promotes leukocyte and cancer cell migration and EC motility. Activation of phospholipase C (PLC) further stimulates PLC/PKC to increase intracellular $Ca^{2+}$ level, which is required for various cellular responses such as insulin secretion. Moreover, $G_{i/o}$ signaling also inhibits adenylyl cyclase (AC) and formation of cyclic adenosine monophosphate (cAMP), which both are important mediators of the cellular response to hormones. $G_q$ also activates PLC/PKC pathway and increases

intracellular $Ca^{2+}$ level. While $G_{12/13}$ signaling activates GTPase Rho and Rho-associated kinase (ROCK), which regulates cytoskeleton structure and cell polarity.[63]

$S1PR_1$ is ubiquitously expressed in various cells, including lymphocytes, smooth muscle cells and endothelial cells. $S1PR_1$ is essential for life, as $S1PR_1$ knockout is embryonically lethal in mice. $S1PR_1$ upregulation and downregulation is required respectively for T lymphocytes migration to and retention in lymph nodes. Transactivation of $S1PR_1$ in vascular endothelial cells enhances hepatocyte growth factor (HGF)-mediated EC barrier integrity, which also regulates egress of lymphocytes.[64] $S1PR_1$ plays an important role in angiogenesis through restricting aberrant sprouting angiogenesis and lymphangiogenesis through activating PLC/$Ca^{2+}$ pathway.[65-66]

$S1PR_2$ also has widespread expression and is crucial for neuronal excitability and development of auditory and vestibular systems. $S1PR_2$ knockout generally does not produce an anatomically or physiologically defected phenotype at birth, but can cause deafness and the death of 14% mice due to sporadic and spontaneous seizures.[67-68] Role of $S1PR_2$ in maintaining vascular barrier function opposes that of $S1PR_1$, since $S1PR_2$ induces adherens junction disruption and thereby increases paracellular permeability of endothelial cells through $S1PR_2$-Rho-Rock signaling.[69] $S1PR_2$-Rho activation is also responsible for reduced vascular muscle cell migration and proliferation, which are observed in neointimal lesions.[70] On the contrary, $S1PR_2$ activation in muscle stem cells (satellite cells) promotes STAT3 activation and expression of smooth muscle differentiating genes to mediate muscle regeneration and proliferation.[71]

High $S1PR_3$ expression can be found in heart, lung, kidney and spleen. $S1PR_3$ knockout does not result in obvious phenotype.[72] However, $S1PR_{2,3}$ dual knockout is

perinatal lethal and $S1PR_{1-3}$ triple knockout is embryonic lethal.[73-74] $S1PR_3$ functions in coordination with $S1PR_{1,2}$. Fingolimod downregulates $S1PR_{1,3}$ to inhibit migration of vascular smooth muscle cells.[75] $S1PR_{2,3}$ synergically regulates embryonic eyelid closure in mice, possibly via $S1PR_{2,3}$-mediated activation of downstream epidermal growth factor receptor (EGFR) signaling.[76] Moreover, opposing the barrier-protective effect of $S1PR_1$-$G_{i/o}$ activation, $S1PR_{2,3}$-$G_{12/13}$ activation induces formation of stress fibres and weakens endothelial barrier. $S1PR_3$ itself also has important role in cancers and inflammatory diseases. Upregulation of $SphK_1$ in cancer stem cells (CSCs) caused increased S1P production. S1P-$S1PR_3$ signaling activates aldehyde dehydrogenase (ALDH) and subsequent notch signaling pathway, which ultimately leads to enhanced tumorigenesis.[77] $S1PR_3$, but not $S1PR_1$, is responsible for migration and endocytosis of dendritic cells.[78] Expression of $S1P_{4,5}$ is much narrower than $S1P_{1-3}$. $S1PR_4$ expression is primarily found in lymphoid tissues and its function is associated with immune cell activation, differentiation and trafficking. $S1PR_4$ knockout does not produce an obvious phenotype but can reduce T helper 17 cell (Th17) differentiation.[79] $S1PR_5$ expression is limited to white matter tracts of the CNS, and knockout produces normal phenotype. S1P-$S1PR_5$ signaling is associated with inhibition of ERK1/2 activity.[80]

### 1.5. Sphingosine-1-phosphate Signaling in Diseases

Due to the pivotal role of S1P signaling in promoting cell proliferation and controlling immune cell trafficking, its upregulation is associated with various of diseases, such as cancer, inflammatory disease, autoimmune disorder, vascular and cardiac disease.

#### 1.5.1. Cancers

Overexpression of SphK1 (~2-3 fold compared with normal tissue) is commonly observed in various cancers, including cancers of breast, prostate, ovary, liver, lung and leukemia. SphK1 overexpression was found to associate with malignant transformation of NIH3T3 fibroblasts and SphK1 activity could be elevated by V12Ras transfection. Administration of SphK1 inhibitor and expression of G82D mutant kinase-dead SphK1 mutant could abolish the cancer transformation. Whether SphK1 counts as an oncogene is still debatable, since inhibition of SphK1 induces death of normal cells as well. But undoubtedly SphK1 plays a significant role in cancer due to cancer cell's non-oncogene addiction for SphK1.

SphK1 upregulation increases production of S1P and reduces levels of Cer and Sph. Alteration of the S1P rheostat resulted in increased cancer cell proliferation and decreased apoptosis. This effect of S1P is, in part, accomplished through S1P-S1PR signaling. ERK1/2 activation, the major determinant of cancer cell proliferation, is induced predominantly by $S1PR_1$ but inhibited by $S1P_5$, indicating the complex role of S1PR signaling.[81-82] $S1PR_1$ couples with Gi and $S1PR_3$ couples with $G_q$ to promote cancer cell migration.[83] However $S1PR_2$ couples with Rho and inhibits migration.[83-84] Although S1P-S1PRs signaling in cancer is complex, signaling through $S1PR_1$ must be overwhelming due to its ubiquitous and high-levels of expression.

As the size of tumors increase, adequate supply of oxygen and nutrients to cancer cells emerges as a demanding requirement. The hypoxia-inducible factor 1α (HIF-1α), a downstream effector of SphK1, can be activated to induce adaptive changes and increase the tolerance of cancer cells for hypoxia condition.[85] $S1P_{1,3}$ promotes while $S1PR_2$ inhibits migration of endothelial cells (ECs). However, the ratio $S1PR_1$:$S1PR_2$ might be

the determinant factor biasing migration and resulting in neovascularization to transport nutrients and provide metastatic pathway to cancer cells.[86]

Crosstalk between growth factor-S1P signaling a key role in regulating tumorigenesis, migration, invasion and neovascularization in cancers. Estrogen-GPR30 interaction induces ERK1/2-mediated SphK1 activation, while the product S1P signals through $S1PR_3$ to promote EGF release for EGFR signaling, further ERK1/2 activation and ultimately leads to tumorigenesis of breast cancer. $S1PR_{1,3}$ are playing multiple roles in interacting with growth factors to promote cancer cell migration. Heregulin-EGFR interaction promotes translocation of SphK1 and facilitates S1P-$S1PR_1$ signaling. $S1PR_1$ can also complex with platelet-derived growth factor receptor (PDGFR) to cause ERK1/2 activation. Lysophosphatidic acid (LPA) signaling promotes SphK1 expression and S1P production, which signals through $S1PR_3$ to promote migration and invasion as well. Activation of ERK1/2 through vascular endothelial growth factor (VEGF)-VEGFR signaling also promotes neovascularization, which is essential for cancer cell proliferation.

### 1.5.2. Inflammatory Diseases and Autoimmune Disorder

The S1P gradient is crucial for immune cell trafficking. Lymphocyte egress depends on S1P-$S1PR_1$ signaling, which requires the existence of regular S1P gradient and surface residency of $S1PR_1$ as the sensor of the gradient.[87] Disruption of the S1P gradient by either reducing S1P levels in blood and lymph or increasing S1P levels in tissues can abort T cell egress and cause lymphopenia. $S1PR_1$ expression is driven by transcription factor KLF2 and can be activated by STAT3 through IL-6-JAK signaling.[88-89] Extended exposure to high-concentration S1P cause $S1PR_1$ to internalize and lose

sensitivity of the S1P gradient. $S1PR_1$ internalization can also be caused by phosphorylated FTY720, which acts as an agonist and functional antagonist.[90]

Evidence has also supported the negative role of S1P-$S1PR_1$ implicated in regulatory T cells ($T_{reg}$ cells) differentiation, which is critical for adaptive immune response. $S1PR_1$ negatively regulates $T_{reg}$ cell population, thymic $T_{reg}$ precursor differentiation, and immune-suppressive effects of $T_{reg}$ cells.[18] Similar negative regulation of $S1PR_1$ is also observed in differentiation of induced $T_{reg}$ cells ($iT_{reg}$ cells), which is associated with autoimmune diseases and transplant rejection.[91] Thus, $S1PR_1$ expression is also positively correlated with autoimmune disorder.

SphK1 catalyzed S1P generation is responsible for inflammatory and allergic responses through signaling pathways implicated in the innate immune system.[16, 92] S1P binds with its intracellular target PKC to activate NF-κB and ultimately stimulate the production of proinflammatory cytokines in patients with severe sepsis.[92] S1P binding with another intracellular target TRAF2 can alsoactivate NF-κB signaling.[16] Moreover, SphK1 activated by protease-activated receptor 1 (PAR1) enables S1P-$S1PR_3$ signaling in dendritic cells to promote systemic coagulation, which is a hallmark of bacterial sepsis inflammatory response.[93] Considering the key roles of SphK1 and S1P in innate immune response, SphK1 and S1PRs are attractive targets for inflammation.

Multiple sclerosis (MS) is an autoimmune disorder caused by lymphocytes attacking neuronal myelin sheath, resulting in permanent damage to nerves. Continuous demyelination requires effective lymphocytes egress from lymphoid into blood, which is stimulated by S1PR1 signaling in response to S1P gradient. **FTY720** (*vide infra*), as the

first-in-class S1PR1 agonist, cause internalization and degradation of S1PR1 in lymphocytes, thus abolishing lymphocyte egress.

### 1.5.3. Vascular and Cardiac Diseases

S1P is essential for the vascular system in regulating development of ECs and vascular smooth muscle cells (VSMCs) through the inside-out signaling processes.[94] While there is evidence showing the vascular endothelium is a contributor of plasma S1P, plasma S1P from erythrocytes is found to be the major source of S1P for maintaining vascular integrity.[94-95] $SphK1^{-/-}/SphK2^{-/-}$ double-knock out mice were not viable due to poorly developed vascular system.[96] $S1PR_{1-5}$ are playing pivotal and complicated roles in controlling vascular development and their effects are receptor subtype-dependent. S1P-$S1PR_1$ signaling in ECs induces formation of adherens junctions, thus increasing vascular integrity.[97] Evidence has shown that $S1PR_1$ was critical for maintaining vascular stability since $S1PR_1^{-/-}$ knockout mice resulted in endothelial hypersprouting.[65] $S1PR_2$ activation in ECs induces permeability, and this contrast was caused by antagonism of different downstream effectors.[69] $S1PR_3$ agonists demonstrated toxicity in mice model and induces bradycardia.[98] Transient receptor potential channels (TRPCs) in VSMCs are also downstream effectors of S1PR. Upon S1P activation, $Ca^{2+}$ permeability into the cell is increased and evoked mobility of VSMCs.[99]

### 1.5.4. Sickle Cell Disease

SphK1-mediated S1P upregulation has been found to promote sickling of erythrocytes in sickle cell disease (SCD).[4] Although the role of S1P in sickling mechanism is still unknown, it has been proposed that S1P is promoting inflammatory response and the polymerization of hemoglobin to form fibrils in SCD.[100] Administration

of selective SphK1 inhibitor **PF-543** ($K_i$=3.6 nM, *vide infra*) to SCD mice model resulted in significant decrease of SphK activity, plasma S1P levels (~50%), intravascular hemolysis and inflammatory cytokines.[4] Similar result of reduced sickling is also observed with another SphK1 inhibitor **SK I-5C** ($IC_{50}$=3.3 μM), which rescued ~30% of red blood cells from sickling. [101] These results highlighted the potential of SphK1 inhibitors in treating SCD.

### 1.6. Therapeutics Modulating Sphingosine-1-phosphate Signaling

Multiple therapeutic strategies have been investigated to modulate the S1P signaling process and can be categorize into two modes of action. The first mode involves developing inhibitors or antibodies to reduce S1P generation, transport and blood concentration. While the second mode targets at S1PRs to modulate signaling response to high levels of S1P.

#### 1.6.1. Sphingolipid Metabolism and Enzyme Inhibitors

S1P levels are directly regulated by SphK, SPPase and S1PL. Inhibition of SphK reduces generation of S1P and abolishes downstream S1P signaling. On the contrary, inhibition of S1PL increases local S1P concentration and provides another strategy to inverse S1P gradient.

##### 1.6.1.1. Sphingosine Kinase Inhibitors

Lipid-like SphK inhibitors were designed to be Sph analogues and took advantage of their structural similarity with Sph for competitive inhibition (Figure 1.7). In general, lipid-like inhibitors have micromolar level $K_i$ values and lack effective potency. Moreover, the limited structural diversity prohibited significant improvement of their pharmaceutical profile.

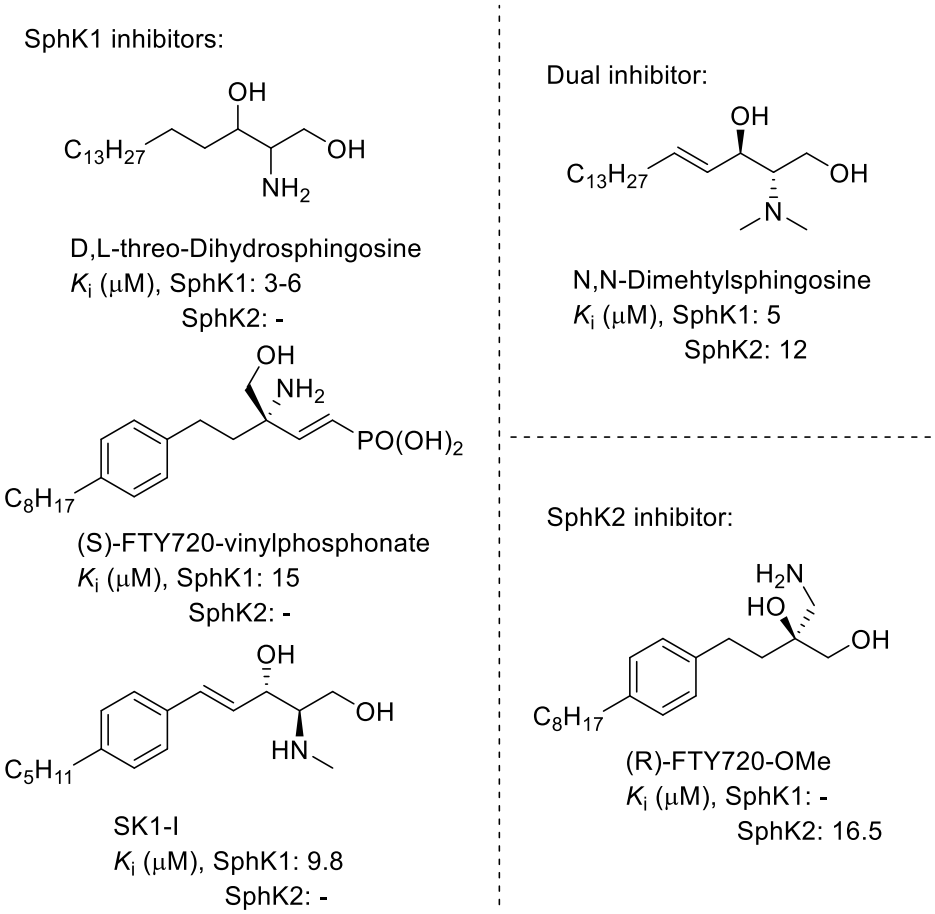


**Figure 1.7.** Structures of select lipid-like SphK inhibitors

On the other hand, non-lipid small molecule inhibitors with diversified pharmacophores were discovered either through rationale design or high-throughput screening (Figure 1.8). Earlier discovered inhibitors like **SKI-II** and **ABC294640** (**Yeliva**®) still lack adequate potency, with their $K_i$ values in the micromolar range. **ABC294640**, as a selective SphK2 inhibitor, has shown antitumor activity in various cancers including prostate, breast, lung cancer and hepatocellular carcinoma. Although its clinical trial for treating Kaposi sarcoma (NCT02229981) has been withdrawn, two trials for treatment of multiple myeloma (NCT02757326) and hepatocellular carcinoma (NCT02939807) are still ongoing and its application has been expanded for treatment of advanced cholangiocarcinoma (NCT03414489). **PF-543** and **Amgen 82**, the two most

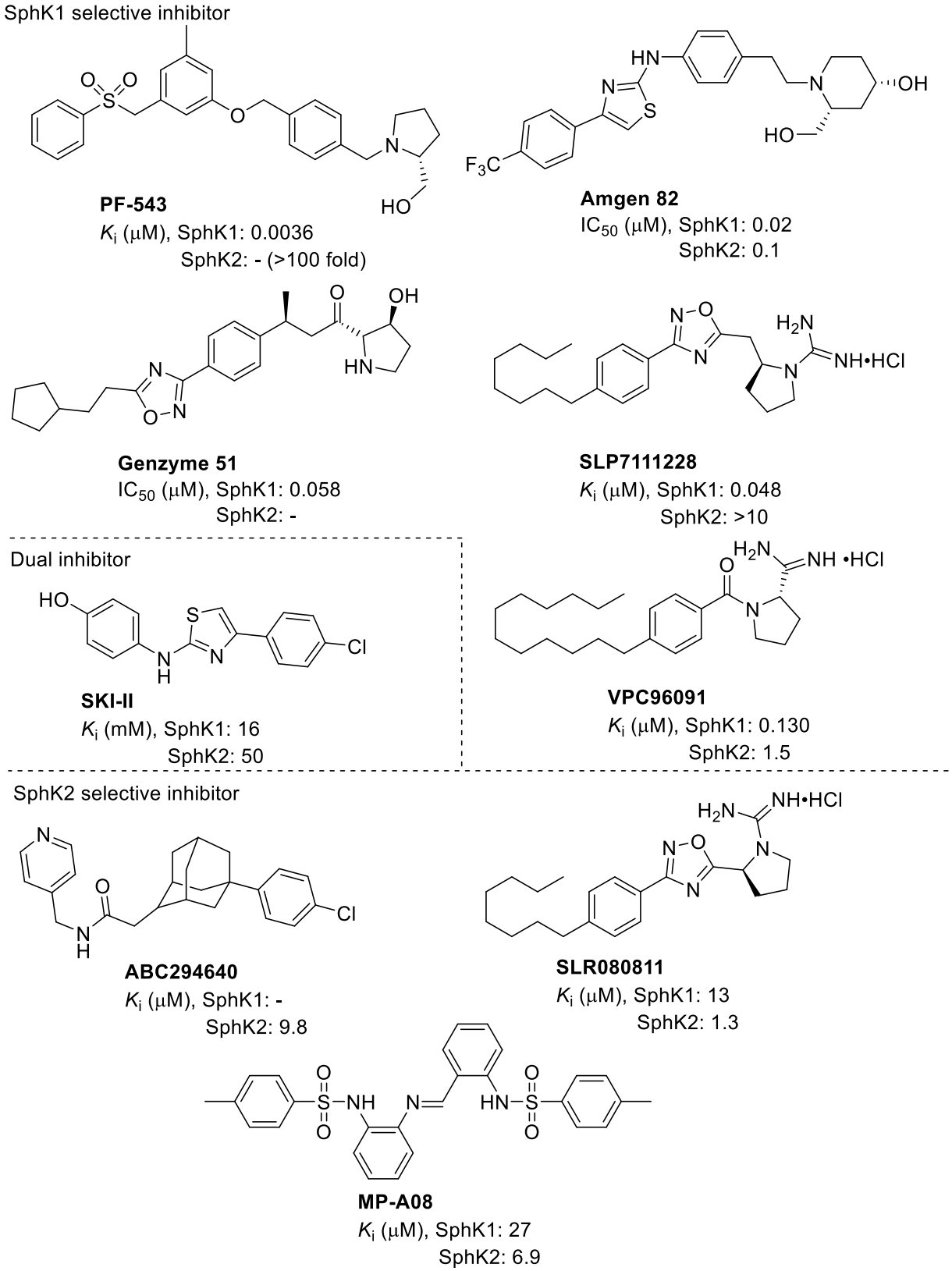


**Figure 1.8.** Structures of select non-lipid like SphK inhibitors

potent SphK1 inhibitors, were discovered by Pfizer and Amgen, respectively. They have unique pyrrolidine- or piperidine-headgroups functionalized by hydroxymethyl group. Oxadiazole/Guanidine-based and amidine-based inhibitors (**SLP7111228**, **SLR080811** and **VPC96091**) has been shown to be successful in selectively inhibiting SphK1 or SphK2. MP-A08 was a competitive inhibitor favoring SphK2 inhibition that binds to the ATP-binding pocket.

#### 1.6.1.2. Sphingosine-1-phosphate Lyase (S1PL) Inhibitors

As the S1P gradient has been shown to play an important role in lymphocyte trafficking, other enzymes affecting S1P gradient are also been investigated for the treatment of autoimmune disorder. A caramel color III component, 2-acetyl-4(5)-(1(*R*),2(*S*),3(*R*),4-tetrahydroxybutyl)-imidazole (**THI**) (Figure 1.9), was found to inhibit S1PL, increase S1P levels in lymphoid tissues, and reduced lymphocyte egress from lymph nodes.[40] Similar results of altered lymphocyte development and egress were also observed in humanized knock-in mice models with less S1PL activity.[102] Structure-activity relationship study afforded more **THI** analogues, among which (*E*)-1-(4-((1*R*,2*S*,3*R*)-1,2,3,4-tetrahydroxybutyl)-1H-imidazol-2-yl)ethanone oxime (**LX2931**) was able to decrease 70% circulating lymphocyte numbers in rodent RA model (18h after 30 mg/kg of oral administration) and has completed phase II clinical trial.[103-104] Moreover, **THI** treatment or siRNA down-regulation of S1PL restored S1P levels in lung tissue and ameliorated lipopolysaccharide-induced inflammation and acute lung injury (ALI) in murine model, validating the potential of S1PL as therapeutic target.[105]

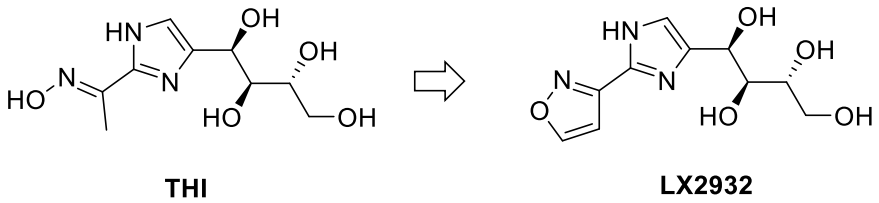


**Figure 1.9.** Development of S1PL inhibitors

### 1.6.2. Sphingosine-1-phosphate Monoclonal Antibodies

The idea of applying S1P antibody as a potential therapeutic for treatment of cancers was first validated by Sabbadini et al. Their work demonstrated that anti-S1P mAb had antiangiogenic and antitumorigenic effects and lead to reduced tumor progress.[106-107] Phase II clinical trials of S1P antibody **ASONEP™** (sonepcizumab/LT1009) for treatment of unresectable and refractory renal cell carcinoma (NCT01762033) and **iSONEP™** (sonepcizumab/LT1009) for treatment of wet age-related macular degeneration (AMD) have been completed (NCT01414153). Although no severe adverse effect has been reported, patients did not display any statistically significant improvement.

### 1.6.3. Sphingosine-1-phosphate Receptor Modulators

S1P receptor modulators provide a different mechanism for treatment of S1P signaling-mediated diseases. Through selectively agonizing or antagonizing S1P receptors, inside-out signaling of S1P can be abolished.

#### 1.6.3.1. Sphingosine-1-phosphate Receptor Agonists

**FTY720** (Fingolimod™/Gilenya®; Novartis; Figure 1.10) was a first-in-class $S1PR_{1,3-5}$ agonist discovered as a chemical derivative of the fungal metabolite myriocin. In a bone marrow transplantation model, **FTY720** demonstrated an immunosuppressive effect in preventing development of graft-versus-host disease. Although it was also found that **FTY720** induced lymphopenia *in vivo*, this effect was not caused by inhibition of the

activation and proliferation of lymphocytes but by sequestering lymphocytes into lymph nodes. This mechanism was not fully elucidated until it was found that **FTY720** was a substrate of SphK2. The corresponding product **FTY720** phosphate is an agonist of S1P receptors and disrupts chemotaxis of lymphocytes towards high blood S1P levels. The potency of **FTY720** was validated by bioassay, with sub-nanomolar $EC_{50}$ values for $S1PR_{1,4,5}$ (~0.3-0.6 nM), nanomolar $EC_{50}$ for $S1PR_3$ (~3 nM), and no activity against $S1PR_2$. Key features of **FTY720** are: a polar aminodiol head group allowing for forming hydrogen bonds with Arg120 and Glu121 residues of $S1PR_1$ and $S1PR_3$, a rigid 1,4-disubstitued phenyl ring as liker group, and a flexible hydrophobic alkyl chain mimicking natural S1P. Treatment of mice with **FTY720** caused $S1PR_1$ internalization and reduced lymphocyte egress from lymph nodes. $S1PR1^{-/-}$ knockout also induced similar effects, indicating the essential role of $S1PR_1$ in lymphocytes trafficking. **FTY720** was capable of penetrating into central nerve system (CNS) and showed glioprotective effects in reducing toxic demyelination murine demyelinating cuprizone model. Pre-clinical evidence further validated efficacy of **FTY720** in preventing neurodegeneration and paralysis in induced experimental autoimmune encephalitis (EAE) model of multiple sclerosis (MS). In 2010, **FTY720** was approved by FDA as a first-in-line drug for treating relapsing-remitting multiple sclerosis (RRMS).

The success of **FTY720** revealed the druggability of targeting S1P receptors. However, certain problems remain to be solved: 1) improved selectivity of S1P receptor agonists since side effect (transient, asymptomatic bradycardia) of **FTY720** was believed to be caused by $S1PR_3$ agonism; 2) development of S1P receptor agonists with different blood-brain barrier (BBB) permeability profile for treatment of CNS diseases.

The majority of second generation S1PR agonists are direct agonists inspired by the triaryl scaffold discovered by Merck.[108] Further modification of the reported scaffolds yielded selective and potent agonists of S1PRs. **Siponimod**® was discovered by Novartis as a selective agonist of $S1PR_1$ and has successfully finished phase III clinical trials for treatment of RRMS (NCT02330965), with its new drug application in progress.

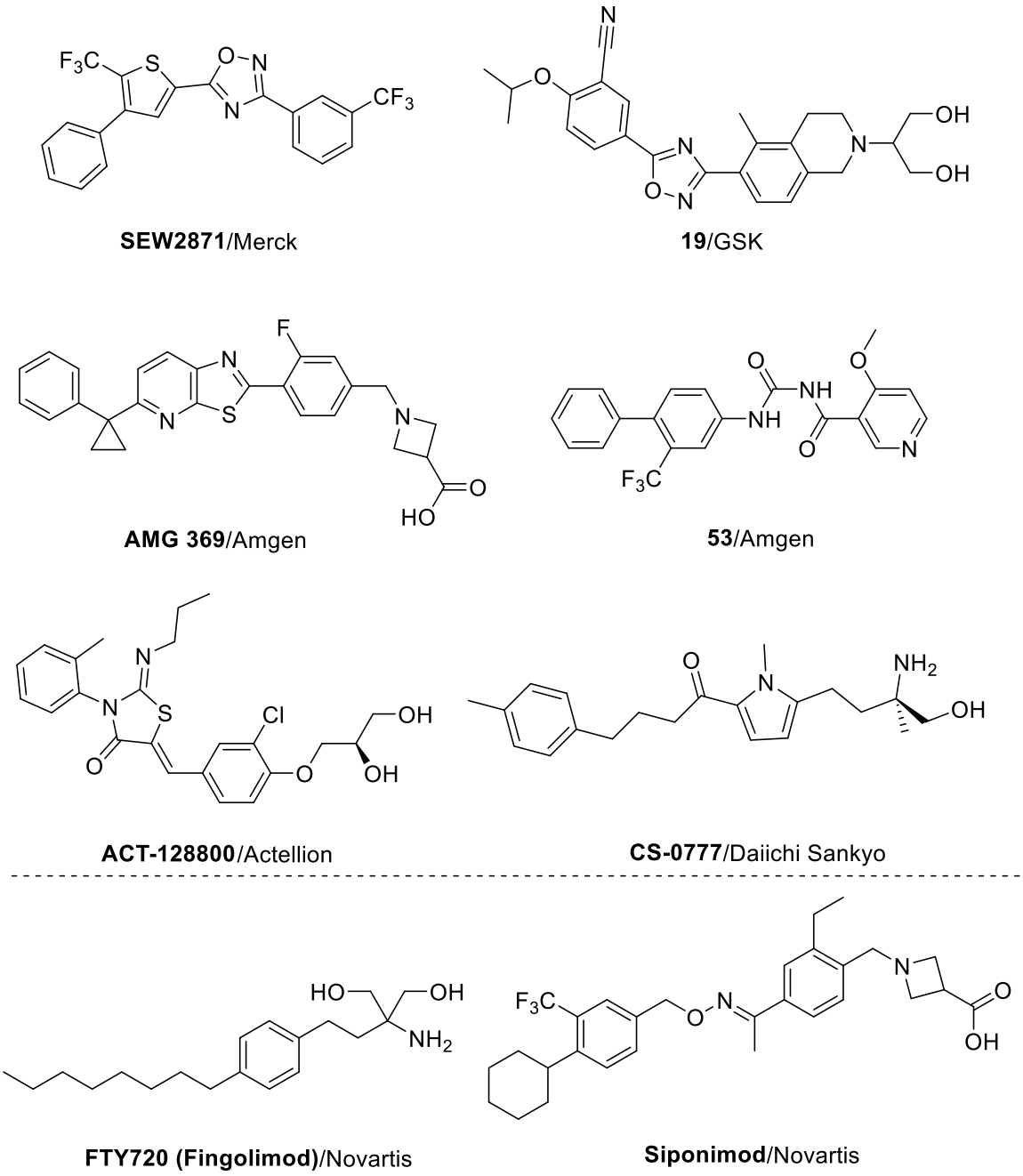


**Figure 1.10.** Structure of select scaffolds of S1P receptor agonists (up) and drug candidate $S1PR_1$ agonist Siponimod® (down)

### 1.6.3.2. Sphingosine-1-phosphate Receptor Antagonists

Due to the observation that extended exposure of $S1PR_1$ to an agonist caused receptor internalization and degradation, the concept of "functional antagonist" has been

proposed to rationalize the pharmacodynamic effects. It has been hypothesized that application of direct antagonists should elicit similar beneficial clinical outcome. Agonist **54** was discovered as a phosphate ester analogue of **FTY720** and acted as a $S1PR_1$ antagonist. Antagonist **54** was capable of inhibit $S1PR_1$ signaling and downstream ERK activity *in vivo*.[109]

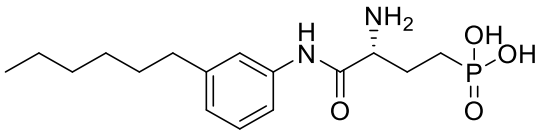


54

**Figure 1.11.** Structure of $S1PR_1$ antagonist **54**

## 1.7. Conclusions

S1P signaling is crucial for cell survival, migration and development, and dysregulated S1P signaling can cause numerous diseases. Various strategies, targeting different S1P modulators have been investigated for the treatment of S1P related diseases and disorders. Developing selective SphK inhibitors and S1PR modulators has been the most attractive and developed strategy, which has been validated by the clinical approval of **FTY720**. However, there is still need for in-depth investigation of the S1P signaling pathway and the development of more drugs for treating S1P-related diseases.

## 1.8. References

1. Maceyka, M.; Spiegel, S., Sphingolipid metabolites in inflammatory disease. *Nature* **2014,** *510* (7503), 58.
2. Pitson, S. M., Regulation of sphingosine kinase and sphingolipid signaling. *Trends Biochem. Sci.* **2011,** *36* (2), 97-107.
3. Van Brocklyn, J. R.; Williams, J. B., The control of the balance between ceramide and sphingosine-1-phosphate by sphingosine kinase: oxidative stress and the seesaw of cell survival and death. *Comp. Biochem. Physiol. B Biochem. Mol. Biol.* **2012,** *163* (1), 26-36.
4. Zhang, Y.; Berka, V.; Song, A.; Sun, K.; Wang, W.; Zhang, W.; Ning, C.; Li, C.; Zhang, Q.; Bogdanov, M.; Alexander, D. C.; Milburn, M. V.; Ahmed, M. H.; Lin, H.; Idowu, M.; Zhang, J.; Kato, G. J.; Abdulmalik, O. Y.; Zhang, W.; Dowhan, W.; Kellems,

R. E.; Zhang, P.; Jin, J.; Safo, M.; Tsai, A. L.; Juneja, H. S.; Xia, Y., Elevated sphingosine-1-phosphate promotes sickling and sickle cell disease progression. *J. Clin. Invest.* **2014,** *124* (6), 2750-61.
5. Schnute, M. E.; McReynolds, M. D.; Carroll, J.; Chrencik, J.; Highkin, M. K.; Iyanar, K.; Jerome, G.; Rains, J. W.; Saabye, M.; Scholten, J. A.; Yates, M.; Nagiec, M. M., Discovery of a Potent and Selective Sphingosine Kinase 1 Inhibitor through the Molecular Combination of Chemotype-Distinct Screening Hits. *J. Med. Chem.* **2017,** *60* (6), 2562-2572.
6. Brinkmann, V.; Billich, A.; Baumruker, T.; Heining, P.; Schmouder, R.; Francis, G.; Aradhye, S.; Burtin, P., Fingolimod (FTY720): discovery and development of an oral drug to treat multiple sclerosis. *Nat. Rev. Drug Discovery* **2010,** *9* (11), 883-97.
7. D Mullen, T.; M Obeid, L., Ceramide and apoptosis: exploring the enigmatic connections between sphingolipid metabolism and programmed cell death. *Anticancer Agents Med. Chem.* **2012,** *12* (4), 340-363.
8. Ponnusamy, S.; Meyers-Needham, M.; Senkal, C. E.; Saddoughi, S. A.; Sentelle, D.; Selvam, S. P.; Salas, A.; Ogretmen, B., Sphingolipids and cancer: ceramide and sphingosine-1-phosphate in the regulation of cell death and drug resistance. *Future Oncol.* **2010,** *6* (10), 1603-1624.
9. McNaughton, M.; Pitman, M.; Pitson, S. M.; Pyne, N. J.; Pyne, S., Proteasomal degradation of sphingosine kinase 1 and inhibition of dihydroceramide desaturase by the sphingosine kinase inhibitors, SKi or ABC294640, induces growth arrest in androgen-independent LNCaP-AI prostate cancer cells. *Oncotarget* **2016,** *7* (13), 16663.
10. Andrieu-Abadie, N.; Gouazé, V.; Salvayre, R.; Levade, T., Ceramide in apoptosis signaling: relationship with oxidative stress. *Free Radical Biol. Med.* **2001,** *31* (6), 717-728.
11. Haimovitz-Friedman, A.; Kan, C.-C.; Ehleiter, D.; Persaud, R. S.; Mcloughlin, M.; Fuks, Z.; Kolesnick, R. N., Ionizing radiation acts on cellular membranes to generate ceramide and initiate apoptosis. *J. Exp. Med.* **1994,** *180* (2), 525-535.
12. Ohtani, R.; Tomimoto, H.; Kondo, T.; Wakita, H.; Akiguchi, I.; Shibasaki, H.; Okazaki, T., Upregulation of ceramide and its regulating mechanism in a rat model of chronic cerebral ischemia. *Brain Res.* **2004,** *1023* (1), 31-40.
13. Chmura, S. J.; Nodzenski, E.; Beckett, M. A.; Kufe, D. W.; Quintans, J.; Weichselbaum, R. R., Loss of ceramide production confers resistance to radiation-induced apoptosis. *Cancer Res.* **1997,** *57* (7), 1270-1275.
14. Cuvillier, O., Sphingosine in apoptosis signaling. *Biochim. Biophys. Acta, Mol. Cell. Biol. Lipids* **2002,** *1585* (2), 153-162.
15. Melendez, A. J.; Carlos-Dias, E.; Gosink, M.; Allen, J. M.; Takacs, L., Human sphingosine kinase: molecular cloning, functional characterization and tissue distribution. *Gene* **2000,** *251* (1), 19-26.
16. Alvarez, S. E.; Harikumar, K. B.; Hait, N. C.; Allegood, J.; Strub, G. M.; Kim, E. Y.; Maceyka, M.; Jiang, H.; Luo, C.; Kordula, T.; Milstien, S.; Spiegel, S., Sphingosine-1-phosphate is a missing cofactor for the E3 ubiquitin ligase TRAF2. *Nature* **2010,** *465* (7301), 1084-8.
17. Tanfin, Z.; Serrano-Sanchez, M.; Leiber, D., ATP-binding cassette ABCC1 is involved in the release of sphingosine 1-phosphate from rat uterine leiomyoma ELT3 cells and late pregnant rat myometrium. *Cell. Signal.* **2011,** *23* (12), 1997-2004.

18. Liu, G.; Burns, S.; Huang, G.; Boyd, K.; Proia, R. L.; Flavell, R. A.; Chi, H., The receptor S1P 1 overrides regulatory T cell–mediated immune suppression through Akt-mTOR. *Nat. Immunol.* **2009,** *10* (7), 769.
19. Kohama, T.; Olivera, A.; Edsall, L.; Nagiec, M. M.; Dickson, R.; Spiegel, S., Molecular cloning and functional characterization of murine sphingosine kinase. *J. Biol. Chem.* **1998,** *273* (37), 23722-8.
20. Liu, H.; Sugiura, M.; Nava, V. E.; Edsall, L. C.; Kono, K.; Poulton, S.; Milstien, S.; Kohama, T.; Spiegel, S., Molecular cloning and functional characterization of a novel mammalian sphingosine kinase type 2 isoform. *J. Biol. Chem.* **2000,** *275* (26), 19513-20.
21. Wang, J.; Knapp, S.; Pyne, N. J.; Pyne, S.; Elkins, J. M., Crystal structure of sphingosine kinase 1 with PF-543. *ACS Med. Chem. Lett.* **2014,** *5* (12), 1329-1333.
22. Allende, M. L.; Sasaki, T.; Kawai, H.; Olivera, A.; Mi, Y.; van Echten-Deckert, G.; Hajdu, R.; Rosenbach, M.; Keohane, C. A.; Mandala, S.; Spiegel, S.; Proia, R. L., Mice deficient in sphingosine kinase 1 are rendered lymphopenic by FTY720. *J. Biol. Chem.* **2004,** *279* (50), 52487-92.
23. Wang, Z.; Min, X.; Xiao, S. H.; Johnstone, S.; Romanow, W.; Meininger, D.; Xu, H.; Liu, J.; Dai, J.; An, S.; Thibault, S.; Walker, N., Molecular basis of sphingosine kinase 1 substrate recognition and catalysis. *Structure* **2013,** *21* (5), 798-809.
24. Pitson, S. M.; Moretti, P. A.; Zebol, J. R.; Lynn, H. E.; Xia, P.; Vadas, M. A.; Wattenberg, B. W., Activation of sphingosine kinase 1 by ERK1/2 - mediated phosphorylation. *EMBO J.* **2003,** *22* (20), 5491-5500.
25. Adams, D. R.; Pyne, S.; Pyne, N. J., Sphingosine kinases: emerging structure–function insights. *Trends Biochem. Sci.* **2016,** *41* (5), 395-409.
26. Stahelin, R. V.; Hwang, J. H.; Kim, J.-H.; Park, Z.-Y.; Johnson, K. R.; Obeid, L. M.; Cho, W., The mechanism of membrane targeting of human sphingosine kinase 1. *J. Biol. Chem.* **2005**.
27. Shen, H.; Giordano, F.; Wu, Y.; Chan, J.; Zhu, C.; Milosevic, I.; Wu, X.; Yao, K.; Chen, B.; Baumgart, T., Coupling between endocytosis and sphingosine kinase 1 recruitment. *Nat. Cell Biol.* **2014,** *16* (7), 652.
28. Jarman, K. E.; Moretti, P. A.; Zebol, J. R.; Pitson, S. M., Translocation of sphingosine kinase 1 to the plasma membrane is mediated by calcium- and integrin-binding protein 1. *J. Biol. Chem.* **2010,** *285* (1), 483-92.
29. Zhu, W.; Gliddon, B. L.; Jarman, K. E.; Moretti, P. A.; Tin, T.; Parise, L. V.; Woodcock, J. M.; Powell, J. A.; Ruszkiewicz, A.; Pitman, M. R., CIB1 contributes to oncogenic signalling by Ras via modulating the subcellular localisation of sphingosine kinase 1. *Oncogene* **2017,** *36* (18), 2619.
30. Barr, R. K.; Lynn, H. E.; Moretti, P. A.; Khew-Goodall, Y.; Pitson, S. M., Deactivation of sphingosine kinase 1 by protein phosphatase 2A. *J. Biol. Chem.* **2008,** *283* (50), 34994-35002.
31. Safadi-Chamberlain, F.; Li-Ping, W.; Payne, S. G.; Chang-Uk, L.; Stratford, S.; Chavez, J. A.; Spiegel, S.; Summers, S. A., Effect of a membrane-targeted sphingosine kinase 1 on cell proliferation and survival. *Biochem. J.* **2005,** *388* (3), 827-834.
32. Pitson, S. M.; Xia, P.; Leclercq, T. M.; Moretti, P. A.; Zebol, J. R.; Lynn, H. E.; Wattenberg, B. W.; Vadas, M. A., Phosphorylation-dependent translocation of sphingosine kinase to the plasma membrane drives its oncogenic signalling. *J. Exp. Med.* **2005,** *201* (1), 49-54.

33. Venkataraman, K.; Thangada, S.; Michaud, J.; Oo, M. L.; Ai, Y.; Lee, Y.-M.; Wu, M.; Parikh, N. S.; Khan, F.; Proia, R. L., Extracellular export of sphingosine kinase-1a contributes to the vascular S1P gradient. *Biochem. J.* **2006,** *397* (3), 461-471.
34. Igarashi, N.; Okada, T.; Hayashi, S.; Fujita, T.; Jahangeer, S.; Nakamura, S., Sphingosine kinase 2 is a nuclear protein and inhibits DNA synthesis. *J. Biol. Chem.* **2003,** *278* (47), 46832-9.
35. Hait, N. C.; Allegood, J.; Maceyka, M.; Strub, G. M.; Harikumar, K. B.; Singh, S. K.; Luo, C.; Marmorstein, R.; Kordula, T.; Milstien, S.; Spiegel, S., Regulation of histone acetylation in the nucleus by sphingosine-1-phosphate. *Science* **2009,** *325* (5945), 1254-7.
36. Hait, N. C.; Bellamy, A.; Milstien, S.; Kordula, T.; Spiegel, S., Sphingosine kinase type 2 activation by ERK-mediated phosphorylation. *J. Biol. Chem.* **2007,** *282* (16), 12058-12065.
37. Le Stunff, H.; Giussani, P.; Maceyka, M.; Lépine, S.; Milstien, S.; Spiegel, S., Recycling of sphingosine is regulated by the concerted actions of sphingosine-1-phosphate phosphohydrolase 1 and sphingosine kinase 2. *J. Biol. Chem.* **2007,** *282* (47), 34372-34380.
38. Paugh, S. W.; Payne, S. G.; Barbour, S. E.; Milstien, S.; Spiegel, S., The immunosuppressant FTY720 is phosphorylated by sphingosine kinase type 2. *FEBS Lett.* **2003,** *554* (1-2), 189-193.
39. Johnson, K. R.; Johnson, K. Y.; Becker, K. P.; Bielawski, J.; Mao, C.; Obeid, L. M., Role of human sphingosine-1-phosphate phosphatase 1 in the regulation of intra-and extracellular sphingosine-1-phosphate levels and cell viability. *J. Biol. Chem.* **2003,** *278* (36), 34541-34547.
40. Schwab, S. R.; Pereira, J. P.; Matloubian, M.; Xu, Y.; Huang, Y.; Cyster, J. G., Lymphocyte sequestration through S1P lyase inhibition and disruption of S1P gradients. *Science* **2005,** *309* (5741), 1735-9.
41. Xia, P.; Wang, L.; Moretti, P. A.; Albanese, N.; Chai, F.; Pitson, S. M.; D'Andrea, R. J.; Gamble, J. R.; Vadas, M. A., Sphingosine kinase interacts with TRAF2 and dissects tumor necrosis factor-alpha signaling. *J. Biol. Chem.* **2002,** *277* (10), 7996-8003.
42. Strub, G. M.; Paillard, M.; Liang, J.; Gomez, L.; Allegood, J. C.; Hait, N. C.; Maceyka, M.; Price, M. M.; Chen, Q.; Simpson, D. C.; Kordula, T.; Milstien, S.; Lesnefsky, E. J.; Spiegel, S., Sphingosine-1-phosphate produced by sphingosine kinase 2 in mitochondria interacts with prohibitin 2 to regulate complex IV assembly and respiration. *FASEB J.* **2011,** *25* (2), 600-12.
43. Takasugi, N.; Sasaki, T.; Suzuki, K.; Osawa, S.; Isshiki, H.; Hori, Y.; Shimada, N.; Higo, T.; Yokoshima, S.; Fukuyama, T.; Lee, V. M.; Trojanowski, J. Q.; Tomita, T.; Iwatsubo, T., BACE1 activity is modulated by cell-associated sphingosine-1-phosphate. *J. Neurosci.* **2011,** *31* (18), 6850-7.
44. Sato, K.; Malchinkhuu, E.; Horiuchi, Y.; Mogi, C.; Tomura, H.; Tosaka, M.; Yoshimoto, Y.; Kuwabara, A.; Okajima, F., Critical role of ABCA1 transporter in sphingosine 1-phosphate release from astrocytes. *J. Neurochem.* **2007,** *103* (6), 2610-9.
45. Mitra, P.; Oskeritzian, C. A.; Payne, S. G.; Beaven, M. A.; Milstien, S.; Spiegel, S., Role of ABCC1 in export of sphingosine-1-phosphate from mast cells. *Proc. Nat. Acad. Sci.* **2006,** *103* (44), 16394-9.
46. Nieuwenhuis, B.; Luth, A.; Chun, J.; Huwiler, A.; Pfeilschifter, J.; Schafer-Korting, M.; Kleuser, B., Involvement of the ABC-transporter ABCC1 and the

sphingosine 1-phosphate receptor subtype S1P(3) in the cytoprotection of human fibroblasts by the glucocorticoid dexamethasone. *J. Mol. Med.* **2009,** *87* (6), 645-57.
47. Takabe, K.; Kim, R. H.; Allegood, J. C.; Mitra, P.; Ramachandran, S.; Nagahashi, M.; Harikumar, K. B.; Hait, N. C.; Milstien, S.; Spiegel, S., Estradiol induces export of sphingosine 1-phosphate from breast cancer cells via ABCC1 and ABCG2. *J. Biol. Chem.* **2010,** *285* (14), 10477-86.
48. Kawahara, A.; Nishi, T.; Hisano, Y.; Fukui, H.; Yamaguchi, A.; Mochizuki, N., The sphingolipid transporter spns2 functions in migration of zebrafish myocardial precursors. *Science* **2009,** *323* (5913), 524-7.
49. Hisano, Y.; Kobayashi, N.; Kawahara, A.; Yamaguchi, A.; Nishi, T., The sphingosine 1-phosphate transporter, SPNS2, functions as a transporter of the phosphorylated form of the immunomodulating agent FTY720. *J. Biol. Chem.* **2011,** *286* (3), 1758-66.
50. Hisano, Y.; Kobayashi, N.; Yamaguchi, A.; Nishi, T., Mouse SPNS2 functions as a sphingosine-1-phosphate transporter in vascular endothelial cells. *PLoS One* **2012,** *7* (6), e38941.
51. Mendoza, A.; Breart, B.; Ramos-Perez, W. D.; Pitt, L. A.; Gobert, M.; Sunkara, M.; Lafaille, J. J.; Morris, A. J.; Schwab, S. R., The transporter Spns2 is required for secretion of lymph but not plasma sphingosine-1-phosphate. *Cell Rep.* **2012,** *2* (5), 1104-10.
52. Fukuhara, S.; Simmons, S.; Kawamura, S.; Inoue, A.; Orba, Y.; Tokudome, T.; Sunden, Y.; Arai, Y.; Moriwaki, K.; Ishida, J.; Uemura, A.; Kiyonari, H.; Abe, T.; Fukamizu, A.; Hirashima, M.; Sawa, H.; Aoki, J.; Ishii, M.; Mochizuki, N., The sphingosine-1-phosphate transporter Spns2 expressed on endothelial cells regulates lymphocyte trafficking in mice. *J. Clin. Invest.* **2012,** *122* (4), 1416-26.
53. Nijnik, A.; Clare, S.; Hale, C.; Chen, J.; Raisen, C.; Mottram, L.; Lucas, M.; Estabel, J.; Ryder, E.; Adissu, H.; Sanger Mouse Genetics, P.; Adams, N. C.; Ramirez-Solis, R.; White, J. K.; Steel, K. P.; Dougan, G.; Hancock, R. E., The role of sphingosine-1-phosphate transporter Spns2 in immune system function. *J. Immunol.* **2012,** *189* (1), 102-11.
54. Nagahashi, M.; Kim, E. Y.; Yamada, A.; Ramachandran, S.; Allegood, J. C.; Hait, N. C.; Maceyka, M.; Milstien, S.; Takabe, K.; Spiegel, S., Spns2, a transporter of phosphorylated sphingoid bases, regulates their blood and lymph levels, and the lymphatic network. *FASEB J.* **2013,** *27* (3), 1001-11.
55. Bradley, E.; Dasgupta, S.; Jiang, X.; Zhao, X.; Zhu, G.; He, Q.; Dinkins, M.; Bieberich, E.; Wang, G., Critical role of Spns2, a sphingosine-1-phosphate transporter, in lung cancer cell survival and migration. *PLoS One* **2014,** *9* (10), e110119.
56. Vu, T. M.; Ishizu, A. N.; Foo, J. C.; Toh, X. R.; Zhang, F.; Whee, D. M.; Torta, F.; Cazenave-Gassiot, A.; Matsumura, T.; Kim, S.; Toh, S. E. S.; Suda, T.; Silver, D. L.; Wenk, M. R.; Nguyen, L. N., Mfsd2b is essential for the sphingosine-1-phosphate export in erythrocytes and platelets. *Nature* **2017,** *550* (7677), 524-528.
57. Kobayashi, N.; Kawasaki-Nishi, S.; Otsuka, M.; Hisano, Y.; Yamaguchi, A.; Nishi, T., MFSD2B is a sphingosine 1-phosphate transporter in erythroid cells. *Sci. Rep.* **2018,** *8* (1), 4969.
58. Liu, M.; Seo, J.; Allegood, J.; Bi, X.; Zhu, X.; Boudyguina, E.; Gebre, A. K.; Avni, D.; Shah, D.; Sorci-Thomas, M. G., Hepatic apolipoprotein M (apoM)

overexpression stimulates formation of larger apoM/sphingosine 1-phosphate-enriched plasma high density lipoprotein. *J. Biol. Chem.* **2014,** *289* (5), 2801-2814.
59. Mulya, A.; Seo, J.; Brown, A. L.; Gebre, A. K.; Boudyguina, E.; Shelness, G. S.; Parks, J. S., Apolipoprotein M expression increases the size of nascent preβ HDL formed by ATP binding cassette transporter A1. *J. Lipid. Res.* **2010,** *51* (3), 514-524.
60. Christoffersen, C.; Obinata, H.; Kumaraswamy, S. B.; Galvani, S.; Ahnström, J.; Sevvana, M.; Egerer-Sieber, C.; Muller, Y. A.; Hla, T.; Nielsen, L. B., Endothelium-protective sphingosine-1-phosphate provided by HDL-associated apolipoprotein M. *Proc. Nat. Acad. Sci.* **2011,** *108* (23), 9613-9618.
61. Galvani, S.; Sanson, M.; Blaho, V. A.; Swendeman, S. L.; Obinata, H.; Conger, H.; Dahlbäck, B.; Kono, M.; Proia, R. L.; Smith, J. D., HDL-bound sphingosine 1-phosphate acts as a biased agonist for the endothelial cell receptor S1P1 to limit vascular inflammation. *Sci. Signal.* **2015,** *8* (389), ra79-ra79.
62. Blaho, V. A.; Galvani, S.; Engelbrecht, E.; Liu, C.; Swendeman, S. L.; Kono, M.; Proia, R. L.; Steinman, L.; Han, M. H.; Hla, T., HDL-bound sphingosine-1-phosphate restrains lymphopoiesis and neuroinflammation. *Nature* **2015,** *523* (7560), 342.
63. Amano, M.; Nakayama, M.; Kaibuchi, K., Rho‐kinase/ROCK: a key regulator of the cytoskeleton and cell polarity. *Cytoskeleton* **2010,** *67* (9), 545-554.
64. Ephstein, Y.; Singleton, P. A.; Chen, W.; Wang, L.; Salgia, R.; Kanteti, P.; Dudek, S. M.; Garcia, J. G.; Jacobson, J. R., Critical role of S1PR1 and integrin β4 in HGF/c-Met-mediated increases in vascular integrity. *J. Biol. Chem.* **2013,** *288* (4), 2191-2200.
65. Gaengel, K.; Niaudet, C.; Hagikura, K.; Laviña, B.; Muhl, L.; Hofmann, J. J.; Ebarasi, L.; Nyström, S.; Rymo, S.; Chen, L. L., The sphingosine-1-phosphate receptor S1PR1 restricts sprouting angiogenesis by regulating the interplay between VE-cadherin and VEGFR2. *Dev. Cell* **2012,** *23* (3), 587-599.
66. Yoon, C. M.; Hong, B. S.; Moon, H. G.; Lim, S.; Suh, P.-G.; Kim, Y.-K.; Chae, C.-B.; Gho, Y. S., Sphingosine-1-phosphate promotes lymphangiogenesis by stimulating S1P1/Gi/PLC/Ca2+ signaling pathways. *Blood* **2008,** *112* (4), 1129-1138.
67. Lorenz, J. N.; Arend, L. J.; Robitz, R.; Paul, R. J.; MacLennan, A. J., Vascular dysfunction in S1P2 sphingosine 1-phosphate receptor knockout mice. *Am. J. Physiol. Regul. Integr. Comp. Physiol.* **2007,** *292* (1), R440-R446.
68. Kono, M.; Belyantseva, I. A.; Skoura, A.; Frolenkov, G. I.; Starost, M. F.; Dreier, J. L.; Lidington, D.; Bolz, S.-S.; Friedman, T. B.; Hla, T., Deafness and stria vascularis defects in S1P2 receptor-null mice. *J. Biol. Chem.* **2007,** *282* (14), 10690-10696.
69. Sanchez, T.; Skoura, A.; Wu, M. T.; Casserly, B.; Harrington, E. O.; Hla, T., Induction of vascular permeability by the sphingosine-1-phosphate receptor–2 (S1P2R) and its downstream effectors ROCK and PTEN. *Arter. Thromb. Vasc. Biol.* **2007,** *27* (6), 1312-1318.
70. Grabski, A. D.; Shimizu, T.; Deou, J.; Mahoney Jr, W. M.; Reidy, M. A.; Daum, G., Sphingosine-1-phosphate receptor-2 regulates expression of smooth muscle alpha-actin after arterial injury. *Arter. Thromb. Vasc. Biol.* **2009,** *29* (10), 1644-1650.
71. Loh, K. C.; Leong, W.-I.; Carlson, M. E.; Oskouian, B.; Kumar, A.; Fyrst, H.; Zhang, M.; Proia, R. L.; Hoffman, E. P.; Saba, J. D., Sphingosine-1-phosphate enhances satellite cell activation in dystrophic muscles through a S1PR2/STAT3 signaling pathway. *PloS one* **2012,** *7* (5), e37218.

72. Ishii, I.; Friedman, B.; Ye, X.; Kawamura, S.; McGiffert, C.; Contos, J. J.; Kingsbury, M. A.; Zhang, G.; Brown, J. H.; Chun, J., Selective loss of sphingosine 1-phosphate signaling with no obvious phenotypic abnormality in mice lacking its G protein-coupled receptor, LPB3/EDG-3. *J. Biol. Chem.* **2001,** *276* (36), 33697-33704.
73. Ishii, I.; Ye, X.; Friedman, B.; Kawamura, S.; Contos, J. J.; Kingsbury, M. A.; Yang, A. H.; Zhang, G.; Brown, J. H.; Chun, J., Marked perinatal lethality and cellular signaling deficits in mice null for the two sphingosine 1-phosphate (S1P) receptors, S1P2/LPB2/EDG-5 and S1P3/LPB3/EDG-3. *J. Biol. Chem.* **2002,** *277* (28), 25152-25159.
74. Kono, M.; Mi, Y.; Liu, Y.; Sasaki, T.; Allende, M. L.; Wu, Y.-P.; Yamashita, T.; Proia, R. L., The sphingosine-1-phosphate receptors S1P1, S1P2, and S1P3 function coordinately during embryonic angiogenesis. *J. Biol. Chem.* **2004,** *279* (28), 29367-29373.
75. Mousseau, Y.; Mollard, S.; Richard, L.; Nizou, A.; Faucher-Durand, K.; Cook-Moreau, J.; Qiu, H.; Baaj, Y.; Funalot, B.; Fourcade, L., Fingolimod inhibits PDGF-B-induced migration of vascular smooth muscle cell by down-regulating the S1PR1/S1PR3 pathway. *Biochimie* **2012,** *94* (12), 2523-2531.
76. Herr, D. R.; Lee, C.-W.; Wang, W.; Ware, A.; Rivera, R.; Chun, J., Sphingosine 1-phosphate receptors are essential mediators of eyelid closure during embryonic development. *J. Biol. Chem.* **2013,** *288* (41), 29882-29889.
77. Hirata, N.; Yamada, S.; Shoda, T.; Kurihara, M.; Sekino, Y.; Kanda, Y., Sphingosine-1-phosphate promotes expansion of cancer stem cells via S1PR3 by a ligand-independent Notch activation. *Nat. Commun.* **2014,** *5*, 4806.
78. Maeda, Y.; Matsuyuki, H.; Shimano, K.; Kataoka, H.; Sugahara, K.; Chiba, K., Migration of CD4 T cells and dendritic cells toward sphingosine 1-phosphate (S1P) is mediated by different receptor subtypes: S1P regulates the functions of murine mature dendritic cells via S1P receptor type 3. *J. Immunol.* **2007,** *178* (6), 3437-3446.
79. Schulze, T.; Golfier, S.; Tabeling, C.; Räbel, K.; Gräler, M. H.; Witzenrath, M.; Lipp, M., Sphingosine-1-phospate receptor 4 (S1P4) deficiency profoundly affects dendritic cell function and TH17-cell differentiation in a murine model. *FASEB J.* **2011,** *25* (11), 4024-4036.
80. Niedernberg, A.; Blaukat, A.; Schöneberg, T.; Kostenis, E., Regulated and constitutive activation of specific signalling pathways by the human S1P5 receptor. *Br. J. Pharmacol.* **2003,** *138* (3), 481-493.
81. Van Brocklyn, J. R.; Letterle, C. A.; Snyder, P. J.; Prior, T. W., Sphingosine-1-phosphate stimulates human glioma cell proliferation through Gi-coupled receptors: role of ERK MAP kinase and phosphatidylinositol 3-kinase β. *Cancer Lett.* **2002,** *181* (2), 195-204.
82. Hu, W.-M.; Li, L.; Jing, B.-Q.; Zhao, Y.-S.; Wang, C.-L.; Feng, L.; Xie, Y.-E., Effect of S1P5 on proliferation and migration of human esophageal cancer cells. *World J. Gastroenterol.* **2010,** *16* (15), 1859.
83. Okamoto, H.; Takuwa, N.; Yokomizo, T.; Sugimoto, N.; Sakurada, S.; Shigematsu, H.; Takuwa, Y., Inhibitory regulation of Rac activation, membrane ruffling, and cell migration by the G protein-coupled sphingosine-1-phosphate receptor EDG5 but not EDG1 or EDG3. *Mol. Cell. Biol.* **2000,** *20* (24), 9247-9261.

84. Lepley, D.; Paik, J.-H.; Hla, T.; Ferrer, F., The G Protein–Coupled Receptor S1P2 Regulates Rho/Rho Kinase Pathway to Inhibit Tumor Cell Migration. *Cancer Res.* **2005,** *65* (9), 3788-3795.
85. Ader, I.; Malavaud, B.; Cuvillier, O., When the sphingosine kinase 1/sphingosine 1-phosphate pathway meets hypoxia signaling: new targets for cancer therapy. *Cancer Res.* **2009,** *69* (9), 3723-3726.
86. Nishida, N.; Yano, H.; Nishida, T.; Kamura, T.; Kojiro, M., Angiogenesis in cancer. *Vasc. Health Risk Manag.* **2006,** *2* (3), 213.
87. Chi, H., Sphingosine-1-phosphate and immune regulation: trafficking and beyond. *Trends Pharmacol. Sci.* **2011,** *32* (1), 16-24.
88. Skon, C. N.; Lee, J.-Y.; Anderson, K. G.; Masopust, D.; Hogquist, K. A.; Jameson, S. C., Transcriptional downregulation of S1pr1 is required for the establishment of resident memory CD8+ T cells. *Nat. Immunol.* **2013,** *14* (12), 1285.
89. Lee, H.; Deng, J.; Kujawski, M.; Yang, C.; Liu, Y.; Herrmann, A.; Kortylewski, M.; Horne, D.; Somlo, G.; Forman, S., STAT3-induced S1PR1 expression is crucial for persistent STAT3 activation in tumors. *Nat. Med.* **2010,** *16* (12), 1421.
90. Gräler, M. H.; Goetzl, E. J., The immunosuppressant FTY720 down-regulates sphingosine 1-phosphate G-protein-coupled receptors. *FASEB J.* **2004,** *18* (3), 551-553.
91. Liu, G.; Yang, K.; Burns, S.; Shrestha, S.; Chi, H., The S1P 1-mTOR axis directs the reciprocal differentiation of T H 1 and T reg cells. *Nat. Immunol.* **2010,** *11* (11), 1047.
92. Puneet, P.; Yap, C. T.; Wong, L.; Yulin, L.; Koh, D. R.; Moochhala, S.; Pfeilschifter, J.; Huwiler, A.; Melendez, A. J., SphK1 regulates proinflammatory responses associated with endotoxin and polymicrobial sepsis. *Science* **2010,** *328* (5983), 1290-1294.
93. Niessen, F.; Schaffner, F.; Furlan-Freguia, C.; Pawlinski, R.; Bhattacharjee, G.; Chun, J.; Derian, C. K.; Andrade-Gordon, P.; Rosen, H.; Ruf, W., Dendritic cell PAR1–S1P3 signalling couples coagulation and inflammation. *Nature* **2008,** *452* (7187), 654.
94. Venkataraman, K.; Lee, Y.-M.; Michaud, J.; Thangada, S.; Ai, Y.; Bonkovsky, H. L.; Parikh, N. S.; Habrukowich, C.; Hla, T., Vascular endothelium as a contributor of plasma sphingosine 1-phosphate. *Circ. Res.* **2008,** *102* (6), 669-676.
95. Camerer, E.; Regard, J. B.; Cornelissen, I.; Srinivasan, Y.; Duong, D. N.; Palmer, D.; Pham, T. H.; Wong, J. S.; Pappu, R.; Coughlin, S. R., Sphingosine-1-phosphate in the plasma compartment regulates basal and inflammation-induced vascular leak in mice. *J. Clin. Invest.* **2009,** *119* (7), 1871-1879.
96. Mizugishi, K.; Yamashita, T.; Olivera, A.; Miller, G. F.; Spiegel, S.; Proia, R. L., Essential role for sphingosine kinases in neural and vascular development. *Mol. Cell. Biol.* **2005,** *25* (24), 11113-21.
97. Allende, M. L.; Proia, R. L., Sphingosine-1-phosphate receptors and the development of the vascular system. *Biochim. Biophys. Acta, Mol. Cell. Biol. Lipids* **2002,** *1582* (1), 222-227.
98. Forrest, M.; Sun, S.-Y.; Hajdu, R.; Bergstrom, J.; Card, D.; Doherty, G.; Hale, J.; Keohane, C.; Meyers, C.; Milligan, J., Immune cell regulation and cardiovascular effects of sphingosine 1-phosphate receptor agonists in rodents are mediated via distinct receptor subtypes. *J. Pharmacol. Exp. Ther.* **2004,** *309* (2), 758-768.
99. Xu, S.-Z.; Muraki, K.; Zeng, F.; Li, J.; Sukumar, P.; Shah, S.; Dedman, A. M.; Flemming, P. K.; McHugh, D.; Naylor, J., A Sphingosine-1–phosphate-activated calcium

channel controlling vascular smooth muscle cell motility. *Circ. Res.* **2006,** *98* (11), 1381-1389.
100. Sun, K.; Zhang, Y.; Bogdanov, M. V.; Wu, H.; Song, A.; Li, J.; Dowhan, W.; Idowu, M.; Juneja, H. S.; Molina, J. G., Elevated adenosine signaling via adenosine A2B receptor induces normal and sickle erythrocyte sphingosine kinase 1 activity in human and mice. *Blood* **2015**, blood-2014-08-595751.
101. Darrow, M. C.; Zhang, Y.; Cinquin, B. P.; Smith, E. A.; Boudreau, R.; Rochat, R. H.; Schmid, M. F.; Xia, Y.; Larabell, C. A.; Chiu, W., Visualizing red blood cell sickling and the effects of inhibition of sphingosine kinase 1 using soft X-ray tomography. *J. Cell Sci.* **2016,** *129* (18), 3511-7.
102. Vogel, P.; Donoviel, M. S.; Read, R.; Hansen, G. M.; Hazlewood, J.; Anderson, S. J.; Sun, W.; Swaffield, J.; Oravecz, T., Incomplete inhibition of sphingosine 1-phosphate lyase modulates immune system function yet prevents early lethality and non-lymphoid lesions. *PLoS One* **2009,** *4* (1), e4112.
103. Bagdanoff, J. T.; Donoviel, M. S.; Nouraldeen, A.; Tarver, J.; Fu, Q.; Carlsen, M.; Jessop, T. C.; Zhang, H.; Hazelwood, J.; Nguyen, H.; Baugh, S. D.; Gardyan, M.; Terranova, K. M.; Barbosa, J.; Yan, J.; Bednarz, M.; Layek, S.; Courtney, L. F.; Taylor, J.; Digeorge-Foushee, A. M.; Gopinathan, S.; Bruce, D.; Smith, T.; Moran, L.; O'Neill, E.; Kramer, J.; Lai, Z.; Kimball, S. D.; Liu, Q.; Sun, W.; Yu, S.; Swaffield, J.; Wilson, A.; Main, A.; Carson, K. G.; Oravecz, T.; Augeri, D. J., Inhibition of sphingosine-1-phosphate lyase for the treatment of autoimmune disorders. *J. Med. Chem.* **2009,** *52* (13), 3941-53.
104. Bagdanoff, J. T.; Donoviel, M. S.; Nouraldeen, A.; Carlsen, M.; Jessop, T. C.; Tarver, J.; Aleem, S.; Dong, L.; Zhang, H.; Boteju, L.; Hazelwood, J.; Yan, J.; Bednarz, M.; Layek, S.; Owusu, I. B.; Gopinathan, S.; Moran, L.; Lai, Z.; Kramer, J.; Kimball, S. D.; Yalamanchili, P.; Heydorn, W. E.; Frazier, K. S.; Brooks, B.; Brown, P.; Wilson, A.; Sonnenburg, W. K.; Main, A.; Carson, K. G.; Oravecz, T.; Augeri, D. J., Inhibition of sphingosine 1-phosphate lyase for the treatment of rheumatoid arthritis: discovery of (E)-1-(4-((1R,2S,3R)-1,2,3,4-tetrahydroxybutyl)-1H-imidazol-2-yl)ethanone oxime (LX2931) and (1R,2S,3R)-1-(2-(isoxazol-3-yl)-1H-imidazol-4-yl)butane-1,2,3,4-tetraol (LX2932). *J. Med. Chem.* **2010,** *53* (24), 8650-62.
105. Zhao, Y.; Gorshkova, I. A.; Berdyshev, E.; He, D.; Fu, P.; Ma, W.; Su, Y.; Usatyuk, P. V.; Pendyala, S.; Oskouian, B.; Saba, J. D.; Garcia, J. G.; Natarajan, V., Protection of LPS-induced murine acute lung injury by sphingosine-1-phosphate lyase suppression. *Am. J. Respir. Cell Mol. Biol.* **2011,** *45* (2), 426-35.
106. Caballero, S.; Swaney, J.; Moreno, K.; Afzal, A.; Kielczewski, J.; Stoller, G.; Cavalli, A.; Garland, W.; Hansen, G.; Sabbadini, R.; Grant, M. B., Anti-sphingosine-1-phosphate monoclonal antibodies inhibit angiogenesis and sub-retinal fibrosis in a murine model of laser-induced choroidal neovascularization. *Exp. Eye. Res.* **2009,** *88* (3), 367-77.
107. Visentin, B.; Vekich, J. A.; Sibbald, B. J.; Cavalli, A. L.; Moreno, K. M.; Matteo, R. G.; Garland, W. A.; Lu, Y.; Yu, S.; Hall, H. S.; Kundra, V.; Mills, G. B.; Sabbadini, R. A., Validation of an anti-sphingosine-1-phosphate antibody as a potential therapeutic in reducing growth, invasion, and angiogenesis in multiple tumor lineages. *Cancer Cell* **2006,** *9* (3), 225-38.
108. Hale, J. J.; Lynch, C. L.; Neway, W.; Mills, S. G.; Hajdu, R.; Keohane, C. A.; Rosenbach, M. J.; Milligan, J. A.; Shei, G.-J.; Parent, S. A., A rational utilization of high-

throughput screening affords selective, orally bioavailable 1-benzyl-3-carboxyazetidine sphingosine-1-phosphate-1 receptor agonists. *J. Med. Chem.* **2004,** *47* (27), 6662-6665.
109. Sanna, M. G.; Wang, S.-K.; Gonzalez-Cabrera, P. J.; Don, A.; Marsolais, D.; Matheu, M. P.; Wei, S. H.; Parker, I.; Jo, E.; Cheng, W.-C., Enhancement of capillary leakage and restoration of lymphocyte egress by a chiral S1P 1 antagonist in vivo. *Nat. Chem. Biol.* **2006,** *2* (8), 434.

# Chapter 2. Design, Synthesis and Biological Evaluation of (*R*)-Prolinol Based Sphingosine Kinase 1 Inhibitors

## 2.1. Contribution

The work in this chapter was conducted in collaboration with Laura G. Wonilowicz, Dr. Yugesh Kharel, and Dr. Anne M. Brown. The author is responsible for the synthesis of all final compounds except for **2.14**, **2.17a-b** and the corresponding intermediate structures. Laura G. Wonilowicz is responsible for final compounds **2.14**, **2.17a-b** and their corresponding intermediates. All biological assays were conducted by Dr. Yugesh Kharel at the University of Virginia. All molecular modeling studies were conducted by Dr. Anne Brown in the Biochemistry Department at Virginia Tech. The final manuscript is currently being prepared by the author.

## 2.2. Abstract

Sphingosine kinase 1 (SphK1) is the major sphingosine kinase (SphK) isoform that catalyzes formation of sphingosine-1-phosphate (S1P), an important signaling molecule which interacts with multiple cellular targets. The potential of inhibiting SphK1 as an alternative therapeutic treatment for diseases such as sickle cell disease and human breast cancers has been under systematic investigation. PF-543 has been shown to be effective in reducing S1P levels and slow down the sickling process *in vivo*. However, potent SphK1 inhibitors with an adequate metabolic profile are still lacking. Herein, we report the synthesis and evaluation of **PF-543** analogues and the structure-activity relationship profile for modification of the tail region.

## 2.3. Introduction

Sphingosine-1-phosphate, a downstream catabolite of ceramide and sphingosine, has been shown to promote cell proliferation while sphingosine and ceramide are pro-apoptotic.[1] S1P functions as a ligand with multiple intracellular and extracellular targets including five G-protein coupled receptors ($S1PR_{1-5}$).[2] Interaction with these different targets regulate different cellular processes such as survival, migration, and proliferation.[3] S1P has been implicated in several diseases including cancer,[4-5] fibrosis,[6] and sickle cell diseases (SCD).[7] Thus, significant attention has been focused on controlling S1P generation, especially through selective inhibition of sphingosine kinase (SphK), which catalyze the formation of S1P.[8]

Synthesis of S1P is regulated by two isoforms of SphK. SphK1 and SphK2 have different subcellular distribution, substrate selectivity, and cellular function.[9-10] Encoded by different genes, SphK1 and SphK2 share some functional redundancy as mice with gene deletions of either isoenzyme are still viable and fertile.[11] However, circulating levels of S1P in SphK1-null mice are decreased significantly whereas SphK2-null mice have increased S1P level compared to wild type, indicating a key role of SphK1 in S1P biosynthesis.[12-13]

As such, various sphingosine kinase inhibitors have been developed. Among these, **PF-543** was discovered through combining fragments of two hits (**12** and **20a**), which were identified via high-throughput screening (Figure 2.1).[14] Brief structure-activity relationships were also investigated (Fig 2.2). The study indicated that (*R*)-prolinol and other hydroxylpyrrolidine groups were all potent and selective head

groups for SphK1 inhibition (Figure 2.1B). As for the tail groups, the 3-methyl group substitution seemed to be unnecessary for inhibition. Sulfonyl group was essential for selectivity, whereas replacing the sulfonyl group with cyclohexyl or isopropanyl group maintained inhibition but also lost selectivity (Figure 2.1B). Among those compounds, **PF-543** was determined to have a $K_i$ of 3.6 nM[15] and a >100 fold selectivity over SphK2. An *in vivo* mice model also demonstrated its capability of reducing more than half erythrocyte and plasma S1P concentration in SCD Tg mice at a dose of 0.93 mg/kg over a period of four weeks.[7] It was also shown to be efficacious as in reducing sickling of red blood cells.[16] Moreover, the crystal structure of **PF-543** bound to SphK1 revealed a strong hydrogen bond between (*R*)-prolinol head group and residual Asp264 in SphK1.[17] However, the need for a continuous dose of **PF-543** over four weeks via an osmotic pump device might be an indicator of its short half-life and low metabolic stability.

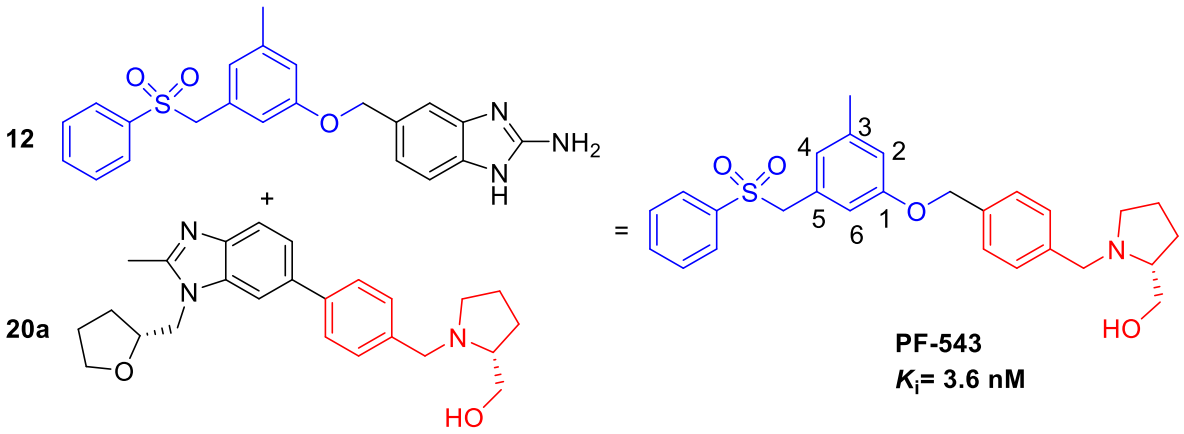


**Figure 2.1.** Molecular combination of identified fragments to yield structure of **PF-543**

We herein discuss the synthesis of analogs of **PF-543** with retained head group and different tail groups, with the interest of probing the lipophilic binding pocket in order to explore the metabolic profile. In this current report, we

investigated novel analogs of **PF-543** wherein changes in the lipophilic tail were introduced to improve the compound's binding affinity and selectivity.

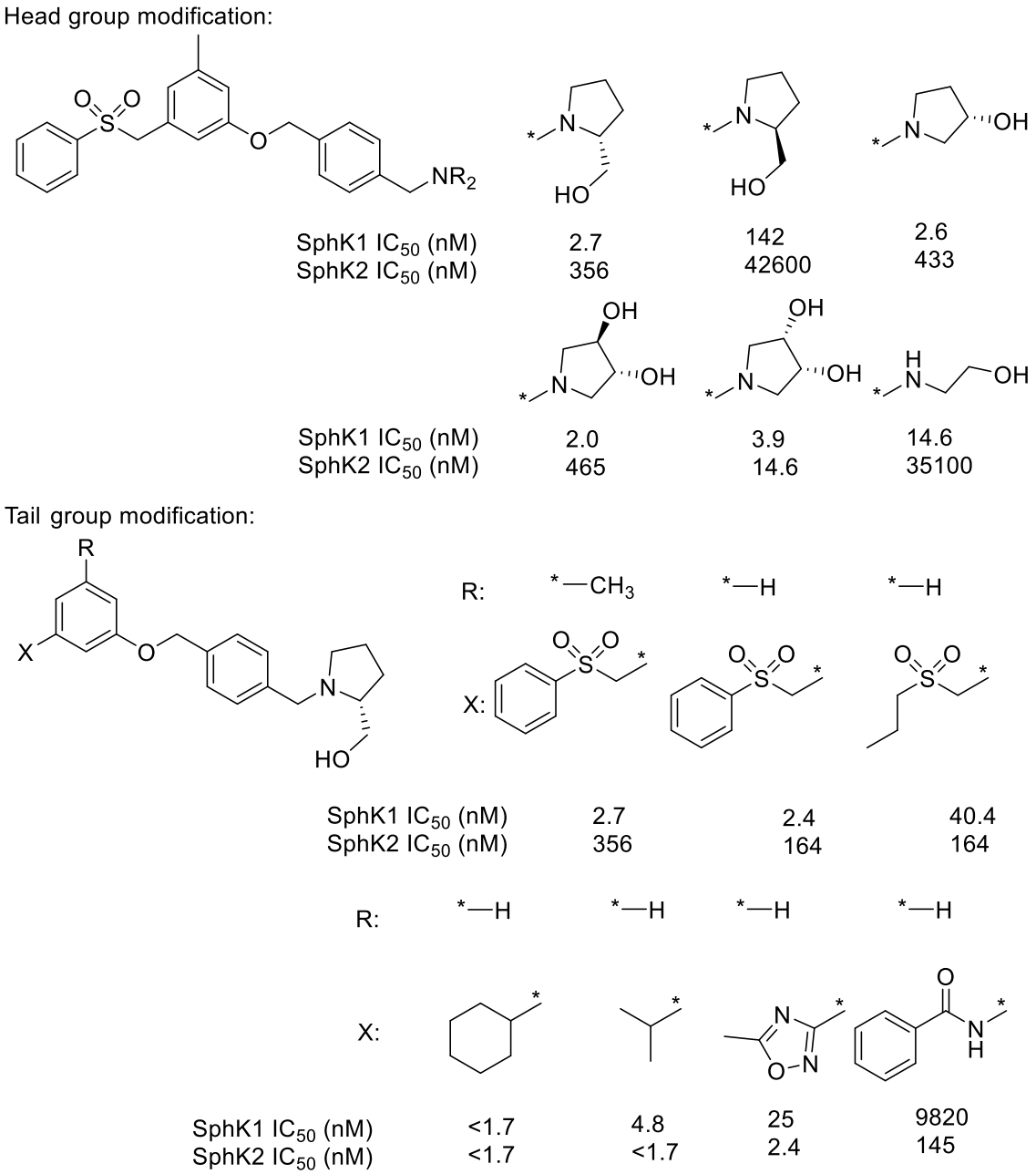


**Figure 2.2** Brief structure-activity relationship analysis for head-group and tail-group modifications of **PF-543**

## 2.4. Drug Design

In this study, different tail groups, such as alkoxy groups, alkyl groups, phenoxy groups and phenethyl groups were incorporated into the proposed structure (Figure 2.2). **PF-543** analogues with alkoxy tails were incorporated to mimic the structure of sphingosine. In consideration of *in vivo* stability, analogues with phenoxy tail groups were designed for the purpose of reducing the chance of being enzymatically metabolized. Analogues with alkyl and phenethyl tail groups without an ether moiety were also investigated to study the effect of added rigidity and potential π-π stacking interactions.

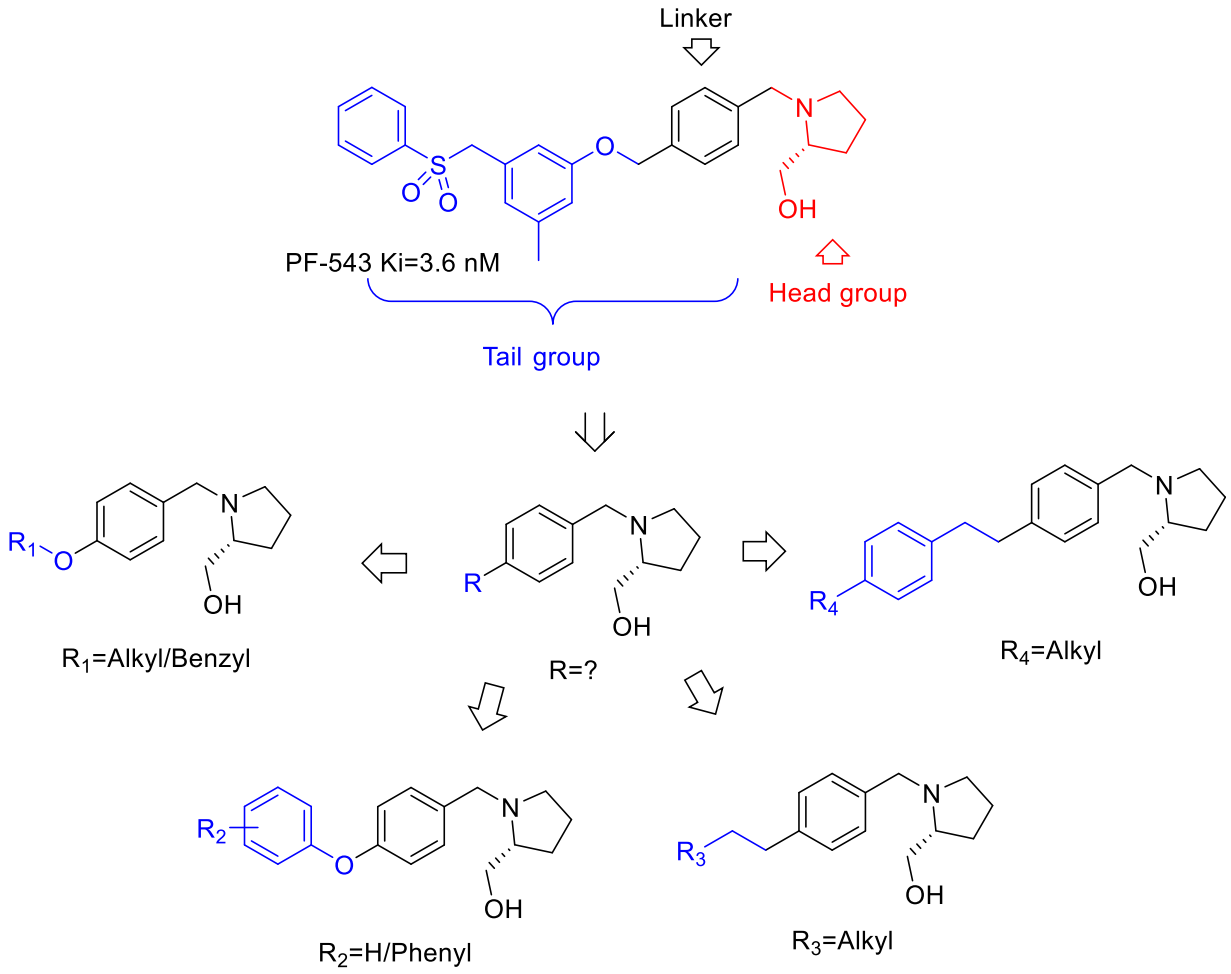


**Figure 2.3.** Compound design for modification of tail group region

## 2.5. Synthesis of Putative Inhibitors

The syntheses of inhibitors with different tail groups are shown in Scheme 2.1-2.3. Typically, the molecules were synthesized from the non-polar tail group region to the polar head group region to facilitate the purification of the final product. For compounds with alkoxy groups (Scheme 2.1), the benzaldehyde intermediates **2.2a-d** were generated through Williamson ether synthesis by reacting 4-hydroxybenzaldehyde **2.1** with alkyl bromides. The resulting benzaldehydes (**2.2a-e**) reacted with (*R*)-prolinol through reductive amination to afford the tertiary amine products **2.3a-e**. The free amine products

were then treated with HCl in MeOH to yield corresponding salts **2.4a-e** to improve stability and solubility. For compounds with a phenyl ether moiety **2.5a-e**, different phenol analogs were used to react with 4-fluorobenzonitrile through an $S_NAr$ reaction (Scheme 2.2). The benzonitrile intermediates **2.6a-e** were reduced by DIBAL-H to afford the corresponding benzaldehyde intermediates **2.7a-e** bearing *t*-butyl-, phenyl-, bromo- or iodo-substitution. With bromo- or iodo-substitution, the aldehyde intermediates were further modified with trifluoromethylphenyl groups through Suzuki coupling. For other compounds without a typical ether moiety (**2.14a-h**, **2.17a-b**, **2.20a-c**, **2.22a-c**), tail groups were incorporated through different Pd-catalyzed cross coupling reactions (Scheme 2.3). Alkyl tail groups were generated through Suzuki coupling (**2.14a-h**). Tail groups with internal doubles bond or triple bonds were generated through Heck coupling (**2.17a-b**) or Sonogashira coupling (**2.20a-c**). And after the tertiary amines have been generated, the internal triple bonds could be further reduced to single bonds through catalytic hydrogenation (**2.22a-c**).

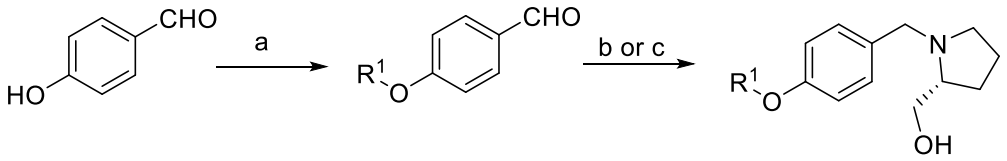


**2.1**

**2.2a-d**
**2.2a**: R1=heptyl
**2.2b**: R1=octyl
**2.2c**: R1=nonyl
**2.2d**: R1=decyl
**2.2e**: R1=4-trifluoromethylbenzyl

**2.3a-f**

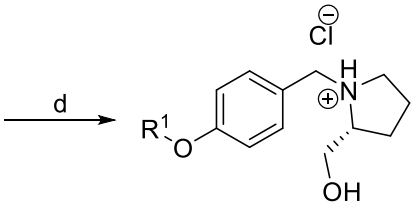


**2.4a-e**
**2.4a**: R1=heptyl
**2.4b**: R1=octyl
**2.4c**: R1=nonyl
**2.4d**: R1=decyl
**2.4e**: R1=decyl with (S)-prolinol head group
**2.4f**: R1=4-trifluoromethylbenzyl

**Scheme 2.1.** Reagents and conditions: (a) RBr, $K_2CO_3$, DMF, reflux, 12-16 h; (b) (i) (*D*)-Proline methyl ester hydrochloride, $NaBH(OAc)_3$, acetic acid, molecular sieves, DCM, rt, 12-16 h; (ii) $LiAlH_4$, THF, -70 °C to rt, 6 h; (c) (*R*)-Prolinol, $TsOH•H_2O$, $NaCNBH_3$, acetic acid, molecular sieves, DCM, rt, 12-16 h; (d) HCl, MeOH, rt, 11 min.

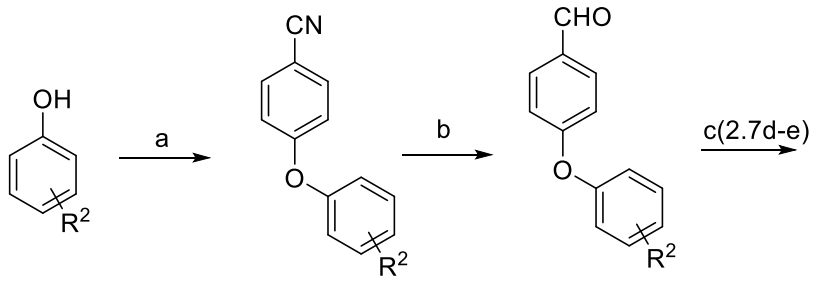


**2.5a-e** **2.6a-e** **2.7a-e**

**2.7a**: $R^2$=H
**2.7b**: $R^2$=3-t-butyl
**2.7c**: $R^2$=4-t-buyl
**2.7d**: $R^2$=3-bromo
**2.7e**: $R^2$=4-iodo

d (**2.7a-c**)

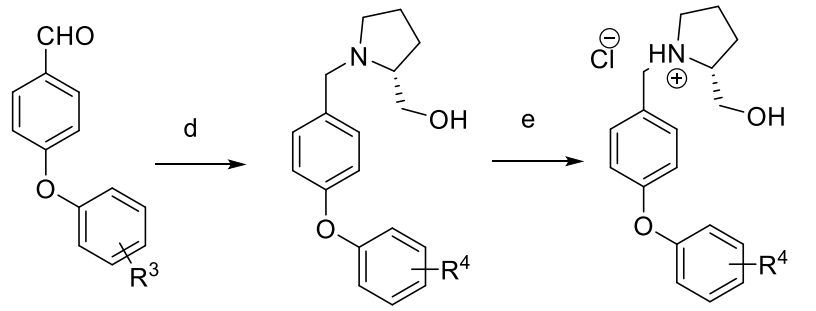


**2.8d-i** **2.9a-i** **2.10a-i**

**2.8d**: $R^3$=3-Ph
**2.8e**: $R^3$=3-Ph(3'-$CF_3$)
**2.8f**: $R^3$=3-Ph(4'-$CF_3$)
**2.8g**: $R^3$= 4-Ph
**2.8h**: $R^3$=4-Ph(3'-$CF_3$)
**2.8i**: $R^3$=4-Ph(4'-$CF_3$)

**2.10a**: $R^4$=H
**2.10b**: $R^4$=3-t-butyl
**2.10c**: $R^4$=3-Ph
**2.10d**: $R^4$=3-Ph(3'-$CF_3$)
**2.10e**: $R^4$=3-Ph(4'-$CF_3$)
**2.10f**: $R^4$=4-t-buyl
**2.10g**: $R^4$=4-Ph
**2.10h**: $R^4$=4-Ph(3'-$CF_3$)
**2.10i**: $R^4$=4-Ph(4'-$CF_3$)

**Scheme 2.2.** Reagent and conditions: (a) 4-Fluorobenzonitrile, $Cs_2CO_3$, DMF, reflux, 12-16h; (b) DIBAL-H, DCM, -70 °C to rt, 4-6 h; (c) Arylboronic acid, Pd(dppf)$Cl_2$, NaOH, THF/$H_2O$ = 5/1, 100 °C, 30 min, microwave; (d) (*R*)-Prolinol, $NaCNBH_3$, TsOH•$H_2O$, MeOH, rt, 12-16 h; (e) HCl, MeOH, rt, 11 min.

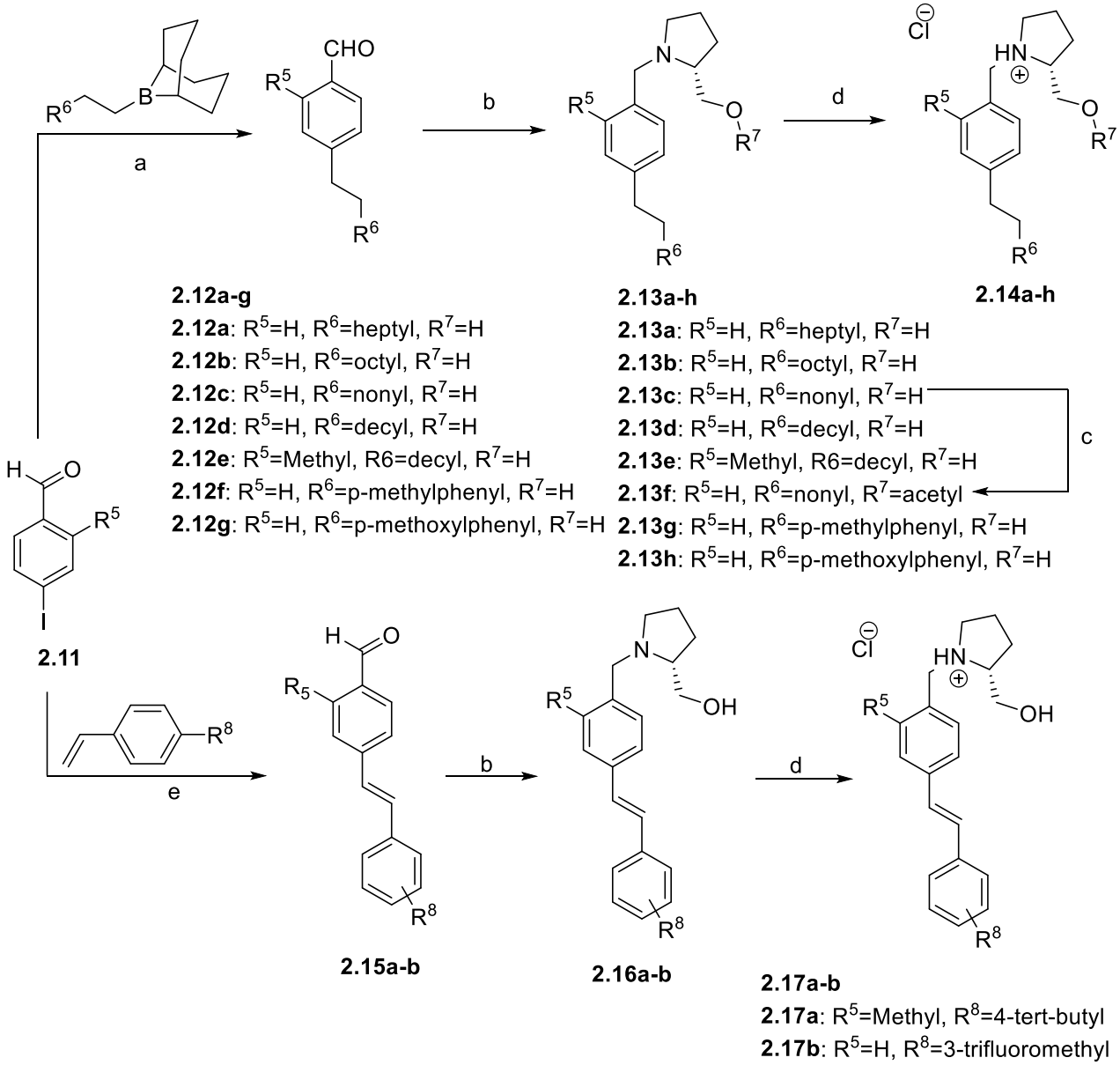


**Scheme 2.3.** Reagent and conditions: (a) (i) Alkene, 9-BBN, THF, 100 °C, 30 min, microwave; (ii) 4-Iodobenzaldehyde, $Pd(dppf)Cl_2$, NaOH, $THF/H_2O$ = 5/1, 100 °C, 30 min, microwave; (b) (*R*)-Prolinol, $NaCNBH_3$, $TsOH•H_2O$, MeOH, rt, 12-16 h; (c) Acetyl chloride, pyridine, rt, 16 h; (d) HCl, MeOH, rt, 11 min; (e) 4-Iodobenzaldehyde, alkene, $Pd(PPh_3)_2Cl_2$, $K_2CO_3$, DMF, reflux, 16 h.

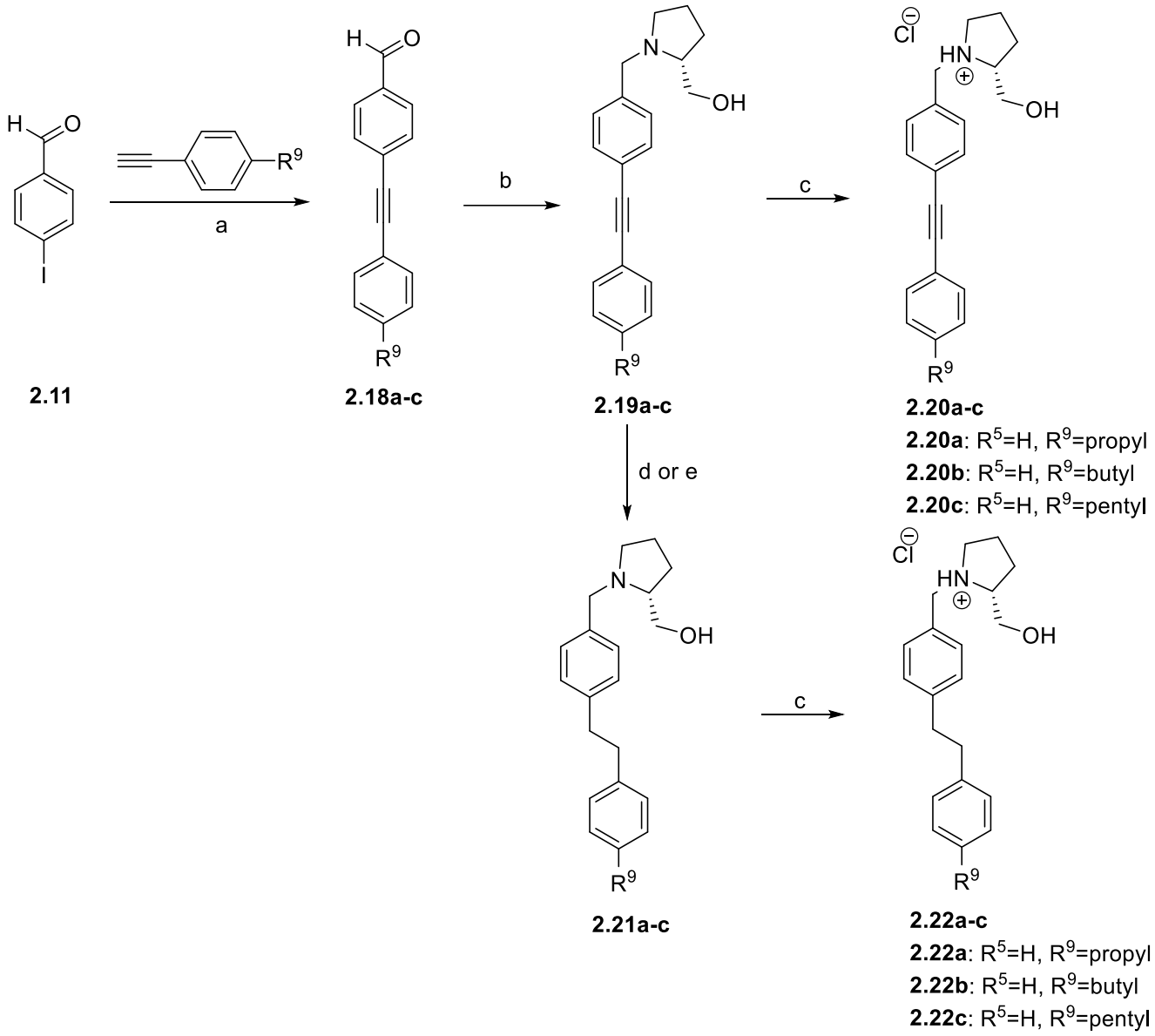


**Scheme 2.4.** Reagent and conditions: (a) 4-Iodobenzaldehyde, alkyne, $Pd(PPh_3)_2Cl_2$, CuI, TEA, THF, 50 °C, 1 h, microwave; (b) (*R*)-Prolinol, $NaCNBH_3$, $TsOH•H_2O$, MeOH, rt, 12-16 h; (c) Acetyl chloride, pyridine, rt, 16 h; (c) HCl, MeOH, rt, 11 min; (d) $H_2$ (*g*), 10% Pd /C, MeOH, rt, 0.5-2 h; (d) $Et_3SiH$, $H_2$ (*g*), 10% Pd /C, MeOH, rt, 5-30 min.

## 2.6. Biological Evaluation of Putative Inhibitors

### 2.6.1. Sphingosine Kinase Broken-cell Assay and Structure-activity Relationship

With the putative inhibitors in hand, their effect on S1P production was investigated using a previously reported broken-cell assay.[18] Recombinant human

SphK1 and SphK2 were expressed and isolated from cell lysate. $K_m$ values for SphK1/2 were determined by fixing the concentration of ATP at 250 μM and varying substrate Sph concentration at a range of 0-50 μM. $K_m$ values were found to be 10 μM and 5 μM, respectively for SphK1 and SphK2, agreeing with literature reports (5-17 μM for SphK1 and 3-5 μM for SphK2).[19-21] For following biological evaluation of putative inhibitors, Sph concentration was fixed at the $K_m$ value of SphK1/2. Inhibitors were assayed at 1 μM for human SphK1 and 0.3 μM for human SphK2.

Briefly, isolated enzymes, sphingosine substrate and $\gamma$-[$^{32}$P]ATP were incubated for 20 min with or without the presence of an inhibitor. The reaction mixture was extracted and separated by thin layer chromatography, and quantified by scintillation counting. SphK activity was determined by the amount of $\gamma$-[$^{32}$P]-S1P produced. SphK1/2 incubated without inhibitor was considered as a control with 100% enzyme activity, and SphK1/2 activity in the presence of inhibitor was represented as percent $\gamma$-[$^{32}$P]-S1P production relative to control.

The results of the inhibition assay are shown in Table 2.1. Starting with compound **2.4a,** which has a linear alkoxy tail mimicking the tail region of natural sphingosine, minimal inhibitory effect was achieved. The low inhibition might be due to the shortness of the tail, as indicated in a previous study with a similar scaffold with (*R*)-prolinol head group.[22] Increasing the tail length of the aliphatic chain from heptoxy (**2.4a**) to decoxy (**2.4d**) group showed a length-dependent inhibition pattern, in which the optimal inhibition was achieved with **2.4c** bearing a nonoxy tail group.

Compound **2.4e**, which is the enantiomer of **2.4d**, was synthesized to investigate the effect of head group chirality, which demonstrated a significant loss of inhibition, indicating the (*R*)-prolinol head group was crucial for binding with SphK. The *p*-trifluromethylbenzyl group has been reported to be a good tail group for designing SphK inhibitors; however, incorporation of this moiety did not improve the binding affinity as shown in **2.4f**.

**Table 2.1.** General inhibitor structure and inhibitory effects of compounds with SphK1 and SphK2[a]

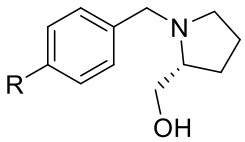


| Compd | R | % Activity | | Compd | R | % Activity | |
|---|---|---|---|---|---|---|---|
| | | SphK1 | SphK2 | | | SphK1 | SphK2 |
| **2.4a** | $C_7H_{15}O$—* | 95 | 104 | **2.10c** | 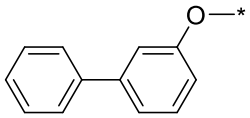 | 93 | 100 |
| **2.4b** | $C_8H_{17}O$—* | 64 | 99 | **2.10d** | 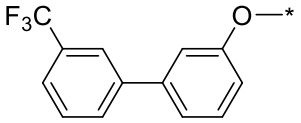 | 81 | 89 |
| **2.4c** | $C_9H_{19}O$—* | 16 | 56 | **2.10e** | 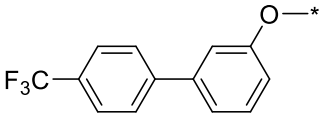 | 88 | 99 |
| **2.4d** | $C_{10}H_{21}O$—* | 38 | 89 | **2.10f** | 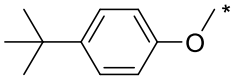 | 58 | 78 |
| **2.4e**[b] | $C_9H_{19}O$—* | 39 | 91[c] | **2.10g** | 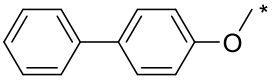 | 65 | 91 |
| **2.4f** | 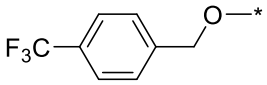 | 86 | 107 | **2.10h** | 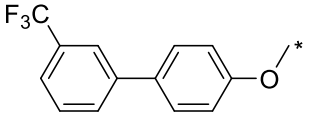 | 30 | 48 |
| **2.10a** | 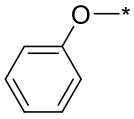 | 96 | 87 | **2.10j** | 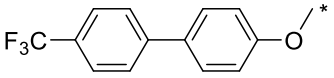 | 93 | 105 |
| **2.10b** | 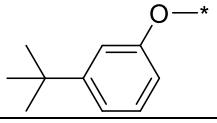 | 102 | 89 | | | | |

[a]Values represent percent activity of hSphK1 and hSphK2 with 10 μM and 5 μM of sphingosine, respectively. Each compound was assayed at 1 μM for human SphK1 and 0.3 μM for human SphK2 in duplicate and the values are the average of duplicate experiments. Lower values indicate better inhibition.
[b]Compound head group has inverted chirality.
[c]Compound assayed at 1 μM concentration.

Next, the effect of replacing the alkoxy group with phenoxy or biphenoxy group was explored. Replacement of a simple phenoxy group (**2.10a)** resulted in poor inhibition, so tail groups were built with more substitutions to probe the binding pocket.

Analogues bearing a *tert*-butyl (**2.10b**) and phenyl group (**2.10c**) at the meta-position gave minimal inhibition. This result is thought to be due to the large angle caused by 1,3-disubstitution pattern. Incorporating an additional trifluoromethyl group to the end phenyl group on either the *meta*- or *para*- position (**2.10d**, **2.10e**) only slightly increased inhibition potency. When the *tert*-butyl (**2.10f**) and phenyl groups (**2.10g**) were incorporated at the *para*-position, both compounds showed significantly increased inhibition potency. An additional trifluoromethyl group on the end phenyl group at the *meta*-position (**2.10h**) improved inhibition potency further, while a trifluoromethyl group on the *para*-position (**2.10i**) led to significant loss of inhibition, indicating that the *meta*-substitution of the end phenyl ring plays an important role for favorable binding.

Analogues with alkyl groups were also investigated (Table 2.2). As expected, increasing the tail length of the aliphatic chain from nonyl to dodecyl group (**2.14a-d**) showed a length-dependent inhibition pattern as well, in which the optimal inhibition was achieved with the dodecyl group (**2.14d**). However, there was also an observed lower selectivity for SphK1 of **2.14d**, comparing to its alkoxy counterpart **2.4c**. Compound **2.14e** was designed with a methyl group as $R_2$ since it has been hypothesized that the methyl group should shield the benzyl amine moiety from being oxidized by the enzyme. Compound **2.14e** still turned out to be potent inhibitor, although not comparable to **2.14d**, indicating there should be more space close to the benzylic position in the binding pocket to be exploited. Protecting the head group alcohol of **2.14d** with acetyl group afforded compound **2.14f**, which demonstrated loss of inhibition, suggesting the free alcohol for forming hydrogen bonding is essential for binding. However, the protection still retained moderate inhibition and might be an advantageous prodrug strategy for drug

administration. Introducing phenyl groups in **2.14g-h**, which might form π-π interactions with SphK1 Phe303 residue, lead to a significant loss of potency that might be caused by the shortness of tail group.

**Table 2.2.** General inhibitor structure and inhibitory effects of compounds with SphK1 and SphK2[a]

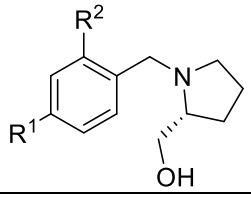


| Compd | $R^1$ | $R^2$ | % Activity | | Compd | $R^1$ | $R^2$ | % Activity | |
|---|---|---|---|---|---|---|---|---|---|
| | | | SphK1 | SphK2 | | | | SphK1 | SphK2 |
| **2.14a** | $C_9H_{19}$—* | H | 38 | 56 | **2.17a** | 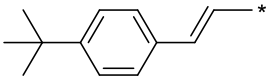 | Me | 77 | 100 |
| **2.14b** | $C_{10}H_{21}$—* | H | 24 | 46 | **2.17b** | 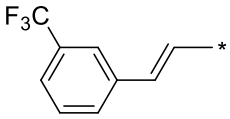 | H | 55 | 87 |
| **2.14c** | $C_{11}H_{23}$—* | H | 25 | 82 | **2.20a** | 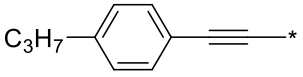 | H | 84 | 100 |
| **2.14d** | $C_{12}H_{25}$—* | H | 22 | 63 | **2.20b** | 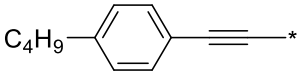 | H | 47 | 75 |
| **2.14e** | $C_{12}H_{25}$—* | Me | 33 | 62 | **2.20c** | 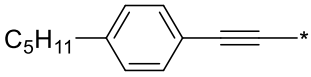 | H | 51 | 81 |
| **2.14f**[b] | $C_{11}H_{23}$—* | H | 53 | 74 | **2.22a** | 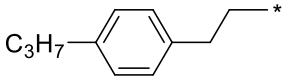 | H | 71 | 97 |
| **2.14g** | 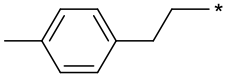 | H | 96 | 97 | **2.22b** | 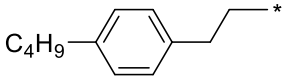 | H | 69 | 100 |
| **2.14h** | 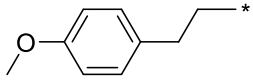 | H | 92 | 98 | **2.22c** | 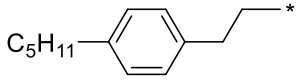 | H | 64 | 85 |

[a]Values represent percent activity of hSphK1 and hSphK2 with 10 μM and 5 μM of sphingosine, respectively. Each compound was assayed at 1 μM for human SphK1 and 0.3 μM for human SphK2 in duplicate and the values are the average of duplicate experiments. Lower values indicate better inhibition.
[b]Compound head group was protected with acetyl group

Inhibitors with rigid tail groups bearing internal double/triple bonds with relatively short length were also evaluated (Table 2.2). Loss of inhibition was observed,

potentially because the linear internal triple bonds prevents the tail group from fitting well into the binding pocket (**2.20a-c**). Increasing the tail length helped to improve the binding affinity slightly, however, the weak to moderate inhibitions were not comparable to the alkyl analogues (**2.22a-c**).

Values of inhibition constant ($K_i$) for hit compounds **2.14c** and **2.14d** were determined with same assay, due to their high potency and dual selectivity. $K_i$ values were determined through a reported method.[18] This method used less-expensive highly expressed crude enzyme instead of pure enzyme. Moreover, compared to traditional method, this method is more efficient in that it doesn't require incubation with multiple substrate concentrations at multiple inhibitor concentrations. Briefly, highly expressed enzyme SphK1/2 was used for incubation and kinetic study was carried out. Initial velocity of catalysis (less than 5% substrate consumption) was measured and SphK1/2 kinetic constants were obtained. The data was fitted to the Michaelis-Menten equation by non-linear regression using GraphPad Prism 5.01 (GraphPad Software). $K_i$ values were calculated using the following equation:[18]

$$K_i = [I]/(K'_m/K_m\text{-}1)$$

Where [I] is the concentration of inhibitor; and $K'_m$ and $K_m$ are the Michaelis-Menten constants in the presence and absence of inhibitor, respectively.

Results indicated their inhibition potency were in sub-micromolar range and confirmed their selectivity of SphK1 over SphK2 (Table 2.3). Moreover, **2.14c-d** were both SphK1 selective, although their selectivity varied. **2.14c** has a >2 fold selectivity for SphK1. However, when the tail group length was increased by one carbon, as in **2.14d**, the selectivity dropped to <2 fold.

**Table 2.3.** $K_i$ values against recombinant hSphK

| Compounds | hSphK1 $K_i$ (μM) | hSphK2 $K_i$ (μM) |
|---|---|---|
| **2.14c** | 0.39 ± 0.02 | 0.87 ± 0.03 |
| **2.14d** | 0.68 ± 0.01 | 0.95 ± 0.03 |

### 2.6.2. Sphingosine Kinase Yeast Assay

Hit compounds **2.10h**, **2.14a-d** were further evaluated via human SphK recombinant yeast assay to determine $EC_{50}$ values for hSphK1 and hSphK2 (Table 2.4), according to a previous reported hSphK recombinant yeast assay.[23] *Saccharomyces cerevisiae* was used as the platform for compound screening, and the assay take advantage of toxicity of S1P to yeast cells. Mutant strains are forced to express hSphK1 and are knocked out of their wild-type genes expressing a phosphatase and a lyase, the two catabolic enzymes that degrade S1P. After incubation, the accumulation of S1P causes retarded cell growth. However, incubation with SphK1 inhibitor can rescue cell growth in a dose dependent manner. Cell growth is determined indirectly through measuring the absorbance of the buffer media, and is proportionally correlated with measured optical density. Based on the dose dependent optical density data, $EC_{50}$ values (dose of inhibitor at which yeast growth was rescued by 50%) can be calculated from the sigmoid curve. Compared to the broken-cell assay (20 min incubation), the yeast cell assay requires longer incubation (24-48 h). Moreover, there's also possibility that compounds might not penetrate through yeast cell membrane, although the chance is very rare. On the other hand, there's also significant advantage for the yeast cell assay. This assay doesn't consume radioactive ATP, and no control experiment is required. In addition, due to the ease of culturing and low cost, multiple compounds can be assayed

at varied concentrations for both SphK isoforms, which allowed for higher throughput screening for inhibitors.

Briefly, yeast containing hSphK plasmid was incubated with various concentrations of inhibitors for 24-48 h, and the absorbance of the culture was measured. Inhibitors were assayed at different concentrations, and $EC_{50}$ values were calculated from the concentration-absorbance diagram. $EC_{50}$ values in the sub-micromolar range are consistent with $K_i$ values generated by the aforementioned broken-cell assay, further confirming the potency and permeability of these compounds. However, compounds **2.14b** and **2.14d** with even numbers of tail length showed around 2 fold selectivity for SphK1, while compounds **2.14a** and **2.14c** with odd numbers of tail length have less selectivity. Compound **2.14c** even had reversed selectivity and favored Sphk2 inhibition. This inconsistency of selectivity, comparing to results based on broken-cell assay, might be attributed to the complex biology of yeast cells.

**Table 2.4.** $EC_{50}$ values of hit compounds

| Compounds | hSphK1 $EC_{50}$ (μM) | hSphK2 $EC_{50}$ (μM) |
|---|---|---|
| **2.10h** | 0.30 ± 0.02 | 0.49 ± 0.04 |
| **2.14a** | 0.31 ± 0.04 | 0.39 ± 0.03 |
| **2.14b** | 0.20 ± 0.03 | 0.40 ± 0.05 |
| **2.14c** | 0.28 ± 0.02 | 0.25 ± 0.02 |
| **2.14d** | 0.15 ± 0.01 | 0.29 ± 0.03 |

### 2.6.3. U937 Cell Culture Assay

Due to the different nature of the yeast cell and eukaryotic cell membranes, compound **2.14d** was also evaluated in U973 cell lines to investigate its SphK1 inhibitory effect and permeability (Figure 2.4). The administration of **2.14d** lead to a dose-dependent reduction of S1P levels, indicating a dose-dependent SphK1 inhibition. At a 1

μM inhibitor level, S1P production was reduced by 90%, indicating that **2.14d** was potent SphK1 inhibitor and was permeable through human cell membrane.

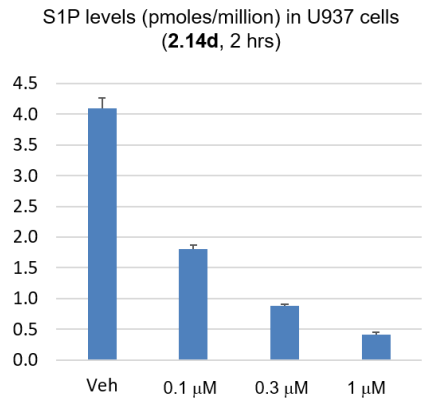


**Figure 2.4.** Dose-dependent reduction of S1P levels by **2.14d** in U937 cell line

### 2.6.4. Mouse Study

Compound **2.14a** was also evaluated with a mouse model to demonstrate its capability of reducing S1P production *in vivo* (Figure 2.5). Three hours after intraperitoneal injection of compound **2.14a** into C57BL/6j mice, blood was collected. The collected blood was either lysed directly or used for isolation of plasma. Lysed blood and isolated plasma were quantified separately for S1P concentration to compare their difference of S1P levels.

Compound **2.14a** was selected instead of hit compound **2.14c** due to its shorter tail group and resultingly lower hydrophobicity, which could potentially improve its bioavailability. Reduction of blood and plasma S1P was expected as the characteristic of a SphK dual inhibitors. However, to our surprise, administration of **2.14c** results in a 20% reduction in plasma S1P after 3 hours of single dose at 10 mg/kg but also slight increase of blood S1P. This result was very consistent with the control compound **SLC4101553**, which was a known SphK2 selective inhibitor (91% SphK1 activity at 1

μM inhibitor concentration and 53% SphK2 activity at 0.3 μM inhibitor concentration). The mechanism behind their similar biological function is not known, but the plasma S1P reduction result was still encouraging, due to the essential role of plasma S1P in inducing lymphocyte trafficking. Although this mouse study could not be directly compared with that of **PF-543** due to different dose, duration and administration method, the *in vivo* activity of **2.14c** still allowed for further improvement.

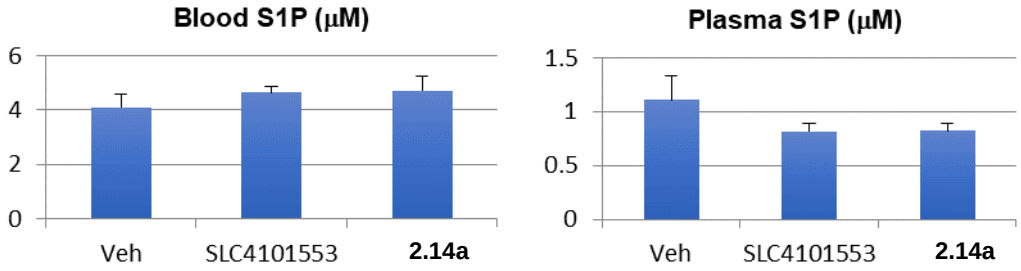


**Figure 2.5.** Effect of compound **2.14a** in reducing plasma S1P level in mice (10 mg/kg, IP, 3 h)

## 2.7. Molecular Modeling

Molecular docking of **2.14d** into SphK1 revealed its binding position in the enzyme (Figure 2.6). The modeling study was performed with hSphK1 (PDB: 3VZB) and ADP (PDB: 3VZD) overlaid. ADP was converted to ATP and binding energy was minimized to generate the docking structure. Strong hydrogen bonds formed between the head group of the inhibitor with polar region of the binding pocket: the primary alcohol formed a 3.0 Å hydrogen bond with Ser168 residue and the tertiary ammonium formed two 3.6 Å hydrogen bonds with Asp178. This suggested the (*R*)-prolinol head group is crucial for binding potency. Also, this typical binding pattern (hydrogen bonding with Ser168) favors SphK1 selectivity, which is consistent with our assay result. The lipophilic alkyl tail group formed a J-shape structure and fitted into the hydrophobic binding pocket to produce maximal hydrophobic interaction, similar to the observed

conformation in crystal structure of SphK1 with sphingosine.[24] The different inhibitory effects of **2.10h** and **2.10i** can also be explained by this modeling study. As the *meta*-trifluoromethyl group of **2.10h** can assume the bended structure, the resultingly stronger hydrophobic interaction improved inhibition. However, the *para*-trifluoromethyl group of **2.10i** might have steric interaction with the amino acid residues, which prohibited optimal binding of the inhibitor.

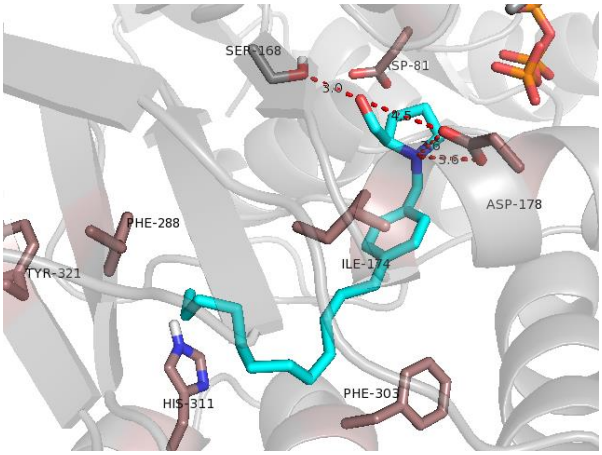


**Figure 2.6.** Molecular docking of compound **2.14c** into SphK1

## 2.8. Conclusion

In conclusion, compounds with different types of tail groups were synthesized and tested for inhibition against SphK and two hit compounds were found: **2.10h** and **2.14d** ($K_i$=0.68 μM for recombinant SphK1 and $EC_{50}$=0.15 μM for yeast assay with recombinant SphK1). Structure-activity relationship analysis revealed that compounds with linear tail groups tend to favor SphK1 inhibition and yield an optimal inhibition at a tail length of 10-12 atoms. Analogues incorporating a biphenyl group into the mid-region of the binding pocket are promising, as they displayed dual inhibition. Yeast cell assay and U937 cell line study confirmed potency and permeability of **2.14d** and its analogues with different tail length. A

mouse study indicated that designed inhibitor **2.14a** (an analogue of **2.14d** with shorter tail length) was able to reduce plasma S1P level but also increase S1P level, which resembled biological function of SphK2 inhibitor and the mechanism was not known yet. A modeling study revealed favorable binding of **2.14d** with SphK1, including hydrogen bonding of the head group and hydrophobic interaction of the lipid-like tail group.

## 2.9. References


1. Spiegel, S.; Milstien, S., Sphingosine 1-phosphate, a key cell signaling molecule. *J. Biol. Chem.* **2002,** *277* (29), 25851-4.
2. Sanchez, T.; Hla, T., Structural and functional characteristics of S1P receptors. *J. Cell. Biochem.* **2004,** *92* (5), 913-22.
3. Van Brocklyn, J. R.; Williams, J. B., The control of the balance between ceramide and sphingosine-1-phosphate by sphingosine kinase: oxidative stress and the seesaw of cell survival and death. *Comp. Biochem. Physiol. B Biochem. Mol. Biol.* **2012,** *163* (1), 26-36.
4. Pyne, N. J.; Pyne, S., Sphingosine 1-phosphate and cancer. *Nat. Rev. Cancer* **2010,** *10* (7), 489-503.
5. Visentin, B.; Vekich, J. A.; Sibbald, B. J.; Cavalli, A. L.; Moreno, K. M.; Matteo, R. G.; Garland, W. A.; Lu, Y.; Yu, S.; Hall, H. S.; Kundra, V.; Mills, G. B.; Sabbadini, R. A., Validation of an anti-sphingosine-1-phosphate antibody as a potential therapeutic in reducing growth, invasion, and angiogenesis in multiple tumor lineages. *Cancer Cell* **2006,** *9* (3), 225-38.
6. Li, C.; Kong, Y.; Wang, H.; Wang, S.; Yu, H.; Liu, X.; Yang, L.; Jiang, X.; Li, L.; Li, L., Homing of bone marrow mesenchymal stem cells mediated by sphingosine 1-phosphate contributes to liver fibrosis. *J. Hepatol.* **2009,** *50* (6), 1174-83.
7. Zhang, Y.; Berka, V.; Song, A.; Sun, K.; Wang, W.; Zhang, W.; Ning, C.; Li, C.; Zhang, Q.; Bogdanov, M.; Alexander, D. C.; Milburn, M. V.; Ahmed, M. H.; Lin, H.; Idowu, M.; Zhang, J.; Kato, G. J.; Abdulmalik, O. Y.; Zhang, W.; Dowhan, W.; Kellems, R. E.; Zhang, P.; Jin, J.; Safo, M.; Tsai, A. L.; Juneja, H. S.; Xia, Y., Elevated sphingosine-1-phosphate promotes sickling and sickle cell disease progression. *J. Clin. Invest.* **2014,** *124* (6), 2750-61.
8. Gustin, D. J.; Li, Y.; Brown, M. L.; Min, X.; Schmitt, M. J.; Wanska, M.; Wang, X.; Connors, R.; Johnstone, S.; Cardozo, M.; Cheng, A. C.; Jeffries, S.; Franks, B.; Li, S.; Shen, S.; Wong, M.; Wesche, H.; Xu, G.; Carlson, T. J.; Plant, M.; Morgenstern, K.; Rex, K.; Schmitt, J.; Coxon, A.; Walker, N.; Kayser, F.; Wang, Z., Structure guided design of a series of sphingosine kinase (SphK) inhibitors. *Bioorg. Med. Chem. Lett.* **2013,** *23* (16), 4608-16.

9. Jarman, K. E.; Moretti, P. A.; Zebol, J. R.; Pitson, S. M., Translocation of sphingosine kinase 1 to the plasma membrane is mediated by calcium- and integrin-binding protein 1. *J. Biol. Chem.* **2010,** *285* (1), 483-92.
10. Igarashi, N.; Okada, T.; Hayashi, S.; Fujita, T.; Jahangeer, S.; Nakamura, S., Sphingosine kinase 2 is a nuclear protein and inhibits DNA synthesis. *J. Biol. Chem.* **2003,** *278* (47), 46832-9.
11. Mizugishi, K.; Yamashita, T.; Olivera, A.; Miller, G. F.; Spiegel, S.; Proia, R. L., Essential role for sphingosine kinases in neural and vascular development. *Mol. Cell. Biol.* **2005,** *25* (24), 11113-21.
12. Allende, M. L.; Sasaki, T.; Kawai, H.; Olivera, A.; Mi, Y.; van Echten-Deckert, G.; Hajdu, R.; Rosenbach, M.; Keohane, C. A.; Mandala, S.; Spiegel, S.; Proia, R. L., Mice deficient in sphingosine kinase 1 are rendered lymphopenic by FTY720. *J. Biol. Chem.* **2004,** *279* (50), 52487-92.
13. Zemann, B.; Kinzel, B.; Muller, M.; Reuschel, R.; Mechtcheriakova, D.; Urtz, N.; Bornancin, F.; Baumruker, T.; Billich, A., Sphingosine kinase type 2 is essential for lymphopenia induced by the immunomodulatory drug FTY720. *Blood* **2006,** *107* (4), 1454-8.
14. Schnute, M. E.; McReynolds, M. D.; Carroll, J.; Chrencik, J.; Highkin, M. K.; Iyanar, K.; Jerome, G.; Rains, J. W.; Saabye, M.; Scholten, J. A.; Yates, M.; Nagiec, M. M., Discovery of a Potent and Selective Sphingosine Kinase 1 Inhibitor through the Molecular Combination of Chemotype-Distinct Screening Hits. *J. Med. Chem.* **2017,** *60* (6), 2562-2572.
15. Schnute, M. E.; McReynolds, M. D.; Kasten, T.; Yates, M.; Jerome, G.; Rains, J. W.; Hall, T.; Chrencik, J.; Kraus, M.; Cronin, C. N.; Saabye, M.; Highkin, M. K.; Broadus, R.; Ogawa, S.; Cukyne, K.; Zawadzke, L. E.; Peterkin, V.; Iyanar, K.; Scholten, J. A.; Wendling, J.; Fujiwara, H.; Nemirovskiy, O.; Wittwer, A. J.; Nagiec, M. M., Modulation of cellular S1P levels with a novel, potent and specific inhibitor of sphingosine kinase-1. *Biochem. J.* **2012,** *444* (1), 79-88.
16. Darrow, M. C.; Zhang, Y.; Cinquin, B. P.; Smith, E. A.; Boudreau, R.; Rochat, R. H.; Schmid, M. F.; Xia, Y.; Larabell, C. A.; Chiu, W., Visualizing red blood cell sickling and the effects of inhibition of sphingosine kinase 1 using soft X-ray tomography. *J. Cell Sci.* **2016,** *129* (18), 3511-7.
17. Wang, J.; Knapp, S.; Pyne, N. J.; Pyne, S.; Elkins, J. M., Crystal Structure of Sphingosine Kinase 1 with PF-543. *ACS Med. Chem. Lett.* **2014,** *5* (12), 1329-33.
18. Kharel, Y.; Mathews, T. P.; Kennedy, A. J.; Houck, J. D.; Macdonald, T. L.; Lynch, K. R., A rapid assay for assessment of sphingosine kinase inhibitors and substrates. *Anal. Rev. Biochem.* **2011,** *411* (2), 230-5.
19. Kohama, T.; Olivera, A.; Edsall, L.; Nagiec, M. M.; Dickson, R.; Spiegel, S., Molecular cloning and functional characterization of murine sphingosine kinase. *J. Biol. Chem.* **1998,** *273* (37), 23722-8.
20. PITSON, S. M.; D'ANDREA, R. J.; VANDELEUR, L.; MORETTI, P. A.; Pu, X.; GAMBLE, J. R.; VADAS, M. A.; WATTENBERG, B. W., Human sphingosine kinase: purification, molecular cloning and characterization of the native and recombinant enzymes. *Biochem. J.* **2000,** *350* (2), 429-441.

21. Liu, H.; Sugiura, M.; Nava, V. E.; Edsall, L. C.; Kono, K.; Poulton, S.; Milstien, S.; Kohama, T.; Spiegel, S., Molecular cloning and functional characterization of a novel mammalian sphingosine kinase type 2 isoform. *J. Biol. Chem.* **2000,** *275* (26), 19513-20.
22. Baek, D. J.; MacRitchie, N.; Anthony, N. G.; Mackay, S. P.; Pyne, S.; Pyne, N. J.; Bittman, R., Structure-activity relationships and molecular modeling of sphingosine kinase inhibitors. *J. Med. Chem.* **2013,** *56* (22), 9310-27.
23. Kharel, Y.; Agah, S.; Huang, T.; Mendelson, A. J.; Eletu, O. T.; Barkey-Bircann, P.; Gesualdi, J.; Smith, J. S.; Santos, W. L.; Lynch, K. R., Saccharomyces cerevisiae as a platform for assessing sphingolipid lipid kinase inhibitors. *PLoS One* **2018,** *13* (4), e0192179.
24. Wang, Z.; Min, X.; Xiao, S. H.; Johnstone, S.; Romanow, W.; Meininger, D.; Xu, H.; Liu, J.; Dai, J.; An, S.; Thibault, S.; Walker, N., Molecular basis of sphingosine kinase 1 substrate recognition and catalysis. *Structure* **2013,** *21* (5), 798-809.

# Chapter 3. Design, Synthesis and Biological Evaluation of Selective Sphingosine Kinase Inhibitors through Head Group Modifications

### 3.1. Contributions

The work in this chapter was conducted in collaboration with Dr. Yugesh Kharel, and Dr. Kevin Lynch. The author is solely responsible for the synthesis of all final compounds and the corresponding intermediate structures. All biological assays were conducted by Dr. Yugesh Kharel at the University of Virginia. The final manuscript is currently being prepared by the author

## 3.2. Abstract

Through tail modifications of **PF-543**, compounds with $K_i$ values in the sub-micromolar range were discovered. However, the limitation of **PF-543** caused by low *in vivo* stability was not improved. Tertiary benzyl amine moiety in the head group of **PF-543** was found to be metabolized and cause the loss of potency. In this chapter, compounds with head group modification was carried out and two series of compounds were designed. The first series of compounds without the benzyl amine moiety were not able to maintain potency. However, the second series of compounds with an altered benzyl amine moiety maintained sub-micromolar potency. Compound **3.14c** had a $K_i$ value of 0.29 μM and was able to reduce plasma S1P by 15% without increasing blood S1P in mice (10mg/kg, I.P., 6 hours).

### 3.3. Introduction

**PF-543** was a SphK1 inhibitor with high *in vitro* potency and selectivity, and part of its inhibitory effect resulted from its capability of inducing proteasomal degradation of SphK1.[1-2] **PF-543** was also found to be effective in mouse models. For example, it was first found that **PF-543** was active in SCD Tg mice model to inhibit erythrocyte SphK1 and reduce plasma S1P levels (50%), which resulted in significant reduction of the sickling of red blood cells.[3] In another mouse hypoxic model, **PF-543** inhibited SphK1 to induce a protective effect against right ventricular hypertrophy and hypertrophic-induced myocardial apoptosis, which were associated with death caused by pulmonary arterial hypertension.[4]

However, the requirement of administering **PF-543** through an osmotic pump device implanted in the neck of the mice for continuous dose indicated its potential low metabolic stability.[3] In the SCD mouse study, osmotic minipumps were implanted subcutaneously in the nape of the neck, and **PF-543** was delivered at a rate of 0.93 mg/kg bodyweight per day into mice for 28 days. The continuous dose might be required due to quick metabolic breakdown of the drug, potentially through oxidation. Low metabolic stability significantly thwarted its further application for treatment of diseases.

Previous research work of our group focused on developing SphK2 selective inhibitors with quaternary ammonium or guanidine head groups.[5-9] Potent and selective SphK1 inhibitor was also discovered through homologation of the guanidine-based SphK2 inhibitor.[10] To develop SphK1 selective inhibitors with a different scaffold, **PF-543** was chosen as the lead compound and modifications were carried out. With the aim of improving metabolic stability of **PF-543**, head group modification was carried out. In

brief, two series of compounds with a dodecyl tail group were designed and synthesized. Their inhibitory effects were then evaluated through yeast cell assay. The hit compound was also tested in a mouse model to validate its *in vivo* activity and stability.

### 3.4. Drug Design

**PF-543** was found to bind with SphK1 through multiple interactions including hydrogen bond, π-π interaction and hydrophobic interaction.[11] The (*D*)-prolinol head group and (*R*)-3-hydroxylpyrrolidine group turned out to be comparable for inhibition due to their similar conformation that favors formation of hydrogen bonds with SphK1.[12] In order to mimic this structure, the first series of compounds was designed. These compounds had reversed positioning of the hydroxyl and amino group (Figure 3.1). Inspired by the previously reported inhibitor **Amgen 26**, the phenyl ring and hydroxyl group were respectively designed to be three carbon and two carbon atoms away from the amino group, which could possibly maintain the head group's capability for hydrogen bond formation (Figure 3.2).[13] Moreover, synthesis of this 1-amino-2-hydroxyethyl moiety could be facilitated by an epoxide ring opening reaction. The cyclic amino group can be functionalized with heteroatoms or substitutions as hydrogen bond donor or acceptor, as shown SphK1 inhibitor **RB-005**.[14]

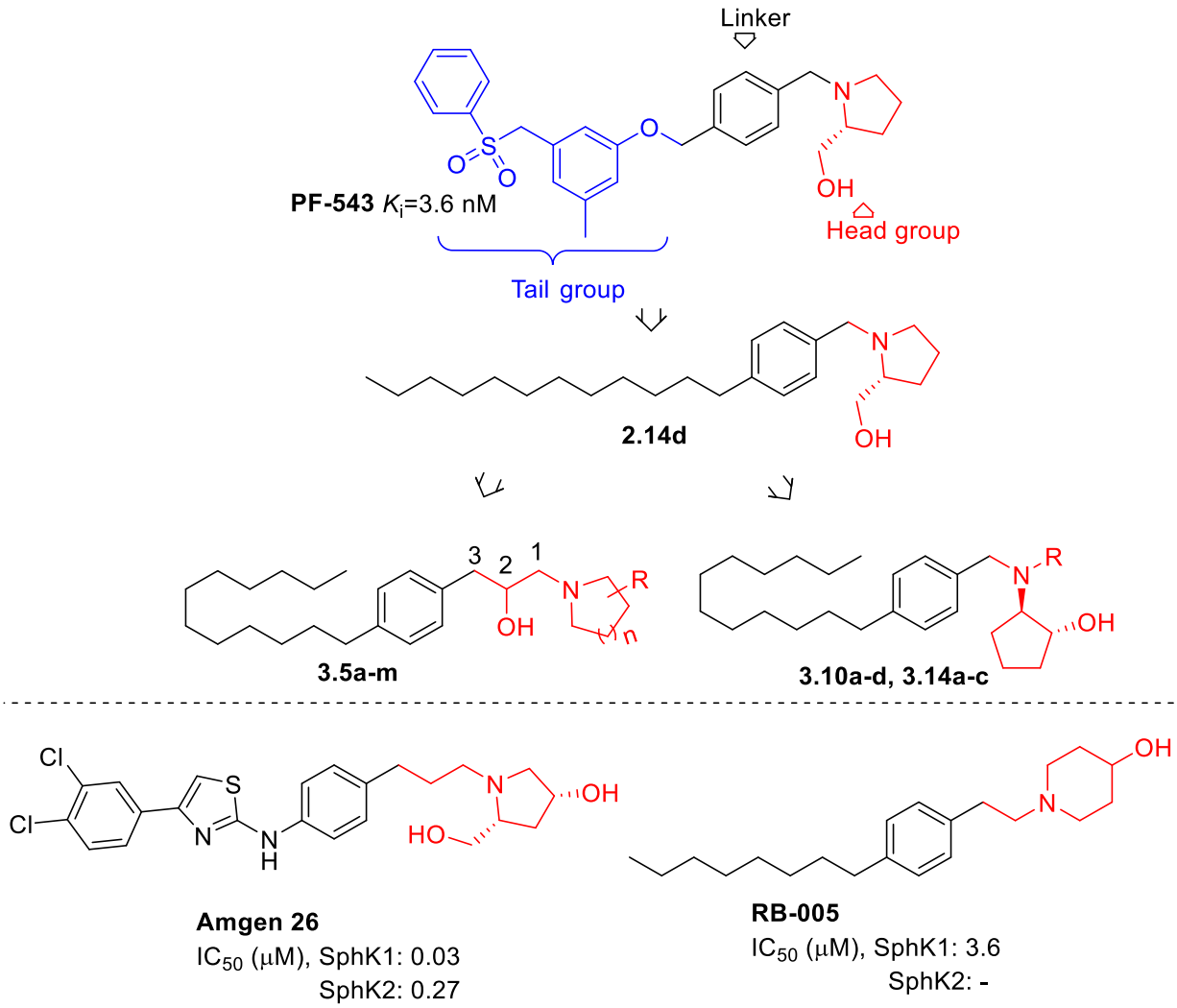


**Figure 3.1.** Compound series designed for head group modification, among which the first series of compounds were inspired by head group structures of **RB-005** and **Amgen 26**. (All compounds were evaluated as racemic or diastereomeric mixture)

In addition to the series of compounds without benzyl tertiary amine moiety, a second series of compounds with altered benzyl amine moiety was also designed. Essentially, these compounds had benzyl amine moiety with altered cyclic system. These compounds with altered benzyl amine moiety might have different metabolic profile and potentially improved metabolic stability.

### 3.5. Synthesis of putative inhibitors

Compound **3.6a-m** were synthesized as shown in Scheme 3.1. Undecyl bromide was converted to its Grignard reagent and reacted with 1,3- or 1,4-dibromobenzene to give mono-alkylated products **3.2a-b**, which were then converted to their Grignard reagents for substitution with allyl bromide. The resulting alkene **3.3a-b** were oxidized with mCPBA to give the corresponding racemic epoxides. Epoxide ring opening reaction was performed with different secondary amines to give amino alcohol products, which were further converted to the corresponding HCl salts. Synthesis of compounds with altered benzyl amine groups is shown in Scheme 3.2. Epoxide ring opening reaction of *N*-methyl-4-bromobenzylamine **3.7** with cyclopentene oxide or cyclohexene oxide gave tertiary amino cyclopentanol intermediate **3.8**, which was then reacted through Suzuki coupling (with 9-alkyl-9-borabicyclo[3.3.1]nonane, $Pd^{II}$ catalyst and base) to incorporate tail groups and afford compounds **3.9a-d**. Synthesis of secondary amino cyclopentanol products **3.14a-c** were accomplished by Suzuki coupling followed by reductive amination with either *trans*- or *cis*-2-aminocyclopentanol. Compound **3.17** with extended length was synthesized differently. 4-Bromophenethylamine was cross coupled followed by epoxide ring opening to afford intermediate **3.16**. However, purification of **3.16** was an issue, so it was N-boc protected and treated with HCl to yield the final product.

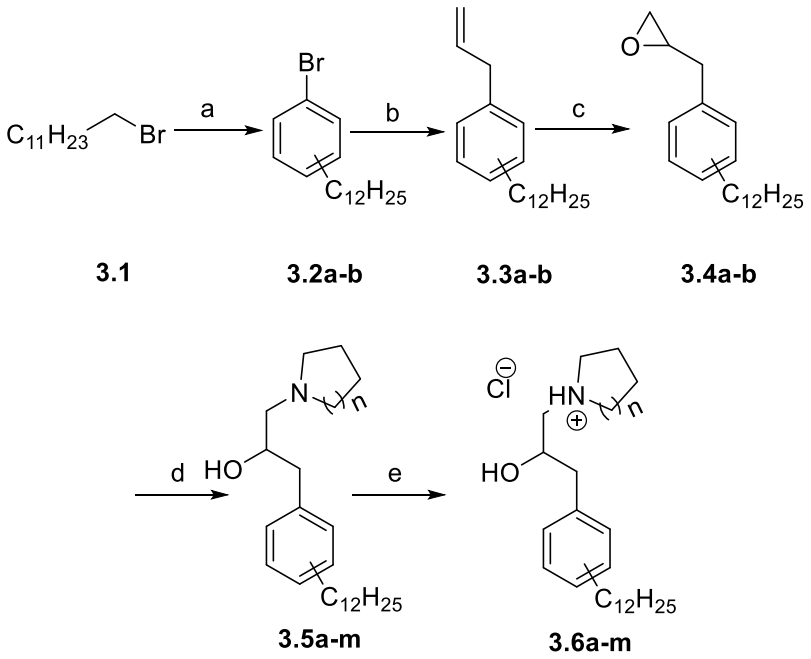


**Scheme 3.1.** Conditions: (a) (i) Mg, THF, rt to reflux, 6-8 h; (ii) 1,4-dibromobenzene or 1,3-dibromobenzene, $Pd(dppf)Cl_2$, THF, 0 °C to reflux, 16 h; (b) (i) Mg, THF, r.t. to reflux, 6-8 h; (ii) Allyl bromide, THF, 0 °C to rt, 6-8 h; (c) mCPBA, DCM, 0 °C to rt, 6 h; (d) amine, EtOH, 80 °C, 30 min, microwave. (e) HCl, MeOH, rt, 10 min.

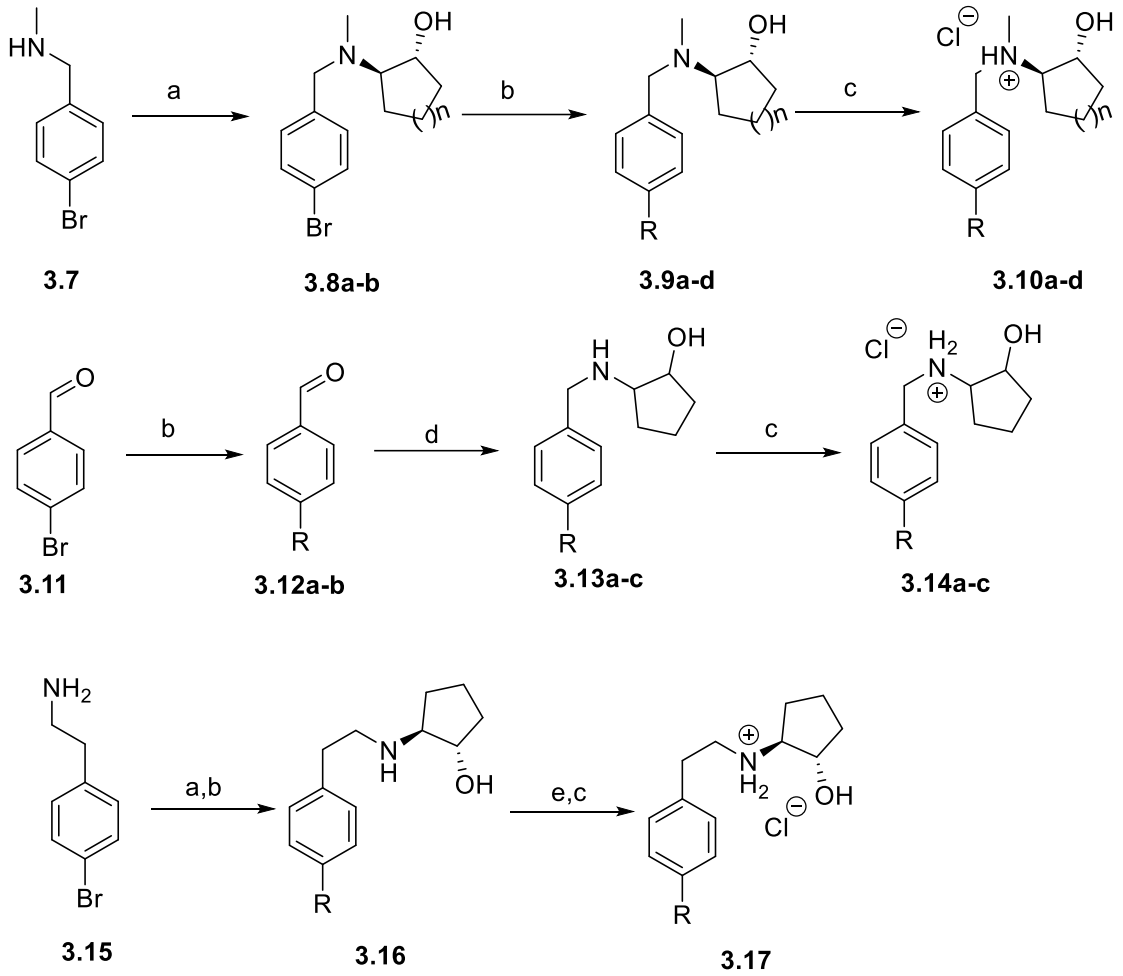


**Scheme 3.2.** Conditions: (a) cyclopentene oxide or cyclohexene oxide, EtOH, 80 °C, 30 min, microwave; (b) (i) alkene, 9-BBN, THF, 100 °C, 30 min; (ii) substrate, NaOH, $Pd(dppf)Cl_2$, $THF/H_2O$ =5/1, 100 °C, 30 min; (c) HCl, MeOH, rt, 11 min; (d) *trans*- or *cis*-aminocyclopentanol, $NaCNBH_3$, $TsOH•H_2O$, MeOH, rt, 12-16 h; (e) $Boc_2O$, TEA, rt, 6-8 h.

### 3.6. Biological Evaluation of Putative Inhibitors

With the synthesized compounds at hand, the inhibitory effects of the compounds were evaluated for hSphK1 and hSphK2 using a reported yeast cell assay.[15] Briefly, yeast containing hSphK plasmid was incubated with different concentrations of compounds for 24-48 h, and the absorbance at 600 nm was measured as an indicator of yeast growth and hSphK inhibition. Compounds were assayed at a concentration range of 0.1-3 μM and $EC_{50}$ values were calculated from inhibition data collected at different concentrations.

Compounds that did not display full sigmoidal inhibition curves were denoted as $EC_{50}$>3 μM. Hit compounds with SphK inhibition potency would be further evaluated in a mouse model, in order to validate their *in vivo* activity of reducing S1P levels, through quantification of blood and plasma S1P concentration by LC/MS

### 3.6.1. Yeast Cell Assay and Structure-Activity Relationship

Compounds **3.5a-g** with modified piperidine moiety in head group did not inhibit either SphK1 or SphK2. Incorporating pyrrolidine moiety into the head group resulted in no improvement of inhibition (**3.5h-j**). Their lack of inhibition could be caused by either their incapability of binding with SphK or poor cell permeability into yeast cells. The later possibility has been validated by our previous SphK2 inhibitor, which had no effect in yeast cell assay. In order to rule out this possibility, these compounds were further tested against recombinant SphK enzymes and he results revealed that they had minimal inhibition against SphK. Generally, they had <5% inhibition at 1 μM concentration for both SphK1 and SphK2, and only **3.5h-i** showed ~10% inhibition at 1 μM concentration for SphK1 (data not shown). Hypothesizing that altering positioning of the tail group might improve the inhibition, compounds **3.5k-m** with the dodecyl tail group at meta-position were tested since their head group might bind with SphK1 from an altered position. Unfortunately, this modification also did not improve the inhibition.

**Table 3.1.** Inhibitory effect of compounds without benzyl amine moiety[a]

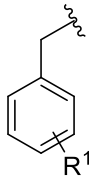

| Compd | $R_1$ | $R_2$ | SphK $EC_{50}$ values (μM) | | Compd | $R_1$ | $R_2$ | SphK $EC_{50}$ values (μM) | |
|---|---|---|---|---|---|---|---|---|---|
| | | | SphK1 | SphK2 | | | | SphK1 | SphK2 |
| **3.5a** | *p*-$C_{12}H_{25}$ | 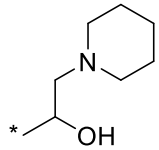 | >3 | >3 | **3.5h** | *p*-$C_{12}H_{25}$ | 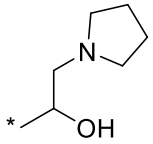 | >3 | >3 |
| **3.5b** | *p*-$C_{12}H_{25}$ | 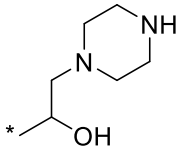 | >3 | >3 | **3.5i** | *p*-$C_{12}H_{25}$ | 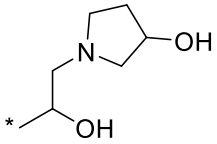 | >3 | >3 |
| **3.5c** | *p*-$C_{12}H_{25}$ | 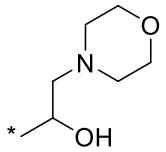 | >3 | >3 | **3.5j** | *p*-$C_{12}H_{25}$ | 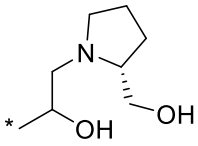 | >3 | >3 |
| **3.5d** | *p*-$C_{12}H_{25}$ | 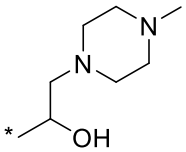 | >3 | >3 | **3.5k** | *m*-$C_{12}H_{25}$ | 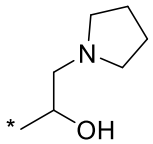 | >3 | >3 |
| **3.5e** | *p*-$C_{12}H_{25}$ | 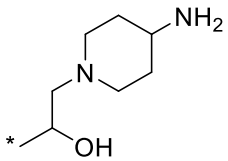 | >3 | >3 | **3.5l** | *m*-$C_{12}H_{25}$ | 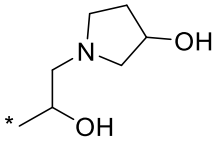 | >3 | >3 |
| **3.5f** | *p*-$C_{12}H_{25}$ | 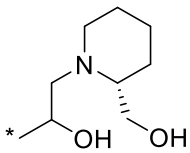 | >3 | >3 | **3.5m** | *m*-$C_{12}H_{25}$ | 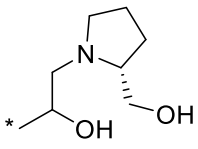 | >3 | >3 |
| **3.5g** | *p*-$C_{12}H_{25}$ | 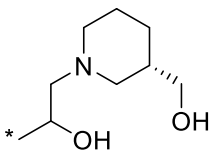 | >3 | >3 | | | | | |

[a]All compounds were assayed as racemic or diastereomeric mixture at a concentration range of 0.1-3 μM

Knowing that removing the benzyl amine moiety would greatly impair enzyme binding, a second series of compounds with altered benzyl amine moieties were tested (Table 3.2). However, compound **3.10a** with amino cyclohexanol head group, as a mimic of the hydroxyl group in SphK, resulted in no improvement of inhibition. When cyclohexanol was replaced with cyclopentanol (**3.10b**), a moderate inhibition was achieved. Further optimization of the tail length (**3.10c-d**) revealed that the undecyl chain (**3.10c**) gave optimal inhibition.

**Table 3.2.** Inhibitory effect of compounds with altered tertiary benzyl amine group[a]

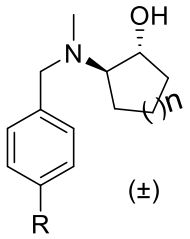


| Compd | n | R | SphK $EC_{50}$ values (μM) | |
|---|---|---|---|---|
| | | | SphK1 | SphK2 |
| **3.10a** | 2 | $-C_{12}H_{25}$ | >3 | >3 |
| **3.10b** | 1 | $-C_{12}H_{25}$ | 3.13 ± 0.34 | >3 |
| **3.10c** | 1 | $-C_{11}H_{23}$ | 1.34 ± 0.15 | >3 |
| **3.10d** | 1 | $-C_{10}H_{21}$ | 2.55 ± 0.30 | >3 |

[a]All compounds were assayed as racemic or diastereomeric mixture at a concentration range of 0.1-3 μM

Compound **3.14a**, synthesized as a comparison compound of **3.10a**, had a secondary amino group in *trans* with the hydroxyl group and improved inhibition significantly (Table 3.3). However, when the head group was changed to *cis*-

aminocyclopentanol, the inhibition was completely lost, indicating that the *trans*-configuration might be essential for hydrogen bond formation. Replacing the dodecyl tail group with undecyl group (**3.14c**) enhanced the inhibition further and resulted in an $EC_{50}$ value of 0.39 μM for SphK1 with no inhibition for SphK2. Although its potency was less than previous hit compound **2.14d** (SphK1 $EC_{50}$=0.15 μM), **3.14c** was able to keep its potency at sub-micromolar level. To study whether an extended length between head group and linker could improve inhibition, a phenethyl version (**3.17**) of **3.12a** was synthesized and tested. The lack of potency of **3.17** indicated the crucial distance between head group and the phenyl ring.

Table 3.3. Inhibitory effect of compounds with secondary benzyl amine group[a]

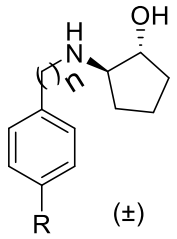


| Compd | n | R | Amino cyclopentanol | SphK $EC_{50}$ values (μM) | |
|---|---|---|---|---|---|
| | | | | SphK1 | SphK2 |
| **3.14a** | 1 | —$C_{12}H_{25}$ | *trans*- | 0.48 ± 0.2 | >3 |
| **3.14b** | 1 | —$C_{12}H_{25}$ | *cis*- | >3 | >3 |
| **3.14c** | 1 | —$C_{11}H_{23}$ | *trans*- | 0.39 ± 0.1 | >3 |
| **3.17** | 2 | —$C_{12}H_{25}$ | *trans*- | >3 | >3 |

[a]All compounds were assayed as racemic or diastereomeric mixture at a concentration range of 0.1-3 μM

### 3.6.2. Mouse study

Since **3.14c** had good potency and selectivity, it was chosen for testing target engagement in vivo wherein S1P levels in blood and plasma were tested. In brief, mice

were dosed with 10 mg/kg inhibitor. Blood was collected after 2 or 6 hours and plasma was isolated after 6 hours. Lipid extraction was carried out and the resulting extract were tested with LC/MS to quantify S1P concentration. According to obtained data (Figure 3.2), there was no significant change in blood S1P levels after 2 or 6 hours, but mouse plasma S1P level was reduced by 15% after 6 hours. Unlike compound **2.14a** ($EC_{50}$ = 0.31 µM**)**, **3.14c** was inactive in increasing blood S1P levels, which indicated that its mode of active more resembled typical SphK1 inhibitors. Its capability to reduce plasma S1P over a longer period of time (15% after 6 hours), compared to **2.14a** (20% after 3 hours), suggested its low potency and possible metabolic instability or poor oral bioavailability. However, a more detailed pharmacokinetic study is needed to definitely make this conclusion.

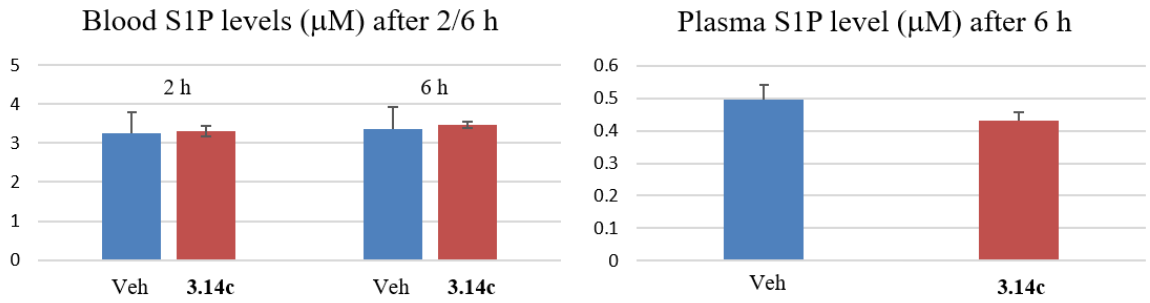


**Figure 3.2.** S1P levels in Blood and Plasma of Drug treated mice (10 mpk, IP, 2/6 h)

### 3.7. Conclusion

With the aim of developing potent SphK1 inhibitors with improved metabolic stability, head group modification was carried out. The designed compound had structures with or without benzyl amine moiety to probe their ability to inhibit SphK. We found that compounds without benzyl amine moiety were poor inhibitors of SphK1. However, hit compound **3.14c** ($EC_{50}$ = 0.39 µM) with secondary benzyl amine and *trans*

amino alcohol configuration was discovered. Mouse study indicated **3.14c** was able to reduce plasma S1P level by 15% after 6 hours without increasing blood S1P level.

### 3.8. References


1. McNaughton, M.; Pitman, M.; Pitson, S. M.; Pyne, N. J.; Pyne, S., Proteasomal degradation of sphingosine kinase 1 and inhibition of dihydroceramide desaturase by the sphingosine kinase inhibitors, SKi or ABC294640, induces growth arrest in androgen-independent LNCaP-AI prostate cancer cells. *Oncotarget* **2016,** *7* (13), 16663.
2. Schnute, M. E.; McReynolds, M. D.; Kasten, T.; Yates, M.; Jerome, G.; Rains, J. W.; Hall, T.; Chrencik, J.; Kraus, M.; Cronin, C. N.; Saabye, M.; Highkin, M. K.; Broadus, R.; Ogawa, S.; Cukyne, K.; Zawadzke, L. E.; Peterkin, V.; Iyanar, K.; Scholten, J. A.; Wendling, J.; Fujiwara, H.; Nemirovskiy, O.; Wittwer, A. J.; Nagiec, M. M., Modulation of cellular S1P levels with a novel, potent and specific inhibitor of sphingosine kinase-1. *Biochem. J.* **2012,** *444* (1), 79-88.
3. Zhang, Y.; Berka, V.; Song, A.; Sun, K.; Wang, W.; Zhang, W.; Ning, C.; Li, C.; Zhang, Q.; Bogdanov, M.; Alexander, D. C.; Milburn, M. V.; Ahmed, M. H.; Lin, H.; Idowu, M.; Zhang, J.; Kato, G. J.; Abdulmalik, O. Y.; Zhang, W.; Dowhan, W.; Kellems, R. E.; Zhang, P.; Jin, J.; Safo, M.; Tsai, A. L.; Juneja, H. S.; Xia, Y., Elevated sphingosine-1-phosphate promotes sickling and sickle cell disease progression. *J. Clin. Invest.* **2014,** *124* (6), 2750-61.
4. MacRitchie, N.; Volpert, G.; Al Washih, M.; Watson, D. G.; Futerman, A. H.; Kennedy, S.; Pyne, S.; Pyne, N. J., Effect of the sphingosine kinase 1 selective inhibitor, PF-543 on arterial and cardiac remodelling in a hypoxic model of pulmonary arterial hypertension. *Cell. Signal.* **2016,** *28* (8), 946-955.
5. Raje, M. R.; Knott, K.; Kharel, Y.; Bissel, P.; Lynch, K. R.; Santos, W. L., Design, synthesis and biological activity of sphingosine kinase 2 selective inhibitors. *Bioorganic Med. Chem.* **2012,** *20* (1), 183-194.
6. Knott, K.; Kharel, Y.; Raje, M. R.; Lynch, K. R.; Santos, W. L., Effect of alkyl chain length on sphingosine kinase 2 selectivity. *Bioorg. Med. Chem. Lett.* **2012,** *22* (22), 6817-20.
7. Congdon, M. D.; Childress, E. S.; Patwardhan, N. N.; Gumkowski, J.; Morris, E. A.; Kharel, Y.; Lynch, K. R.; Santos, W. L., Structure–activity relationship studies of the lipophilic tail region of sphingosine kinase 2 inhibitors. *Bioorganic Med. Chem. Lett.* **2015,** *25* (21), 4956-4960.
8. Congdon, M. D.; Kharel, Y.; Brown, A. M.; Lewis, S. N.; Bevan, D. R.; Lynch, K. R.; Santos, W. L., Structure–activity relationship studies and molecular modeling of naphthalene-based sphingosine kinase 2 inhibitors. *ACS Med. Chem. Lett.* **2016,** *7* (3), 229-234.
9. Childress, E. S.; Kharel, Y.; Brown, A. M.; Bevan, D. R.; Lynch, K. R.; Santos, W. L., Transforming Sphingosine kinase 1 inhibitors into dual and Sphingosine kinase 2 selective inhibitors: design, synthesis, and in vivo activity. *J. Med. Chem.* **2017,** *60* (9), 3933-3957.
10. Patwardhan, N. N.; Morris, E. A.; Kharel, Y.; Raje, M. R.; Gao, M.; Tomsig, J. L.; Lynch, K. R.; Santos, W. L., Structure− activity relationship studies and in vivo

activity of guanidine-based sphingosine kinase inhibitors: discovery of sphK1-and sphK2-selective inhibitors. *J. Med. Chem.* **2015,** *58* (4), 1879-1899.
11. Wang, J.; Knapp, S.; Pyne, N. J.; Pyne, S.; Elkins, J. M., Crystal Structure of Sphingosine Kinase 1 with PF-543. *ACS Med. Chem. Lett.* **2014,** *5* (12), 1329-33.
12. Schnute, M. E.; McReynolds, M. D.; Carroll, J.; Chrencik, J.; Highkin, M. K.; Iyanar, K.; Jerome, G.; Rains, J. W.; Saabye, M.; Scholten, J. A.; Yates, M.; Nagiec, M. M., Discovery of a Potent and Selective Sphingosine Kinase 1 Inhibitor through the Molecular Combination of Chemotype-Distinct Screening Hits. *J. Med. Chem.* **2017,** *60* (6), 2562-2572.
13. Gustin, D. J.; Li, Y.; Brown, M. L.; Min, X.; Schmitt, M. J.; Wanska, M.; Wang, X.; Connors, R.; Johnstone, S.; Cardozo, M.; Cheng, A. C.; Jeffries, S.; Franks, B.; Li, S.; Shen, S.; Wong, M.; Wesche, H.; Xu, G.; Carlson, T. J.; Plant, M.; Morgenstern, K.; Rex, K.; Schmitt, J.; Coxon, A.; Walker, N.; Kayser, F.; Wang, Z., Structure guided design of a series of sphingosine kinase (SphK) inhibitors. *Bioorg. Med. Chem. Lett.* **2013,** *23* (16), 4608-16.
14. Baek, D. J.; MacRitchie, N.; Pyne, N. J.; Pyne, S.; Bittman, R., Synthesis of selective inhibitors of sphingosine kinase 1. *Chem. Comm.* **2013,** *49* (21), 2136-2138.
15. Kharel, Y.; Agah, S.; Huang, T.; Mendelson, A. J.; Eletu, O. T.; Barkey-Bircann, P.; Gesualdi, J.; Smith, J. S.; Santos, W. L.; Lynch, K. R., Saccharomyces cerevisiae as a platform for assessing sphingolipid lipid kinase inhibitors. *PLoS One* **2018,** *13* (4), e0192179.

## Chapter 4. Experimental

### 4.1. General Procedures

All solvents were dried using a PureSolv solvent drying system prior to use. All chemical reagents were purchased from commercial sources and used without further purification. Column chromatography was performed using flash grade silica gel. All reactions utilizing a microwave were conducted in a Discover SP microwave synthesizer (CEM Corporation).

### 4.2. Instrumentation

$^{1}$H NMR spectra were obtained with either a Bruker Advance-II 500 MHz, Agilent 400-MR 400 MHz, or an Agilent U4-DD2 400 MHz spectrometer. Chemical shifts are reported in ppm from tetramethylsilane with the solvent resonance as the internal standard ($CDCl_3$:7.26 ppm, $CD_3OD$: 3:31 ppm). $^{13}$C NMR spectra were obtained with either a Bruker Advance II 500 MHz, Agilent 400-MR 400 MHz, or an Agilent U4-DD2 400 MHz spectrometer with complete proton decoupling. Chemical shifts are reported in ppm with the solvent resonance as the internal standard ($CDCl_3$: 77.2 ppm, $CD_3OD$: 49.0 ppm). $^{19}$F NMR spectra were obtained with either an Agilent 400-MR 400 MHz or an Agilent U4-DD2 400 MHz spectrometer. High-resolution mass spectrometry (HRMS) was performed on a LC-MS time-of-flight mass spectrometer using ESI.

### 4.3. Synthetic procedures and characterization from Chapter 2

4.3.1. General procedure for preparation of **2.2a-d**

4-hydroxybenzaldehyde (1 equiv.), potassium carbonate (5 equiv.) and alkyl halide (1.2 equiv.) were added to a round bottom flask containing DMF. The reaction

mixture was stirred for 16 hours under nitrogen until TLC indicated the starting material had been fully consumed. The reaction was extracted with ethyl acetate and saturated LiBr solution. The combined organic layers were washed with brine and dried over sodium sulfate. After filtration and concentration via reduced pressure, the resulting oil residue was purified on a silica column with hexane and ethyl acetate as the eluent to yield pure product.

4. 3. 1. 1. 4-(heptyloxy)benzaldehyde (**2.2a**)

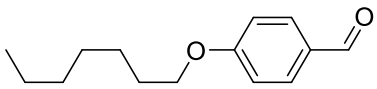

Clear oil, 87%; $^{1}$H NMR (400 MHz, $CDCl_3$) δ: 9.85 (s, 1H), 7.80 (d, J=8.9 Hz, 2H), 6.96 (d, J=8.9 Hz, 2H), 4.01 (t, J=6.6 Hz, 2H), 1.83–1.73 (m, 2H), 1.48–1.39 (m, 2H), 1.39–1.23 (m, 6H), 0.90–0.84 (m, 3H); $^{13}$C NMR (101 MHz, $CDCl_3$) δ: 190.92, 164.37, 132.09, 129.83, 114.84, 68.53, 31.86, 29.17, 29.12, 26.04, 22.71, 14.20; HRMS(ESI): calcd. for $C_{14}H_{21}O_2$+ $[M+1]^+$ 221.1536, found: 221.1548.

4. 3. 1. 2. 4-(octyloxy)benzaldehyde (**2.2b**)

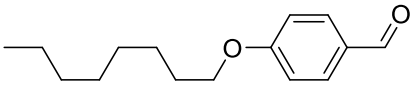

Clear oil, 74%; $^{1}$H NMR (400 MHz, $CDCl_3$) δ: 9.88 (s, 1H), 7.82 (d, J=8.9 Hz, 1H), 6.99 (d, J = 8.7 Hz, 2H), 4.04 (t, J=6.6 Hz, 2H), 1.87–1.75 (m, 2H), 1.47 (dt, J=15.2, 6.8 Hz, 2H), 1.40–1.21(m, 8H), 0.91–0.86(m, 3H); $^{13}$C NMR (101 MHz, $CDCl_3$) δ: 190.94, 164.40, 132.11, 129.86, 68.56, 31.93, 29.44, 29.35, 29.19, 26.10, 22.79, 14.24; HRMS(ESI): calcd. for $C_{15}H_{23}O_2$+ $[M+1]^+$ 235.1693, found: 235.1707.

4. 3. 1. 3. 4-(nonyloxy)benzaldehyde (**2.2c**)

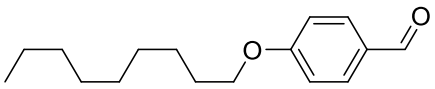

Clear oil, 80%; $^{1}$H NMR (400 MHz, $CDCl_3$) δ: 9.87 (s, 1H), 7.82 (d, J = 8.9 Hz, 2H), 6.98 (d, J = 8.8 Hz, 2H), 4.03 (t, J = 6.6 Hz, 2H), 1.86 – 1.75 (m, 2H), 1.50–1.40 (m, 2H), 1.40–1.21 (m, 10H), 0.92–0.83 (m, 3H); $^{13}$C NMR (101 MHz, $CDCl_3$) δ: 190.94, 164.39, 132.11, 129.84, 114.86, 68.55, 31.99, 29.63, 29.47, 29.37, 29.18, 26.09, 22.80, 14.24; HRMS(ESI): calcd. for $C_{16}H_{25}O_2$+ $[M+1]^+$ 249.1849 , found: 249.1865.

4. 3. 1. 4. 4-(decyloxy)benzaldehyde(**2.2d**)

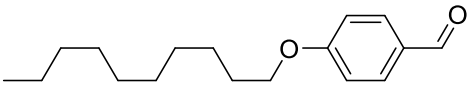

Clear oil, 72%; $^{1}$H NMR (400 MHz, $CDCl_3$) δ: 9.87 (s, 1H), 7.82 (d, J = 8.9 Hz, 2H), 6.99 (d, J = 8.6 Hz, 2H), 4.03 (t, J = 6.6 Hz, 2H), 1.86–1.76 (m, 2H), 1.51–1.41 (m, 2H), 1.29 (dd, J = 14.2, 5.5 Hz, 12H), 0.91–0.84 (m, 3H); $^{13}$C NMR (101 MHz, $CDCl_3$) δ: 190.97, 164.41, 132.13, 129.85, 114.87, 68.57, 32.03, 29.69, 29.68, 29.48, 29.45, 29.19, 26.10, 22.82, 14.26; HRMS(ESI): calcd. for $C_{17}H_{27}O_2$+ $[M+1]^+$ 263.2006, found: 263.2029.

4. 3. 1. 5. 4-((4-(trifluoromethyl)benzyl)oxy)benzaldehyde (**2.2e**)

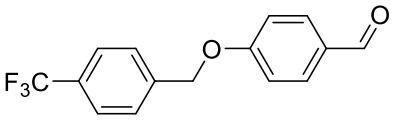

White solid, 65%; $^{1}$H NMR (400 MHz, $CDCl_3$) δ: 9.90 (s, 1H), 7.86 (d, J = 8.8 Hz, 2H), 7.67 (d, J = 8.1 Hz, 2H), 7.56 (d, J = 8.0 Hz, 2H), 7.08 (d, J = 8.8 Hz, 2H), 5.22 (s, 2H); $^{13}$C NMR (101 MHz, $CDCl_3$) δ: 190.84, 163.37, 140.12, 132.18, 130.56, 127.54, 125.89, 125.85, 125.81, 125.78, 115.23, 69.45; HRMS(ESI): calcd. for $C_{30}H_{22}F_6KO_4$+ $[2M+K]^+$ 599.1054, found: 599.1084.

4.3.2. General procedure for preparation of **2.3a-c**

Procedure 1: Aldehyde (1 equiv.) and (*R*)-prolinol (1.3 equiv.) were added to a round bottom flask containing DCM and 100 mg 4 Å molecular sieves. The solution was allowed to be stirred at room temperature under nitrogen for 8 hours before the addition of acetic acid (0.05 equiv.) and sodium trisacetoxyborohydride (1.3 equiv.). The solution was further stirred at room temperature under nitrogen for 16 hours. The solid was removed via filtration and solution was partitioned between ethyl acetate and water. The organic layers were washed with saturated sodium bicarbonate solution and brine, dried over sodium sulfate, and concentrated via reduced pressure. The residue was purified using silica gel column chromatography (30% ethyl acetate/hexanes) to yield the product.

Ester (1 equiv.) was added to a round bottom flask containing THF. The solution was cooled in ice bath for 5 minutes before the addition of lithium aluminium hydride (0.7 equiv.) suspension in THF. The mixture was allowed to rise to room temperature and refluxed for 10 hours under nitrogen. The reaction was cooled in ice bath and quenched with 1 mL ethyl acetate and 20 mL saturated sodium hydroxide solution. The mixture was extracted with ethyl acetate, washed with saturated sodium bicarbonate solution and brine, dried over sodium sulfate, and concentrated via reduced pressure. The residue was purified using silica gel column chromatography (100% ethyl acetate) to yield the product.

Procedure 2: Aldehyde (1 equiv.) and (R)-prolinol (1.3 equiv.) were added to a round bottom flask containing DCM/MeOH=1:1. The solution was allowed to be cooled in ice bath for 5 minutes before the addition of p-toluenesulfonic acid (1 equiv.) and sodium cyanoborohydride (0.7 equiv.). The solution was further stirred at room

temperature for 12-16 hours under nitrogen until TLC indicated that the starting material had been consumed. The solid was removed via filtration and solution was partitioned between ethyl acetate and water. The organic layers were washed with saturated sodium bicarbonate solution, brine and dried over sodium sulfate, and concentrated via reduced pressure. The residue was purified using silica gel column chromatography (5% methanol/dichloromethane) to yield the product.

4.3.2.1. (R)-(1-(4-(heptyloxy)benzyl)pyrrolidin-2-yl)methanol (**2.3a**)

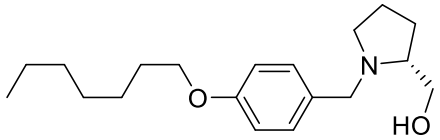


Clear oil, 8 % through procedure 1; $^{1}$H NMR (400 MHz, $CDCl_3$) δ: 7.21 (d, J = 8.7 Hz, 2H), 6.84 (d, J = 8.7 Hz, 2H), 3.95 – 3.89 (m, 3H), 3.64 (dd, J = 11.0, 3.6 Hz, 1H), 3.46 (dd, J = 11.0, 2.8 Hz, 1H), 3.39 (d, J = 12.9 Hz, 1H), 3.00 (dt, J = 9.5, 4.6 Hz, 1H), 2.79 (td, J = 6.0, 3.1 Hz, 1H), 2.35 (q, J = 8.5 Hz, 1H), 1.99–1.87 (m, 1H), 1.86–1.79 (m, 1H), 1.79–1.66 (m, 4H), 1.49–1.39 (m, 2H), 1.38–1.24 (m, 6H), 0.93–0.85 (m, 3H); $^{13}$C NMR (101 MHz, $CDCl_3$) δ: 158.55, 130.20, 129.95, 114.41, 68.04, 64.61, 61.78, 58.00, 54.29, 31.84, 29.13, 27.73, 26.08, 23.41, 22.67, 14.15; HRMS(ESI): calcd. for $C_{19}H_{32}NO_2$+ $[M+1]^+$ 306.2428, found: 306.2425.

4.3.2.2. (R)-(1-(4-(octyloxy)benzyl)pyrrolidin-2-yl)methanol (**2.3b**)

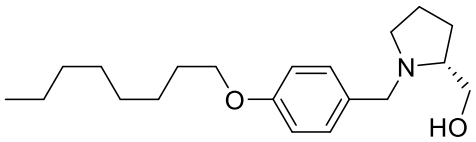


Clear oil, 12 % through procedure 1; $^{1}$H NMR (400 MHz, $CDCl_3$) δ: 7.19 (d, J = 8.6 Hz, 2H), 6.84 (d, J = 8.7 Hz, 2H), 3.93 (t, J = 6.6 Hz, 2H), 3.89 (d, J = 12.8 Hz, 1H), 3.64 (dd, J = 10.7, 3.5 Hz, 1H), 3.41 (dd, J = 10.7, 2.2 Hz, 1H), 3.31 (d, J = 12.8 Hz, 1H), 3.00–

2.92 (m, 2H), 2.75–2.68 (m, 2H), 2.34–2.23 (m, 1H), 1.98–1.85 (m, 1H), 1.85–1.73 (m, 3H), 1.73–1.60 (m, 2H), 1.45 (dt, J = 15.0, 6.9 Hz, 2H), 1.38–1.23 (m, 8H), 0.93–0.84 (m, 3H); $^{13}$C NMR (101 MHz, $CDCl_3$) δ: 158.40, 131.15, 129.96, 114.40, 68.12, 64.18, 61.84, 57.96, 54.46, 31.96, 29.51, 29.45, 29.39, 27.98, 26.21, 23.55, 22.80. 4; HRMS(ESI): calcd. for $C_{20}H_{34}NO_2$+ $[M+1]^+$ 320.2584, found: 320.2563.

4.3.2.3. (R)-(1-(4-(nonyloxy)benzyl)pyrrolidin-2-yl)methanol (**2.3c**)

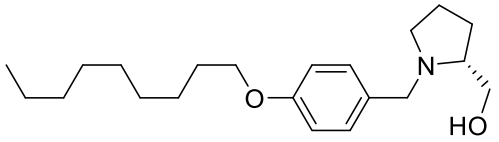


Clear oil, 10 % through procedure 1; $^1$H NMR (400 MHz, $CDCl_3$) δ: 7.19 (d, J = 8.6 Hz, 2H), 6.84 (d, J = 8.7 Hz, 2H), 3.93 (t, J = 6.6 Hz, 2H), 3.88 (d, J = 12.8 Hz, 1H), 3.64 (dd, J = 10.7, 3.5 Hz, 1H), 3.42 (dd, J = 10.7, 2.2 Hz, 1H), 3.30 (d, J = 12.8 Hz, 1H), 3.00–2.91 (m, 1H), 2.75–2.67 (m, 1H), 2.28 (td, J = 9.4, 7.6 Hz, 1H), 1.99–1.82 (m, 1H), 1.85–1.61 (m, 3H), 1.69 (s, 2H), 1.45 (dt, J = 15.0, 7.1 Hz, 2H), 1.39–1.21 (m, 10H), 0.93 – 0.84 (m, 3H); $^{13}$C NMR (101 MHz, $CDCl_3$) δ: 158.38, 131.11, 129.94, 114.37, 68.09, 64.18, 61.87, 57.96, 54.43, 31.99, 29.66, 29.53, 29.43, 29.38, 27.95, 26.18, 23.51, 22.79, 14.23; HRMS(ESI): calcd. for $C_{21}H_{36}NO_2$+ $[M+1]^+$ 334.2741, found: 334.2764.

4.3.2.4. (R)-(1-(4-(docyloxy)benzyl)pyrrolidin-2-yl)methanol (**2.3d**)

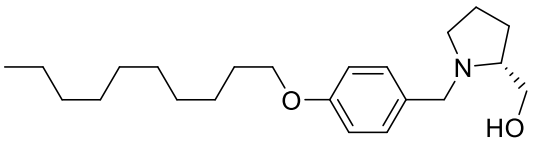


Clear oil, 9 % through procedure 1; $^1$H NMR (400 MHz, $CDCl_3$) δ: 7.36 (d, J = 8.7 Hz, 2H), 6.91 (d, J = 8.7 Hz, 2H), 4.39 (d, J = 13.1 Hz, 1H), 4.12 (d, J = 13.1 Hz, 1H), 3.92 (t, J = 6.6 Hz, 2H), 3.86 – 3.75 (m, 2H), 3.64 – 3.56 (m, 1H), 3.46 – 3.37 (m, 1H), 3.06 – 2.96 (m, 1H), 2.19 – 1.86 (m, 4H), 1.80 – 1.70 (m, 2H), 1.41 (q, J = 7.2 Hz, 2H), 1.37 –

1.19 (m, 12H), 0.89 – 0.82 (m, 3H); $^{13}$C NMR (101 MHz, $CDCl_3$) δ: 160.62, 132.40, 120.92, 115.40, 68.34, 67.96, 60.90, 53.86, 32.03, 29.71, 29.70, 29.53, 29.46, 29.30, 26.60, 26.15, 22.99, 22.82, 14.26; HRMS(ESI): calcd. for $C_{22}H_{38}NO_2$+ $[M+1]^+$ 348.2897, found: 348.2902.

4.3.2.5. (*S*)-(1-(4-(decyloxy)benzyl)pyrrolidin-2-yl)methanol (**2.3e**)

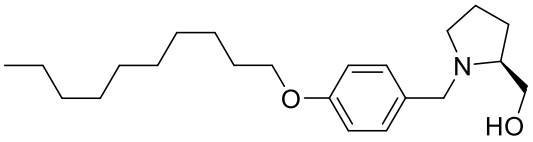


Clear oil, 38% through procedure 2; $^1$H NMR (400 MHz, $CDCl_3$) δ: 7.36 (d, J = 8.7 Hz, 2H), 6.91 (d, J = 8.7 Hz, 2H), 4.39 (d, J = 13.1 Hz, 1H), 4.12 (d, J = 13.1 Hz, 1H), 3.92 (t, J = 6.6 Hz, 2H), 3.86–3.75 (m, 2H), 3.60 (m, 1H), 3.42 (m, 1H), 3.01 (m, 1H), 2.19–1.86 (m, 4H), 1.80–1.70 (m, 1H), 1.41 (m, 2H), 1.37–1.19 (m, 12H), 0.89–0.82 (m, 3H); $^{13}$C NMR (101 MHz, $CDCl_3$) δ: 160.62, 132.40, 120.92, 115.40, 68.34, 67.96, 60.90, 53.86, 32.03, 29.71, 29.70, 29.53, 29.46, 29.30, 26.60, 26.15, 22.99, 22.82, 14.26; HRMS(ESI): calcd. for $C_{22}H_{38}NO_2$+ $[M+1]^+$ 348.2897, found: 348.2902.

4.3.2.6. (R)- (1-(4-((4-(trifluoromethyl)benzyl)oxy)benzyl)pyrrolidin-2-yl)methanol (**2.3f**)

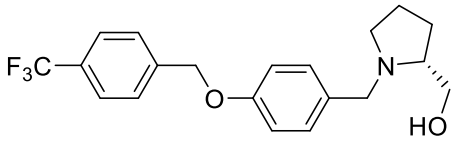


Clear oil, 36 % through procedure 2; $^1$H NMR (400 MHz, $CDCl_3$) δ: 7.64 (d, J = 8.1 Hz, 2H), 7.54 (d, J = 8.7 Hz, 2H), 7.39 (d, J = 8.8 Hz, 2H), 7.00 (d, J = 8.8 Hz, 2H), 5.12 (s, 2H), 4.34 (d, J = 13.1 Hz, 1H), 3.97 (d, J = 13.1 Hz, 1H), 3.78 (d, J = 4.8 Hz, 2H), 3.45 (dq, J = 10.0, 4.9 Hz, 1H), 3.36 (dt, J = 11.0, 5.8 Hz, 1H), 2.88 (dt, J = 11.0, 7.3 Hz, 1H), 2.19 – 2.04 (m, 1H), 2.06 – 1.85 (m, 3H); $^{13}$C NMR (101 MHz, $CDCl_3$) δ: 159.44,

140.66, 132.10, 130.40 (q, J = 32.3 Hz), 127.58, 125.74 (q, J = 3.8 Hz), 124.17 (q, J = 272.0 Hz), 115.60, 77.48, 69.34, 67.55, 61.13, 58.80, 54.08, 26.84, 23.14; HRMS(ESI): calcd. for $C_{20}H_{23}F_3NO_2$+ $[M+1]^+$ 366.1675, found: 366.1709.

4.3.3. General procedure for preparation of **2.6a-e**

Phenol (1.5 equiv.) and sodium bicarbonate (5 equiv.) and 4-fluorobenzonitrile (1 equiv.) were added into a round bottom flask containing DMF. The mixture was refluxed under nitrogen protection for 12-16 hours until TLC indicated the starting material had been fully consumed. Saturated lithium bromide solution was added, and the mixture was extracted with ethyl acetate, washed with brine, dried over sodium sulfate, and concentration via reduced pressure. The residue was purified using silica gel column chromatography (100% ethyl acetate) to yield the product.

4.3.3.1. 4-phenoxybenzonitrile(**2.6a**)

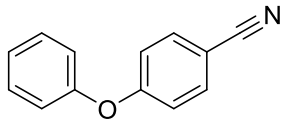


Clear oil, 86 %; $^1$H NMR (400 MHz, $CDCl_3$) δ: 7.57 (d, J = 9.0 Hz, 2H), 7.40 (dd, J = 8.5, 7.6 Hz, 2H), 7.22 (t, J = 7.4 Hz, 1H), 7.06 (dd, J = 8.6, 1.1 Hz, 2H), 6.99 (d, J = 9.0 Hz, 2H); $^{13}$C NMR (101 MHz, $CDCl_3$) δ: 161.56, 154.73, 134.06, 130.19, 125.10, 120.34, 118.77, 117.85, 105.74; HRMS(ESI): calcd. for $C_{13}H_{10}NO$+ $[M+1]^+$ 196.0757, found: 196.0744.

4.3.3.2. 4-(3-(tert-butyl)phenoxy)benzonitrile(**2.6b**)

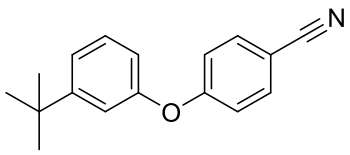


Clear oil, 81 %; $^1$H NMR (400 MHz, CDCl3) δ: 7.58 (d, J = 9.0 Hz, 2H), 7.32 (t, J = 7.9

Hz, 1H), 7.26 – 7.22 (m, 1H), 7.09 (t, J = 2.1 Hz, 1H), 6.98 (d, J = 8.8 Hz, 2H), 6.84 (ddd, J = 7.9, 2.4, 1.1 Hz, 1H), 1.30 (s, 9H); $^{13}$C NMR (101 MHz, $CDCl_3$) δ: 161.99, 154.60, 154.27, 134.20, 129.79, 122.30, 119.02, 117.81, 117.78, 117.38, 105.63, 34.99, 31.35; HRMS(ESI): calcd. for $C_{17}H_{18}NO+$ $[M+1]^+$ 252.1383, found: 252.1363.

4.3.3.3. 4-(4-(tert-butyl)phenoxy)benzonitrile(**2.6c**)

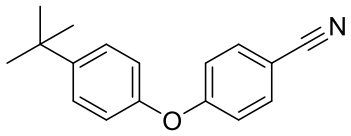


Clear oil, 77 %; $^1$H NMR (400 MHz, $CDCl_3$) δ 7.58 (d, J = 8.9 Hz, 2H), 7.42 (d, J = 8.7 Hz, 2H), 7.00 (d, J = 2.3 Hz, 2H), 6.98 (d, J = 2.2 Hz, 2H), 1.35 (s, 9H); $^{13}$C NMR (101 MHz, $CDCl_3$) δ 162.00, 152.29, 148.19, 134.10, 127.09, 119.96, 118.96, 117.72, 105.52, 34.53, 31.50; HRMS(ESI) $[M+1]^+$ Calcd. for $C_{17}H_{18}NO+$: 251.1383, Found: 252.1366.

4.3.3.4. 4-(3-bromophenoxy)benzonitrile(**2.6d**)

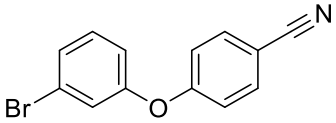


Clear oil, 75 %; $^1$H NMR (400 MHz, $CDCl_3$) δ: 7.62 (d, J = 8.9 Hz, 2H), 7.35 (ddd, J = 8.0, 1.8, 1.1 Hz, 1H), 7.27 (t, J = 8.1 Hz, 1H), 7.23–7.20 (m, 1H), 7.04–6.98(m, 3H); $^{13}$C NMR (101 MHz, $CDCl_3$) δ: 160.87, 155.82, 134.36, 131.39, 128.24, 123.57, 118.93, 118.69, 118.45, 106.74; HRMS(ESI): calcd. for $C_{13}H_9BrNO+$ $[M+1]^+$ 273.9862 , found: 273.9860.

4.3.3.5. 4-(4-iodophenoxy)benzonitrile(**2.6e**)

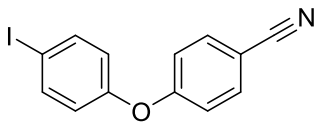


Clear oil, 78 %; $^1$H NMR (400 MHz, $CDCl_3$) δ: 7.68 (d, J = 5.9 Hz, 2H), 7.60 (dd, J =

5.0, 2.3 Hz, 2H), 7.00 (d, J = 8.9 Hz, 2H), 6.82 (d, J = 8.9 Hz, 2H); $^{13}$C NMR (101 MHz, $CDCl_3$) δ: 160.99, 155.01, 139.34, 134.35, 122.51, 118.73, 118.31, 106.54; HRMS(ESI): calcd. for $C_{13}H_9INO+$ $[M+1]^+$ 321.9723, found: 321.9698.

4.3.4. General procedure for preparation of **2.7a-e**

Aryl nitrile (1 equiv.) was added to a round bottom flask containing THF. The solution was cooled to -70 °C before the addition of DIBAL-H (1.1 equiv.) solution (1M in THF). The mixture was stirred at -40 °C for 5 hours under nitrogen until TLC indicated the starting material had been fully consumed. The reaction was cooled in ice bath and quenched with 1 mL ethyl acetate and 20 mL HCl (1 M). The mixture was extracted with ethyl acetate, washed with brine, dried over sodium sulfate and concentrated via reduced pressure. The residue was purified using silica gel column chromatography (5% ethyl acetate/hexanes) to yield the product.

4.3.4.1. 4-phenoxybenzaldehyde(**2.7a**)

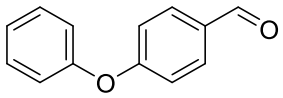

White solid, 82%; $^1$H NMR (400 MHz, $CDCl_3$) δ: 9.92 (s, 1H), 7.84 (d, J = 8.8 Hz, 2H), 7.46–7.37 (m, 2H), 7.23 (t, J = 7.4 Hz, 1H), 7.09 (dd, J = 8.7, 1.1 Hz, 2H), 7.06 (d, J = 8.4 Hz, 2H); $^{13}$C NMR (101 MHz, $CDCl_3$) δ: 190.88, 163.34, 155.20, 132.06, 131.37, 130.26, 125.06, 120.54, 117.68; HRMS(ESI) $[M+1]^+$ calcd. for $C_{13}H_{11}O_2+$: 199.0754, found: 199.0753.

4.3.4.2. 4-(3-(tert-butyl)phenoxy)benzaldehyde (**2.7b**)

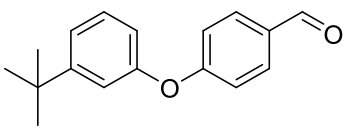

Clear oil, 84%; $^{1}$H NMR (400 MHz, $CDCl_3$) δ: 9.91 (s, 1H), 7.84 (d, J = 8.8 Hz, 2H), 7.33 (t, J = 7.9 Hz, 1H), 7.29–7.22 (m, 1H), 7.14–7.10 (m, 1H), 7.05 (d, J = 8.7 Hz, 1H), 6.91–6.83 (m, 1H), 1.32 (s, 9H); $^{13}$C NMR (101 MHz, $CDCl_3$) δ: 190.85, 163.57, 154.89, 154.14, 132.05, 131.18, 129.70, 122.09, 117.84, 117.45, 117.41, 31.36; HRMS(ESI) $[M+1]^+$ calcd. for $C_{17}H_{19}O_2$+: 255.1380, found: 255.1369.

4.3.4.3. 4-(4-(tert-butyl)phenoxy)benzaldehyde (**2.7c**)

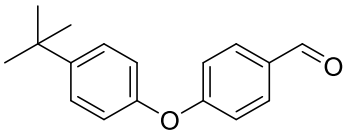


Clear oil, 77%; $^{1}$H NMR (400 MHz, $CDCl_3$) δ: 9.91 (s, 1H), 7.83 (d, J = 8.8 Hz, 2H), 7.42 (d, J = 8.8 Hz, 2H), 7.05 (d, J = 8.4 Hz, 2H), 7.01 (d, J = 8.8 Hz, 2H), 1.35 (s, 9H); $^{13}$C NMR (101 MHz, $CDCl_3$) δ: 190.92, 163.70, 152.68, 148.09, 132.05, 131.18, 127.09, 120.05, 117.48, 34.62, 31.60; HRMS(ESI) $[M+1]^+$ calcd. for $C_{17}H_{19}O_2$+: 255.1380, found: 255.1372.

4.3.4.4. 4-(3-bromophenoxy)benzaldehyde (**2.7d**)

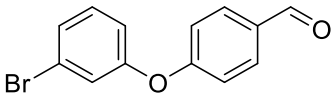


Brown solid, 78%; $^{1}$H NMR (400 MHz, $CDCl_3$) δ: 9.91 (s, 1H), 7.84 (d, J = 8.6 Hz, 2H), 7.34–7.30 (m, 1H), 7.23 (d, J = 5.2 Hz, 1H), 7.21 (dd, J = 3.6, 1.5 Hz, 1H), 7.05 (d, J = 8.7 Hz, 2H), 7.01–6.97 (m, 1H); $^{13}$C NMR (101 MHz, $CDCl_3$) δ: 190.81, 162.43, 156.23, 132.16, 131.97, 131.34, 128.06, 123.61, 123.27, 118.97, 118.21; HRMS(ESI) calcd. for $C_{13}H_{10}BrO_2$+ $[M+1]^+$ 276.9859, found: 276.9860.

4.3.4.5. 4-(4-iodophenoxy)benzaldehyde(**2.7e**)

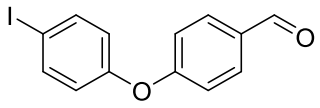

Brown solid, 73%; $^{1}$H NMR (400 MHz, $CDCl_3$) δ: 9.93 (s, 1H), 7.86 (d, J = 8.9 Hz, 2H), 7.71 (d, J = 8.9 Hz, 2H), 7.07 (d, J = 8.4 Hz, 2H), 6.85 (d, J = 8.9 Hz, 2H); $^{13}$C NMR (101 MHz, $CDCl_3$) δ: 190.81, 162.62, 155.37, 139.29, 132.13, 131.82, 122.54, 117.99, 88.32; HRMS(ESI): calcd. for $C_{13}H_{10}IO_2$+ $[M+1]^+$ 324.9720, found: 324.9744.

4.3.5. General procedure for preparation of **2.8d-k**

Aryl halide (1 equiv.), aryl boron species (1.3 equiv.) were added into microwave reaction tube containing THF. The solution was purged with argon for 5 minutes before the addition of sodium hydroxide aqueous solution (3 equiv.) to form THF/$H_2O$=5:1 mixture. The mixture was further purged with argon for 5 minutes before the addition of Pd(dppf)$Cl_2$ (0.1 equiv.). The mixture was heated to 100 °C for 10 minutes in microwave. The solid was removed via filtration and solution was partitioned between ethyl acetate and water. The resulting organic layer was washed with saturated sodium bicarbonate solution and brine, dried over sodium sulfate, and concentrated via reduced pressure. The residue was purified using silica gel column chromatography (5% ethyl acetate/hexanes) to yield the product.

4.3.5.1. 4-([1,1'-biphenyl]-3-yloxy)benzaldehyde (**2.8d**)

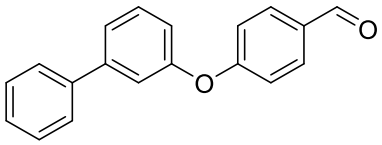

Clear oil, 85%; $^{1}$H NMR (400 MHz, $CDCl_3$) δ: 9.93 (t, J = 0.4 Hz, 1H), 7.87 (d, J = 8.8 Hz, 2H), 7.58 (dd, J = 8.3, 1.4 Hz, 2H), 7.51–7.41 (m, 4H), 7.39–7.34 (m, 1H), 7.33 (ddd, J = 2.3, 1.4, 0.7 Hz, 1H), 7.12 (d, J = 8.4 Hz, 2H), 7.07 (dt, J = 6.8, 2.5 Hz, 1H); $^{13}$C

NMR (101 MHz, $CDCl_3$) δ: 190.90, 163.31, 155.69, 143.70, 140.15, 132.14, 131.48, 130.59, 129.03, 127.98, 127.22, 123.81, 119.22, 117.81; HRMS(ESI): calcd. for $C_{19}H_{15}O_2$+ $[M+1]^+$ 275.1067, found: 275.1077.

4.3.5.2. 4-((3'-(trifluoromethyl)-[1,1'-biphenyl]-3-yl)oxy)benzaldehyde(**2.8e**)

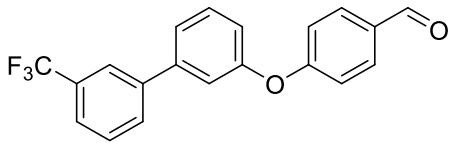


Clear oil, 90%; $^1$H NMR (400 MHz, $CDCl_3$) δ: 9.94 (s, 1H), 7.88 (d, J = 8.7 Hz, 2H), 7.82 (s, 1H), 7.75 (d, J = 7.7 Hz, 1H), 7.63 (d, J = 7.8 Hz, 1H), 7.61–7.51 (m, 1H), 7.51 (t, J = 7.9 Hz, 1H), 7.46 (dt, J = 7.7, 1.6 Hz, 1H), 7.37–7.31 (m, 1H), 7.12 (m, 3H); $^{13}$C NMR (101 MHz, $CDCl_3$) δ: 190.88, 163.09, 155.88, 142.20, 140.95, 132.16, 131.94 (q, *J* = 33.6 Hz), 130.86, 130.52, 130.51, 129.53, 124.63 (q, *J* = 3.8 Hz), 124.02 (q, *J* = 3.9 Hz), 123.82, 122.61, 121.24 (q, *J* = 277.1 Hz), 119.95, 119.27, 117.83.

HRMS(ESI): calcd. for $C_{20}H_{14}F_3O_2$+ $[M+1]^+$ 343.0940, found: 343.0943.

4.3.5.3. 4-((4'-(trifluoromethyl)-[1,1'-biphenyl]-3-yl)oxy)benzaldehyde (**2.8f**)

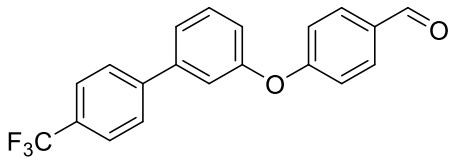


Clear oil, 77%; $^1$H NMR (400 MHz, $CDCl_3$) δ: 9.94 (s, 1H), 7.88 (d, J = 8.8 Hz, 2H), 7.74 – 7.63 (m, 4H), 7.52 (t, J = 7.8 Hz, 1H), 7.50–7.42 (m, 1H), 7.36–7.30 (m, 1H), 7.15–7.09 (m, 3H); $^{13}$C NMR (101 MHz, $CDCl_3$) δ: 190.83, 163.01, 155.93, 143.63, 142.17, 132.14, 131.66, 130.85, 130.01 (q, J = 32.8 Hz), 127.54, 125.97 (q, J = 3.8 Hz), 124.28 (d, J = 272.0 Hz)123.84, 120.04, 119.26, 117.91; HRMS(ESI): calcd. for $C_{20}H_{14}F_3O_2$+ $[M+1]^+$ 343.0940, found: 343.0949.

4.3.5.4. 4-([1,1'-biphenyl]-4-yloxy)benzaldehyde(**2.8g**)

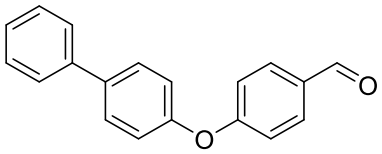

Clear oil, 83%; $^{1}$H NMR (400 MHz, $CDCl_3$) δ: 9.94 (s, 1H), 7.87 (d, J = 8.8 Hz, 2H), 7.63 (d, J = 8.7 Hz, 2H), 7.60 (dd, J = 8.4, 1.3 Hz, 2H), 7.46 (t, J = 7.5 Hz, 2H), 7.41–7.32 (m, 2H), 7.16 (d, J = 8.7 Hz, 2H), 7.12 (d, J = 8.4 Hz, 2H); $^{13}$C NMR (101 MHz, $CDCl_3$) δ: 190.88, 163.26, 154.70, 140.29, 138.16, 132.10, 131.48, 128.99, 128.92, 127.50, 127.11, 120.76, 117.81; HRMS(ESI): calcd. for $C_{19}H_{15}O_2$+ $[M+1]^+$ 275.1067, found: 275.1048.

4.3.5.5. 4-((3'-(trifluoromethyl)-[1,1'-biphenyl]-4-yl)oxy)benzaldehyde(**2.8h**)

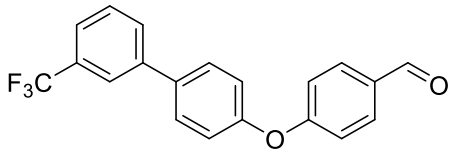

Clear oil, 80%; $^{1}$H NMR (400 MHz, $CDCl_3$) δ: 9.95 (s, 1H), 7.88 (d, J = 8.7 Hz, 2H), 7.83 (s, 1H), 7.76 (d, J = 7.6 Hz, 1H), 7.68–7.53 (m, 4H), 7.19 (d, J = 8.6 Hz, 2H), 7.13 (d, J = 8.7 Hz, 2H); $^{13}$C NMR (101 MHz, $CDCl_3$) δ: 190.86, 162.98, 155.44, 141.13, 136.59, 132.14, 131.70, 131.42 (q, J = 32.1 Hz), 130.37, 129.50, 129.07, 124.26 (q, J = 272.3 Hz), 124.18 (q, J = 3.8 Hz), 123.91 (q, J = 3.8 Hz), 120.90, 117.99; HRMS(ESI): calcd. for $C_{20}H_{14}F_3O_2$+ $[M+1]^+$ 343.0940, found: 343.0946.

4.3.5.6. 4-((4'-(trifluoromethyl)-[1,1'-biphenyl]-4-yl)oxy)benzaldehyde(**2.8i**)

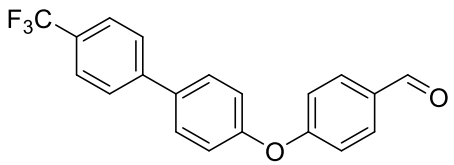

Clear oil, 81%; $^{1}$H NMR (400 MHz, $CDCl_3$) δ: 9.95 (s, 1H), 7.88 (d, J = 8.7 Hz, 2H),

7.70 (d, J = 2.3 Hz, 4H), 7.64 (d, J = 8.6 Hz, 2H), 7.19 (d, J = 8.6 Hz, 2H), 7.13 (d, J = 8.6 Hz, 2H); $^{13}$C NMR (101 MHz, $CDCl_3$) δ: 190.84, 162.91, 155.61, 143.80, 136.52, 132.14, 131.73, 129.57 (q, *J* = 32.5 Hz), 129.14, 127.37, 125.96 (q, J = 3.8 Hz), 124.37 (q, *J* = 272.0 Hz), 120.83, 118.05; HRMS(ESI): calcd. for $C_{20}H_{14}F_3O_2$+ $[M+1]^+$ 343.0940, found: 343.0935.

4.3.6. General procedure for preparation of **2.12a-g**

Alkene (1.3 equiv.) and 9-BBN (1.6 equiv.) were added into microwave reaction tube containing THF. The mixture was heated to 100 °C for 10 minutes in the microwave. The solution was purged with argon for 5 minutes before the addition of sodium hydroxide aqueous solution (3 equiv.) to form THF/$H_2O$=5:1 mixture. The mixture was further purged with argon for 5 minutes before the addition of aryl halide (1 equiv.) and Pd(dppf)$Cl_2$ (0.1 equiv.). The mixture was heated to 100 °C for 10 minutes in the microwave. The solid was removed via filtration and solution was partitioned between ethyl acetate and water. The solid was removed via filtration and solution was partitioned between ethyl acetate and water. The resulting organic layer was washed with saturated sodium bicarbonate solution and brine, dried over sodium sulfate, and concentrated via reduced pressure. The residue was purified using silica gel column chromatography (5% ethyl acetate/hexanes) to yield the product.

4.3.6.1. 4-nonylbenzaldehyde(**2.12a**)

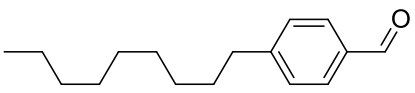

Clear oil, 45%; $^1$H NMR (400 MHz, $CDCl_3$) δ: 9.97 (s, 1H), 7.79 (d, J = 8.3 Hz, 2H), 7.33 (d, J = 7.9 Hz, 2H), 2.72–2.64 (m, 2H), 1.64 (p, J = 7.5 Hz, 2H), 1.36–1.22 (m, 12H), 0.97–0.81 (m, 3H); $^{13}$C NMR (101 MHz, $CDCl_3$) δ: 192.20, 150.66, 134.51,

130.03, 129.22, 36.37, 32.02, 31.23, 29.65, 29.59, 29.44, 29.40, 22.82, 14.26; HRMS(ESI): calcd. for $C_{16}H_{25}O+$ $[M+1]^+$ 233.1990, found: 233.1905.

4.3.6.2. 4-decylbenzaldehyde(**2.12b**)

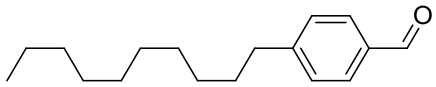

Clear oil, 42%; $^1$H NMR (400 MHz, $CDCl_3$) δ: 9.97 (s, 1H), 7.79 (d, J = 8.2 Hz, 2H), 7.33 (d, J = 8.0 Hz, 2H), 2.95–2.43 (m, 2H), 1.63 (m, 2H), 1.28 (d, J = 20.3 Hz, 14H), 1.15–0.61 (m, 3H); $^{13}$C NMR (101 MHz, $CDCl_3$) δ: 192.19, 150.66, 134.51, 130.03, 129.22, 36.37, 32.04, 31.23, 29.74, 29.69, 29.59, 29.46, 29.40, 22.83, 14.27; HRMS(ESI): calcd. for $C_{17}H_{27}O+$ $[M+1]^+$ 247.2056, found: 247.2059.

4.3.6.3. 4-undecylbenzaldehyde(**2.12c**)

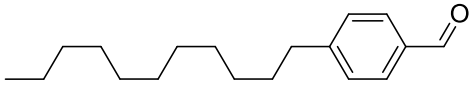

Clear oil, 60%; $^1$H NMR (400 MHz, $CDCl_3$) δ: 9.97 (s, 1H), 7.79 (d, J = 8.2 Hz, 2H), 7.33 (d, J = 8.0 Hz, 2H), 3.00–2.46 (m, 2H), 1.64 (p, J = 7.4 Hz, 2H), 1.45–1.05 (m, 16H), 1.15–0.56 (m, 3H); $^{13}$C NMR (101 MHz, $CDCl_3$) δ: 192.19, 150.66, 134.51, 130.03, 129.22, 36.37, 32.06, 31.24, 29.78, 29.76, 29.69, 29.59, 29.48, 29.41, 22.84, 14.27; HRMS(ESI): calcd. for $C_{18}H_{29}O+$ $[M+1]^+$ 261.2213, found: 261.2214.

4.3.6.4. 4-dodecylbenzaldehyde(**2.12d**)

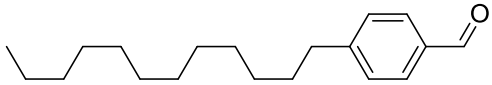

Clear oil, 55%; $^1$H NMR (400 MHz, $CDCl_3$) δ: 9.97 (s, 1H), 7.79 (d, J = 8.2 Hz, 2H), 7.33 (d, J = 8.0 Hz, 2H), 2.72–2.64 (m, 2H), 1.64 (dt, J = 15.0, 7.4 Hz, 2H), 1.37–1.21 (m, 18H), 0.91–0.84 (m, 3H); $^{13}$C NMR (101 MHz, $CDCl_3$) δ: 192.18, 150.66, 134.52,

130.03, 129.21, 36.37, 32.06, 31.23, 29.80, 29.78, 29.69, 29.59, 29.49, 29.40, 22.84, 14.27; HRMS(ESI): calcd. for $C_{19}H_{31}O+$ $[M+1]^+$ 275.2369, found: 275.2371.

4.3.6.5. 4-dodecyl-2-methylbenzaldehyde (**2.12e**)

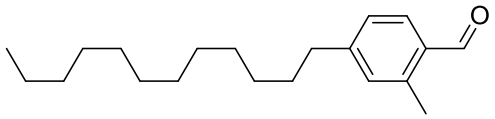

Clear oil, %; $^1$H NMR (400 MHz, $CDCl_3$) δ: 10.21 (s, 1H), 7.71 (d, J = 7.8 Hz, 1H), 7.19 – 7.14 (m, 1H), 7.09 – 7.04 (m, 1H), 2.65 (s, 3H), 2.63 – 2.60 (m, 2H), 1.66 – 1.58 (m, 2H), 1.35 – 1.22 (m, 18H), 0.88 (d, J = 6.9 Hz, 3H); $^{13}$C NMR (101 MHz, $CDCl_3$) δ: 192.60, 149.72, 140.79, 132.57, 132.27, 132.06, 126.56, 36.22, 36.02, 32.07, 31.23, 31.19, 29.81, 29.79, 29.70, 29.62, 29.60, 29.50, 29.46, 22.84, 19.81, 14.27; HRMS(ESI): calcd. for $C_{20}H_{33}O+$ $[M+1]^+$ 289.2526, found: 289.2529.

4.3.6.6. 4-(4-methylphenethyl)benzaldehyde (**2.12f**)

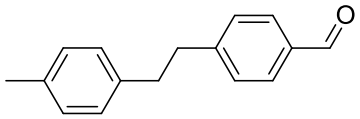

Clear oil, 33%; $^1$H NMR (400 MHz, $CDCl_3$) δ: 9.98 (s, 1H), 7.79 (d, J = 8.2 Hz, 2H), 7.32 (d, J = 7.9 Hz, 2H), 7.09 (d, J = 7.8 Hz, 2H), 7.04 (d, J = 8.1 Hz, 2H), 3.02–2.96 (m, 2H), 2.91 (ddd, J = 8.7, 6.5, 2.0 Hz, 2H), 2.32 (s, 3H); $^{13}$C NMR (101 MHz, $CDCl_3$) δ 192.16, 149.36, 137.97, 135.78, 134.69, 130.04, 129.33, 128.42, 38.32, 37.06, 21.16; HRMS(ESI): calcd. for $C_{16}H_{17}O+$ $[M+1]^+$ 225.1274, found: 225.1285.

4.3.6.7. 4-(4-methoxyphenethyl)benzaldehyde (**2.12g**)

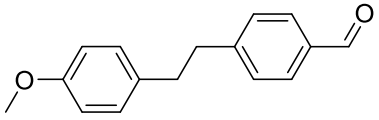

Clear oil, 49%; $^1$H NMR (400 MHz, $CDCl_3$) δ 9.97 (s, 1H), 7.79 (d, J = 8.2 Hz, 2H), 7.30

(d, J = 7.9 Hz, 2H), 7.05 (d, J = 8.8 Hz, 2H), 6.82 (d, J = 8.6 Hz, 2H), 3.79 (s, 3H), 2.97 (ddd, J = 9.0, 6.7, 2.0 Hz, 2H), 2.89 (ddd, J = 8.5, 6.6, 2.0 Hz, 2H); $^{13}$C NMR (101 MHz, $CDCl_3$) δ 192.17, 158.12, 149.32, 134.70, 133.11, 130.03, 129.50, 129.37, 113.95; HRMS(ESI): calcd. for $C_{16}H_{17}O_2$+ $[M+1]^+$ 241.1223 , found: 241.1233.

4.3.7. General procedure for preparation of **2.15a-b**

Aryl halide (1 equiv.), aryl alkene (1.3 equiv.) and potassium carbonate (3 equiv.) were added into microwave reaction tube containing DMF. The mixture was purged with argon for 5 minutes before the addition of $Pd(PPh)_2Cl_2$ (0.1 equiv.) and was heated to 140 °C for 2 h in the microwave. The reaction was extracted with ethyl acetate and saturated LiBr solution. The combined organic layers were washed with brine and dried over sodium sulfate. After filtration and concentration via reduced pressure, the resulting oil residue was purified on a silica column with hexane and ethyl acetate as the eluent to yield pure product. The residue was purified using silica gel column chromatography (5% ethyl acetate/hexanes) to yield the product.

4.3.7.1. (**2.15a**)

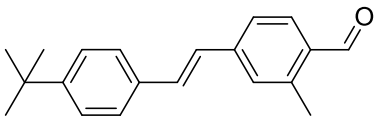

Clear oil, 51%; $^1$H NMR (400 MHz, $CDCl_3$) δ: 10.23 (s, 1H), 7.79 (d, *J* = 8.0 Hz, 1H), 7.51 – 7.39 (m, 5H), 7.37 (s, 1H), 7.25 – 7.14 (m, 1H), 7.06 (d, *J* = 16.3 Hz, 1H), 2.70 (s, 3H), 1.34 (s, 9H); $^{13}$C NMR (101 MHz, $CDCl_3$) δ 192.16, 151.90, 142.84, 141.18, 134.01, 133.14, 132.70, 131.97, 129.82, 126.77, 126.69, 125.92, 124.23, 34.89, 31.40, 19.88; HRMS (ESI+): Calcd for $C_{20}H_{23}O$+ $[M+1]^+$: 279.1749, Found: 279.1739

4.3.7.2. (E)-4-(3-(trifluoromethyl)styryl)benzaldehyde **(2.15b)**

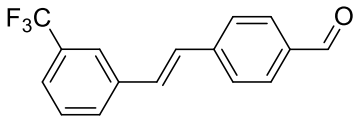

Yellow solid, 43%; $^{1}$H NMR (400 MHz, $CDCl_3$) δ: 10.02 (s, 1H), 7.94 – 7.86 (m, 2H), 7.79 (s, 1H), 7.73 – 7.69 (m, 1H), 7.70 – 7.66 (m, 2H), 7.59 – 7.48 (m, 2H), 7.24 (q, *J* = 16.4 Hz, 2H). $^{13}$C NMR (101 MHz, $CDCl_3$) δ 191.53, 142.62, 137.32, 135.70, 131.13, 130.47, 130.26, 129.94 (q, 4J = 1.3 MHz), 129.93 (q, J = 1.3 MHz), 129.91 (q, J = 1.3 MHz), 129.90 (q, J = 1.3 MHz), 129.29, 129.15, 127.11, 124.92 (q, J = 4.0 MHz), 124.88 (q, J = 4.0 MHz), 124.84 (q, J = 4.0 MHz), 124.80, 123.47 (q, J = 3.7 MHz), 123.43 (q, J = 3.7 MHz), 123.39, 123.36, 109.99; HRMS (ESI+): Calcd for $C_{16}H_{12}F_3O^+$ $[M+1]^+$: 277.0835, Found: 277.0829

General procedure for preparation of **2.18a-c**

Aryl halide (1 equiv.), aryl alkyne (1.3 equiv.) and triethylamine (3 equiv.) were added into microwave reaction tube containing THF. The mixture was purged with argon for 5 minutes before the addition of $Pd(PPh)_3Cl_2$ (0.1 equiv.) and further purged with argon for 5 minutes before the addition of CuI (0.05 equiv.). The mixture was heated to 50 °C for 30 minutes in the microwave. The solvent was removed under reduced pressure. The residue was purified using silica gel column chromatography (5% ethyl acetate/hexanes) to yield the product.

4.3.8.1. 4-((4-propylphenyl)ethynyl)benzaldehyde(**2.18a**)

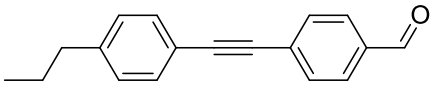

Yellow solid, 94%; $^{1}$H NMR (400 MHz, $CDCl_3$) δ: 10.02 (s, 1H), 7.86 (d, J = 8.5 Hz, 2H), 7.66 (d, J = 8.1 Hz, 2H), 7.47 (d, J = 8.3 Hz, 2H), 7.19 (d, J = 8.4 Hz, 2H), 2.61 (t, J

= 7.6 Hz, 2H), 1.73–1.58 (m, 2H), 0.95 (t, J = 7.3 Hz, 3H); $^{13}$C NMR (101 MHz, $CDCl_3$) δ: 191.59, 144.18, 135.39, 132.17, 131.85, 130.05, 129.72, 128.81, 119.78, 94.00, 88.14, 38.16, 24.46, 13.90; HRMS(ESI): calcd. for $C_{18}H_{17}O^+$ $[M+1]^+$ 249.1274, found: 249.1267.

4.3.8.2. 4-((4-butylphenyl)ethynyl)benzaldehyde(**2.18b**)

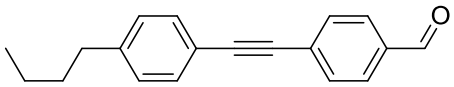

Yellow solid, 92%; $^1$H NMR (400 MHz, Chloroform-d) δ 10.01 (s, 1H), 7.85 (d, J = 8.5 Hz, 2H), 7.66 (d, J = 8.0 Hz, 2H), 7.47 (d, J = 8.4 Hz, 2H), 7.19 (d, J = 8.5 Hz, 2H), 2.66–2.60 (m, 2H), 1.66–1.55 (m, 2H), 1.36 (dq, J = 14.5, 7.3 Hz, 2H), 0.94 (t, J = 7.3 Hz, 3H); $^{13}$C NMR (101 MHz, cdcl3) δ 191.54, 144.39, 135.37, 132.14, 131.84, 130.02, 129.69, 128.73, 119.72, 93.99, 88.13, 35.78, 33.48, 22.44, 14.06; HRMS(ESI): Calcd. for $C_{19}H_{19}O^+$ $[M+1]^+$ 263.1430, found: 263.1426.

4.3.8.3. 4-((4-pentylphenyl)ethynyl)benzaldehyde(**2.18c**)

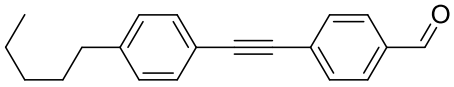

Yellow solid, 89 %; $^1$H NMR (400 MHz, $CDCl_3$) δ: 10.01 (s, 1H), 7.86 (d, J = 8.3 Hz, 2H), 7.66 (d, J = 8.4 Hz, 2H), 7.47 (d, J = 8.2 Hz, 2H), 7.19 (d, J = 8.1 Hz, 2H), 2.67–2.58 (m, 2H), 1.62 (p, J = 7.6 Hz, 2H), 1.40–1.25 (m, 4H), 0.90 (t, J = 6.9 Hz, 3H); $^{13}$C NMR (101 MHz, $CDCl_3$) δ: 191.58, 144.44, 135.35, 132.14, 131.84, 130.02, 129.70, 128.73, 119.71, 93.99, 88.13, 36.06, 31.57, 31.03, 22.65, 14.16; HRMS(ESI): calcd. for $C_{20}H_{21}O^+$ $[M+1]^+$ 277.1587 , found: 277.1590.

4.3.8. General procedure for preparation of **2.9a-i, 2.13a-e, 2.13g-h, 17a-b, and 2.19a-c**

Aldehyde (1 equiv.) and (R)-prolinol (1.3 equiv.) were added to a round bottom

flask containing DCM/MeOH=1:1. The solution was allowed to be cooled in ice bath for 5 minutes before the addition of p-toluenesulfonic acid (1 equiv.) and sodium cyanoborohydride (0.7 equiv.). The solution was further stirred at room temperature for 12-16 hours under nitrogen until TLC indicated that the starting material had been consumed. The solid was removed via filtration and solution was partitioned between ethyl acetate and water. The organic layers were washed with saturated sodium bicarbonate solution, brine and dried over sodium sulfate, and concentrated via reduced pressure. The residue was purified using silica gel column chromatography (5% methanol/dichloromethane) to yield the product.

4.3.9.1. (*R*)-(1-(4-phenoxybenzyl)pyrrolidin-2-yl)methanol (**2.9a**)

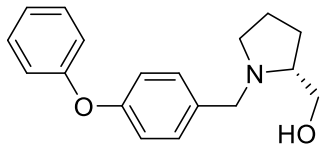


Clear oil, 45%; $^{1}$H NMR (400 MHz, $CDCl_3$) δ 7.33 (dd, J = 8.6, 7.4 Hz, 2H), 7.28 (d, J = 8.5 Hz, 2H), 7.13–7.07 (m, 1H), 7.01 (dd, J = 8.7, 1.1 Hz, 2H), 6.97 (d, J = 8.6 Hz, 2H), 3.98 (d, J = 13.0 Hz, 1H), 3.68 (dd, J = 10.9, 3.5 Hz, 1H), 3.47 (dd, J = 11.0, 2.6 Hz, 1H), 3.40 (d, J = 13.0 Hz, 1H), 3.03 (ddd, J = 9.5, 5.6, 3.8 Hz, 1H), 2.80 (ddt, J = 9.2, 6.1, 3.0 Hz, 1H), 2.35 (td, J = 9.2, 7.8 Hz, 1H), 2.01–1.90 (m, 1H), 1.89–1.80 (m, 1H), 1.78–1.70 (m, 2H); $^{13}$C NMR (101 MHz, $CDCl_3$) δ 157.30, 156.58, 133.44, 130.38, 129.87, 123.38, 118.96, 118.88, 64.68, 61.84, 58.10, 54.49, 27.80, 23.57; HRMS(ESI): calcd. for $C_{18}H_{22}NO_2$+ $[M+1]^+$ 284.1645, found: 284.1656.

4.3.9.2. (*R*)-(1-(4-(3-(tert-butyl)phenoxy)benzyl)pyrrolidin-2-yl)methanol (**2.9b**)

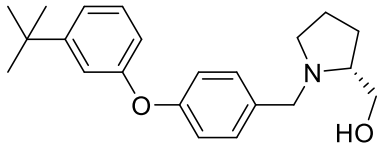


Clear oil, 51%; $^{1}$H NMR (400 MHz, $CDCl_3$) δ: 7.32 (d, J = 8.5 Hz, 2H), 7.30 – 7.27 (m, 1H), 7.19 – 7.15 (m, 1H), 7.11 (dd, J = 2.4, 1.9 Hz, 1H), 6.99 (d, J = 8.5 Hz, 2H), 6.81 (dddd, J = 8.0, 2.4, 1.0, 0.4 Hz, 1H), 4.04 (d, J = 13.0 Hz, 1H), 3.72 (dd, J = 11.1, 3.4 Hz, 1H), 3.56 – 3.46 (m, 1H), 3.14 – 3.05 (m, 2H), 2.89 (td, J = 5.9, 3.0 Hz, 1H), 2.43 (dt, J = 9.5, 8.2 Hz, 1H), 2.03–1.94 (m, 1H), 1.91–1.86 (m, 1H), 1.82–1.75 (m, 2H), 1.33 (s, 9H); $^{13}$C NMR (101 MHz, $CDCl_3$) δ: 157.08, 156.77, 153.67, 130.54, 129.32, 120.61, 118.53, 116.72, 115.91, 110.15, 65.02, 61.78, 58.18, 54.43, 34.94, 31.41, 27.71, 23.56; HRMS(ESI): calcd. for $C_{22}H_{30}NO_2$+ $[M+1]^+$ 340.2271, found: 340.2278.

4.3.9.3. (*R*)-(1-(4-([1,1'-biphenyl]-3-yloxy)benzyl)pyrrolidin-2-yl)methanol (**2.9c**)

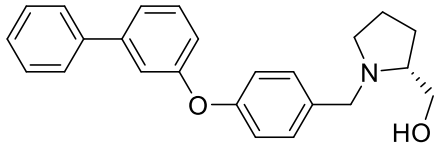


Clear oil, 54%; $^{1}$H NMR (400 MHz, $CDCl_3$) δ: 7.56 (d, J = 7.1 Hz, 1H), 7.26 – 7.25 (m, 1H), 7.03 (d, J = 8.2 Hz, 2H), 7.01 – 6.97 (m, 1H), 4.28 – 4.18 (m, 1H), 3.82 – 3.73 (m, 2H), 3.70 – 3.64 (m, 1H), 3.29 – 3.17 (m, 1H), 2.72 – 2.64 (m, 1H), 2.09 – 2.05 (m, 1H), 1.94 – 1.83 (m, 2H); $^{13}$C NMR (101 MHz, $CDCl_3$) δ: 157.90, 157.06, 143.35, 140.44, 131.55, 130.31, 128.94, 127.78, 127.23, 122.70, 118.86, 118.16, 76.84, 61.39, 58.34, 54.25, 29.82, 27.19, 23.24, 14.33; HRMS(ESI): calcd. for $C_{24}H_{26}NO_2$+ $[M+1]^+$ 360.1958, found: 360.1957.

4.3.9.4. (*R*)-(1-(4-((3'-(trifluoromethyl)-[1,1'-biphenyl]-3-yl)oxy)benzyl)pyrrolidin-2-yl)methanol (**2.9d**)

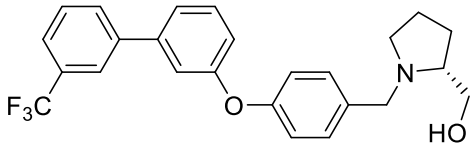


Clear oil, 37%; $^{1}$H NMR (500 MHz, CDCl3) δ 7.79 (s, 1H), 7.73 (d, J = 7.8 Hz, 1H), 7.60 (d, J = 7.8 Hz, 1H), 7.54 (t, J = 7.7 Hz, 1H), 7.44 (t, J = 7.9 Hz, 1H), 7.38 (d, J = 8.5 Hz, 2H), 7.36 (d, J = 8.2 Hz, 1H), 7.25 (t, J = 2.1 Hz, 1H), 7.03 (d, J = 8.6 Hz, 3H), 4.21 (d, J = 13.1 Hz, 1H), 3.77–3.70 (m, 2H), 3.65 (dd, J = 11.7, 4.5 Hz, 1H), 3.21 (td, J = 6.6, 2.8 Hz, 1H), 3.15 (q, J = 5.0 Hz, 1H), 2.66 – 2.60 (m, 1H), 2.06–2.01 (m, 1H), 1.91–1.83 (m, 3H); $^{13}$C NMR (126 MHz, CDCl3) δ: 157.33, 157.26, 141.72, 141.15, 131.34, 131.17 (q, J = 32.3 Hz), 130.44, 129.63, 129.33, 124.30 (q, J = 3.8 Hz), 124.09 (q, J = 272.5 Hz), 123.88 (q, J = 3.8 Hz), 122.48, 118.79, 118.60, 118.00, 66.13, 61.36, 58.20, 54.14, 27.14, 23.21; HRMS(ESI): calcd. for $C_{25}H_{25}F_3NO_2$+ $[M+1]^+$ 428.1832, found $[M+1]^+$ 428.1840.

4.3.9.5. (*R*)-(1-(4-((4'-(trifluoromethyl)-[1,1'-biphenyl]-3-yl)oxy)benzyl)pyrrolidin-2-yl)methanol (**2.9e**)

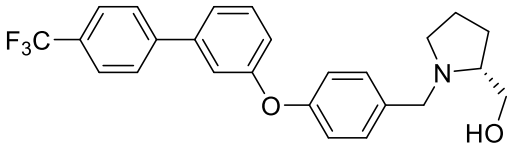


Clear oil, 40%; $^{1}$H NMR (500 MHz, $CDCl_3$) δ 7.71–7.63 (m, 4H), 7.43 (t, J = 7.9 Hz, 1H), 7.39–7.32 (m, 3H), 7.25 (t, J = 2.1 Hz, 1H), 7.06–7.00 (m, 3H), 4.15–4.09 (m, 1H), 3.72 (dd, J = 11.5, 3.4 Hz, 1H), 3.63–3.55 (m, 2H), 3.16 (ddd, J = 10.4, 6.7, 3.7 Hz, 1H), 3.00 (ddt, J = 9.5, 6.5, 3.6 Hz, 1H), 2.55–2.46 (m, 1H), 2.03–1.97 (m, 1H), 1.92–1.77 (m, 3H); 13C NMR (126 MHz, $CDCl_3$) δ: 157.52, 156.80, 143.90, 143.90, 141.66, 130.99, 130.37, 129.65 (q, J = 32.5 Hz), 127.42, 125.75 (q, J = 3.7 Hz), 124.19 (q, J = 272.1 Hz), 122.35, 118.86, 118.54, 117.83, 77.28, 65.63, 61.55, 58.21, 54.22, 27.34, 23.41;

HRMS(ESI): calcd. for $C_{25}H_{25}F_3NO_2$+ $[M+1]^+$ 428.1832, found: 428.1837.

4.3.9.6. (*R*)-(1-(4-(4-(tert-butyl)phenoxy)benzyl)pyrrolidin-2-yl)methanol (**2.9f**)

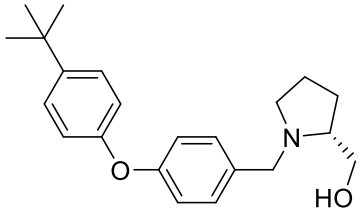


Clear oil, 36%; $^1$H NMR (400 MHz, $CDCl_3$) δ: 7.37 (d, J = 2.1 Hz, 2H), 7.35 (d, J = 2.3 Hz, 2H), 6.97 (d, J = 8.6 Hz, 2H), 6.94 (d, J = 9.0 Hz, 2H), 4.30 (d, J = 13.0 Hz, 1H), 3.89 (d, J = 13.1 Hz, 1H), 3.78 (dd, J = 12.1, 3.6 Hz, 1H), 3.72 (dd, J = 12.1, 5.3 Hz, 1H), 3.38–3.27 (m, 2H), 2.84–2.73 (m, 2H), 2.13–2.05 (m, 1H), 1.98–1.86 (m, 3H), 1.32 (s, 9H); $^{13}$C NMR (101 MHz, $CDCl_3$) δ: 158.70, 153.89, 147.00, 131.78, 126.85, 119.14, 118.53, 66.96, 61.24, 58.41, 54.11, 34.50, 31.60, 26.99, 23.15; HRMS(ESI): calcd. for $C_{22}H_{30}NO_2$+ $[M+1]^+$ 340.2271 , found: 340.2275.

4.3.9.7. (*R*)-(1-(4-((3'-(trifluoromethyl)-[1,1'-biphenyl]-4-yl)oxy)benzyl)pyrrolidin-2-yl)methanol (**2.9h**)

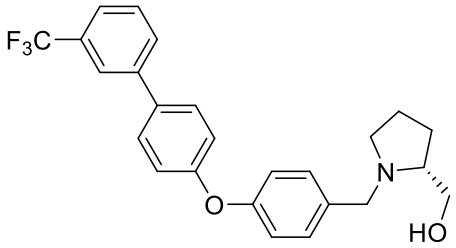


Clear oil, 38%; $^1$H NMR (500 MHz, $CDCl_3$) δ 7.79 (s, 1H), 7.73 (d, J = 7.5 Hz, 1H), 7.61 – 7.51 (m, 4H), 7.40 (d, J = 8.1 Hz, 2H), 7.10 (d, J = 8.3 Hz, 2H), 7.04 (d, J = 8.2 Hz, 2H), 4.26 (d, J = 13.0 Hz, 1H), 3.82–3.75 (m, 2H), 3.69 (dd, J = 11.8, 4.8 Hz, 1H), 3.30–3.21 (m, 2H), 2.74–2.67 (m, 1H), 2.11–2.03 (m, 1H), 1.95–1.83 (m, 3H); $^{13}$C NMR (126 MHz, $CDCl_3$) δ 157.39, 156.79, 141.19, 135.19, 131.50, 131.15 (d, J = 32.1 Hz), 130.18,

129.29, 128.97, 128.66, 124.15 (q, J = 272.4 Hz), 123.77 (q, J = 3.9 Hz), 123.65 (q, J = 3.9 Hz), 119.53, 119.00, 66.45, 61.27, 58.25, 54.14, 27.05, 23.13; HRMS(ESI): calcd. for $C_{25}H_{25}F_3NO_2$+ $[M+1]^+$ 428.1832, found: 428.1839.

4.3.9.8. (*R*)-(1-(4-((4'-(trifluoromethyl)-[1,1'-biphenyl]-4-yl)oxy)benzyl)pyrrolidin-2-yl)methanol (**2.9i**)

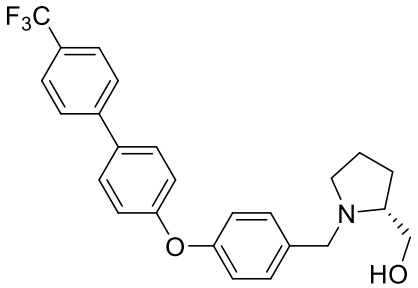


Clear oil, 61%; $^1$H NMR (500 MHz, $CDCl_3$) δ 7.71–7.64 (m, 4H), 7.57 (d, J = 8.6 Hz, 2H), 7.36 (d, J = 8.5 Hz, 2H), 7.10 (d, J = 8.7 Hz, 2H), 7.04 (d, J = 8.5 Hz, 2H), 4.07 (d, J = 13.0 Hz, 1H), 3.71 (dd, J = 11.3, 3.4 Hz, 1H), 3.57–3.51 (m, 2H), 3.13 (dd, J = 6.8, 3.6 Hz, 1H), 2.93 (dt, J = 8.0, 4.3 Hz, 1H), 2.46 (q, J = 8.8 Hz, 1H), 2.05–1.95 (m, 1H), 1.88 (dt, J = 12.4, 6.5 Hz, 1H), 1.84–1.76 (m, 2H); $^{13}$C NMR (126 MHz, $CDCl_3$) δ 157.47, 156.38, 143.97, 143.96, 134.78, 130.73, 129.01 (q, J = 32.5 Hz), 128.66, 127.53, 125.74 (q, J = 3.7 Hz), 124.85 (q, *J* = 271.8 Hz), 119.12, 119.11, 65.27, 61.60, 58.16, 54.32, 27.48, 23.47; HRMS(ESI): calcd. for $C_{25}H_{25}F_3NO_2$+ $[M+1]^+$ 428.1832, found:428.1834.

4.3.9.9. (*R*)-(1-(4-nonylbenzyl)pyrrolidin-2-yl)methanol (**2.13a**)

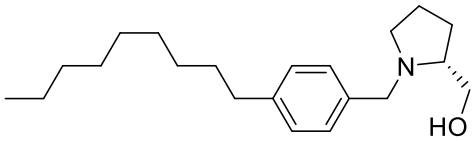


Clear oil, 46%; $^1$H NMR (400 MHz, $CDCl_3$) δ: 7.22 (d, J = 8.0 Hz, 2H), 7.13 (d, J = 8.0 Hz, 2H), 3.96 (d, J = 12.9 Hz, 1H), 3.67 (dd, J = 10.9, 3.5 Hz, 1H), 3.46 (dd, J = 10.9, 2.5 Hz, 1H), 3.39 (d, J = 12.9 Hz, 1H), 3.05–2.98 (m, 1H), 2.78 (ddt, J = 9.1, 6.1, 3.0 Hz,

1H), 2.61–2.55 (m, 2H), 2.34 (td, J = 9.1, 7.9 Hz, 1H), 1.99–1.88 (m, 1H), 1.88–1.77 (m, 1H), 1.76–1.66 (m, 2H), 1.65–1.54 (m, 2H), 1.36–1.22 (m, 12H), 0.91–0.85 (m, 3H); $^{13}$C NMR (101 MHz, $CDCl_3$) δ: 142.07, 135.81, 128.89, 128.49, 64.56, 61.81, 58.37, 54.47, 35.74, 31.99, 31.62, 29.65, 29.62, 29.45, 29.43, 27.80, 23.51, 22.78, 14.22; HRMS(ESI): calcd. for $C_{21}H_{36}NO^+$ $[M+1]^+$ 318.2791, found: 318.2802.

4.3.9.10. (*R*)-(1-(4-decylbenzyl)pyrrolidin-2-yl)methanol (**2.13b**)

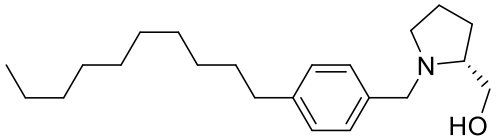


Clear oil, 51%; $^1$H NMR (400 MHz, $CDCl_3$) δ 7.38 (d, J = 8.2 Hz, 2H), 7.16 (d, J = 8.0 Hz, 2H), 4.18 (d, J = 13.1 Hz, 1H), 3.85 (d, J = 13.4 Hz, 1H), 3.76 (dd, J = 12.3, 3.1 Hz, 1H), 3.66 (dd, J = 12.3, 4.6 Hz, 1H), 3.34–3.27 (m, 1H), 3.26–3.20 (m, 1H), 2.69 (dd, J = 8.1, 3.7 Hz, 1H), 2.60–2.54 (m, 2H), 2.03–1.89 (m, 3H), 1.88–1.79 (m, 1H), 1.56 (q, J = 7.2 Hz, 2H), 1.32–1.20 (m, 14H), 0.88–0.83 (m, 3H); $^{13}$C NMR (101 MHz, $CDCl_3$) δ 143.86, 130.27, 128.95, 126.13, 66.97, 61.20, 58.58, 53.95, 35.73, 31.98, 31.42, 29.77, 29.73, 29.69, 29.65, 29.56, 29.41, 26.97, 23.47, 22.75, 14.20; HRMS(ESI): calcd. for $C_{22}H_{38}NO^+$ $[M+1]^+$ 332.2948, found: 332.2955.

4.3.9.11. (*R*)-(1-(4-undecylbenzyl)pyrrolidin-2-yl)methanol (**2.13c**)

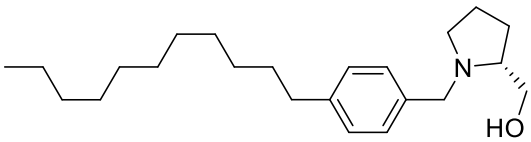


Clear oil, 58%; $^1$H NMR (400 MHz, $CDCl_3$) δ: 7.20 (d, J = 8.0 Hz, 2H), 7.12 (d, J = 7.9 Hz, 2H), 3.92 (d, J = 12.9 Hz, 1H), 3.65 (dd, J = 10.7, 3.4 Hz, 1H), 3.42 (dd, J = 10.7, 2.1 Hz, 1H), 3.32 (d, J = 12.9 Hz, 1H), 2.98 (dq, J = 9.3, 5.6, 4.4 Hz, 1H), 2.77–2.67 (m, 1H), 2.62–2.53 (m, 2H), 2.29 (td, J = 9.3, 7.6 Hz, 1H), 1.93 (dq, J = 12.6, 8.8 Hz, 1H), 1.87–

1.78 (m, 1H), 1.69 (td, J = 8.9, 5.7 Hz, 2H), 1.59 (dt, J = 15.0, 6.2 Hz, 2H), 1.34–1.19 (m, 16H), 0.88 (t, J = 6.9 Hz, 3H); $^{13}$C NMR (101 MHz, $CDCl_3$) δ: 141.93, 136.55, 128.76, 128.48, 64.29, 61.83, 58.34, 54.57, 35.78, 32.07, 31.69, 29.82, 29.78, 29.74, 29.67, 29.51, 29.50, 27.95, 23.60, 22.84, 14.28; HRMS(ESI): calcd. for $C_{23}H_{40}NO+$ $[M+1]^+$ 346.3104, found: 346.3132.

4.3.9.12. (*R*)-(1-(4-dodecylbenzyl)pyrrolidin-2-yl)methanol (**2.13d**)

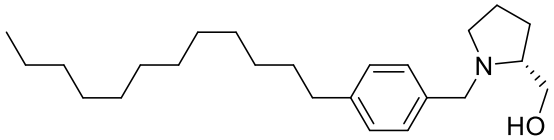


Clear oil, 39%; $^1$H NMR (400 MHz, $CDCl_3$) δ: 7.25 (d, J = 8.3 Hz, 2H), 7.16 (d, J = 8.0 Hz, 2H), 4.07 (d, J = 13.0 Hz, 1H), 3.74–3.66 (m, 1H), 3.55 (dd, J = 11.7, 4.2 Hz, 1H), 3.12 (dt, J = 10.0, 4.9 Hz, 1H), 2.97 (m, 1H), 2.63–2.55 (m, 2H), 2.50 (m, 1H), 2.06–1.92 (m, 2H), 1.92–1.74 (m, 2H), 1.59 (m, 2H), 1.37–1.18 (m, 18H), 0.91–0.81 (m, 3H); $^{13}$C NMR (101 MHz, $CDCl_3$) δ: 142.98, 129.39, 128.81, 110.15, 35.80, 32.07, 31.60, 29.82, 29.81, 29.79, 29.74, 29.65, 29.50, 27.54, 23.46, 22.84, 14.28; HRMS(ESI): calcd. for $C_{24}H_{42}NO+$ $[M+1]^+$ 360.3261, found: 360.3266.

4.3.9.13. (R)-(1-(4-dodecyl-2-methylbenzyl)pyrrolidin-2-yl)methanol (**2.13e**)

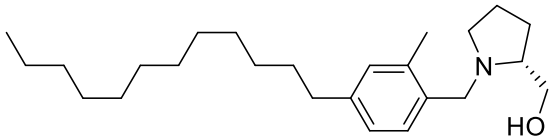


Clear oil, 35%; $^1$H NMR (400 MHz, $CDCl_3$) δ: 7.18 (d, J = 7.5 Hz, 1H), 6.96 (d, J = 7.4 Hz, 2H), 3.94 (d, J = 13.0 Hz, 1H), 3.64 (dd, J = 10.9, 3.4 Hz, 1H), 3.46 – 3.34 (m, 2H), 3.03 – 2.94 (m, 1H), 2.76 (s, 1H), 2.54 (t, J = 8.9, 6.7 Hz, 2H), 2.34 (s, 3H), 2.33 – 2.27 (m, 1H), 2.01 – 1.89 (m, 1H), 1.89 – 1.79 (m, 1H), 1.76 – 1.64 (m, 2H), 1.58 (p, J = 10.6, 4.8 Hz, 2H), 1.37 – 1.20 (m, 19H), 0.88 (t, J = 6.8 Hz, 3H) ; $^{13}$C NMR (101 MHz,

$CDCl_3$) δ: 136.74, 136.44, 130.77, 130.38, 130.02, 126.03, 65.54, 61.99, 56.52, 54.72, 35.73, 32.07, 31.65, 29.83, 29.80, 29.75, 29.68, 29.57, 29.52, 27.75, 23.83, 22.85, 19.48, 14.33, 14.22; HRMS(ESI): calcd. for $C_{25}H_{44}NO^+$ $[M+1]^+$ 374.3417, found: 374.3439.

4.3.9.14. (*R*)-(1-(4-(4-methylphenethyl)benzyl)pyrrolidin-2-yl)methanol (**2.13g**)

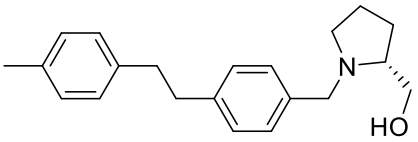


Clear oil, 45%; $^1$H NMR (400 MHz, $CDCl_3$) δ: 7.38 (d, J = 8.2 Hz, 2H), 7.23 (d, J = 8.2 Hz, 2H), 7.08 (d, J = 7.9 Hz, 2H), 7.03 (d, J = 8.2 Hz, 2H), 4.45 (d, J = 13.0 Hz, 1H), 4.15 (d, J = 13.1 Hz, 1H), 3.88–3.74 (m, 2H), 3.66–3.58 (m, 1H), 3.43 (ddd, J = 11.7, 6.8, 4.9 Hz, 1H), 3.02 (ddd, J = 11.3, 8.3, 7.2 Hz, 1H), 2.93–2.82 (m, 4H), 2.31 (s, 3H), 2.21–2.12 (m, 1H), 2.09–1.89 (m, 3H); $^{13}$C NMR (101 MHz, $CDCl_3$) δ: 144.20, 138.23, 135.64, 130.86, 129.64, 129.18, 128.40, 127.21, 68.15, 60.85, 58.94, 54.10, 37.78, 37.19, 26.63, 22.95, 21.15; HRMS(ESI): calcd. for $C_{21}H_{28}NO^+$ $[M+1]^+$ 310.2165, found: 310.2176.

4.3.9.15. (*R*)-(1-(4-(4-methylphenethyl)benzyl)pyrrolidin-2-yl)methanol (**2.13h**)

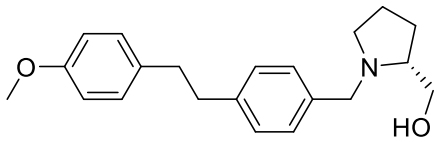


Clear oil, 32%; $^1$H NMR (400 MHz, $CDCl_3$) δ: 7.28 (d, J = 8.0 Hz, 2H), 7.15 (d, J = 8.1 Hz, 2H), 7.08 (d, J = 8.7 Hz, 2H), 6.82 (d, J = 8.6 Hz, 2H), 4.02 (d, J = 13.0 Hz, 1H), 3.79 (s, 3H), 3.69 (dd, J = 11.4, 3.3 Hz, 1H), 3.58 – 3.48 (m, 2H), 3.16 – 3.08 (m, 1H), 2.95 – 2.89 (m, 1H), 2.89 – 2.83 (m, 4H), 2.51 – 2.40 (m, 1H), 2.00 – 1.87 (m, 2H), 1.83 – 1.71 (m, 2H); $^{13}$C NMR (101 MHz, $CDCl_3$) δ: 157.95, 133.84, 129.47, 128.82, 113.84, 61.62, 58.56, 55.38, 54.39, 37.97, 37.05, 27.59, 23.62; HRMS(ESI): calcd. for $C_{21}H_{28}NO_2^+$ $[M+1]^+$ 326.2115, found: 326.2142.

4.3.9.16. (R)-(1-(4-((4-propylphenyl)ethynyl)benzyl)pyrrolidin-2-yl)methanol (**2.16a**)

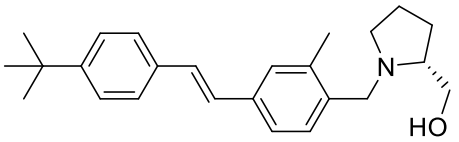


Clear oil, 20%; $^{1}$H NMR (400 MHz, Chloroform-*d*) δ 7.49 – 7.35 (m, 4H), 7.33 – 7.26 (m, 3H), 7.06 (q, *J* = 16.3 Hz, 2H), 3.97 (d, *J* = 13.2 Hz, 1H), 3.66 (dd, *J* = 10.8, 3.4 Hz, 1H), 3.48 – 3.37 (m, 2H), 3.04 – 2.96 (m, 1H), 2.81 – 2.73 (m, 1H), 2.39 (s, 3H), 2.37 – 2.26 (m, 2H), 2.02 – 1.91 (m, 1H), 1.91 – 1.81 (m, 1H), 1.77 – 1.67 (m, 2H), 1.34 (s, 9H). $^{13}$C NMR (101 MHz, Chloroform-*d*) δ 150.81, 137.08, 136.62, 134.78, 130.09, 128.54, 128.27, 127.77, 126.32, 125.74, 124.01, 65.14, 62.18, 56.68, 54.91, 34.76, 31.46, 31.41, 27.94, 23.83, 19.47. HRMS (ESI+): Calcd for $C_{25}H_{34}NO^{+}$ [M+H]: 364.2640, Found: 364.2634.

4.3.9.17. (R)-(1-(4-((4-propylphenyl)ethynyl)benzyl)pyrrolidin-2-yl)methanol (**2.16b**)

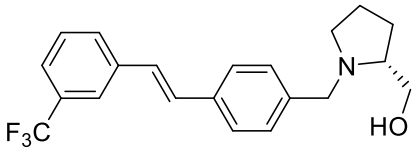


Clear oil, 15%; $^{1}$H NMR (400 MHz, Chloroform-*d*) δ 7.75 (s, 1H), 7.66 (d, *J* = 7.3 Hz, 1H), 7.54 – 7.43 (m, 4H), 7.32 (d, *J* = 7.9 Hz, 2H), 7.13 (q, *J* = 16.4 Hz, 2H), 3.98 (d, *J* = 13.1 Hz, 1H), 3.68 (dd, *J* = 10.8, 3.5 Hz, 1H), 3.46 (dd, *J* = 10.8, 2.3 Hz, 1H), 3.39 (d, *J* = 13.2 Hz, 1H), 3.04 – 2.97 (m, 1H), 2.80 – 2.72 (m, 1H), 2.71 (s, 1H), 2.37 – 2.26 (m, 1H), 2.01 – 1.90 (m, 1H), 1.90 – 1.80 (m, 1H), 1.77 – 1.66 (m, 2H). $^{13}$C NMR (101 MHz, cdcl$_3$) δ 138.17, 136.11, 131.68 (q, J = 32 Hz), 131.36 (q, J = 32 Hz), 131.04 (q, J = 32 Hz), 130.73 (q, J = 32 Hz), 130.16, 129.69 (q, J = 1.0 Hz), 129.68 (q, J = 1.0 Hz), 129.67 (q, 4JCF = 1.0 Hz), 129.64, 129.24, 127.27, 126.91, 125.61, 124.22 (q, J = 3.7

Hz), 124.19 (q, J = 3.7 Hz), 124.15 (q, J = 3.7 Hz), 124.11 (q, J = 3.7 Hz), 123.21 (q, J = 3.7 Hz), 123.18 (q, J = 3.7 Hz), 123.14 (q, J = 3.7 Hz), 123.10 (q, J = 3.7), 122.90, 65.15, 61.81, 58.53, 54.51, 27.66, 23.58; HRMS(ESI): calcd. for $C_{21}H_{23}F_3NO+$ $[M+1]^+$ 362.1726, found: 362.1719.

4.3.9.18. (R)-(1-(4-((4-propylphenyl)ethynyl)benzyl)pyrrolidin-2-yl)methanol (**2.19a**)

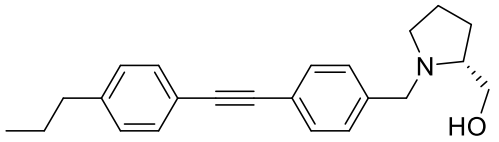


Clear oil, 55%; $^1$H NMR (400 MHz, $CDCl_3$) δ: 7.48 (d, J = 8.2 Hz, 2H), 7.44 (d, J = 8.2 Hz, 2H), 7.28 (d, J = 8.2 Hz, 2H), 7.16 (d, J = 8.3 Hz, 2H), 3.98 (d, J = 13.2 Hz, 1H), 3.66 (dd, J = 10.8, 3.5 Hz, 1H), 3.45 (dd, J = 10.8, 2.2 Hz, 1H), 3.37 (d, J = 13.2 Hz, 1H), 3.00 – 2.94 (m, 1H), 2.77 – 2.70 (m, 1H), 2.62 – 2.57 (m, 2H), 2.32 – 2.24 (m, 1H), 1.99 – 1.89 (m, 1H), 1.85 (dt, J = 13.0, 6.4 Hz, 1H), 1.75 – 1.68 (m, 2H), 1.64 (dt, J = 14.8, 7.4 Hz, 3H), 0.94 (t, J = 7.3 Hz, 3H); $^{13}$C NMR (101 MHz, $CDCl_3$) δ: 143.23, 139.50, 131.67, 131.59, 128.78, 128.63, 122.35, 120.59, 89.63, 88.76, 64.52, 61.96, 58.51, 54.59, 38.08, 27.85, 24.45, 23.59, 13.87; HRMS(ESI): calcd. for $C_{23}H_{28}NO$ $[M+1]^+$ 334.2165, found: 334.2142.

4.3.9.19. (R)-(1-(4-((4-butylphenyl)ethynyl)benzyl)pyrrolidin-2-yl)methanol (**2.19b**)

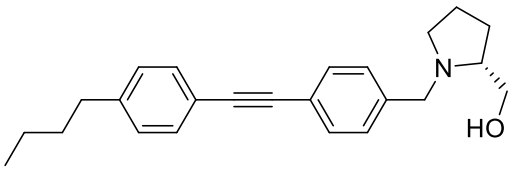


Clear oil, 36%; $^1$H NMR (400 MHz, $CDCl_3$) δ: 7.48 (d, J = 8.1 Hz, 2H), 7.44 (d, J = 8.1 Hz, 2H), 7.28 (d, J = 8.1 Hz, 2H), 7.16 (d, J = 8.0 Hz, 2H), 3.98 (d, J = 13.2 Hz, 1H), 3.66 (dd, J = 10.8, 3.5 Hz, 1H), 3.45 (dd, J = 10.8, 2.3 Hz, 1H), 3.37 (d, J = 13.2 Hz, 1H), 2.98

(dt, J = 9.3, 4.4 Hz, 1H), 2.74 (ddt, J = 9.1, 5.9, 2.9 Hz, 1H), 2.66 – 2.57 (m, 2H), 2.34 – 2.23 (m, 1H), 1.95 (dt, J = 12.6, 8.7 Hz, 1H), 1.84 (td, J = 13.0, 12.6, 7.1 Hz, 1H), 1.71 (tt, J = 8.6, 3.8 Hz, 2H), 1.66 – 1.54 (m, 2H), 1.36 (dq, J = 14.6, 7.3 Hz, 2H), 0.93 (t, J = 7.4 Hz, 3H); $^{13}$C NMR (101 MHz, $CDCl_3$) δ: 143.47, 139.43, 131.65, 131.59, 128.79, 128.57, 122.33, 120.49, 89.63, 88.72, 64.49, 61.91, 58.48, 54.57, 35.71, 33.52, 27.82, 23.58, 22.43, 14.06; HRMS(ESI): calcd. for $C_{24}H_{30}NO$ $[M+1]^+$ 348.2322, found: 348.2342.

4.3.9.20. (R)-(1-(4-((4-pentylphenyl)ethynyl)benzyl)pyrrolidin-2-yl)methanol (**2.19c**)

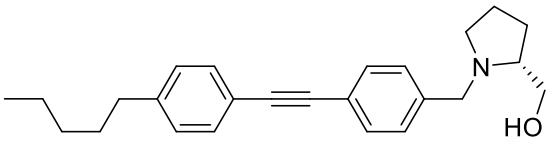


Clear oil, 47%; $^1$H NMR (400 MHz, $CDCl_3$) δ: 7.48 (d, J = 8.3 Hz, 2H), 7.44 (d, J = 8.3 Hz, 2H), 7.28 (d, J = 8.2 Hz, 2H), 7.16 (d, J = 8.4 Hz, 2H), 3.98 (d, J = 13.2 Hz, 1H), 3.66 (dd, J = 10.8, 3.5 Hz, 1H), 3.45 (dd, J = 10.8, 2.2 Hz, 1H), 3.37 (d, J = 13.2 Hz, 1H), 3.03 – 2.93 (m, 1H), 2.80 – 2.69 (m, 1H), 2.66 – 2.57 (m, 2H), 2.35 – 2.23 (m, 1H), 2.02 – 1.78 (m, 2H), 1.77 – 1.66 (m, 2H), 1.62 (dt, J = 15.2, 7.6 Hz, 2H), 1.33 (td, J = 7.8, 6.5, 4.5 Hz, 4H), 0.94 – 0.85 (m, 3H); $^{13}$C NMR (101 MHz, $CDCl_3$) δ: 143.52, 139.49, 131.67, 131.61, 128.79, 128.58, 122.34, 120.52, 89.64, 88.74, 64.50, 61.91, 58.49, 54.60, 36.01, 31.57, 31.07, 27.85, 23.61, 22.66, 14.16; HRMS(ESI): calcd. for $C_{25}H_{32}NO$ $[M+1]^+$ 362.2478, found: 362.2456.

4.3.9. General procedure for preparation of **2.13f**

Alcohol starting material (1 equiv.) was dissolved in DCM and the stirring flask was cooled in ice bath for 5 min. Pyridine (3 equiv.) was added slowly followed by acetic anhydride (2 equiv.). The mixture was allowed to slowly rise to room temperature and

stirred for overnight. The solvent was removed via reduced pressure and the residue was extracted with ethyl acetate. Combined organic layer was washed with brine, dried over $Na_2SO_4$ and concentrated. The residue was purified using silica gel column chromatography (20% ethyl acetate/hexanes) to yield the product.

4.3.9.1. (R)-(1-(4-dodecylbenzyl)pyrrolidin-2-yl)methyl acetate (**2.13f**)

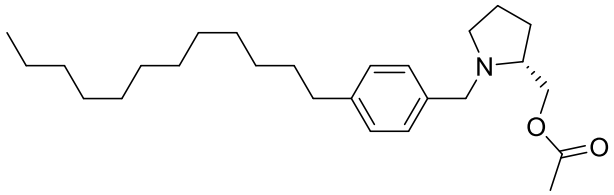


Clear oil, 76%; $^1$H NMR (400 MHz, Chloroform-d) δ 7.21 (d, J = 8.0 Hz, 2H), 7.11 (d, J = 8.2 Hz, 2H), 4.11 (dd, J = 11.0, 5.2 Hz, 1H), 4.05–4.00 (m, 2H), 3.38 (d, J = 12.9 Hz, 1H), 2.93 (ddd, J = 9.4, 6.9, 3.0 Hz, 1H), 2.80 (dq, J = 8.5, 5.7 Hz, 1H), 2.61–2.54 (m, 2H), 2.31–2.18 (m, 1H), 2.06 (s, 3H), 1.98–1.88 (m, 1H), 1.76–1.55 (m, 5H), 1.26 (m, 16H), 0.87 (t, 3H); $^{13}$C NMR (101 MHz, CDCl3) δ 171.24, 141.69, 136.65, 77.16, 67.32, 61.87, 59.30, 54.53, 35.78, 32.06, 31.69, 29.81, 29.77, 29.74, 29.67, 29.49, 28.56, 23.01, 22.83, 21.16, 14.26; HRMS(ESI): calcd. for $C_{26}H_{44}NO_2$ $[M+1]^+$ 402.3367, found: 402.3339.

4.3.10. General procedure for preparation of **2.21a-c**

Starting material (1 equiv.) was added into a round bottom flask containing 10% Pd/C (0.1 equiv.) and methanol. The solution was stirred at room temperature under hydrogen for 1-2 hours until TLC indicated the starting material had been fully consumed. The solid was removed via filtration upon Cilite and the solvent was removed via reduced pressure. The residue was purified using silica gel column chromatography (5% methanol/dichloromethane) to yield the product.

4.3.10.1. (R)-(1-(4-(4-propylphenethyl)benzyl)pyrrolidin-2-yl)methanol(**2.21a**)

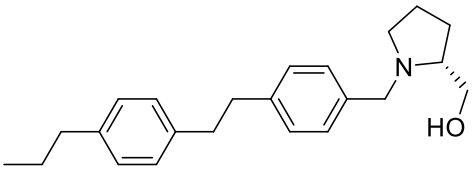


Yellow oil, 48%; $^{1}$H NMR (400 MHz, $CDCl_3$) δ: 7.22 (d, J = 8.0 Hz, 2H), 7.16 (d, J = 8.0 Hz, 2H), 7.11 (s, 4H), 3.94 (d, J = 12.9 Hz, 1H), 3.66 (dd, J = 10.7, 3.5 Hz, 1H), 3.43 (dd, J = 10.7, 2.1 Hz, 1H), 3.35 (d, J = 12.9 Hz, 1H), 3.03–2.94 (m, 1H), 2.90 (s, 4H), 2.79–2.68 (m, 1H), 2.62–2.50 (m, 1H), 2.33-2.27 (m, 1H), 2.02–1.77 (m, 2H), 1.76–1.57 (m, 4H), 0.95 (t, J = 7.3 Hz, 3H); $^{13}$C NMR (101 MHz, $CDCl_3$) δ: 140.90, 140.35, 139.11, 136.94, 128.84, 128.54, 128.51, 128.36, 64.28, 61.85, 58.34, 54.57, 37.82, 37.79, 37.69, 27.96, 24.77, 23.59, 14.01; HRMS(ESI): calcd. for $C_{23}H_{32}NO$ $[M+1]^+$ 338.2478, found: 338.2480.

4.3.10.2. (R)-(1-(4-(4-butylphenethyl)benzyl)pyrrolidin-2-yl)methanol (**2.21b**)

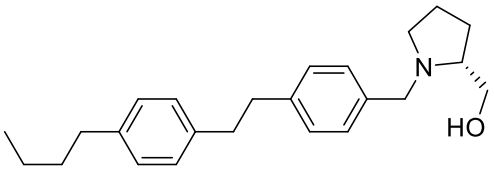


Yellow oil, 55%; $^{1}$H NMR (400 MHz, $CDCl_3$) δ: 7.22 (d, J = 8.1 Hz, 2H), 7.15 (d, J = 8.1 Hz, 2H), 7.10 (s, 4H), 3.94 (d, J = 12.9 Hz, 1H), 3.66 (dd, J = 10.8, 3.4 Hz, 1H), 3.43 (dd, J = 10.8, 2.2 Hz, 1H), 3.35 (d, J = 12.9 Hz, 1H), 2.99 (dt, J = 9.3, 4.4 Hz, 1H), 2.88 (d, J = 1.5 Hz, 4H), 2.78 – 2.71 (m, 1H), 2.63 – 2.55 (m, 2H), 2.30 (td, J = 9.3, 7.7 Hz, 1H), 1.99 – 1.78 (m, 2H), 1.76 – 1.66 (m, 2H), 1.64 – 1.54 (m, 2H), 1.41 – 1.31 (m, 2H), 0.93 (t, J = 7.3 Hz, 3H); HRMS(ESI): calcd. for $C_{24}H_{34}NO$ $[M+1]^+$ 352.2635, found: 352.2633.

4.3.10.3. (R)-(1-(4-(4-pentylphenethyl)benzyl)pyrrolidin-2-yl)methanol (**2.21c**)

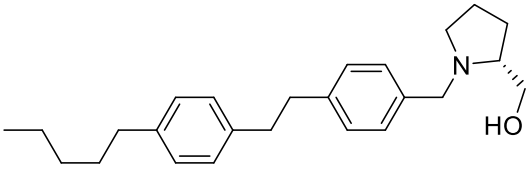


Clear oil, 51%; $^{1}$H NMR (400 MHz, $CDCl_3$) δ: 7.25 (d, J = 8.3 Hz, 2H), 7.16 (d, J = 8.1 Hz, 2H), 7.10 (s, 4H), 4.00 (d, J = 13.0 Hz, 1H), 3.68 (dd, J = 11.1, 3.4 Hz, 1H), 3.53–3.43 (m, 2H), 3.07 (dd, J = 9.7, 5.5 Hz, 1H), 2.93–2.81 (m, 5H), 2.62–2.53 (m, 2H), 2.45–2.34 (m, 1H), 2.00–1.79 (m, 2H), 1.81–1.68 (m, 2H), 1.60 (dt, J = 15.2, 7.5 Hz, 2H), 1.36–1.28 (m, 4H), 0.94–0.85 (m, 3H); $^{13}$C NMR (101 MHz, $CDCl_3$) δ: 141.43, 140.66, 139.00, 132.19, 129.25, 128.67, 128.49, 128.39, 64.95, 61.76, 58.48, 54.44, 37.82, 37.64, 35.68, 31.69, 31.41, 27.73, 23.60, 22.70, 14.20, 7.26; HRMS(ESI): calcd. for $C_{25}H_{36}NO$ $[M+1]^+$ 366.2791, found: 366.2763.

4.3.11. General procedure for preparation amine salt

Tertiary amine (1 equiv.) was dissolved in MeOH. HCl gas was purged into the solution for 1 minute. The solution was stirred for 5-10 minutes until TLC indicated that the starting material had been consumed. The solvent was removed via reduced pressure. The resulting white to brown oil or solid was washed with diethyl ether to yield pure product.

**4.4. Synthetic procedures and characterization from Chapter 3**

4.4.1. General procedure for preparation of **3.2a-b**

Magnesium turnings (1.5 equiv.) and catalytic amount of iodine were added followed by dry THF and the mixture was stirred for 30 min under nitrogen. Dodecyl bromide (1 equiv.) was added dropwise as THF solution through addition funnel over 30 min. Meanwhile the system was gently heated to mild reflux for 6-8 h to generate Grignard reagent. In a different container 1,4-dibromobenzene or 1,3-dibromobenzene

(0.9 equiv.) was dissolved in dry THF, followed by addition of $Pd(dppf)Cl_2$ (0.09 equiv.). The system was cooled in ice bath for 5 min. The generated Grignard reagent was slowed added through syringe over a period of 5 min. The system was removed from ice bath and heated to reflux for 16 h. After the mixture cooled to room temperature, iced water was slowly added to quench residue Grignard reagent and the resulting mixture was partitioned between ethyl acetate and water. Collected organic layer was washed with brine, dried over sodium sulfate, filtered and concentrated. The residue was purified using silica gel column chromatography (100% hexanes) to yield the product.

4.4.2. General procedure for preparation of **3.3a-b**

Magnesium turnings (1.5 equiv.) and catalytic amount of iodine were added followed by dry THF and the mixture was stirred for 30 min under nitrogen. 1-Bromo-4-dodecylbenzene (1 equiv.) was added dropwise as THF solution through addition funnel over 30 min. Meanwhile the system was gently heated to mild reflux for 6-8 h to generate Grignard reagent. The system was cooled in ice bath and allyl bromide (1.3 equiv.) was added dropwise as THF solution through addition funnel over 30 min. The system was stirred for 16 h and the temperature was slowly raised to room temperature. Iced water was slowly added to quench residue Grignard reagent and the resulting mixture was partitioned between ethyl acetate and water. Collected organic layer was washed with brine, dried over sodium sulfate, filtered and concentrated. The residue was purified using silica gel column chromatography (100% hexanes) to yield the product.

4.4.3. General procedure for preparation of **3.4a-b**

Alkene reactant (1 equiv.) was dissolved in dry DCM and the solution was cooled in ice bath for 5 min. Oxidizer mCPBA (1.5 equiv.) was added in four portions over 6 h.

The mixture was partitioned between ethyl acetate and water. Collected organic layer was washed with saturated sodium bicarbonate and brine, dried over sodium sulfate, filtered and concentrated. The residue was purified using silica gel column chromatography (5% ethyl acetate/hexane) to yield the product.

4.4.4. General procedure for preparation of **3.5a-m** and **3.8a-b**

Epoxide reactant (1 equiv.) was dissolved in ethanol followed by addition of cyclic amine (1.5 equiv.). The resulting solution was microwaved at 80 °C for 30 min. The residue was purified using silica gel column chromatography (5% methanol/DCM) to yield the product.

4.4.5. General procedure for preparation of **3.9a-d** and **3.12a-b**

Alkene (1.3 equiv.) and 9-BBN (1.6 equiv.) were added into microwave reaction tube containing THF. The mixture was heated to 100 °C for 10 minutes in the microwave. The solution was purged with argon for 5 minutes before the addition of sodium hydroxide aqueous solution (3 equiv.) to form THF/$H_2O$=5:1 mixture. The mixture was further purged with argon for 5 minutes before the addition of aryl halide (1 equiv.) and Pd(dppf)$Cl_2$ (0.1 equiv.). The mixture was heated to 100 °C for 10 minutes in the microwave. The solid was removed via filtration and solution was partitioned between ethyl acetate and water. The solid was removed via filtration and solution was partitioned between ethyl acetate and water. The resulting organic layer was washed with saturated sodium bicarbonate solution and brine, dried over sodium sulfate, and concentrated via reduced pressure. The residue was purified using silica gel column chromatography (5% ethyl acetate/hexanes) to yield the product.

4.4.5.1. *Rac*-(1R,2R)-2-((4-decylbenzyl)(methyl)amino)cyclopentan-1-ol (**3.9b**)

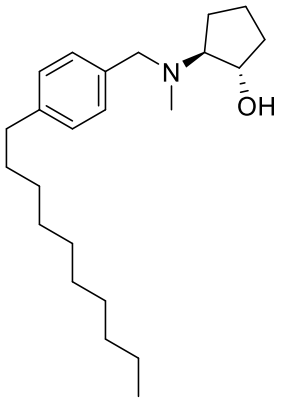


Clear oil, 35%; 1H NMR (400 MHz, Chloroform-d) δ 7.23 (d, J = 8.0 Hz, 2H), 7.12 (d, J = 8.0 Hz, 2H), 4.12 (q, J = 6.6 Hz, 1H), 3.55 (s, 2H), 2.77 (ddd, J = 8.8, 7.6, 6.3 Hz, 1H), 2.60 – 2.55 (m, 2H), 2.41 (s, 1H), 2.19 (s, 4H), 1.98 – 1.91 (m, 1H), 1.86 – 1.80 (m, 1H), 1.73 – 1.51 (m, 4H), 1.28 (d, J = 16.2 Hz, 15H), 0.92 – 0.85 (m, 3H). 13C NMR (101 MHz, cdcl3) δ 141.79, 136.49, 129.01, 128.42, 74.83, 73.45, 59.79, 38.68, 35.78, 33.17, 32.04, 31.68, 29.76, 29.73, 29.66, 29.50, 29.47, 24.72, 22.82, 20.99, 14.25. HRMS(ESI): calcd. for $C_{23}H_{40}NO+$ $[M+1]^+$ 346.3104, found: 346.3130.

4.4.5.2. *Rac*-(1S,2S)-2-(methyl(4-undecylbenzyl)amino)cyclopentan-1-ol (**3.9c**)

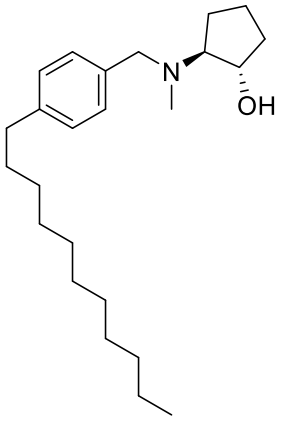


Clear oil, 21%; 1H NMR (400 MHz, Chloroform-d) δ 7.23 (d, J = 8.0 Hz, 2H), 7.12 (d, J = 8.0 Hz, 2H), 4.12 (q, J = 6.6 Hz, 1H), 3.55 (s, 2H), 2.77 (ddd, J = 8.9, 7.6, 6.4 Hz, 1H), 2.61 – 2.56 (m, 2H), 2.32 (s, 1H), 2.19 (s, 3H), 2.01 – 1.88 (m, 1H), 1.88 – 1.77 (m, 1H),

1.76 – 1.49 (m, 4H), 1.34 – 1.22 (m, 14H), 0.92 – 0.85 (m, 2H). 13C NMR (101 MHz, cdcl3) δ 141.79, 136.54, 129.00, 128.42, 74.84, 73.45, 59.80, 38.70, 35.78, 32.05, 31.69, 29.81, 29.77, 29.74, 29.66, 29.51, 29.48, 24.71, 22.82, 20.97, 14.26. HRMS(ESI): calcd. for $C_{24}H_{42}NO+$ $[M+1]^+$ 360.3261, found: 360.3233.

4.4.5.3. *Rac*-(1R,2R)-2-((4-undecylbenzyl)amino)cyclopentan-1-ol (**3.10a**)

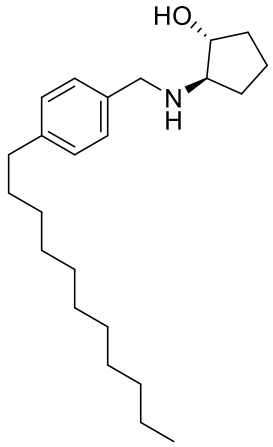


Clear oil, 5%; $^1$H NMR (400 MHz, Chloroform-d) δ 7.13 (s, 4H), 4.41 (s, 2H), 4.15 – 3.98 (m, 2H), 2.61 – 2.54 (m, 2H), 1.92 – 1.76 (m, 1H), 1.63 – 1.55 (m, 1H), 1.47 – 1.41 (m, 9H), 1.33 – 1.23 (m, 17H), 0.91 – 0.85 (m, 3H). $^{13}$C NMR (101 MHz, cdcl3) δ 141.83, 136.97, 128.70, 126.59, 80.44, 77.48, 66.68, 48.65, 35.70, 32.40, 32.05, 31.62, 29.80, 29.77, 29.73, 29.64, 29.48, 29.45, 28.56, 27.90, 22.82, 14.26. HRMS(ESI): calcd. for $C_{23}H_{40}NO+$ $[M+1]^+$ 346.3104, found: 46.3121.

4.4.5.4. *Rac*-(1R,2R)-2-((4-dodecylbenzyl)amino)cyclopentan-1-ol (**3.10b**)

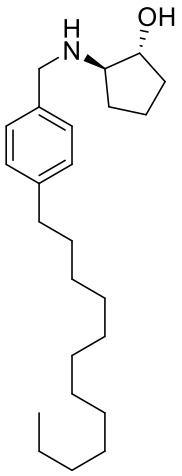


Clear oil, 8%; 1H NMR (400 MHz, Chloroform-d) δ 7.29 (d, J = 8.1 Hz, 2H), 7.17 (d, J = 8.1 Hz, 2H), 3.94 (d, J = 13.0 Hz, 1H), 3.79 (d, J = 13.0 Hz, 1H), 3.00 (td, J = 8.1, 6.4 Hz, 1H), 2.59 – 2.53 (m, 2H), 2.08 – 1.94 (m, 2H), 13C NMR (101 MHz, cdcl3) δ 143.54, 132.19, 129.23, 129.07, 76.65, 66.13, 51.53, 35.80, 32.25, 32.07, 31.55, 29.85, 29.83, 29.82, 29.79, 29.74, 29.64, 29.51, 28.32, 22.84, 20.35, 14.27. 1.78 – 1.66 (m, 2H), 1.66 – 1.49 (m, 5H), 1.33 – 1.21 (m, 16H), 0.90 – 0.86 (m, 3H). HRMS(ESI): calcd. for $C_{24}H_{42}NO+$ $[M+1]^+$ 360.3261, found: 360.3266.

4.4.6. General procedure for preparation of **3.13a-c**

Aldehyde (1 equiv.) and (R)-prolinol (1.3 equiv.) were added to a round bottom flask containing DCM/MeOH=1:1. The solution was cooled in ice bath for 5 minutes before the addition of p-toluenesulfonic acid (1 equiv.) and sodium cyanoborohydride (0.7 equiv.). The solution was further stirred at room temperature for 12-16 hours under nitrogen until TLC indicated that the starting material had been consumed. The solid was removed via filtration and solution was partitioned between ethyl acetate and water. The organic layers were washed with saturated sodium bicarbonate solution, brine and dried over sodium sulfate, and concentrated via reduced pressure. The residue was purified

using silica gel column chromatography (5% methanol/dichloromethane) to yield the product.

4.4.7. General procedure for preparation of **3.16a-m**

Epoxide reactant (1 equiv.) was dissolved in ethanol followed by addition of cyclic amine (1.5 equiv.). The resulting solution was microwaved at 80 °C for 30 min. The product didn't separate with excess amine reactant, so the mixture was directly used for cross coupling reaction. Alkene (1.3 equiv.) and 9-BBN (1.6 equiv.) were added into microwave reaction tube containing THF. The mixture was heated to 100 °C for 10 minutes in the microwave. The solution was purged with argon for 5 minutes before the addition of sodium hydroxide aqueous solution (3 equiv.) to form THF/$H_2O$=5:1 mixture. The mixture was further purged with argon for 5 minutes before the addition of aryl halide (1 equiv.) and Pd(dppf)$Cl_2$ (0.1 equiv.). The mixture was heated to 100 °C for 10 minutes in the microwave. The solid was removed via filtration and solution was partitioned between ethyl acetate and water. The solid was removed via filtration and solution was partitioned between ethyl acetate and water. The resulting organic layer was washed with saturated sodium bicarbonate solution and brine, dried over sodium sulfate, and concentrated via reduced pressure. The residue was purified using silica gel column chromatography (5% ethyl acetate/hexanes) to yield a mixture of the product and excess amine. To separate the product, boc-protection was carried out. In brief, the mixture (1 equiv.) was dissolved in DCM and $Boc_2O$ was added and the mixture was stirred for 8 h. The solution was concentrated, and the residue was purified using silica gel column chromatography (10% ethyl acetate/hexane) to yield the product.

4.4.7.1. 1-(4-dodecylphenyl)-3-(piperidin-1-yl)propan-2-ol (**3.5a**)

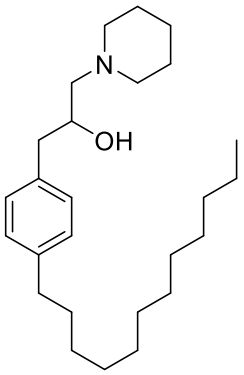


Clear oil, 11%; $^{1}$H NMR (400 MHz, Chloroform-d) δ 7.11 (d, J = 8.5 Hz, 2H), 7.08 (d, J = 8.5 Hz, 2H), 3.99 (q, J = 6.6 Hz, 1H), 2.81 (dd, J = 13.7, 6.8 Hz, 1H), 2.71–2.63 (m, 1H), 2.60 (dd, J = 13.7, 6.2 Hz, 1H), 2.56–2.52 (m, 2H), 2.47–2.36 (m, 4H), 1.64 (p, J = 4.8, 3.4 Hz, 4H), 1.59–1.50 (m, 2H), 1.45 (q, J = 5.8 Hz, 2H), 1.23 (s, 18H), 0.89–0.82 (m, 3H). 13C NMR (101 MHz, cdcl3) δ 141.13, 135.21, 129.24, 128.58, 67.21, 64.31, 54.80, 41.22, 35.72, 32.06, 31.68, 29.82, 29.81, 29.78, 29.75, 29.67, 29.52, 29.50, 25.46, 23.85, 22.84, 14.28. HRMS(ESI): calcd. for $C_{26}H_{46}NO^{+}$ $[M+1]^{+}$ 388.3574, found: 388.3598.

4.4.7.2. *Tert*-butyl 4-(3-(4-dodecylphenyl)-2-hydroxypropyl)piperazine-1-carboxylate (**3.5b**)

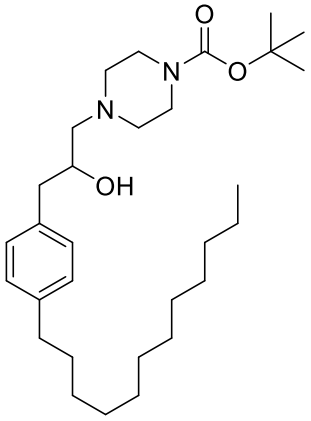


Clear oil, 22%; $^{1}$H NMR (400 MHz, Chloroform-d) δ 7.11 (d, J = 1.8 Hz, 4H), 4.01–3.90 (m, 1H), 3.46 (q, J = 3.8 Hz, 4H), 2.80 (dd, J = 13.7, 6.9 Hz, 1H), 2.70–2.53 (m, 5H),

2.46–2.32 (m, 4H), 1.58 (p, J = 7.1 Hz, 2H), 1.45 (s, 9H), 1.25 (s, 18H), 0.91–0.83 (m, 3H). 13C NMR (101 MHz, $CDCl_3$) δ 154.74, 141.23, 135.08, 129.26, 128.61, 80.02, 67.41, 63.78, 53.16, 41.02, 35.73, 32.07, 31.69, 29.82, 29.79, 29.75, 29.68, 29.53, 29.50, 28.53, 22.84, 14.29. HRMS(ESI): calcd. for $C_{20}H_{53}N_2O_3$+ $[M+1]^+$ 489.4051, found: 489.4033.

4.4.7.3. 1-(4-dodecylphenyl)-3-morpholinopropan-2-ol (**3.5c**)

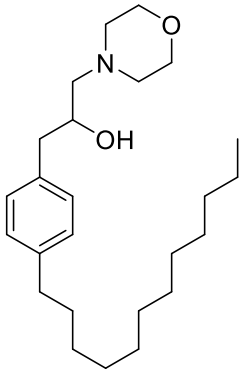


Clear oil, 13%; $^1$H NMR (400 MHz, Chloroform-d) δ 7.13 (d, J = 8.5 Hz, 2H), 7.10 (d, J = 8.5 Hz, 2H), 3.92 (dddd, J = 10.5, 7.0, 5.7, 3.5 Hz, 1H), 3.75–3.64 (m, 4H), 2.80 (dd, J = 13.7, 7.0 Hz, 1H), 2.68–2.59 (m, 3H), 2.59–2.54 (m, 2H), 2.42–2.28 (m, 4H), 1.59 (dq, J = 9.7, 7.2 Hz, 2H), 1.37–1.21 (m, 18H), 0.93–0.83 (m, 3H). 13C NMR (101 MHz, cdcl3) δ 141.12, 135.26, 129.27, 128.56, 67.15, 64.16, 53.74, 41.01, 35.73, 32.06, 31.69, 22.84, 14.28. HRMS(ESI): calcd. for $C_{25}H_{44}NO_2$+ $[M+1]^+$ 390.3367, found: 390.3352.

4.4.7.4. 1-(4-dodecylphenyl)-3-(4-methylpiperazin-1-yl)propan-2-ol (**3.5d**)

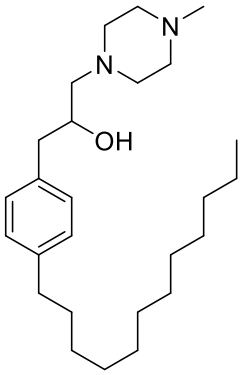


Clear oil, 16%; $^{1}$H NMR (400 MHz, Chloroform-d) δ 7.13 (d, J = 8.3 Hz, 2H), 7.10 (d, J = 8.3 Hz, 2H), 3.95 – 3.86 (m, 1H), 2.78 (dd, J = 13.7, 7.0 Hz, 1H), 2.65 (dt, J = 13.7, 6.0 Hz, 4H), 2.56 (dd, J = 8.9, 6.7 Hz, 2H), 2.51 – 2.33 (m, 6H), 2.30 (s, 3H), 1.57 (q, J = 7.4 Hz, 2H), 1.25 (s, 18H), 0.88 (t, J = 6.7 Hz, 3H). 13C NMR (101 MHz, CDCl3) δ 141.07, 135.35, 129.26, 128.54, 67.41, 63.50, 55.22, 46.02, 41.08, 35.73, 32.06, 31.68, 29.82, 29.78, 29.74, 29.67, 29.53, 29.50, 22.84, 14.28. HRMS(ESI): calcd. for $C_{26}H_{47}N_2O^+$ $[M+1]^+$ 403.3683, found: 403.3689.

4.4.7.5. *Tert*-butyl (1-(3-(4-dodecylphenyl)-2-hydroxypropyl)piperidin-4-yl)carbamate (**3.16e**)

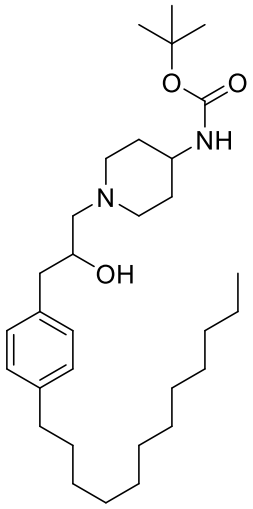

Clear oil, 10%; $^{1}$H NMR (400 MHz, Chloroform-*d*) δ 7.09 (d, *J* = 2.1 Hz, 4H), 4.48–4.39 (m, 1H), 3.95–3.87 (m, 1H), 3.45 (s, 1H), 2.98–2.90 (m, 1H), 2.78 (dd, *J* = 13.7, 6.9 Hz, 2H), 2.64–2.51 (m, 3H), 2.43–2.31 (m, 3H), 2.04 (t, *J* = 11.5 Hz, 1H), 1.91 (d, *J* = 12.5 Hz, 2H), 1.55 (dt, *J* = 9.5, 6.3 Hz, 2H), 1.41 (s, 9H), 1.31–1.21 (m, 18H), 0.86 (t, *J* = 6.8 Hz, 3H). $^{13}$C NMR (101 M Hz, $cdcl_3$) δ 155.12, 140.97, 135.06, 129.08, 128.41, 79.33, 67.38, 63.44, 53.92, 51.06, 47.37, 40.96, 35.57, 32.55, 32.23, 31.90, 31.53, 29.66, 29.62, 29.59, 29.51, 29.37, 29.34, 28.37, 22.68, 14.13. HRMS(ESI): calcd. for $C_{30}H_{53}N_2O_3$+ $[M+1]^+$ 489.4051, found: 489.4078.

4.4.7.6. 1-(4-dodecylphenyl)-3-(pyrrolidin-1-yl)propan-2-ol (**3.5h**)

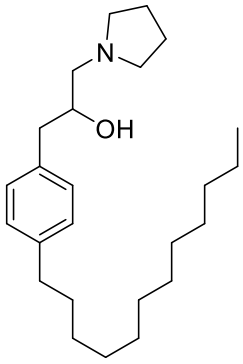


Clear oil, 21%; $^{1}$H NMR (400 MHz, Chloroform-d) δ 7.11 (s, 4H), 4.22 (ddt, J = 9.1, 6.6, 3.4 Hz, 1H), 3.18–3.05 (m, 2H), 3.00–2.86 (m, 4H), 2.78–2.62 (m, 1H), 2.59–2.52 (m, 1H), 2.01–1.95 (m, 2H), 1.62–1.53 (m, 4H), 1.35–1.20 (m, 18H), 0.87 (t, 3H). 13C NMR (101 MHz, cdcl3) δ 141.60, 134.33, 129.28, 128.83, 68.63, 61.85, 54.79, 41.26, 35.72, 32.07, 31.66, 29.83, 23.46, 22.85, 14.29; HRMS(ESI): calcd. for $C_{25}H_{44}NO$+ $[M+1]^+$ 374.3417, found: 374.3398.

4.4.7.7. 1-(4-dodecylphenyl)-3-((R)-2-(hydroxymethyl)pyrrolidin-1-yl)propan-2-ol (**3.5j**)

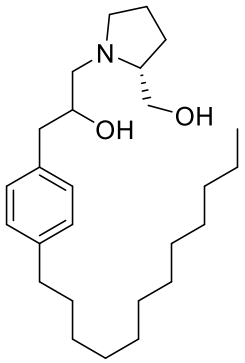


Clear oil, 33%; $^{1}$H NMR (400 MHz, Chloroform-*d*) δ 7.11 (s, 4H), 4.22 (q, *J* = 7.8 Hz, 1H), 3.90 (dd, *J* = 12.7, 3.2 Hz, 1H), 3.78 (dd, *J* = 12.8, 6.0 Hz, 1H), 3.74–3.63 (m, 1H), 3.37–3.28 (m, 1H), 3.21 (dd, *J* = 12.7, 10.0 Hz, 1H), 2.93 (dd, *J* = 13.8, 6.7 Hz, 1H), 2.83–2.76 (m, 1H), 2.68 (dd, *J* = 13.8, 7.1 Hz, 1H), 2.61–2.52 (m, 3H), 2.06–1.96 (m, 2H), 1.91 (dt, *J* = 12.7, 6.1 Hz, 2H), 1.57 (q, *J* = 7.4 Hz, 2H), 1.25 (s, 18H), 0.90–0.85 (m, 3H). $^{13}$C NMR (101 MHz, cdcl$_3$) δ 141.52, 134.00, 129.09, 128.72, 77.19, 68.58, 62.41, 61.16, 55.27, 40.94, 35.55, 31.90, 31.49, 29.66, 29.62, 29.60, 29.51, 29.35, 29.34, 26.47, 23.52, 22.68, 14.12. HRMS(ESI): calcd. for $C_{26}H_{46}NO_2$+ $[M+1]^+$ 404.3523, found: 404.3536.

4.4.8. General procedure for preparation of **3.1a-d**, **3.14a-c** and **3.17**

Amine (1 equiv.) was dissolved in MeOH. HCl gas was purged into the solution for 1 minute. The solution was stirred for 5-10 minutes until TLC indicated that the starting material had been consumed. The solvent was removed via reduced pressure. The resulting white to brown oil or solid was washed with diethyl ether to yield pure product.

4.5. Biological evaluation procedures

4.5.1. SphK broken-cell assay

The inhibitory effects of the synthesized compounds were investigated using a previously reported broken-cell assay[1]. Recombinant human SphK1 and SphK2 were

isolated from SF9 cells expressing respective plasmid DNAs. SphK activity was measured in kinase buffer that consisted of 20 mM Tris-Cl (pH 7.4), 1 mM 2-mercaptoethanol, 1 mM EDTA, 5 mM sodium orthovanadate, 40 mM β-glycerophosphate, 15 mM NaF, 1 mM phenylmethylsulfonyl fluoride, 10 mM $MgCl_2$, 0.5 mM 4-deoxypyridoxine, 10% glycerol, and 0.1 mg/ml each leupeptin, aprotinin, and soybean trypsin inhibitor. For SphK2 activity, the buffer was supplemented with 1 M KCl. The buffer was supplemented with substrate (D-erythro-sphingosine, 5-10 μM; 1 μM FTY720, with or without inhibitors), [γ-$^{32}$P]ATP (10 μM, specific activity=8.3 Ci/mmol), and cell or tissue extract (0.02–0.03 mg of total protein). After 30 min at 37 °C, the reaction mixture was stopped on ice. One eighth of kinase reaction content was spotted on labeled P81 phosphocellulose paper. P81 paper was washed 3 times with 75 mM orthophosphoric acid followed by soaking in acetone for 2 minutes. Dried P81 paper was placed in a 7 ml scintillation vial and add 5 ml of scintillation fluid and counted in a liquid scintillation counter. SphK activity was determined by the amount of $\gamma$-[$^{32}$P]-S1P as a function of inhibitor concentration. Inhibitors were assayed at 1 μM for human SphK1 and 0.3 μM for human SphK2.

4.5.2. SphK yeast-cell assay

The $EC_{50}$ values of selected compounds were determined using a previous reported hSphK recombinant yeast assay[2]. Yeast strains containing plasmids *pGAL-HsSPHK1* and *pGAL-HsSPHK2* were used to measure the $EC_{50}$ values as described. Briefly, yeast harboring SphK plasmids were cultured in synthetic complete media lacking uracil (SC-URA) with 2% glucose as the fermentable carbon source. After overnight growth at 30°C in this media, the cultures were diluted 1:100 into SC-URA

media supplemented with 2% galactose and inhibitors at concentration of 0.005-3 μM. After a further 24–48 hours' incubation at 30°C, the extent of growth was assessed by measuring absorbance at 600 nm, and $EC_{50}$ values were calculated from the concentration-absorbance diagram.

4.5.3. U937 cell culture assay

U937 cells were grown in RPMI 1640 media supplemented with (*L*)-glutamate, 10% fetal bovine serum (FBS) and 1% penicillin/streptomycin at 37 °C in an atmosphere containing 5% $CO_2$. Twenty-four hours before adding inhibitors, the growth media was replaced with media containing 0.5% FBS. Cells were treated with compound **14a** for 2 hours before being harvested and lipids were extracted for LC/MS analysis as described previously.

4.5.4. Mouse study

C57BL/6j mice (6-8 weeks old, n=4-6, male) were injected i.p. with vehicle (2% solution of hydroxypropyl-β-cyclodextrin; Cargill Cavitron 82004; Cargill Inc., Cedar Rapids, IA) or 10 mg/kg control compound or compound **14a.** After 3 hours, blood was collected, and plasma was isolated and processed for LC/MS analysis as described below. The use of mice for these studies was approved by the University of Virginia's School of Medicine Animal Care and Use Committee.

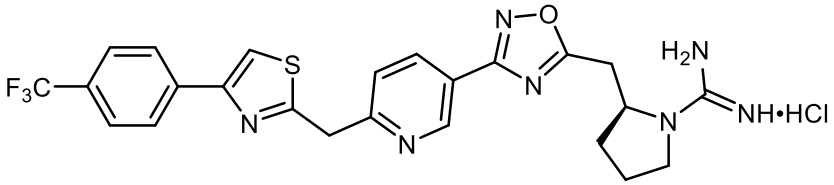


**SLC4101553**
SphK activity: 91% for SphK1 (1 μM)
53% for SphK2 (0.3 μM)

Figure: Structure and inhibition data of **SLC4101553**

4.5.5. LC/MS sample preparation and analysis

LC/MS sample preparation and analysis were carried out as described previously.[3] Cell pellets ($2 \times 10^6$ to $4 \times 10^6$ cells) or plasma blood (10 μl) were mixed with 2 ml of methanol/chloroform (3:1) and transferred to a capped glass vial. 10 μl of an internal standard solution containing 10 pmol of deuterated (D7) $C_{18}$-S1P was added in each sample. Mixtures were briefly sonicated and incubated at 48°C for 16 hours. For saponification, 200 μl of 1 M KOH in methanol was added in each sample and incubated for further 2 hours at 37°C. Samples were neutralized by the addition of 20 μl of glacial acetic acid, transferred to 2-ml microcentrifuge tubes, and centrifuged at 12,000g for 12 minutes. The supernatant fluid was collected in a separate glass vial and evaporated under a stream of nitrogen gas. Immediately prior to LC/MS analysis, the dried material was dissolved in 0.3 ml of methanol and centrifuged at 12,000*g* for 12 minutes. 150 microliters of the resulting supernatant fluid were analyzed by LC/MS.

Analyses were performed by LC-MS using a triple quadrupole mass spectrometer (AB-Sciex 4000 Q-Trap) coupled to a Shimadzu LC-20AD LC system). The following analytes were monitored using MRM (multiple reaction monitoring) for S1P (380.4, 264.4) anf D7-S1P (387.4, 271.3).

4.6. References

1. Kharel, Y.; Mathews, T. P.; Kennedy, A. J.; Houck, J. D.; Macdonald, T. L.; Lynch, K. R., A rapid assay for assessment of sphingosine kinase inhibitors and substrates. *Anal. Rev. Biochem.* **2011,** *411* (2), 230-5.
2. Kharel, Y.; Agah, S.; Huang, T.; Mendelson, A. J.; Eletu, O. T.; Barkey-Bircann, P.; Gesualdi, J.; Smith, J. S.; Santos, W. L.; Lynch, K. R., Saccharomyces cerevisiae as a platform for assessing sphingolipid lipid kinase inhibitors. *PLoS One* **2018,** *13* (4), e0192179.
3. Kharel, Y.; Mathews, T. P.; Gellett, A. M.; Tomsig, J. L.; Kennedy, P. C.; Moyer, M. L.; Macdonald, T. L.; Lynch, K. R., Sphingosine kinase type 1 inhibition reveals rapid turnover of circulating sphingosine 1-phosphate. *Biochem. J.* **2011,** *440* (3), 345-53.

# Appendix A NMR Spectra for Chapter 2

$^{1}H$ and $^{13}C$ spectra of 4-(heptyloxy)benzaldehyde (**2.2a**)

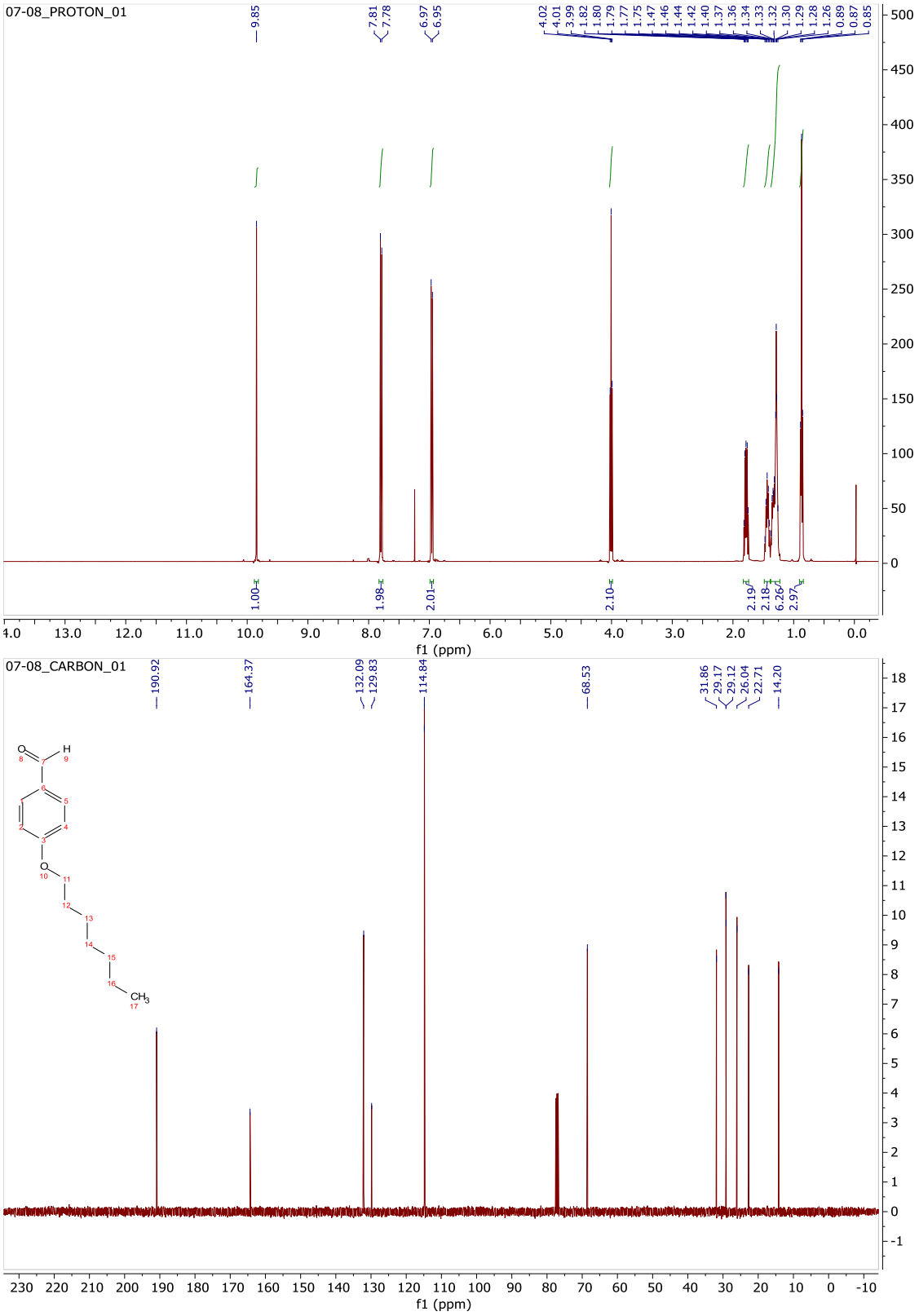

$^{1}H$ and $^{13}C$ spectra of 4-(octyloxy)benzaldehyde (**2.2b**)

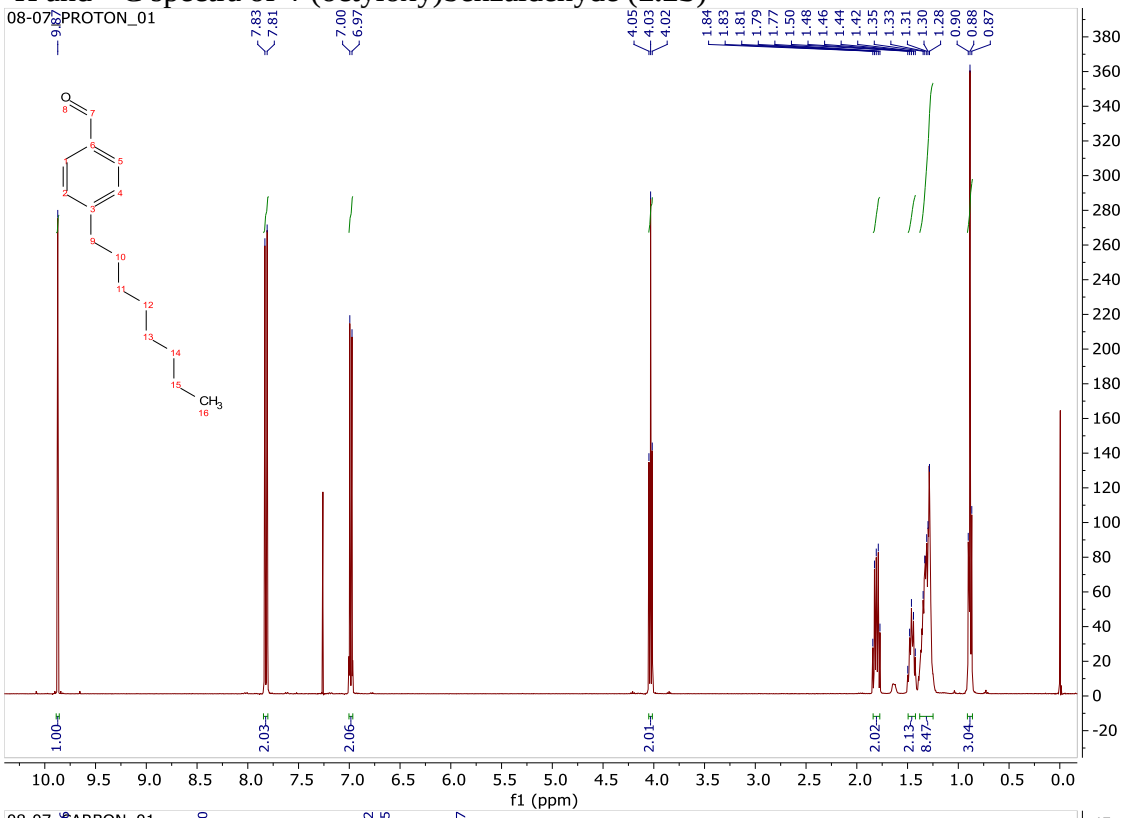


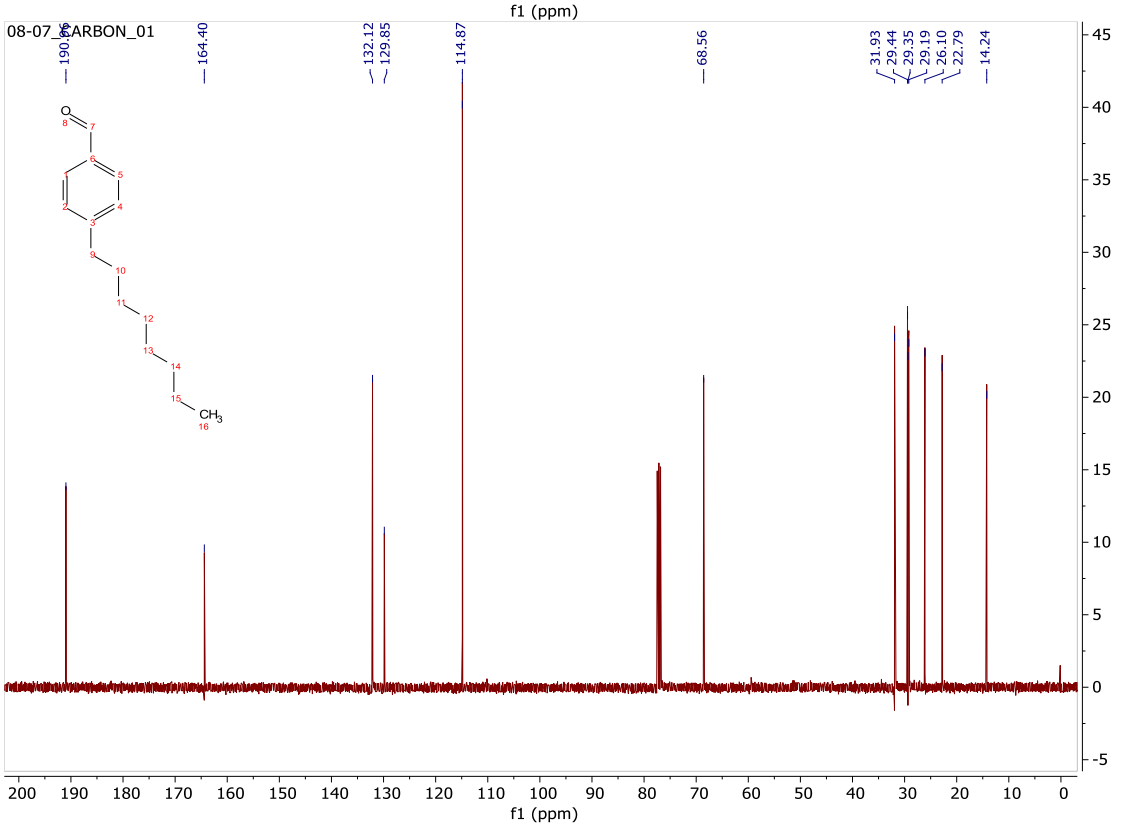

$^{1}H$ and $^{13}C$ spectra of 4-(nonyloxy)benzaldehyde (**2.2c**)

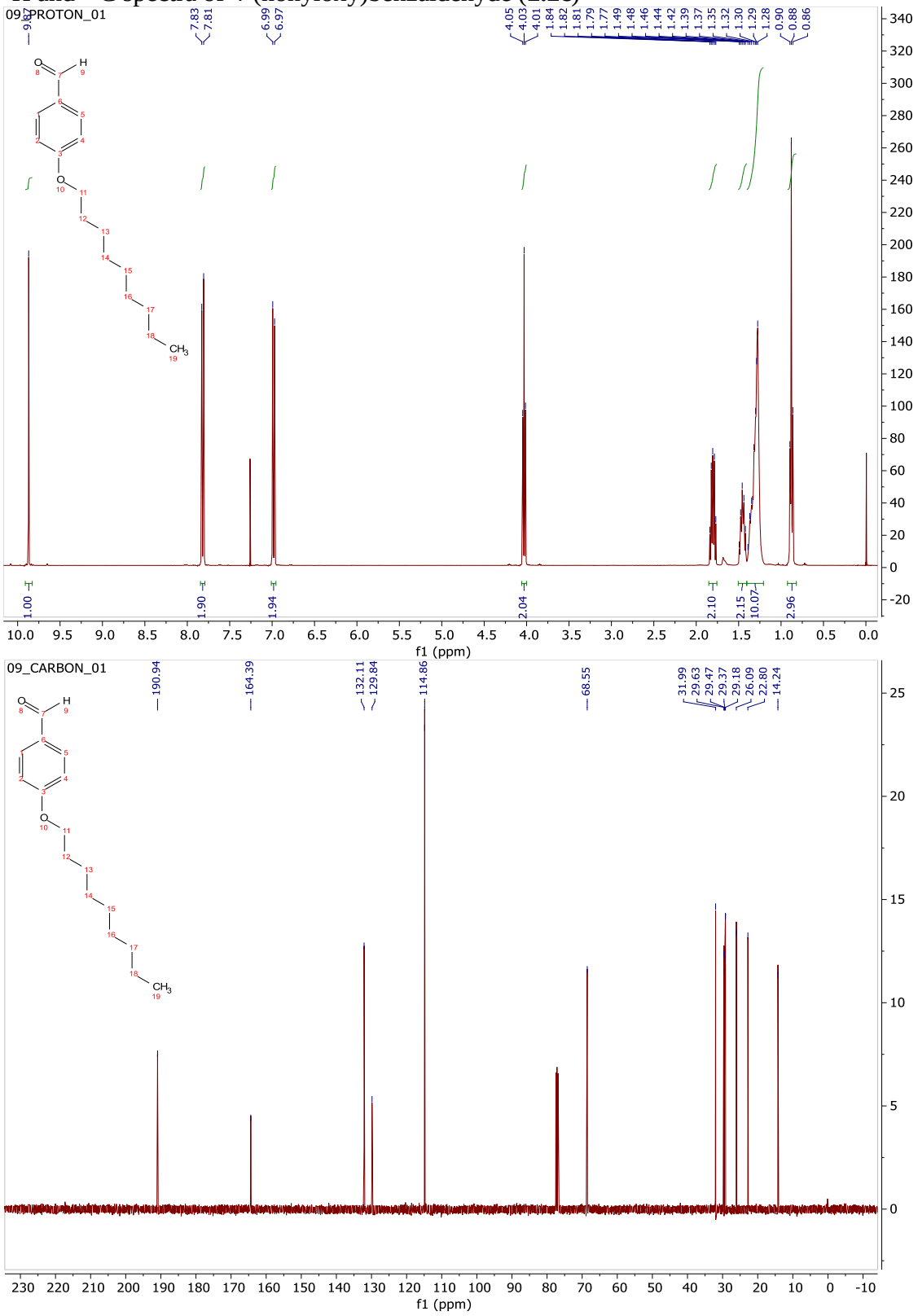

$^{1}H$ and $^{13}C$ spectra of 4-(decyloxy)benzaldehyde(**2.2d**)

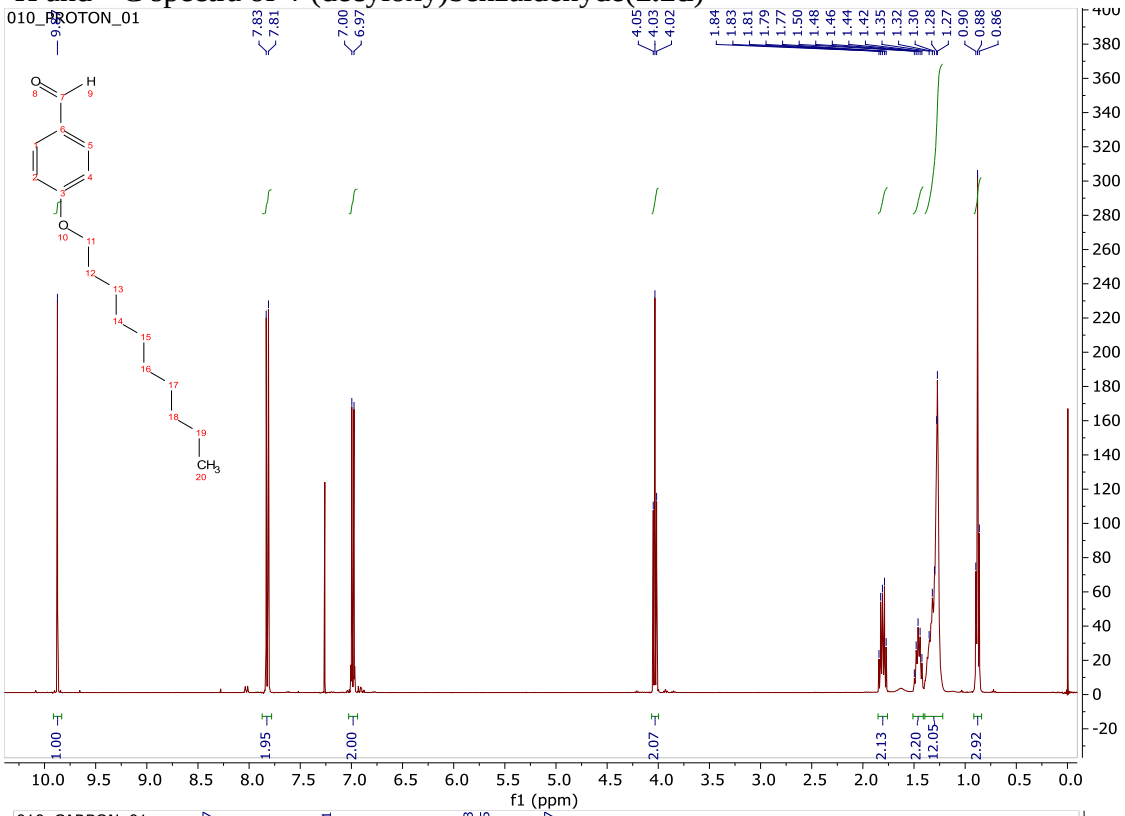


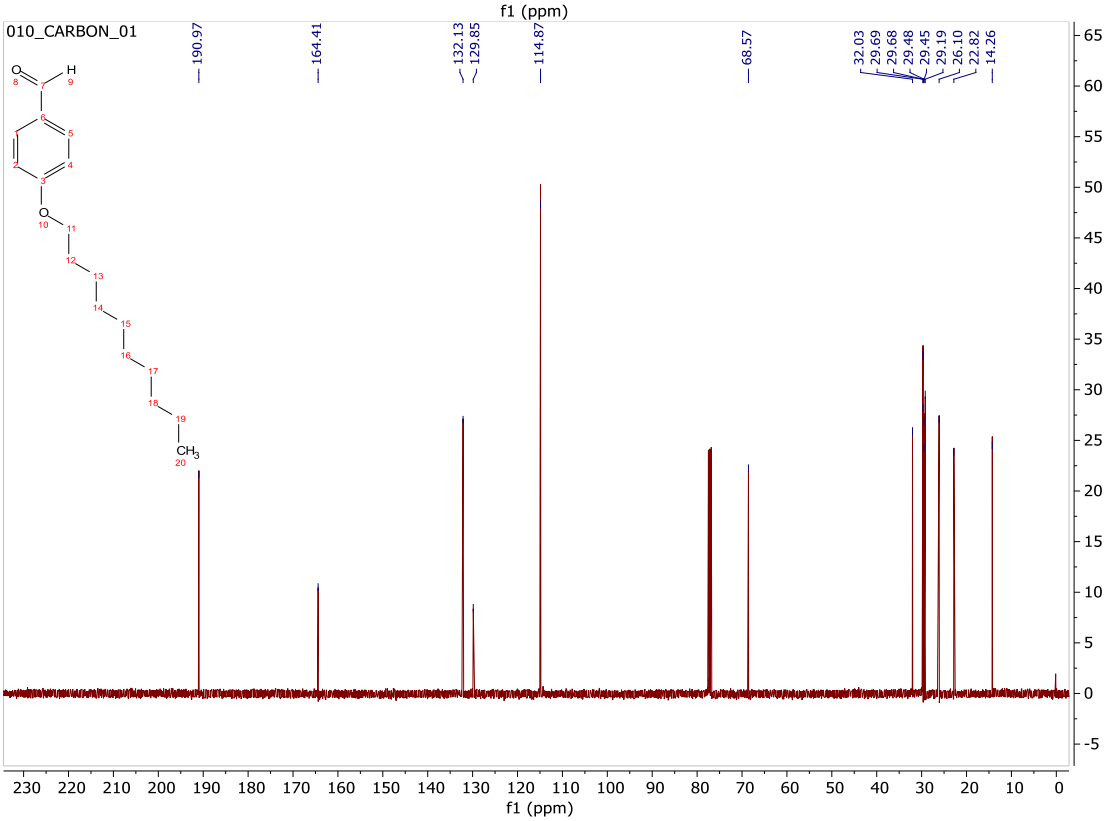

$^{1}H$ and $^{13}C$ spectra of 4-((4-(trifluoromethyl)benzyl)oxy)benzaldehyde (**2.2e**)

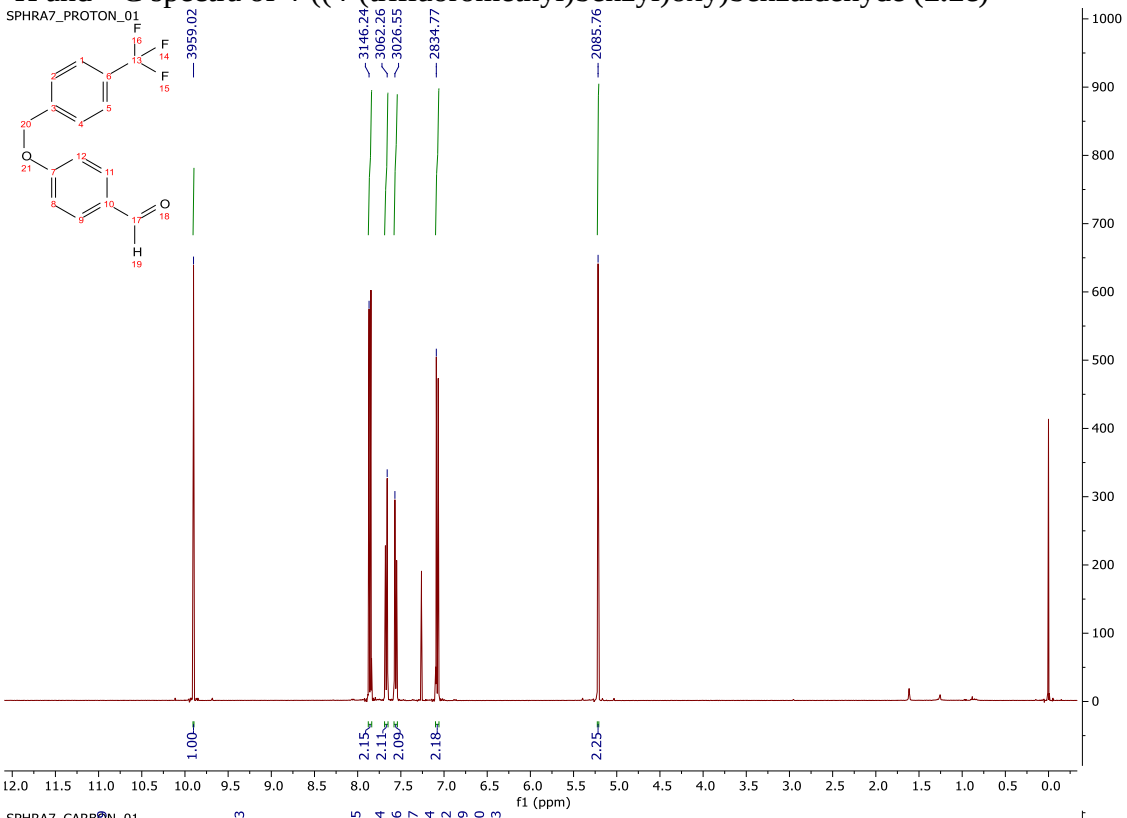


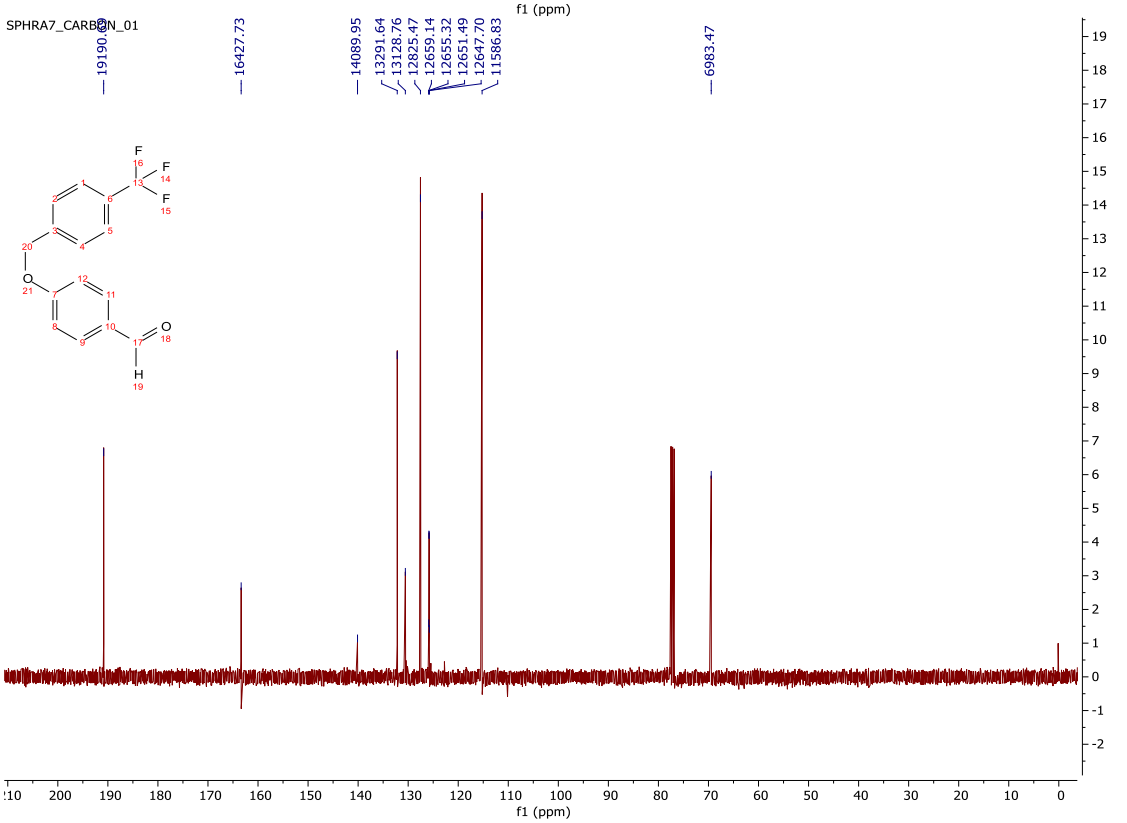

$^{1}H$ and $^{13}C$ spectra of (R)-(1-(4-(heptyloxy)benzyl)pyrrolidin-2-yl)methanol (**2.3a**)

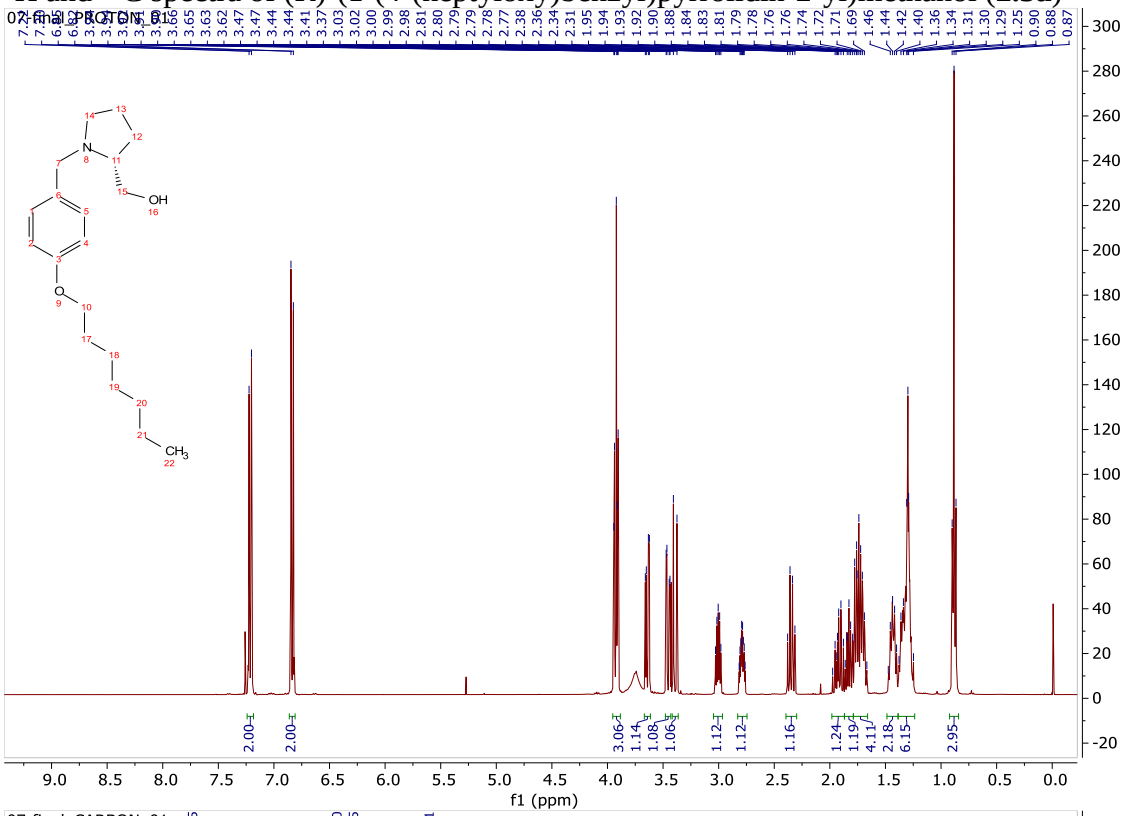


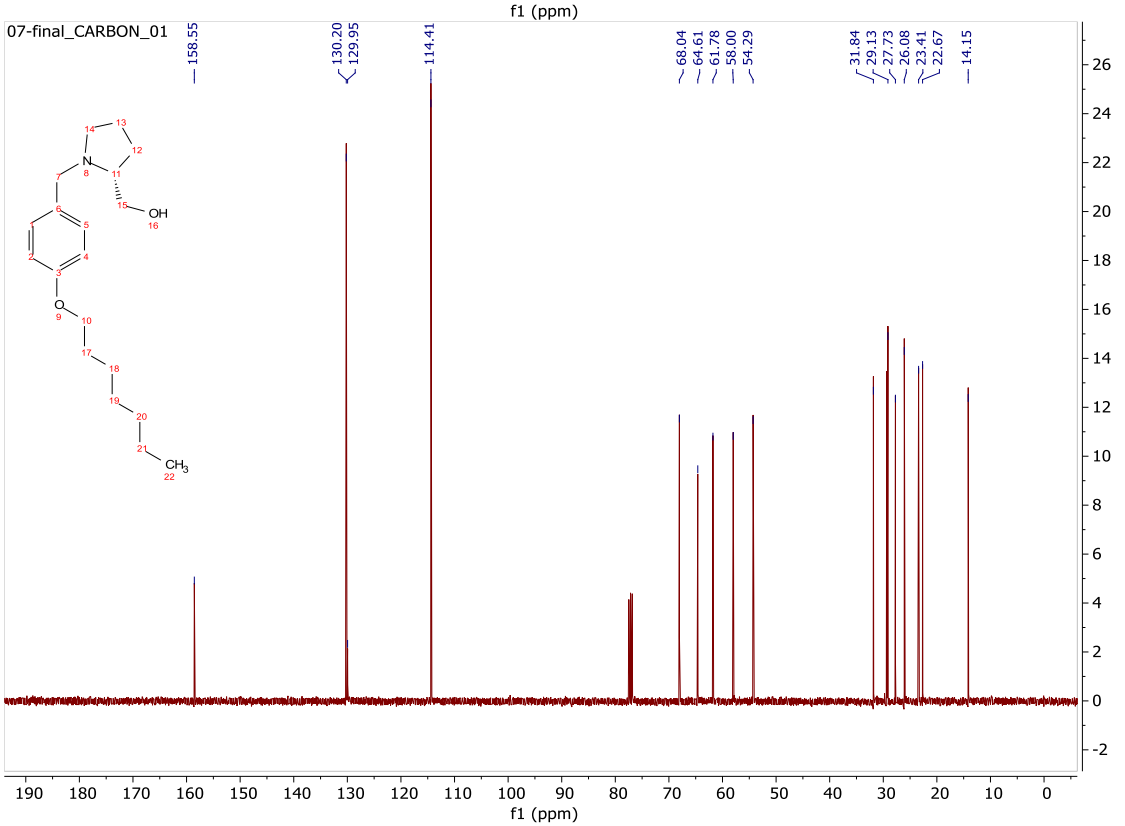

$^{1}H$ and $^{13}C$ spectra of (R)-(1-(4-(octyloxy)benzyl)pyrrolidin-2-yl)methanol (**2.3b**)

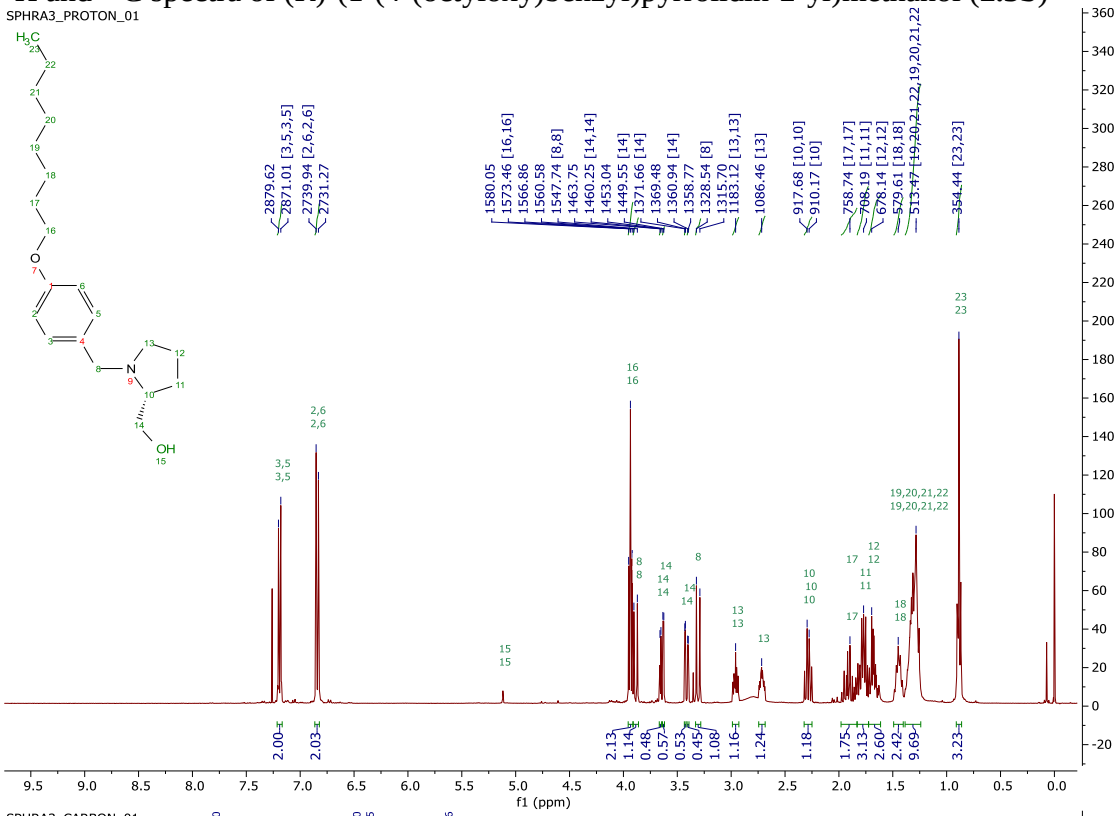


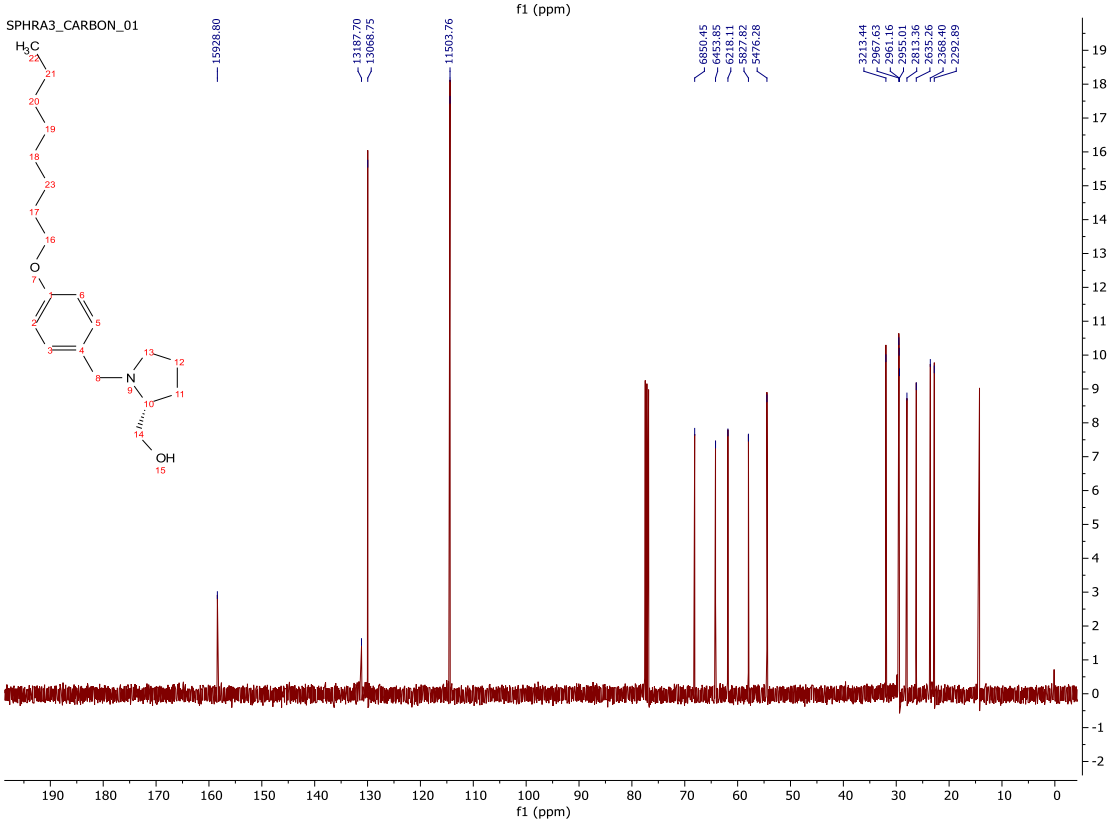

$^{1}H$ and $^{13}C$ spectra of (R)-(1-(4-(nonyloxy)benzyl)pyrrolidin-2-yl)methanol (**2.3c**)

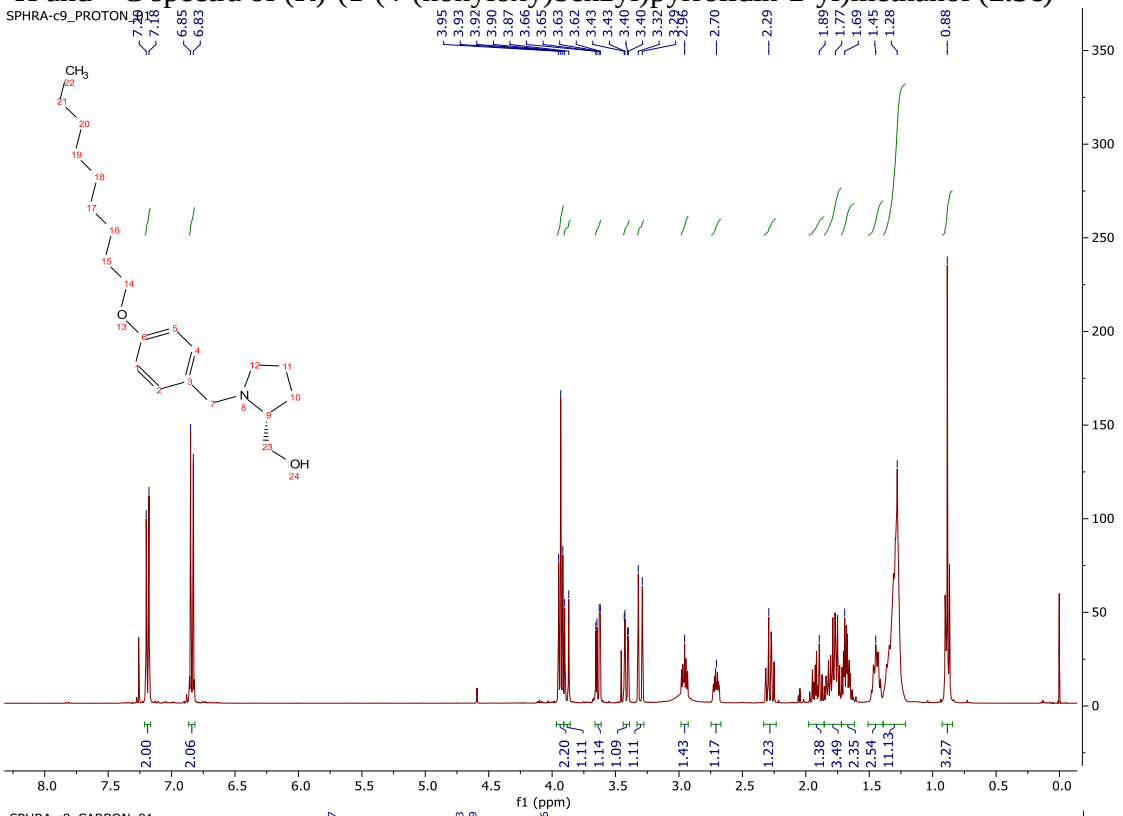


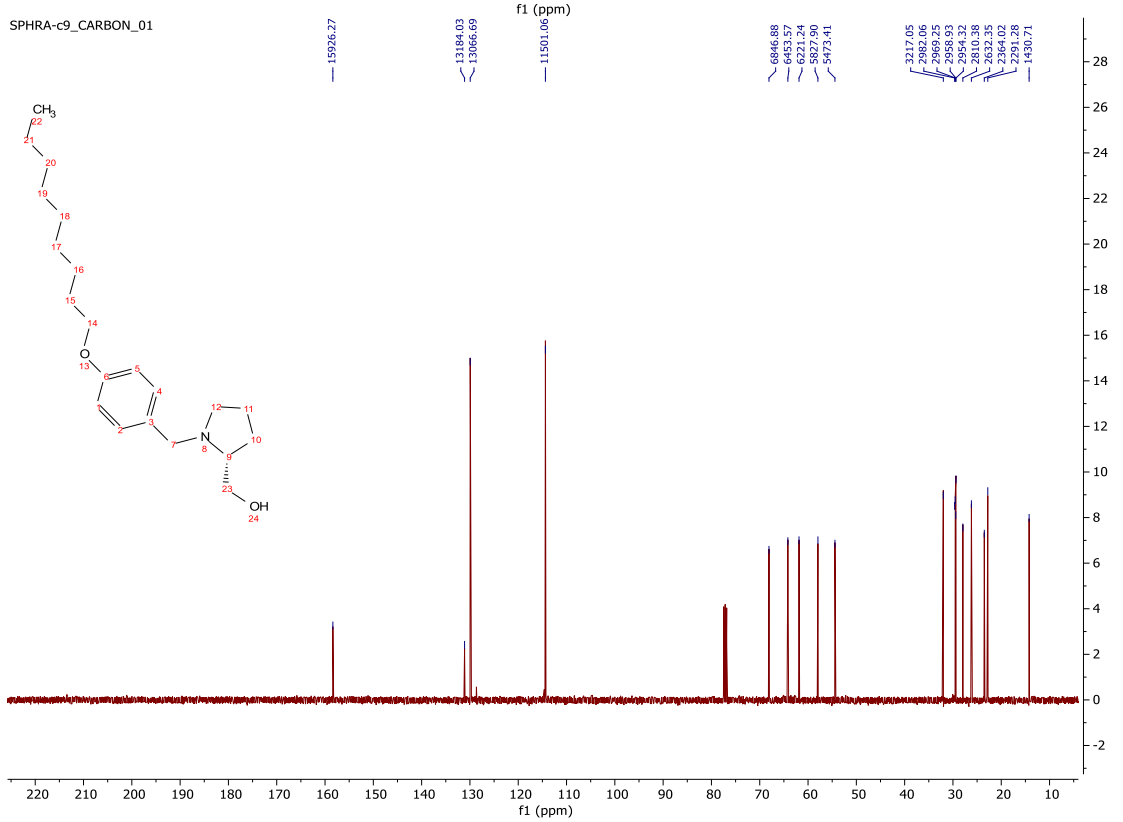

$^{1}H$ and $^{13}C$ spectra of (R)-(1-(4-(docyloxy)benzyl)pyrrolidin-2-yl)methanol (**2.3d**)

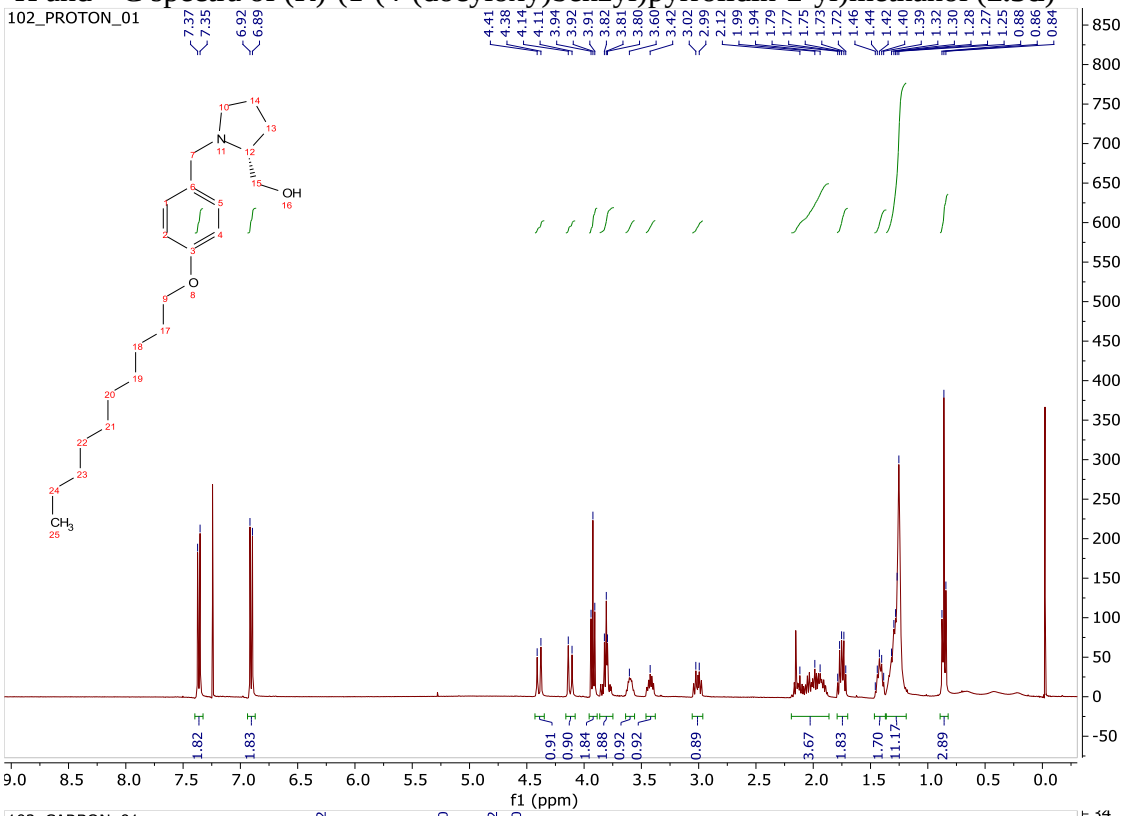


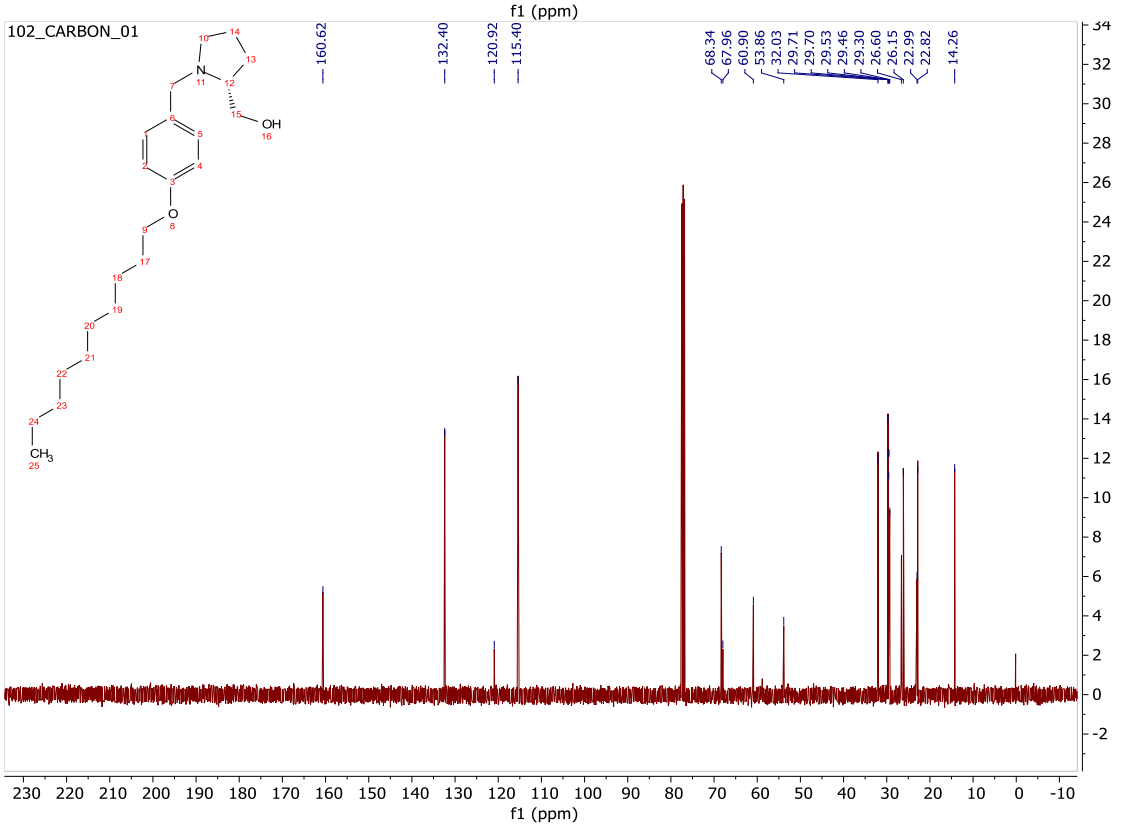

$^{1}H$ and $^{13}C$ spectra of 4-phenoxybenzonitrile(**2.6a**)

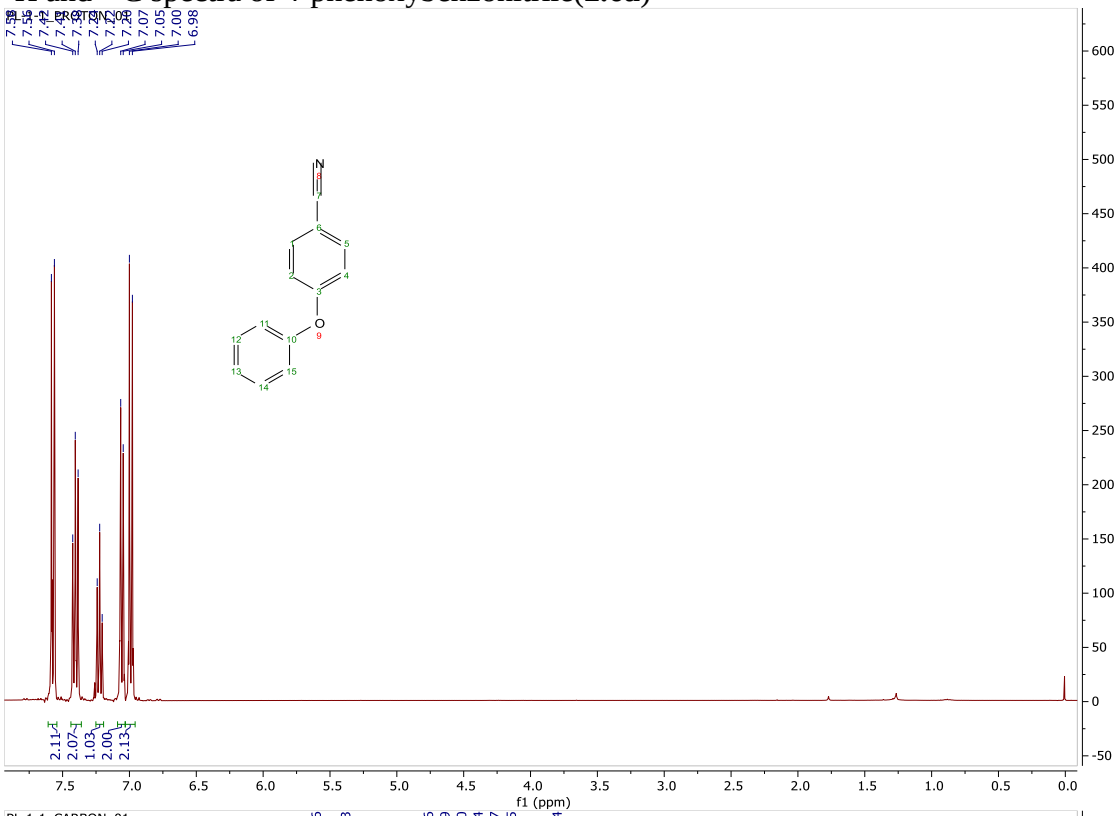


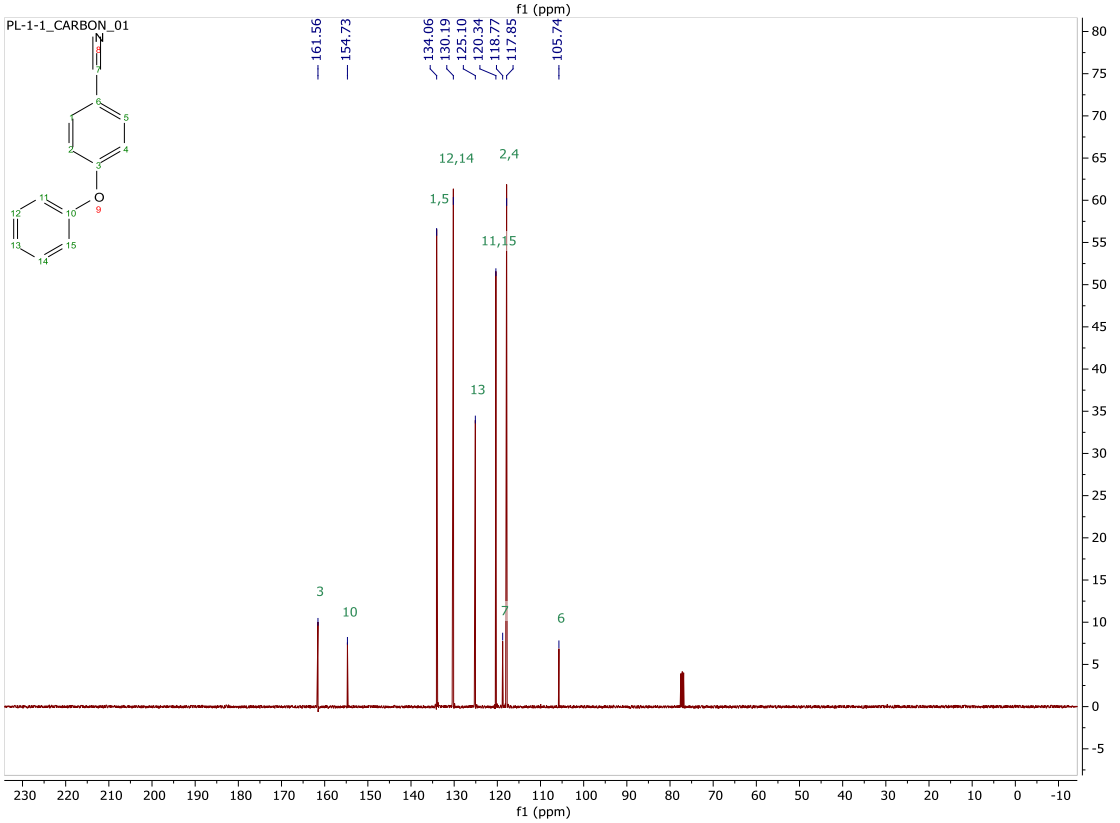

$^{1}H$ and $^{13}C$ spectra of 4-(3-(tert-butyl)phenoxy)benzonitrile(**2.6b**)

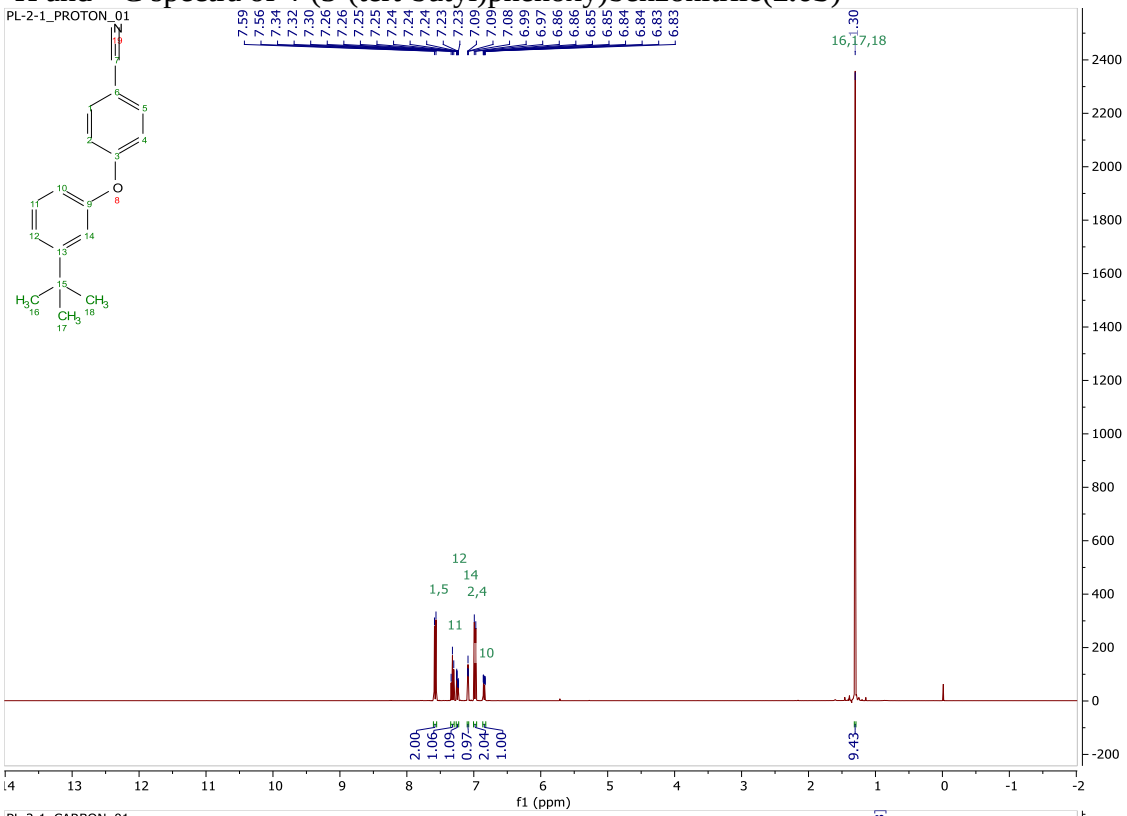


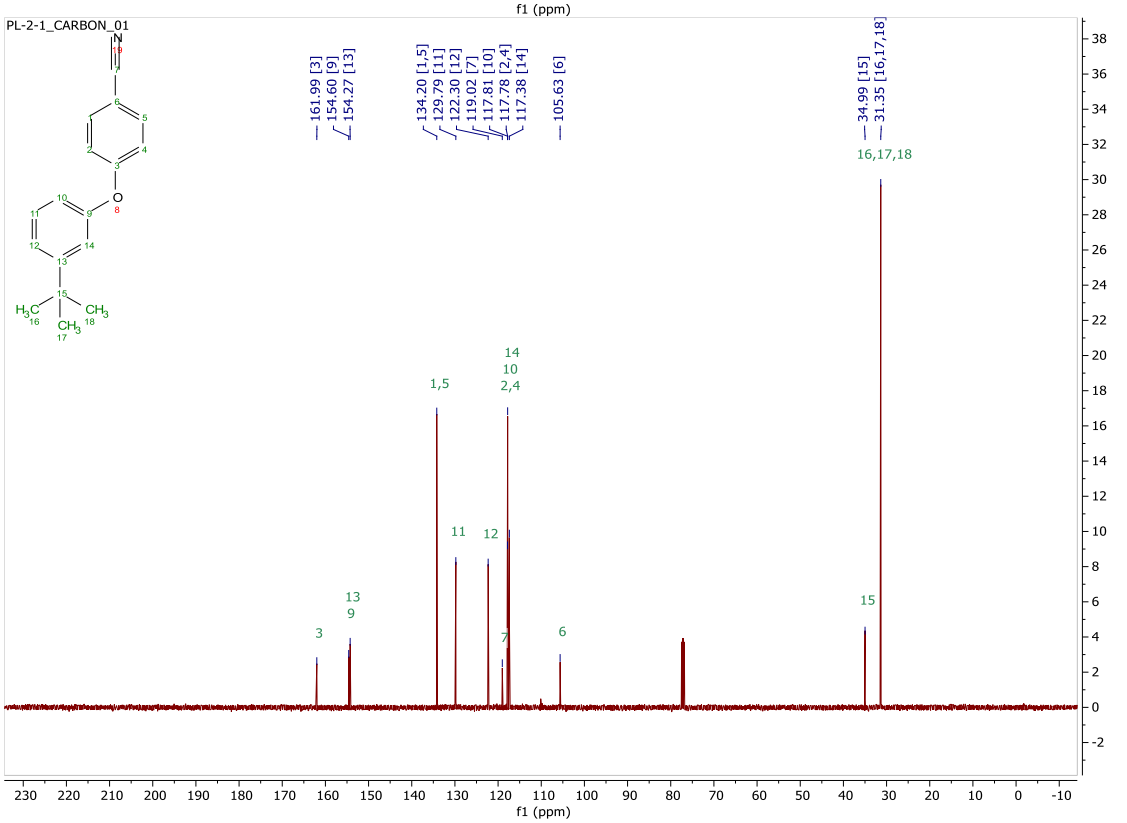

$^{1}H$ and $^{13}C$ spectra of 4-(4-(tert-butyl)phenoxy)benzonitrile(**2.6c**)

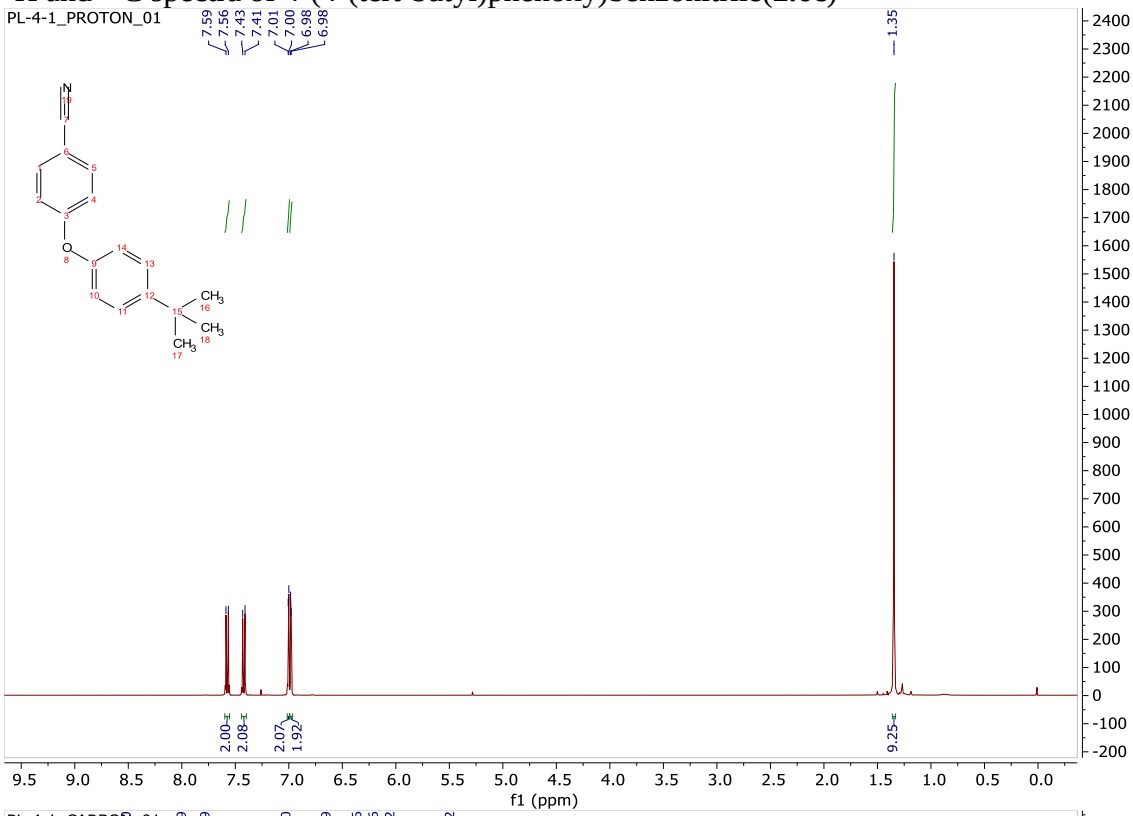


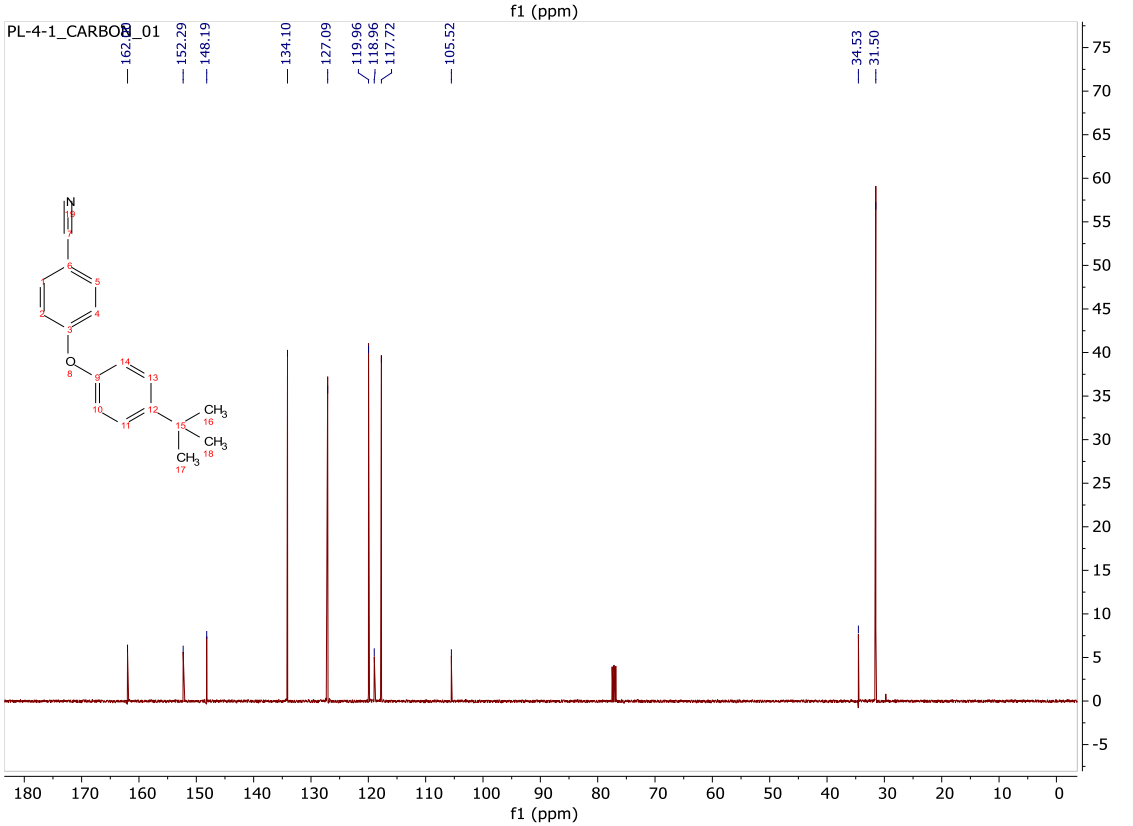

$^{1}H$ and $^{13}C$ spectra of 4-(3-bromophenoxy)benzonitrile(**2.6d**)

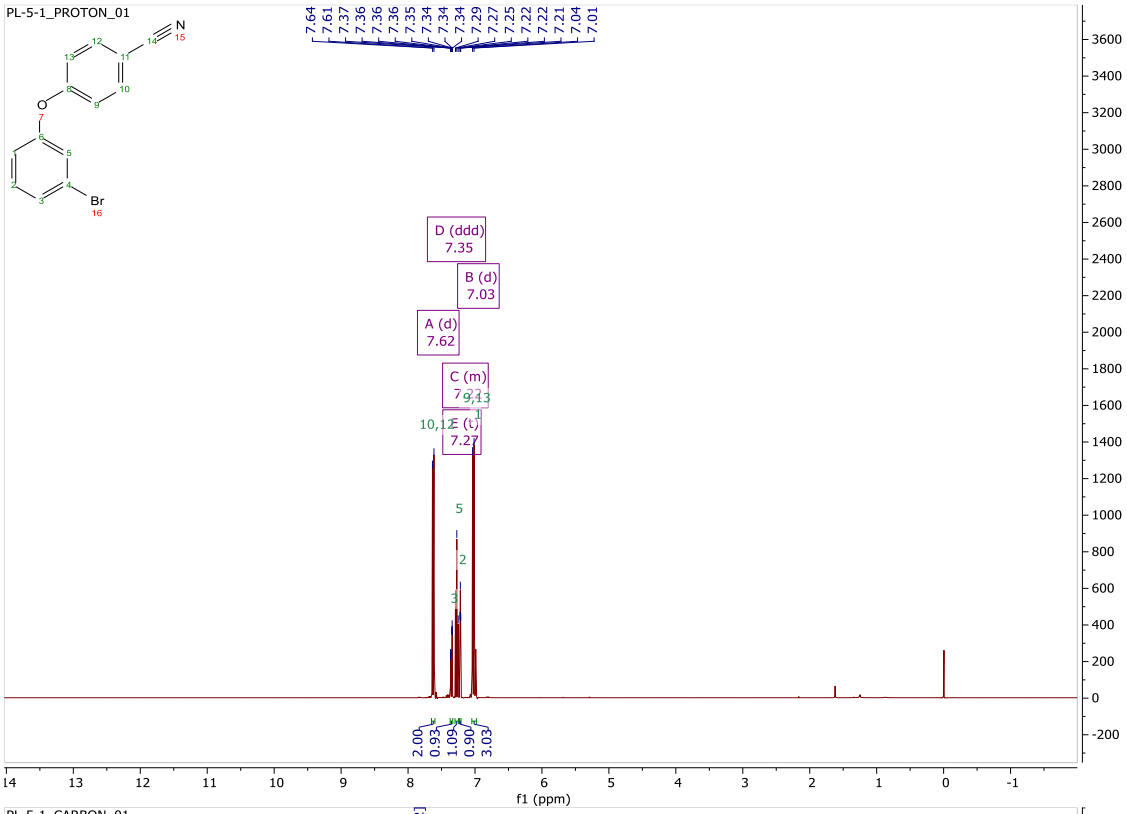


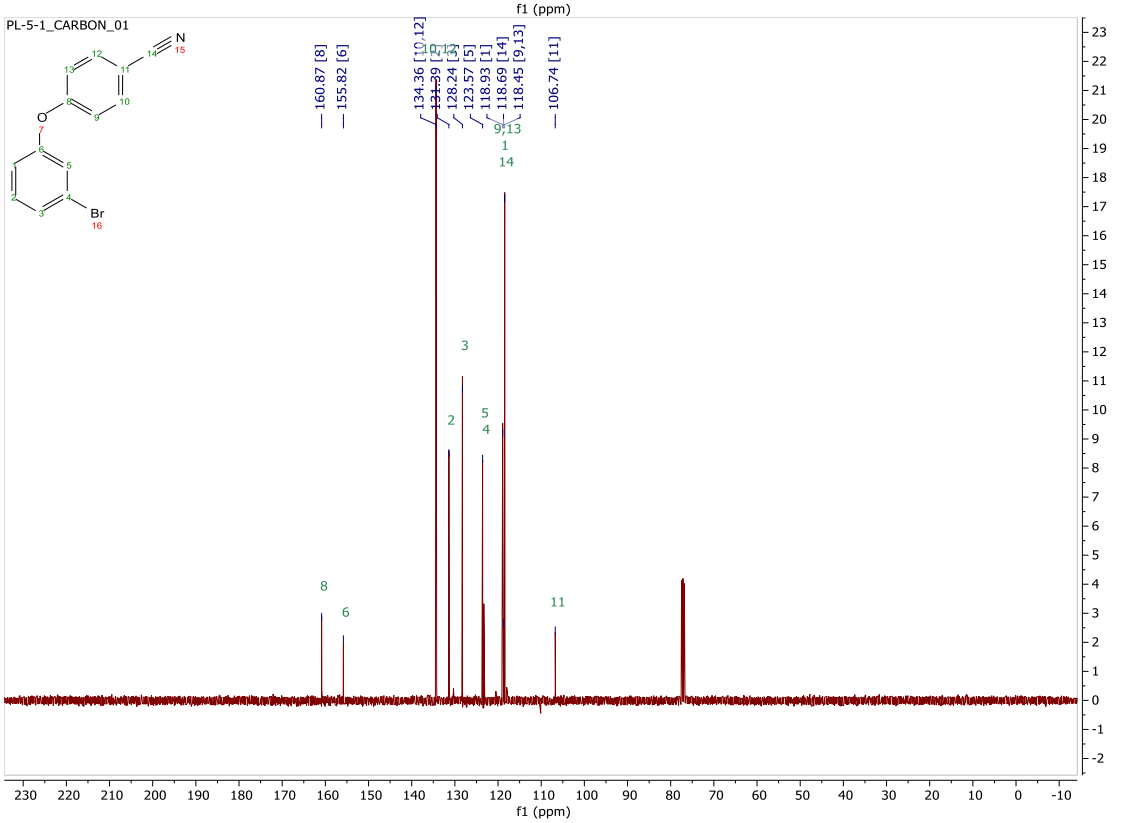

$^{1}H$ and $^{13}C$ spectra of 4-(4-iodophenoxy)benzonitrile(**2.6e**)

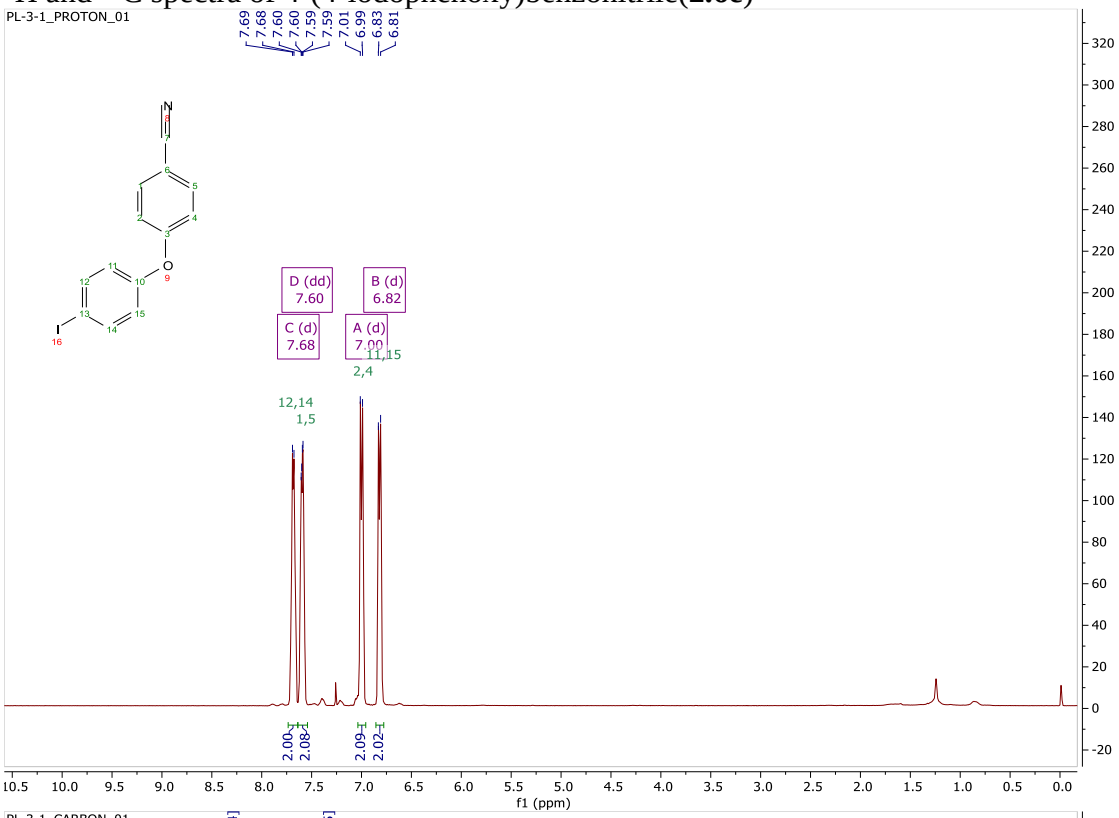


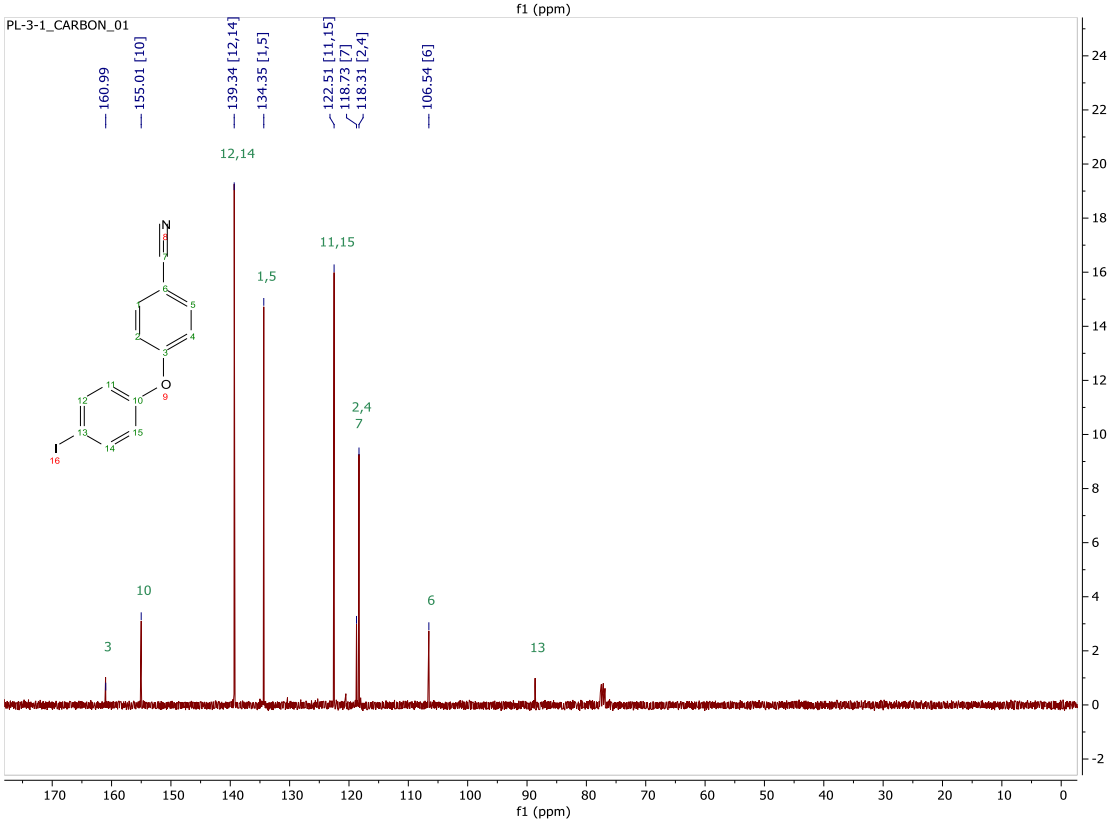

$^{1}H$ and $^{13}C$ spectra of 4-phenoxybenzaldehyde(**2.7a**)

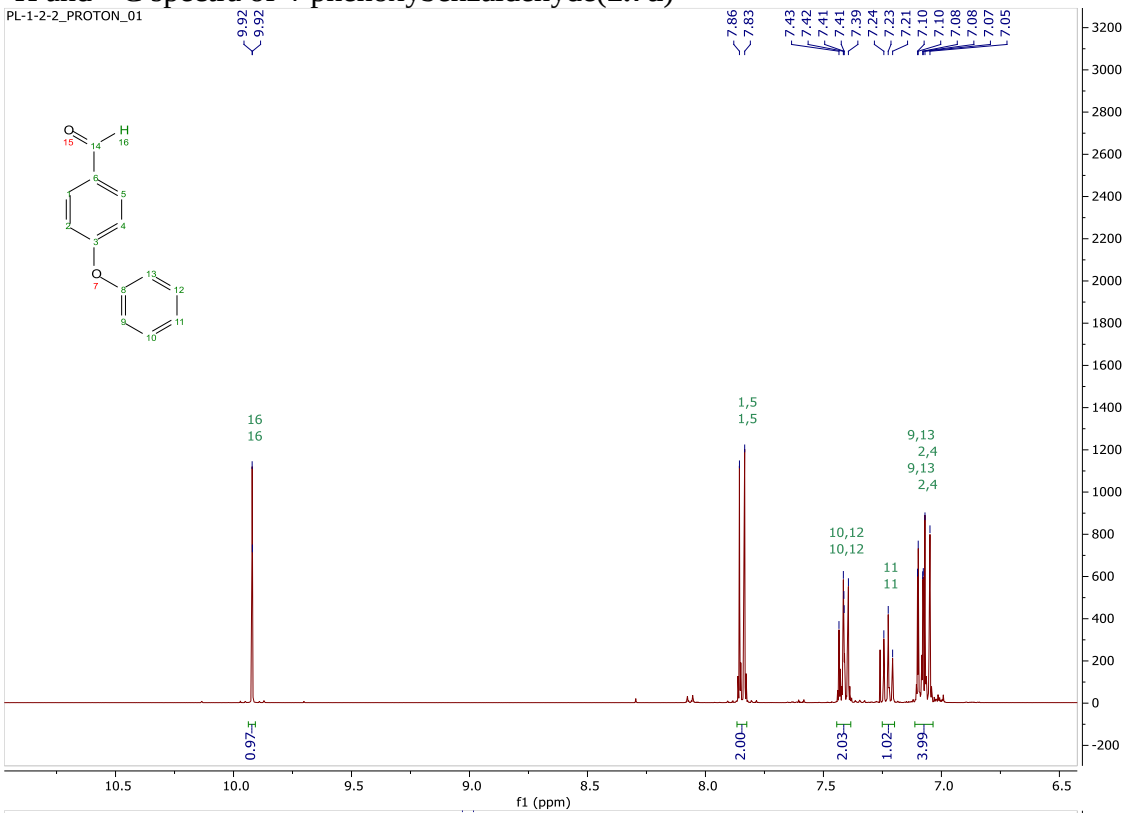


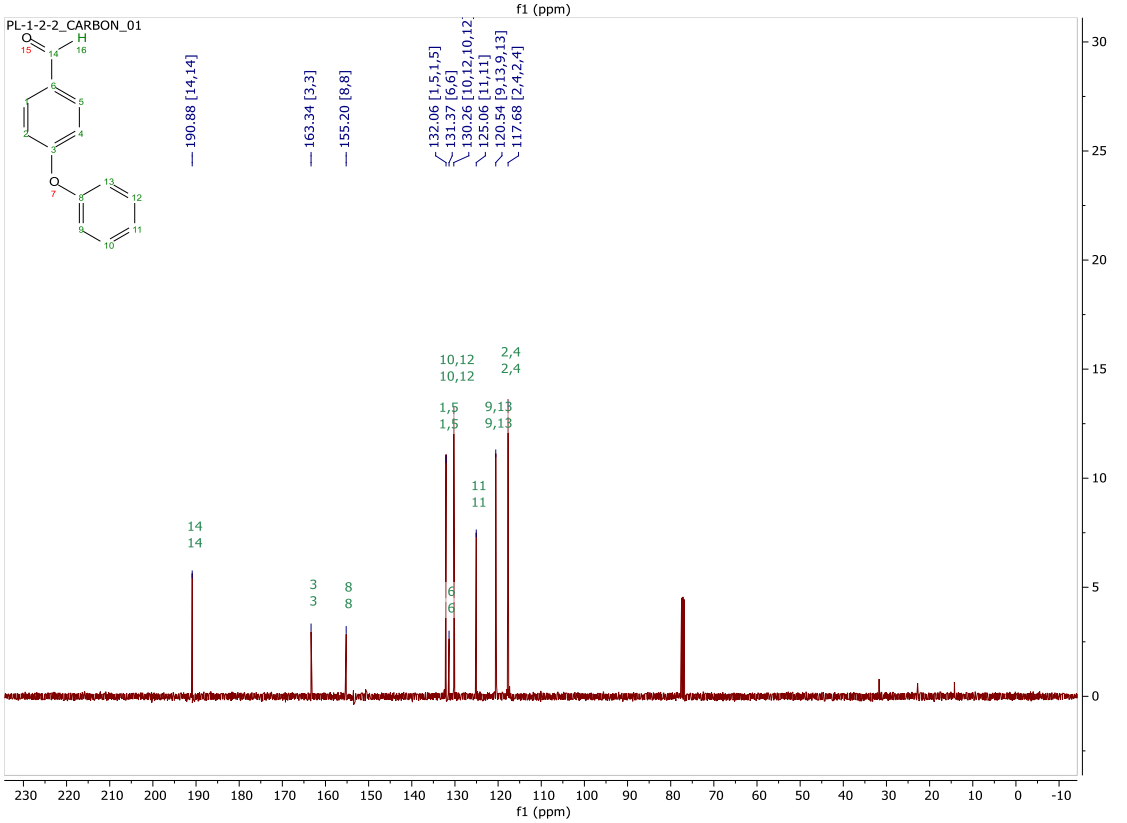

$^{1}H$ and $^{13}C$ spectra of 4-(3-(tert-butyl)phenoxy)benzaldehyde (**2.7b**)

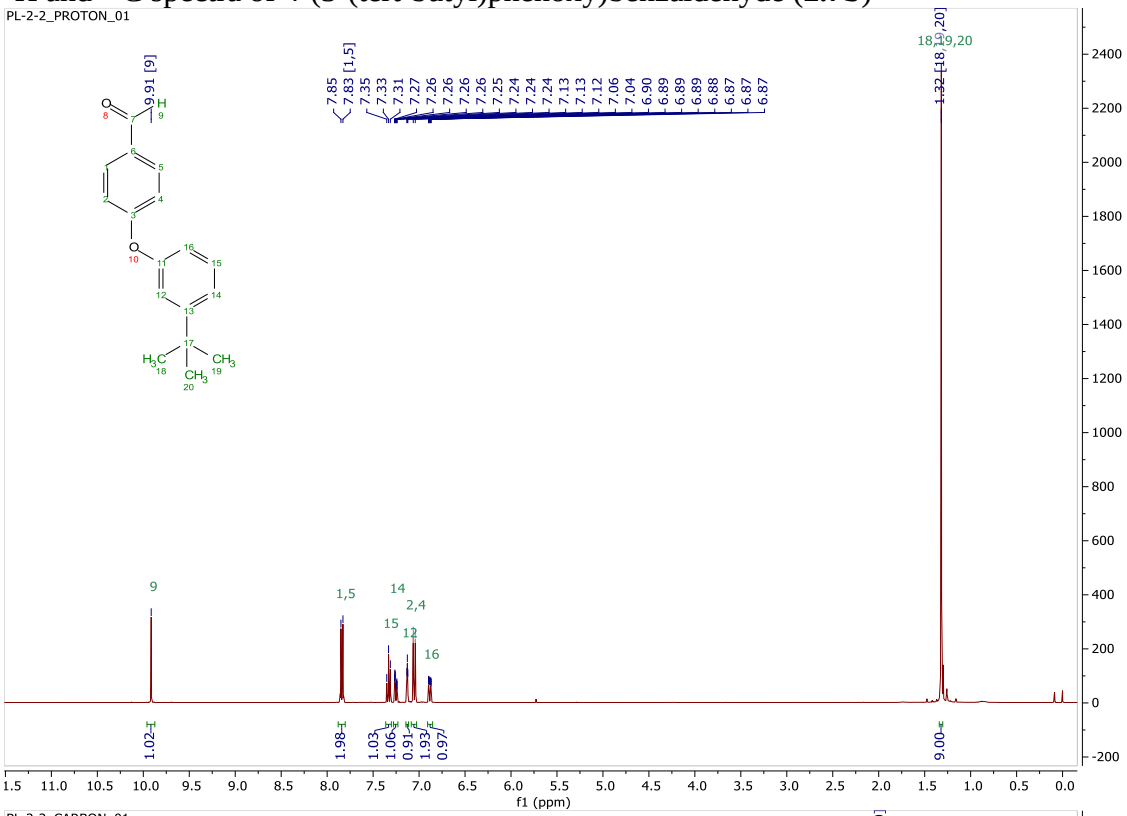


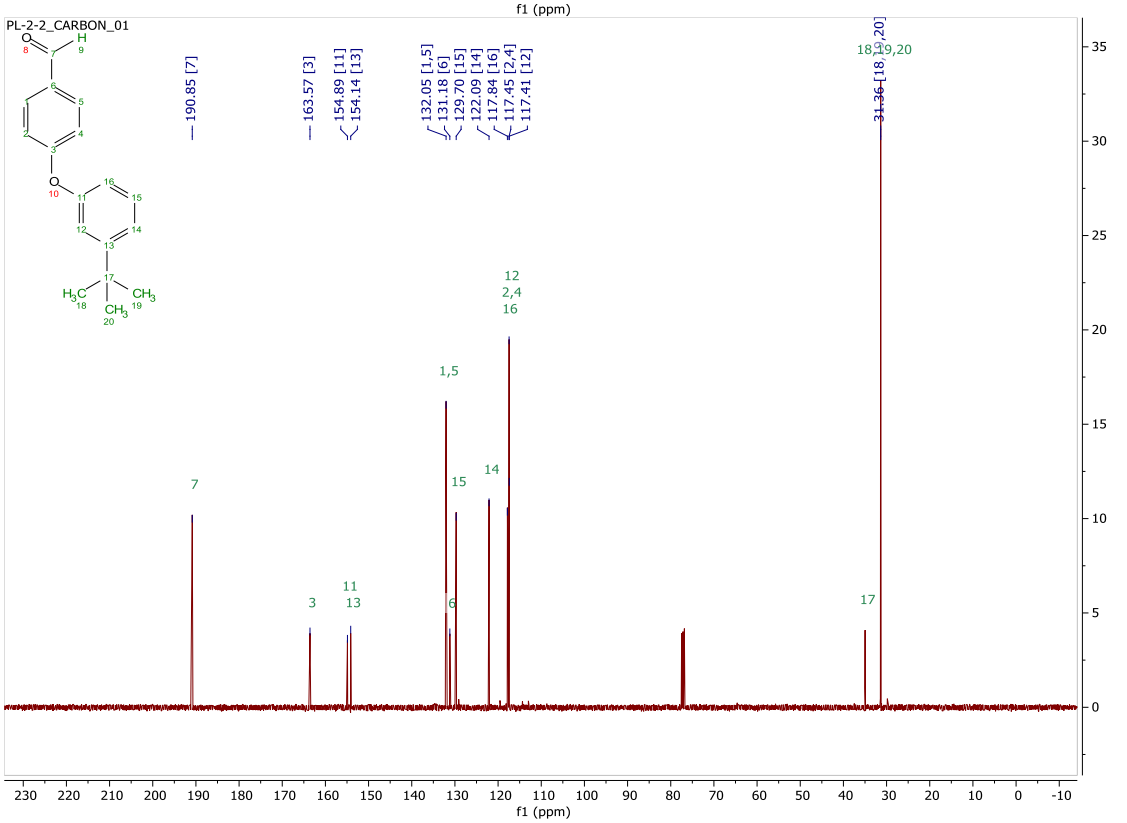

$^{1}H$ and $^{13}C$ spectra of 4-(4-(tert-butyl)phenoxy)benzaldehyde (**2.7c**)

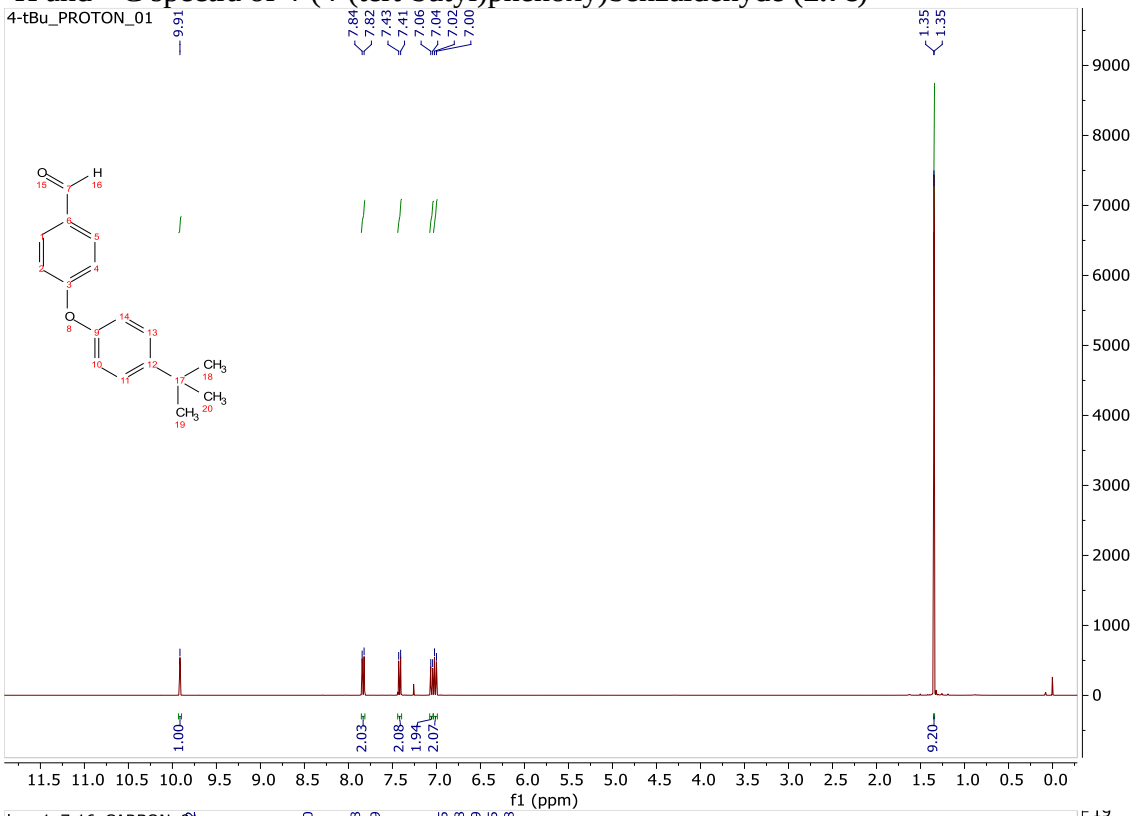


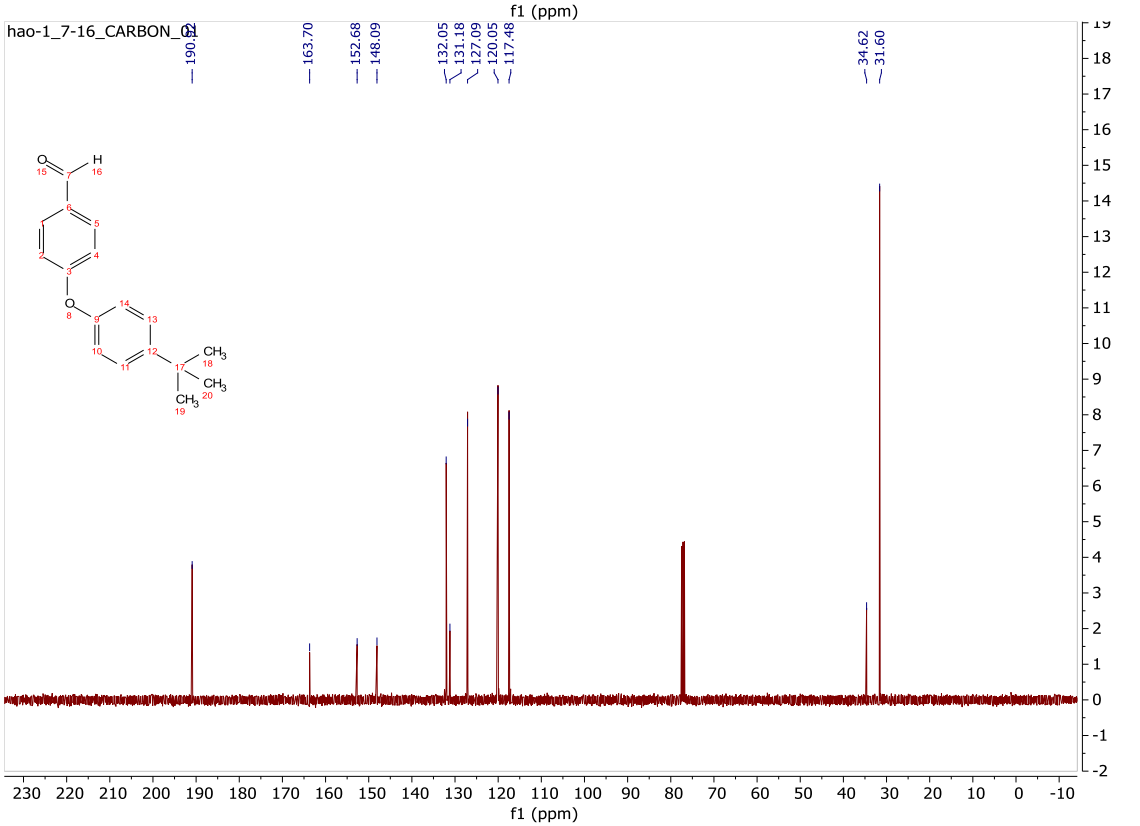

$^{1}H$ and $^{13}C$ spectra of 4-(3-bromophenoxy)benzaldehyde (**2.7d**)

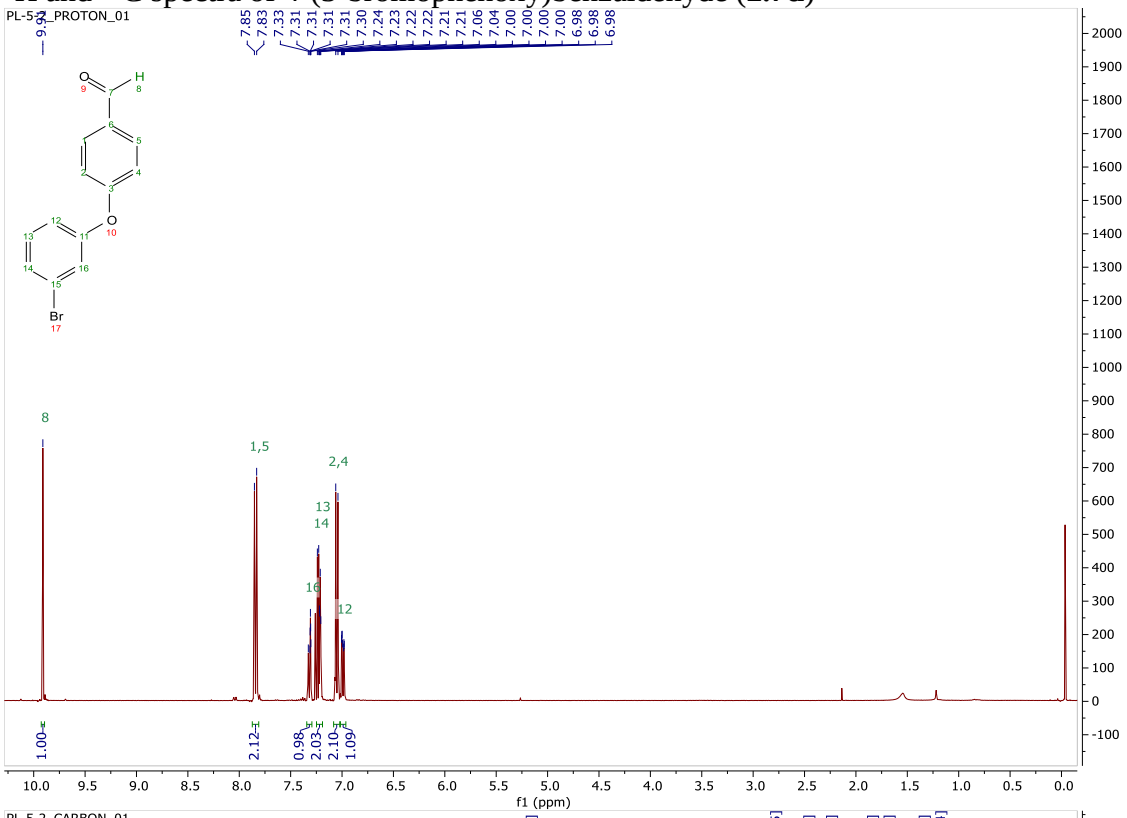


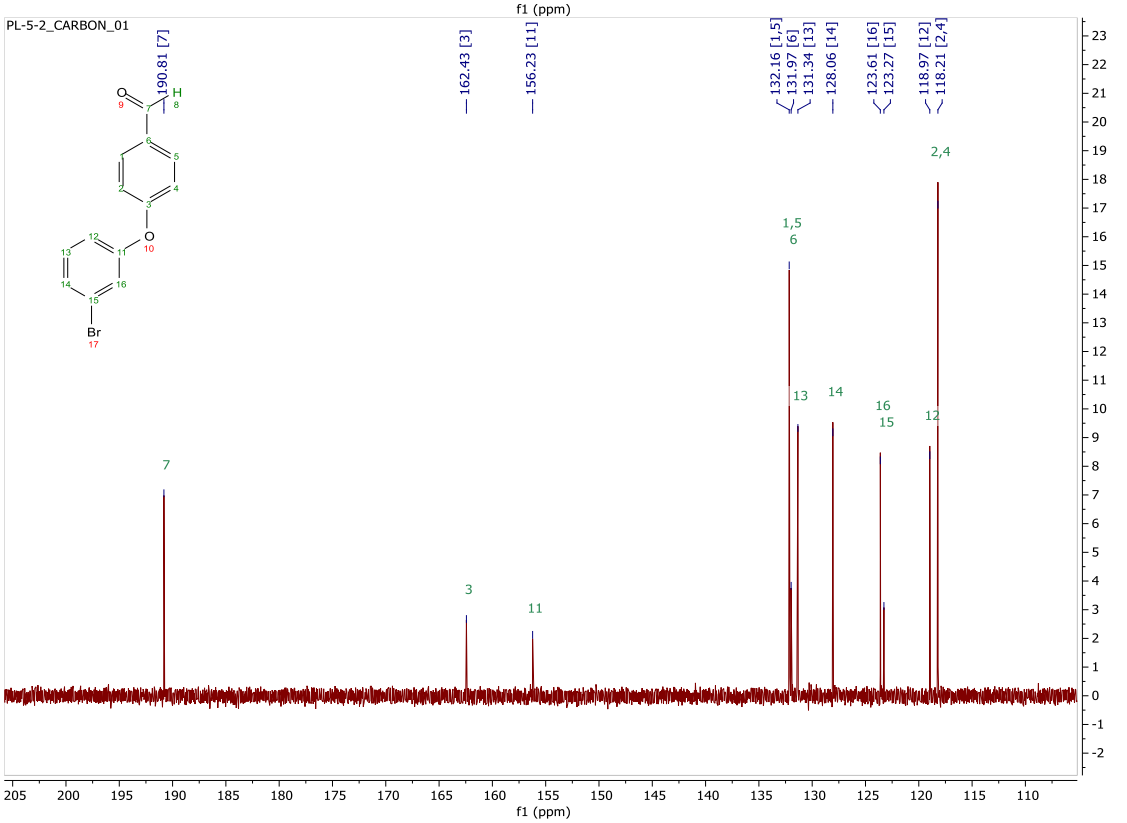

$^{1}H$ and $^{13}C$ spectra of 4-(4-iodophenoxy)benzaldehyde(**2.7e**)

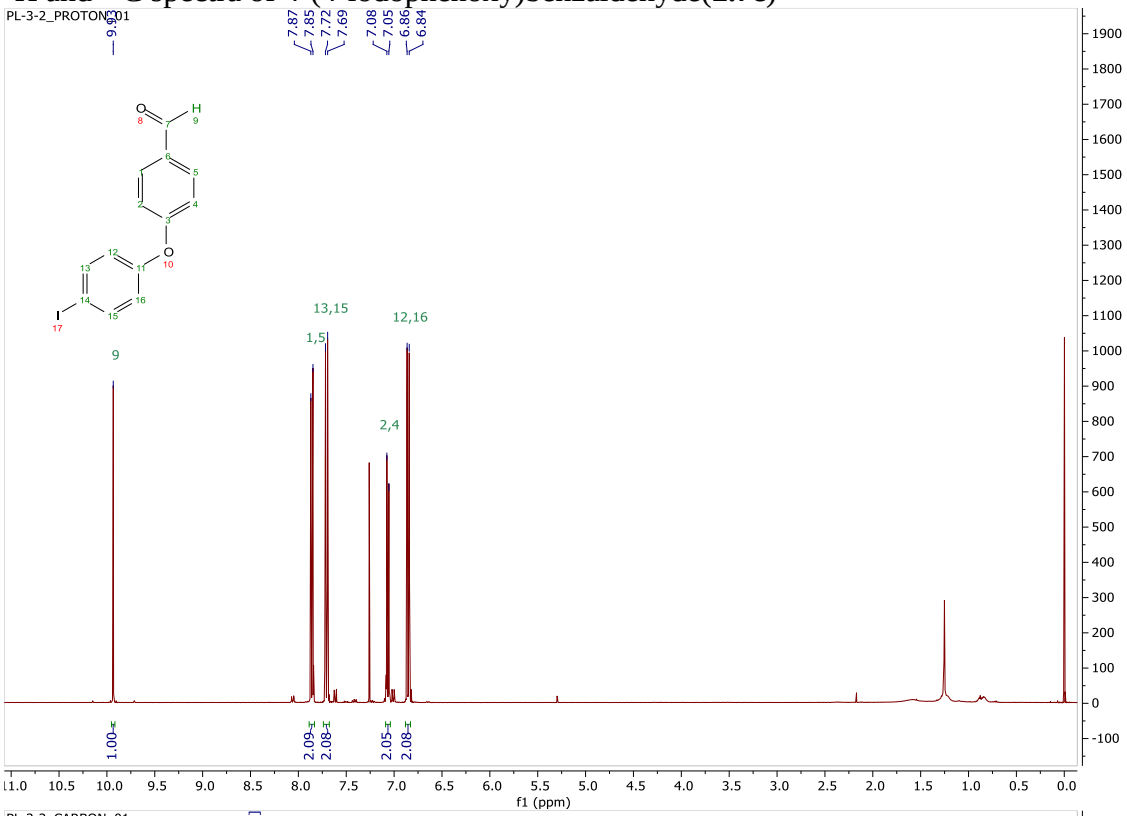


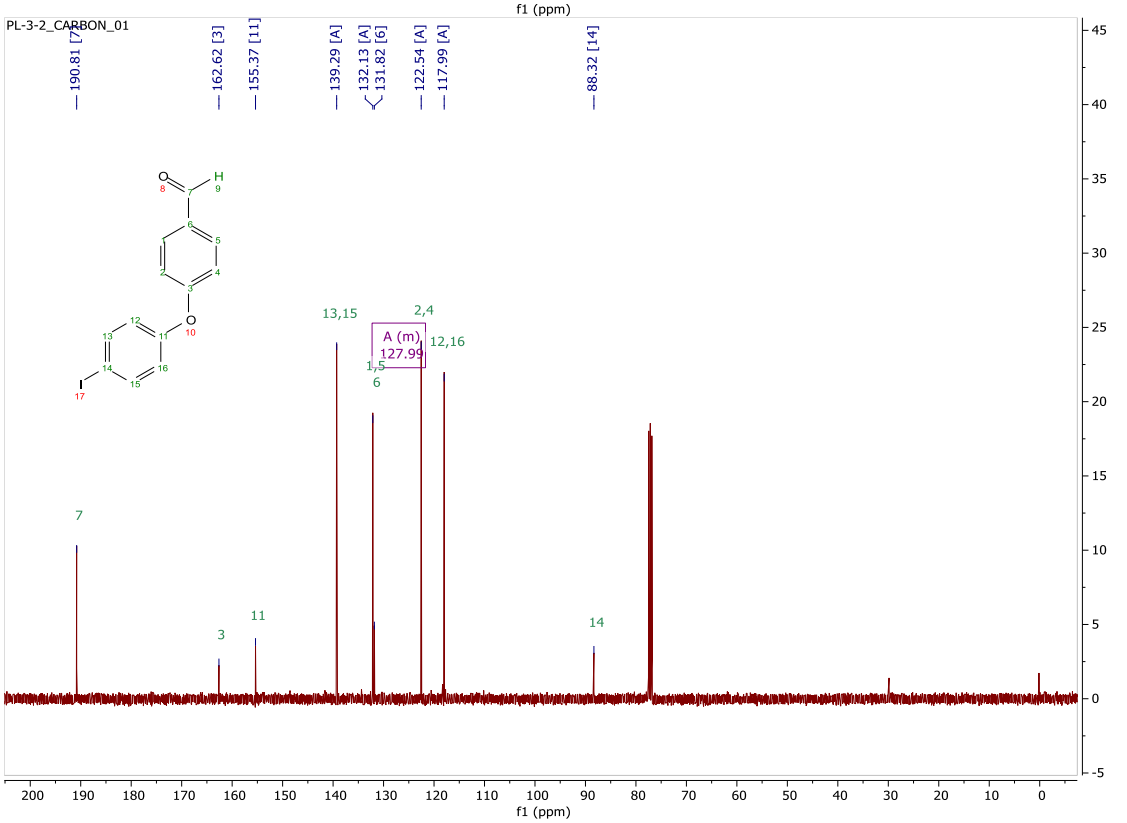

$^{1}H$ and $^{13}C$ spectra of 4-([1,1'-biphenyl]-3-yloxy)benzaldehyde(**2.8d**)

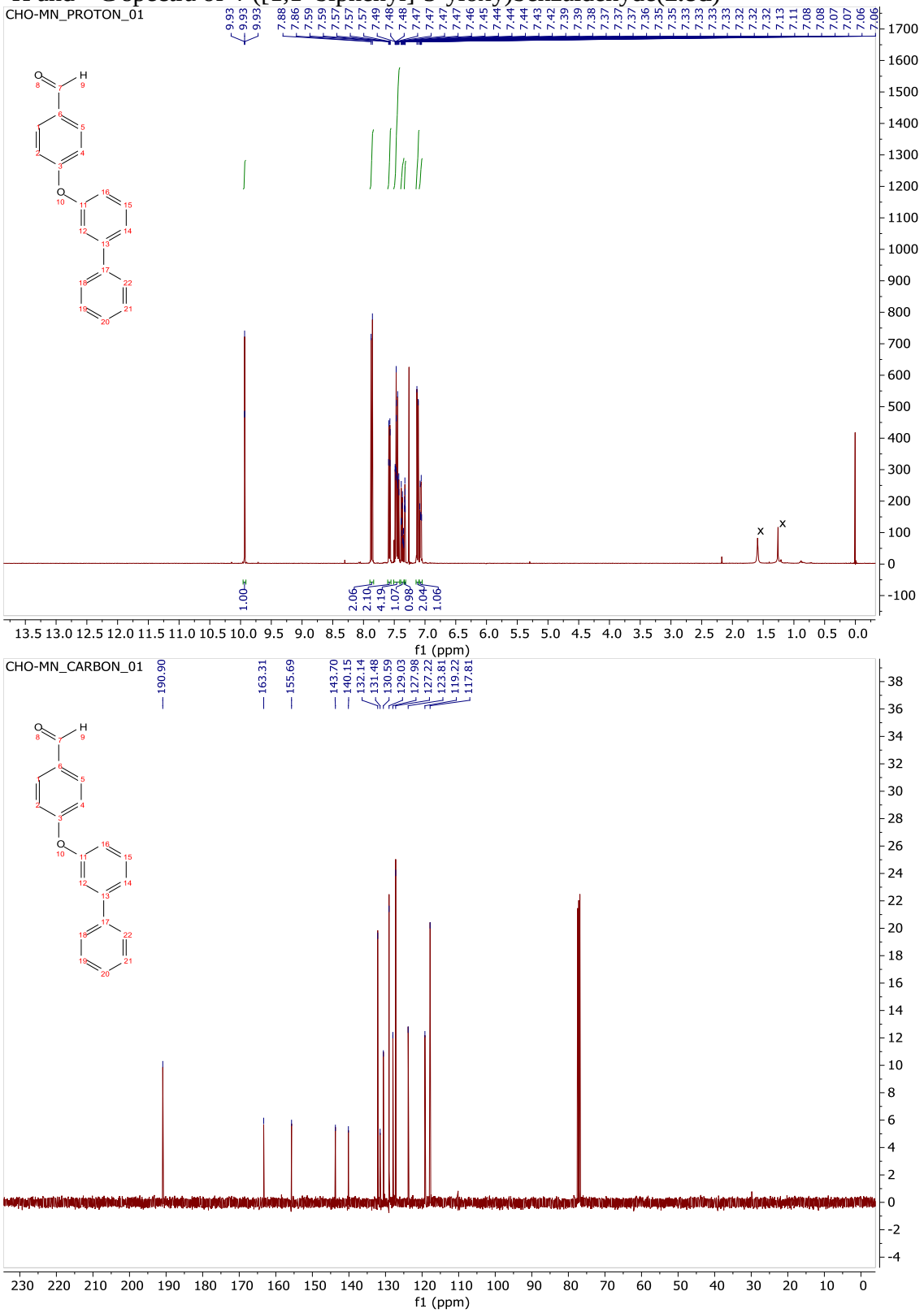

$^{1}H$ and $^{13}C$ spectra of 4-((3'-(trifluoromethyl)-[1,1'-biphenyl]-3-yl)oxy)benzaldehyde(**2.8e**)

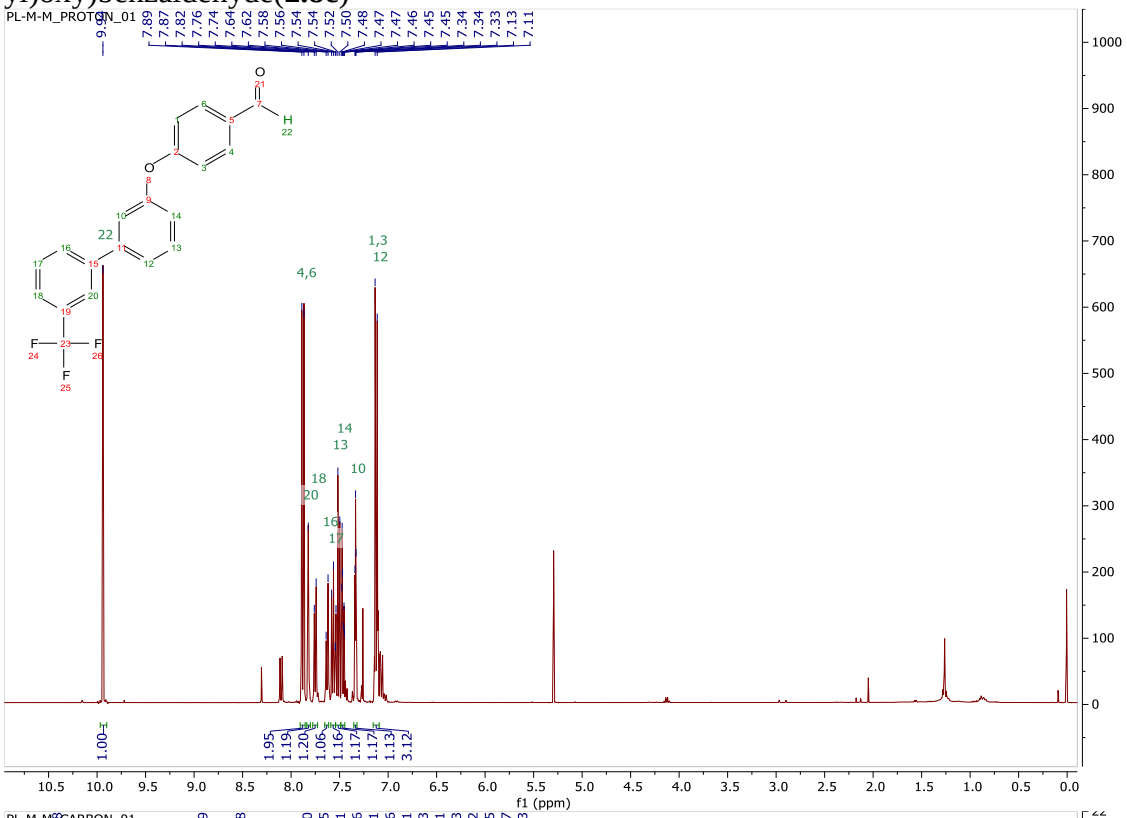


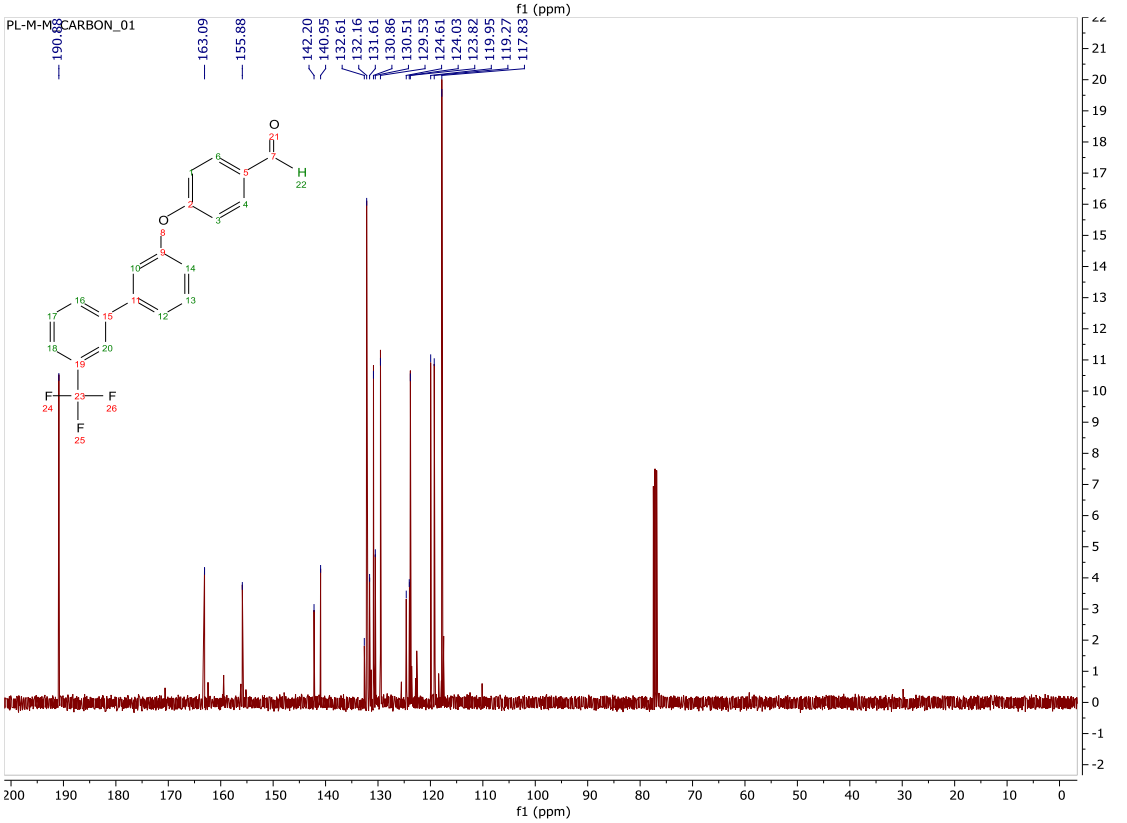

$^{1}H$ and $^{13}C$ spectra of 4-((4'-(trifluoromethyl)-[1,1'-biphenyl]-3-yl)oxy)benzaldehyde(**2.8f**)

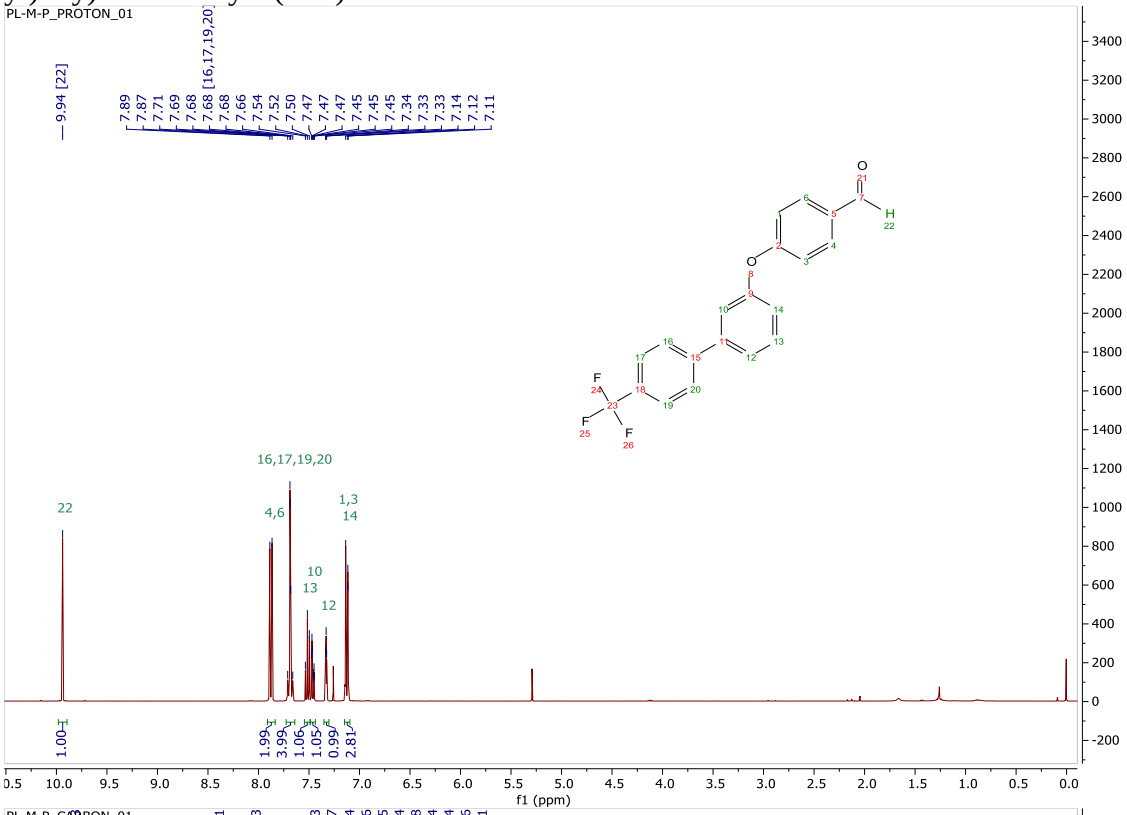


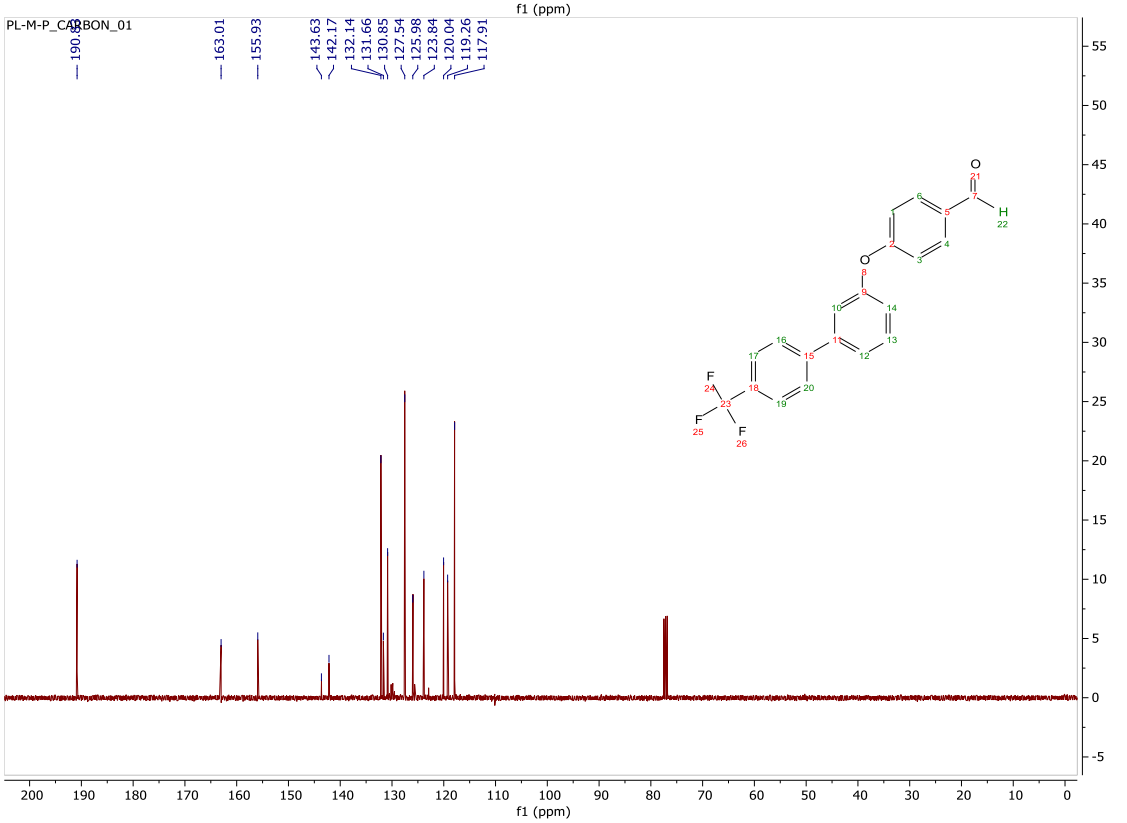

$^{1}H$ and $^{13}C$ spectra of 4-([1,1'-biphenyl]-4-yloxy)benzaldehyde(**2.8g**)

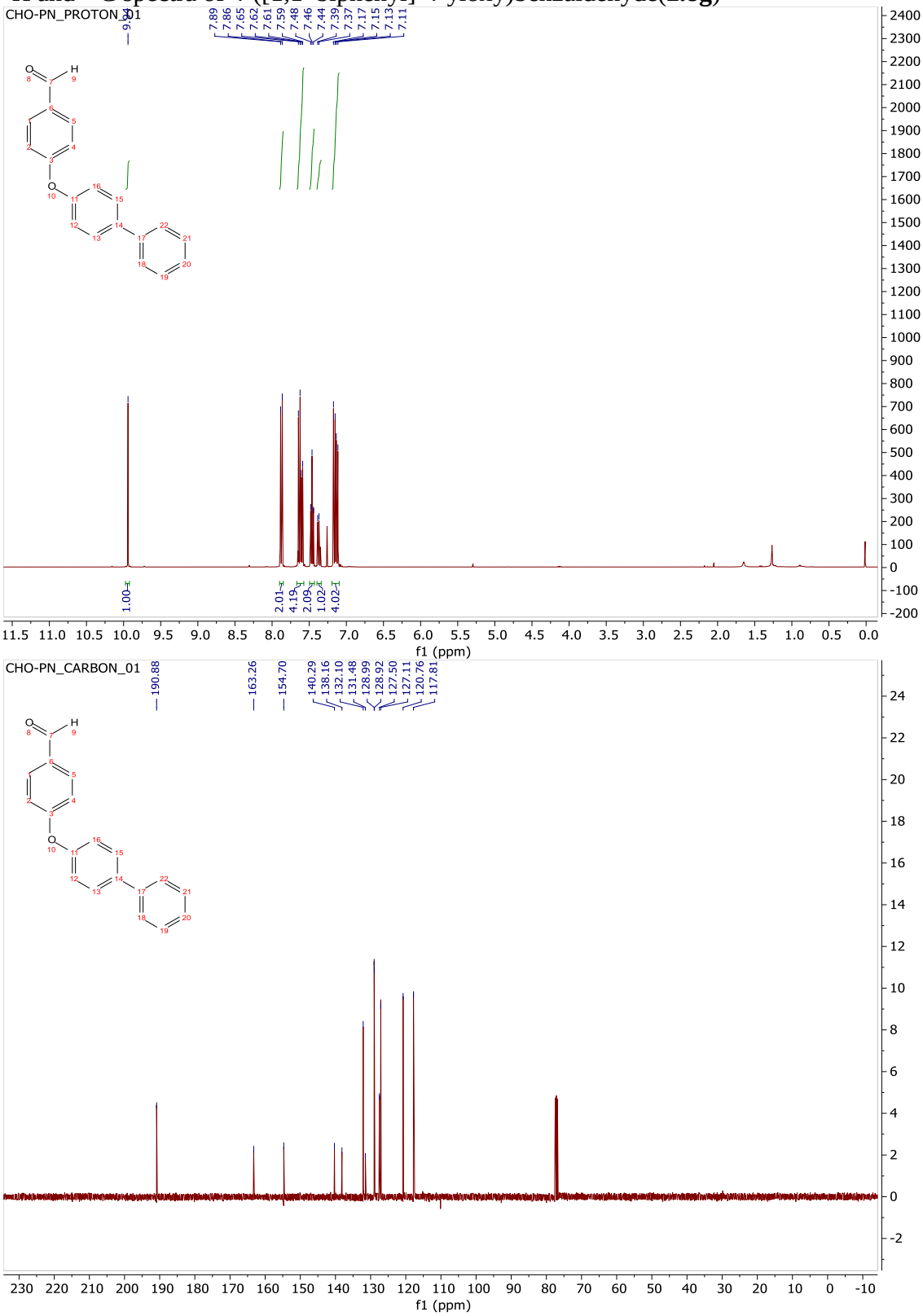

$^{1}H$ and $^{13}C$ spectra of 4-((3'-(trifluoromethyl)-[1,1'-biphenyl]-4-yl)oxy)benzaldehyde(**2.8h**)

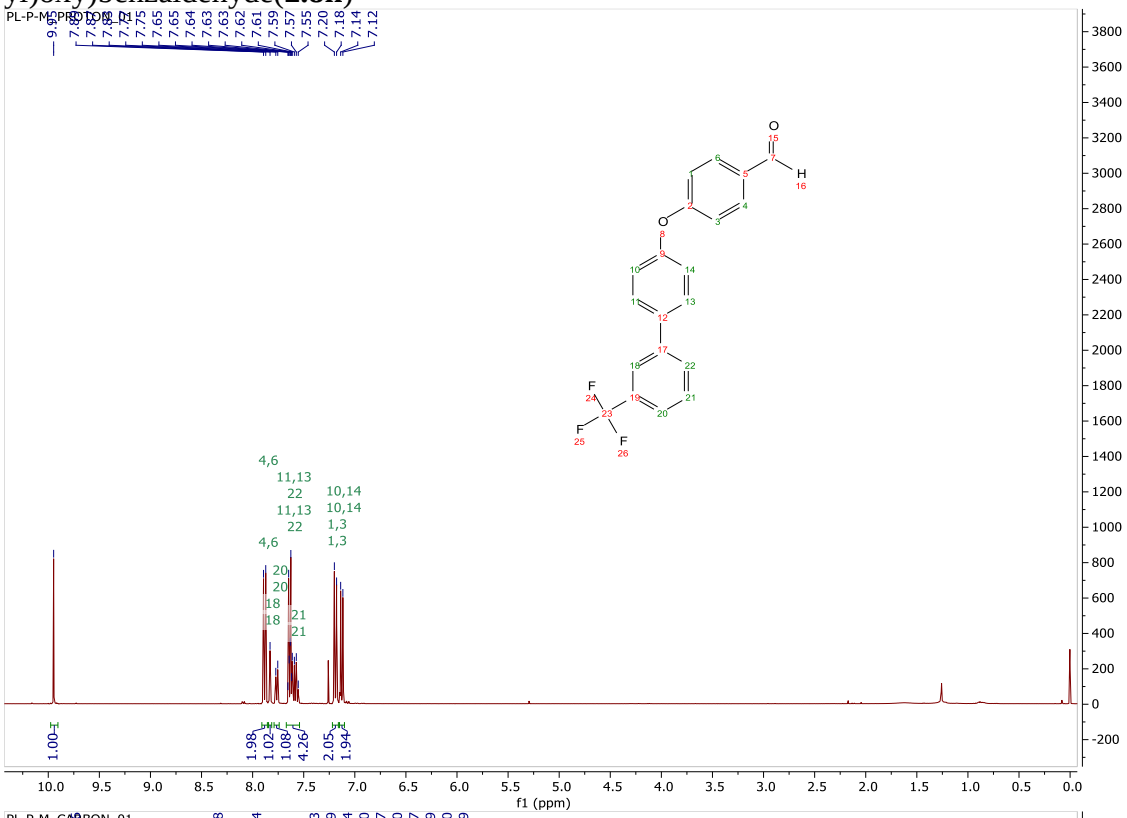


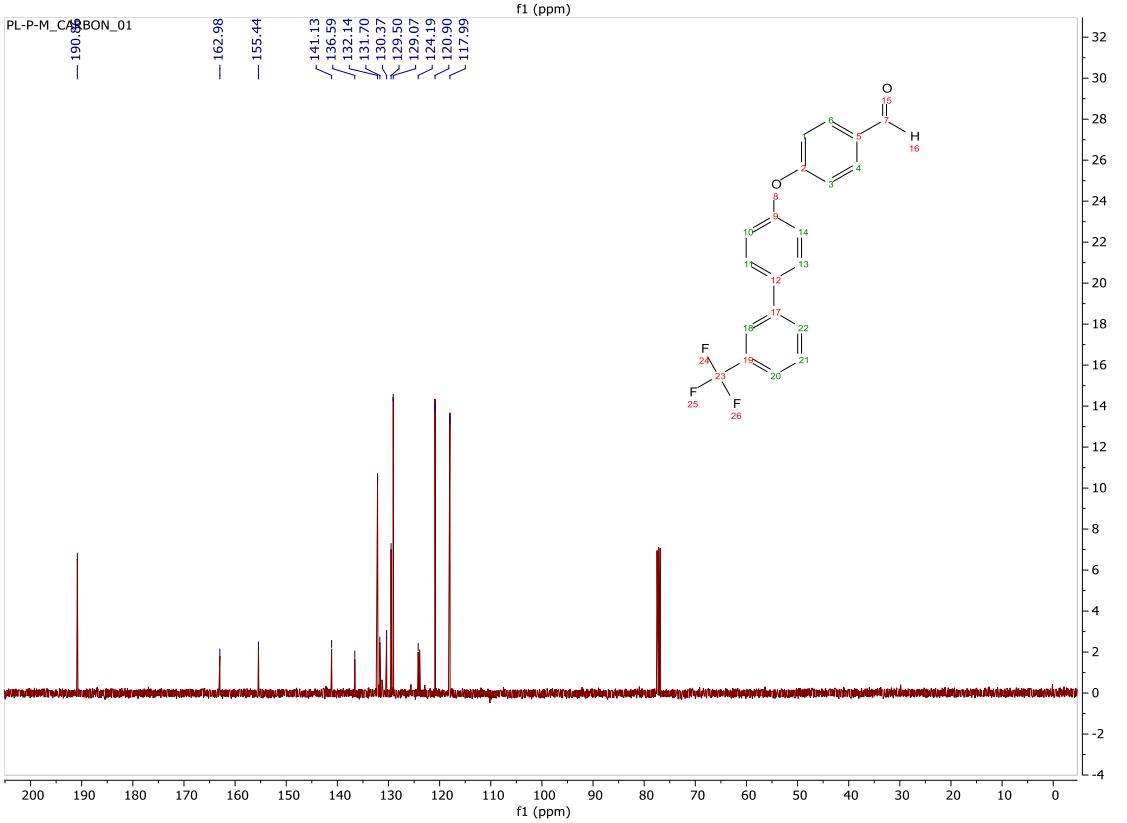

$^{1}H$ and $^{13}C$ spectra of 4-((4'-(trifluoromethyl)-[1,1'-biphenyl]-4-yl)oxy)benzaldehyde(**2.8i**)

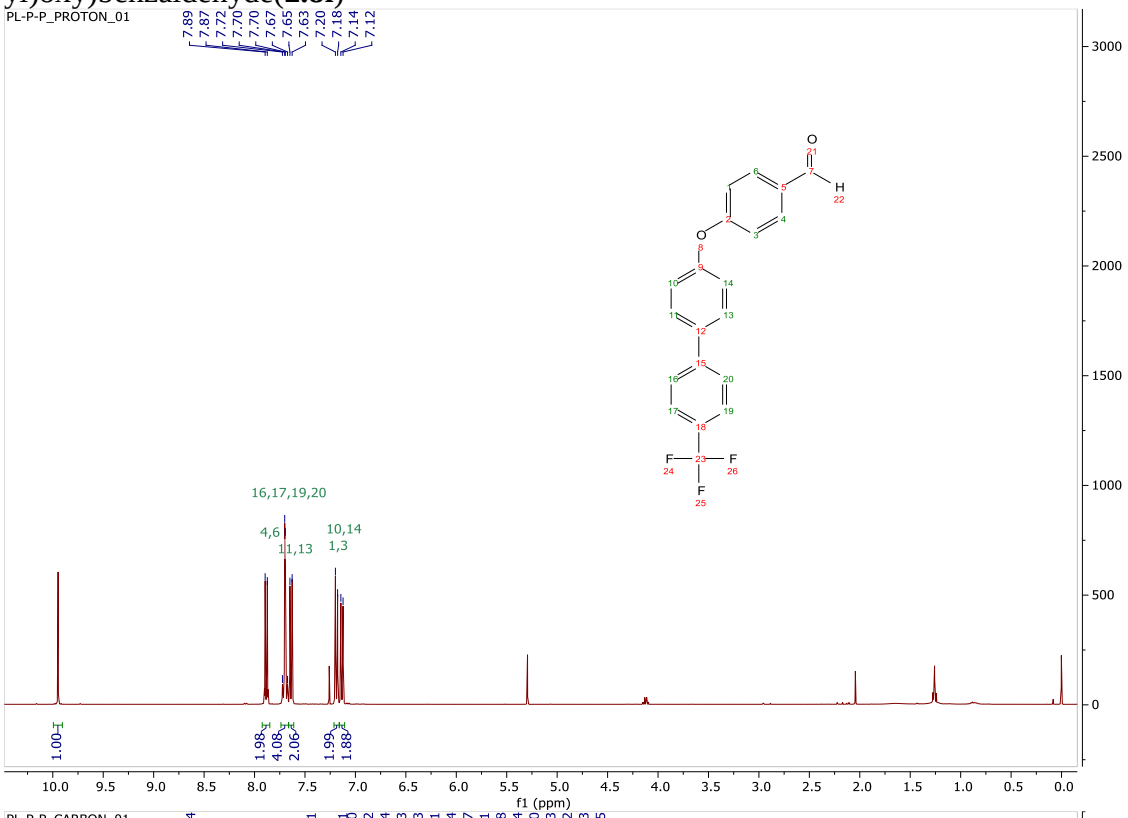


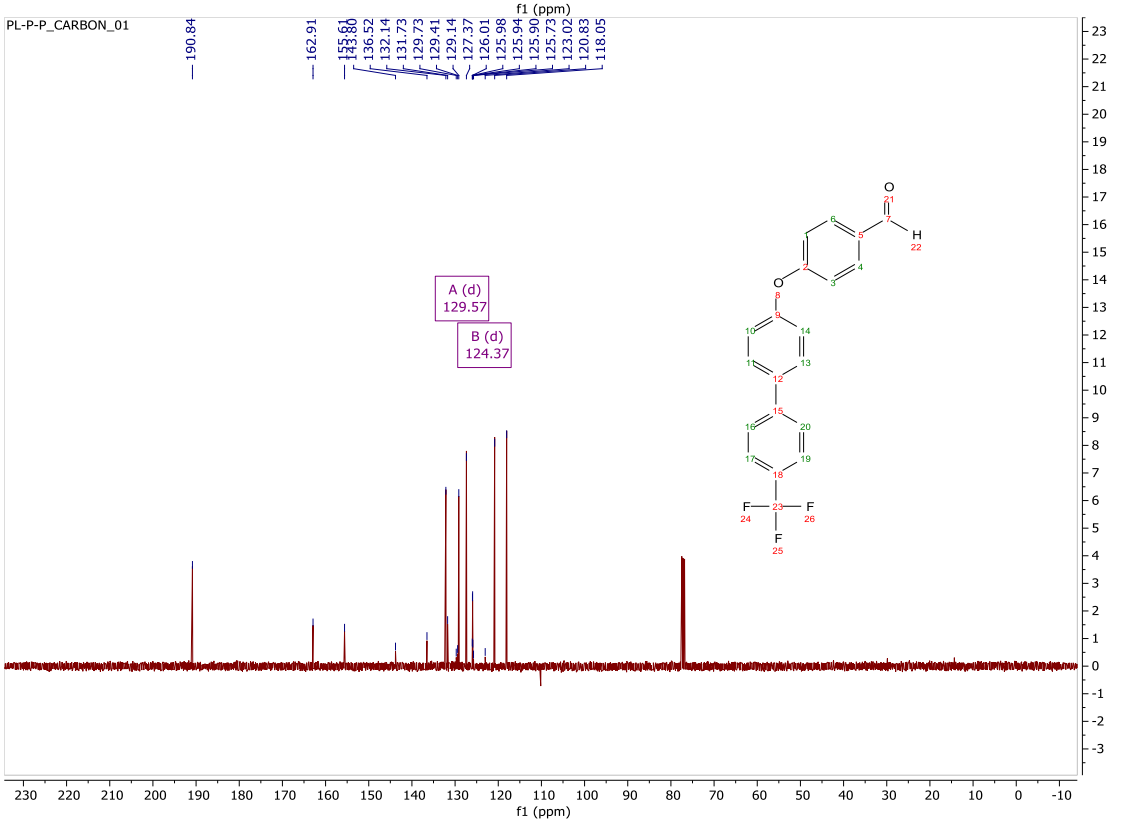

$^{1}H$ and $^{13}C$ spectra of 4-nonylbenzaldehyde(**2.12a**)

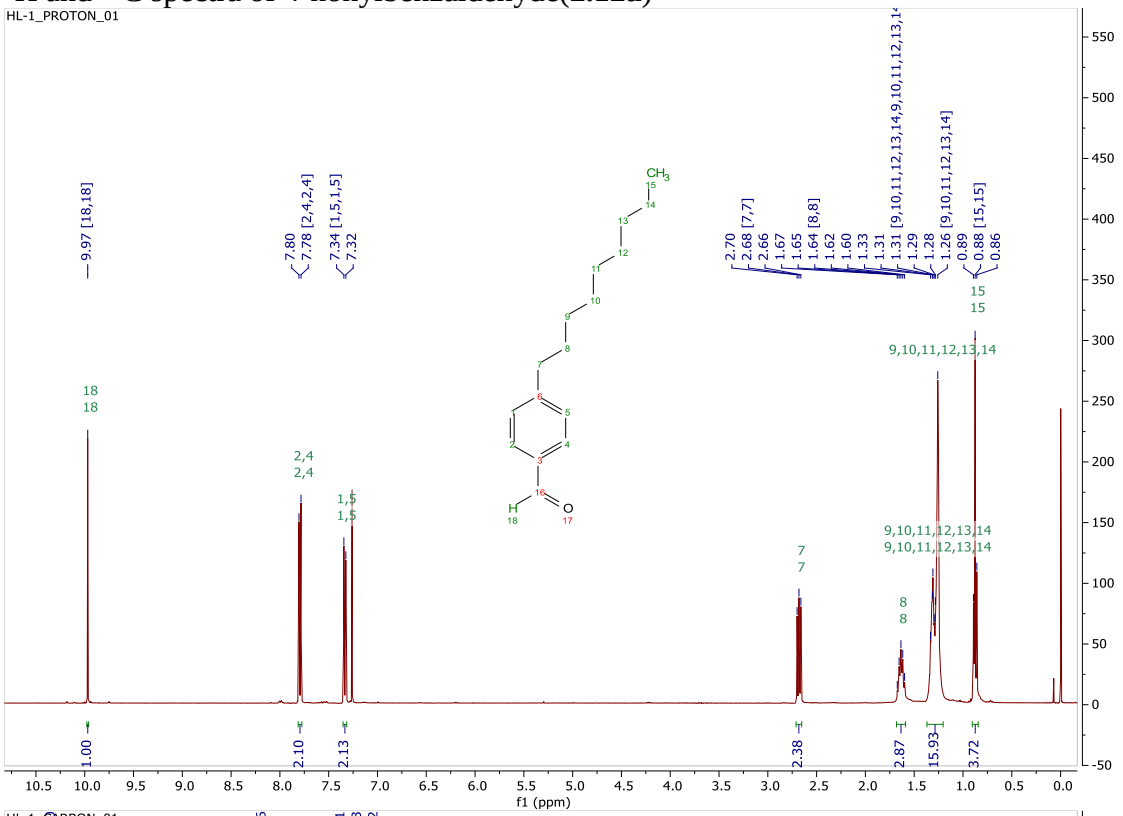


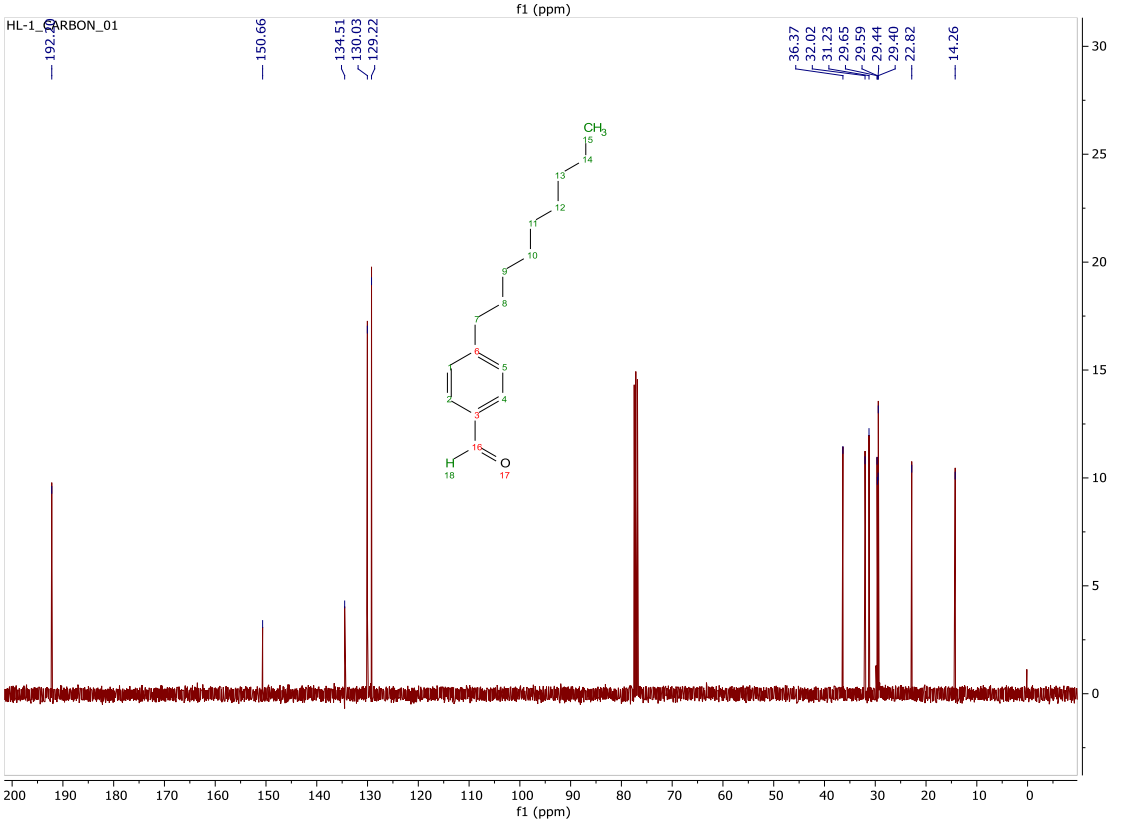

$^{1}H$ and $^{13}C$ spectra of 4-decylbenzaldehyde(**2.12b**)

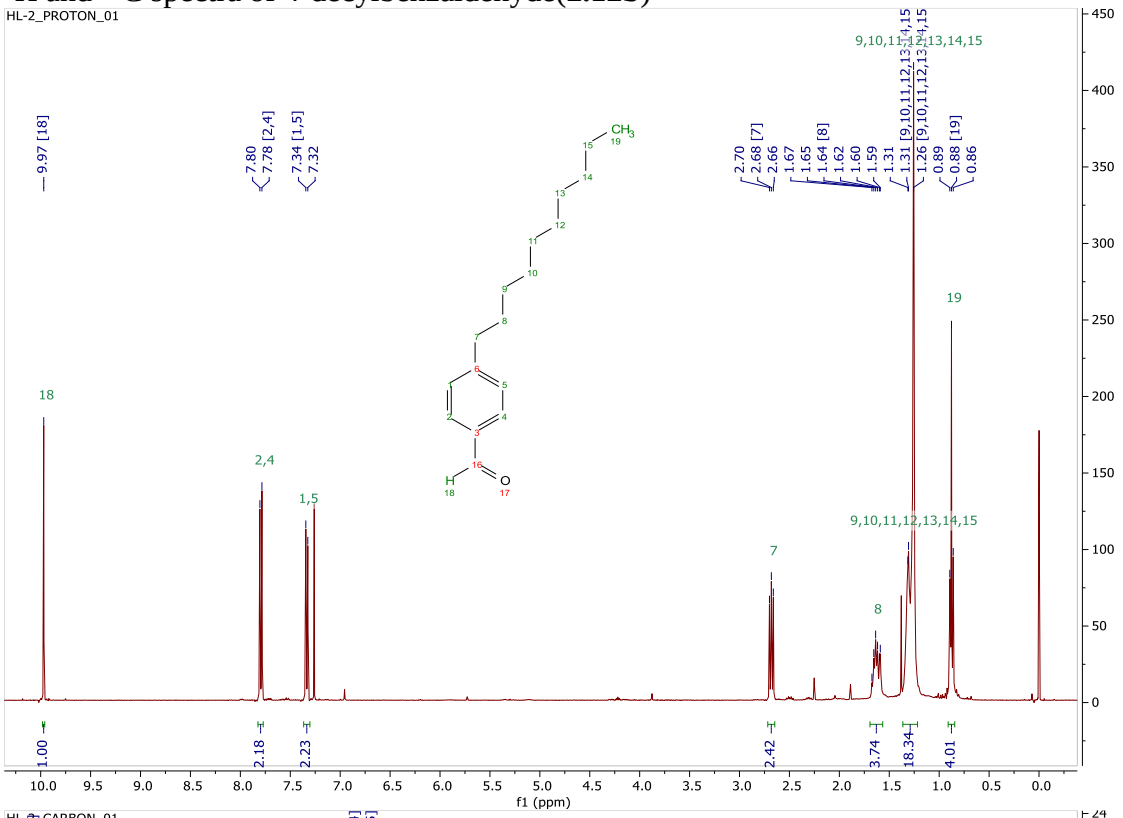


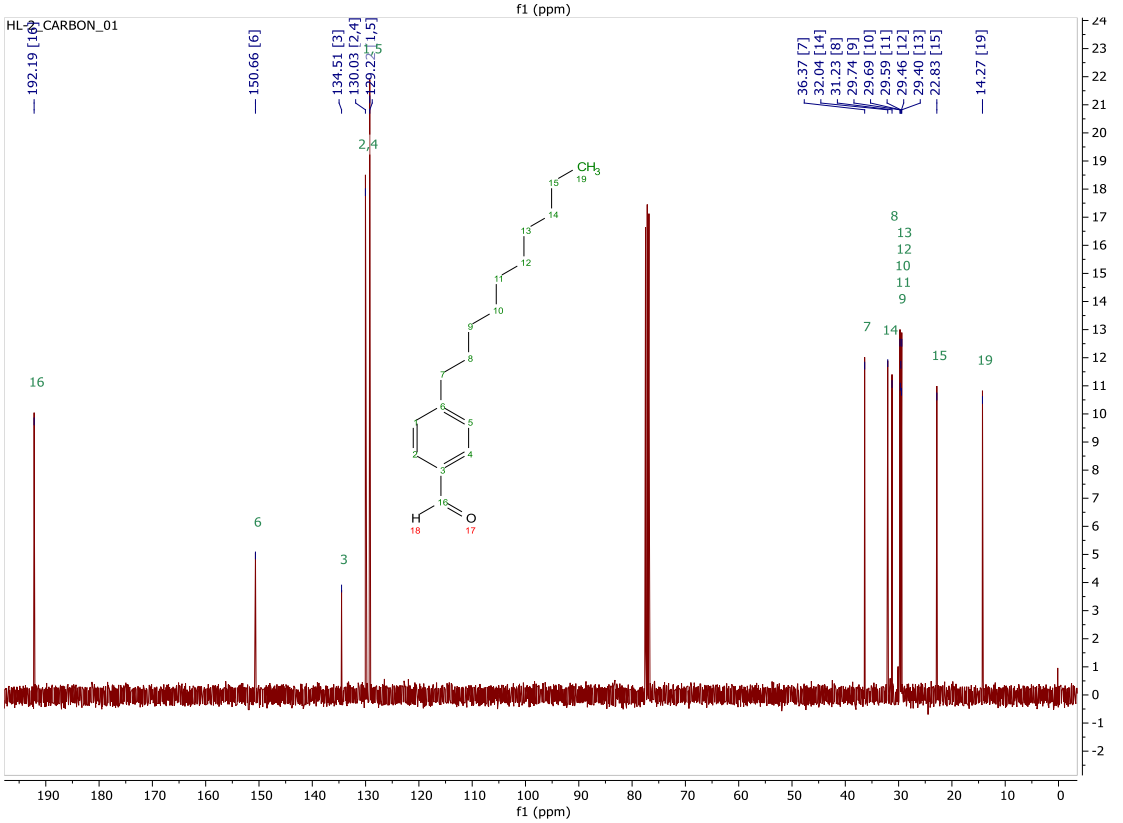

$^{1}H$ and $^{13}C$ spectra of 4-undecylbenzaldehyde(**2.12c**)

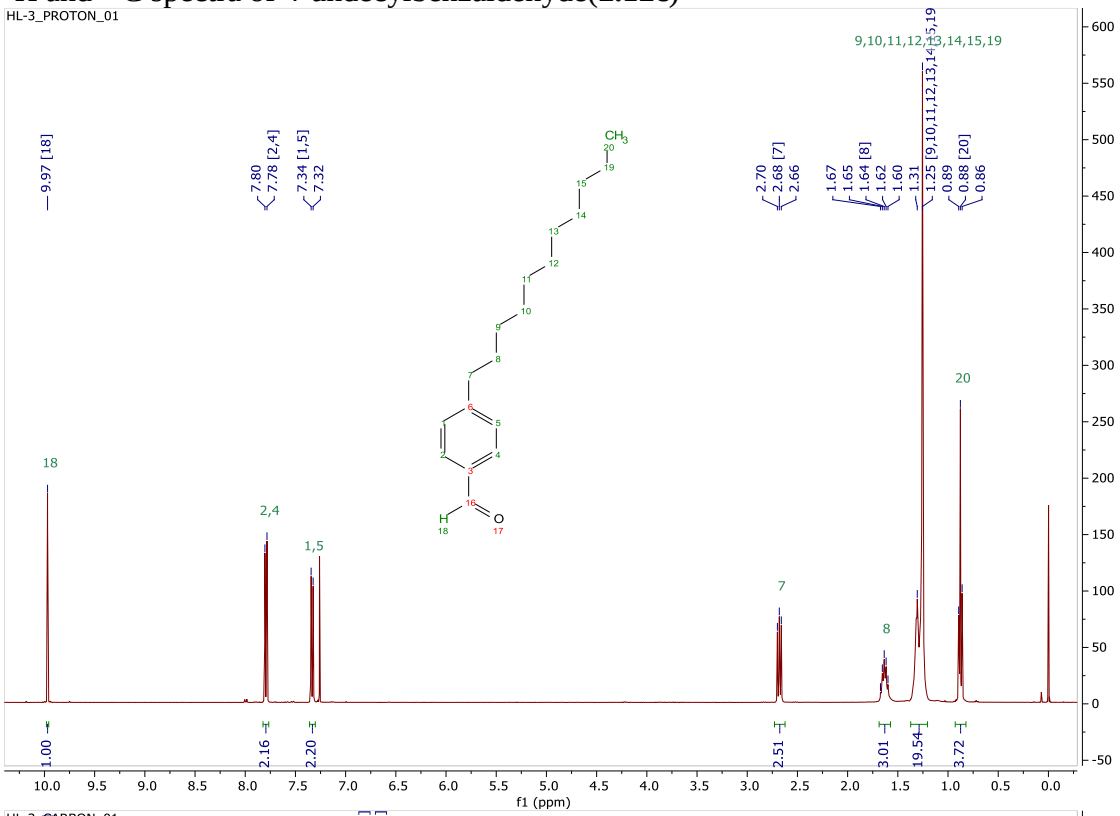


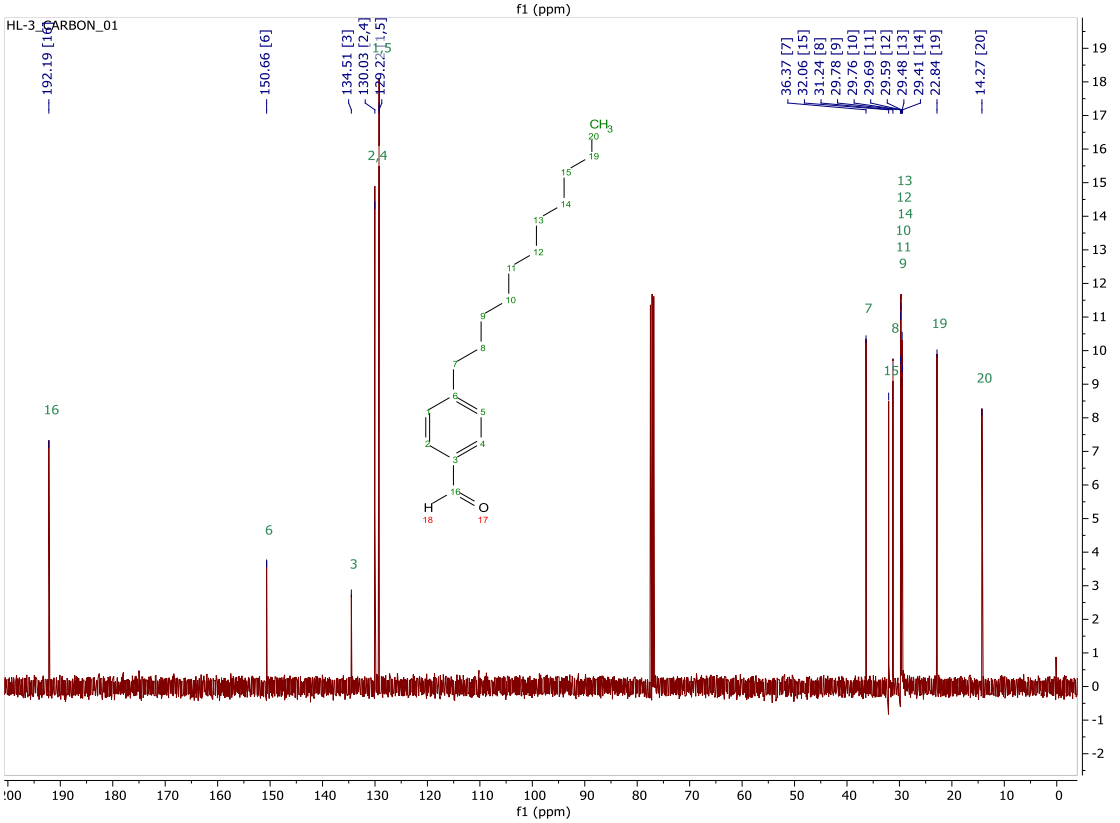

$^{1}H$ and $^{13}C$ spectra of 4-dodecylbenzaldehyde(**2.12d**)

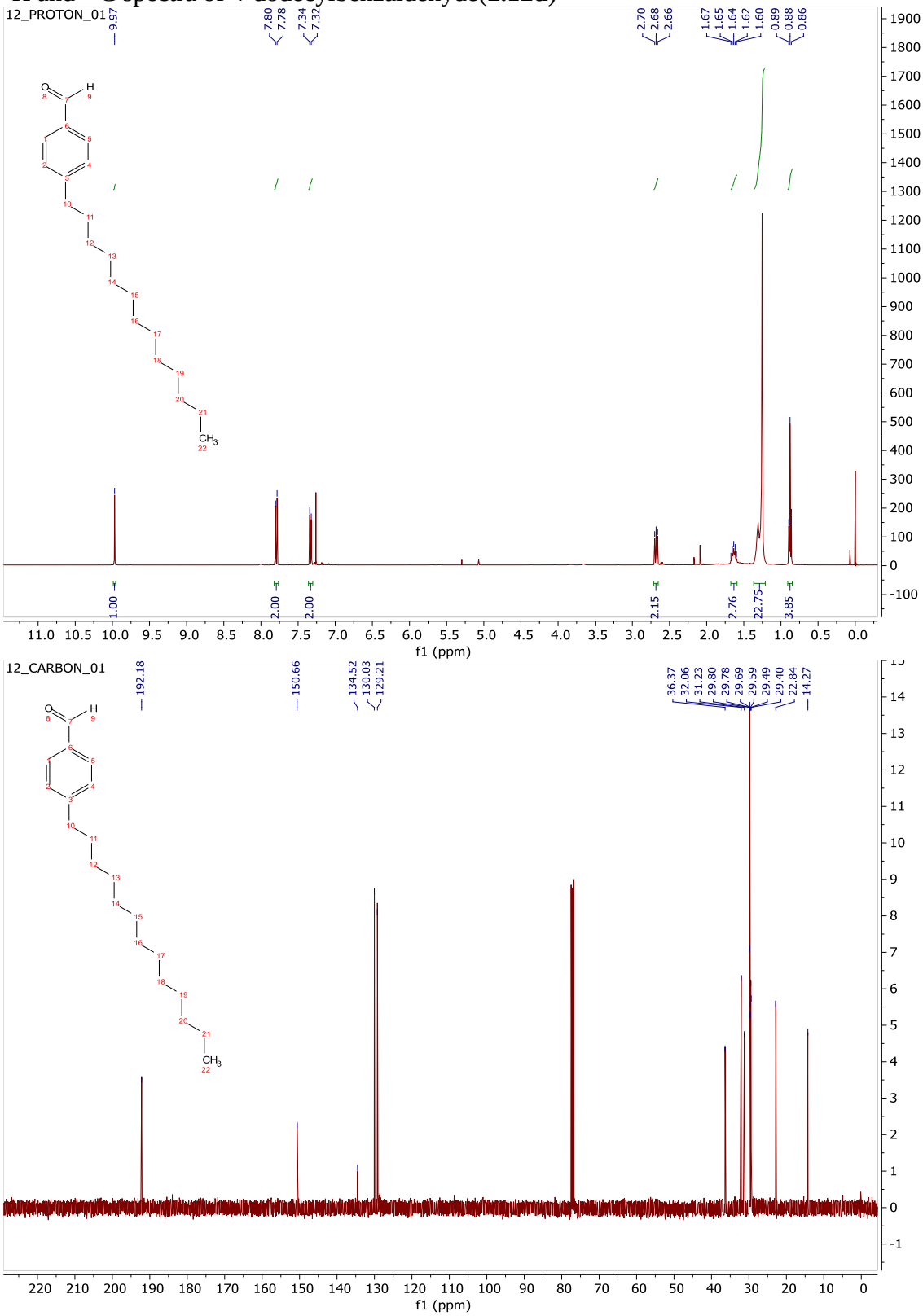

$^{1}H$ and $^{13}C$ spectra of 4-dodecyl-2-methylbenzaldehyde (**2.12e**)

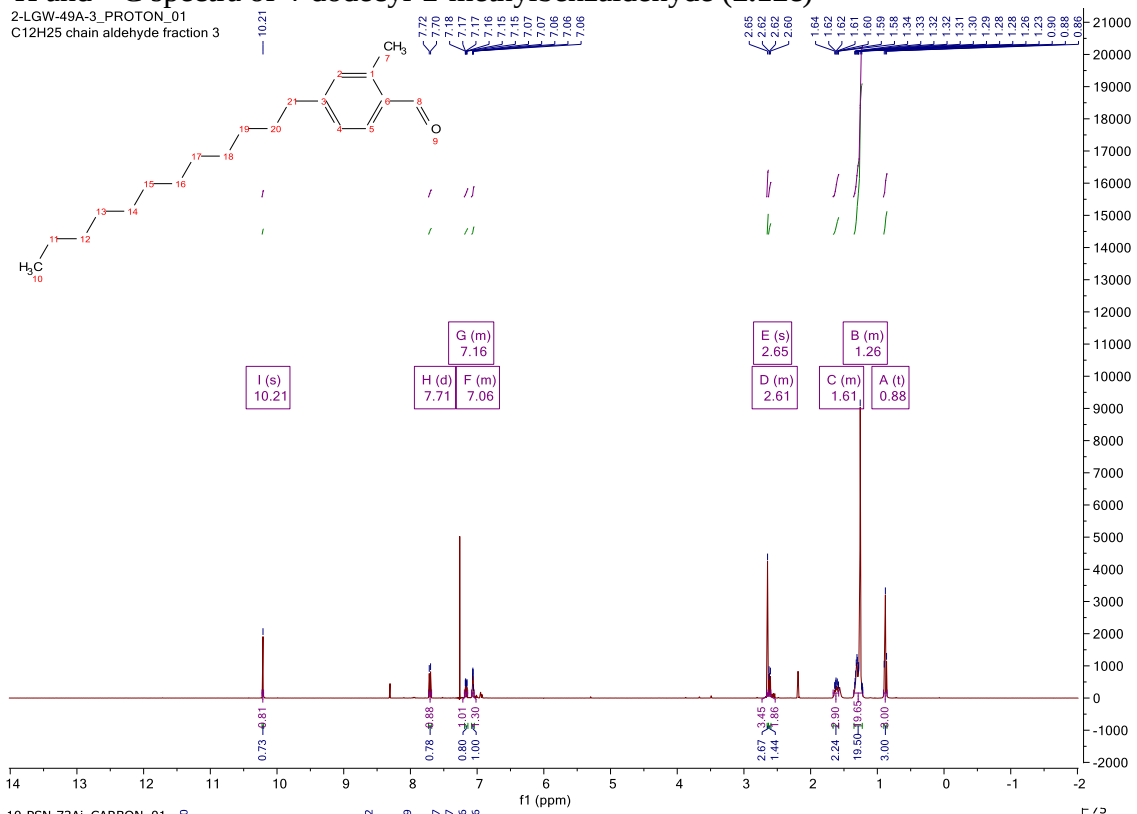


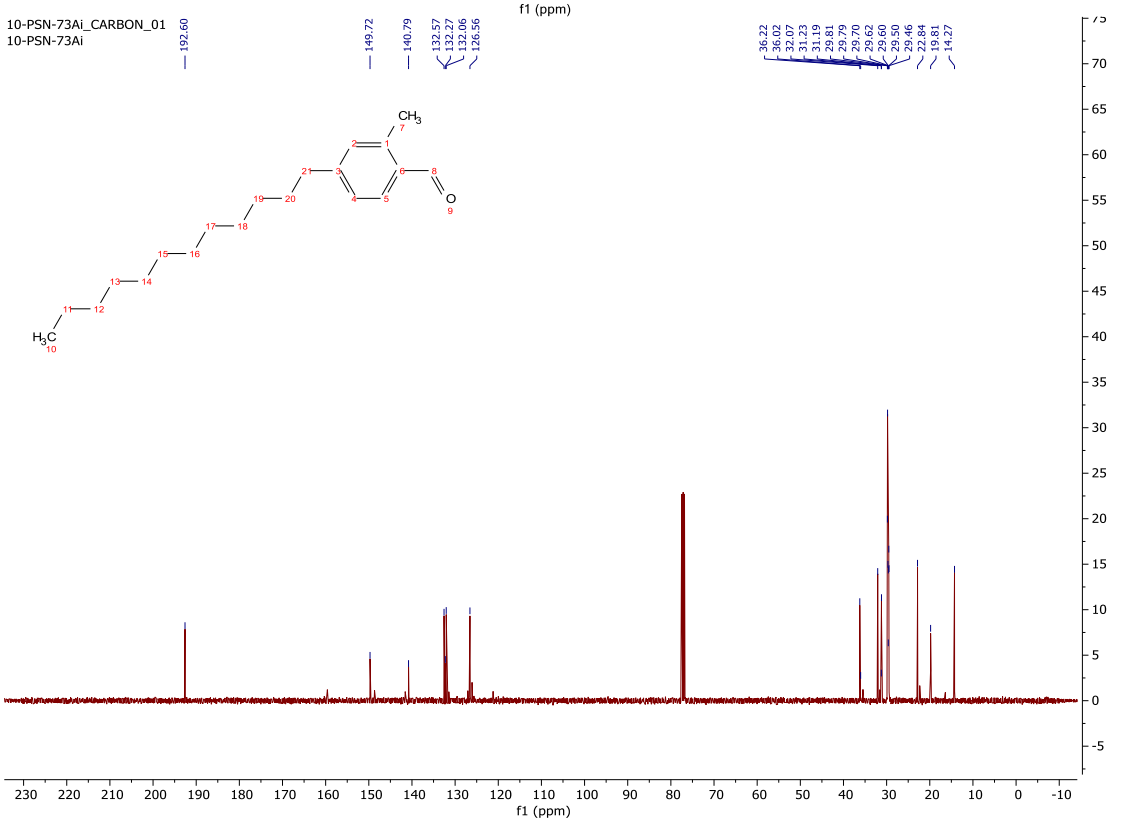

$^{1}H$ and $^{13}C$ spectra of 4-(4-methylphenethyl)benzaldehyde (**2.12f**)

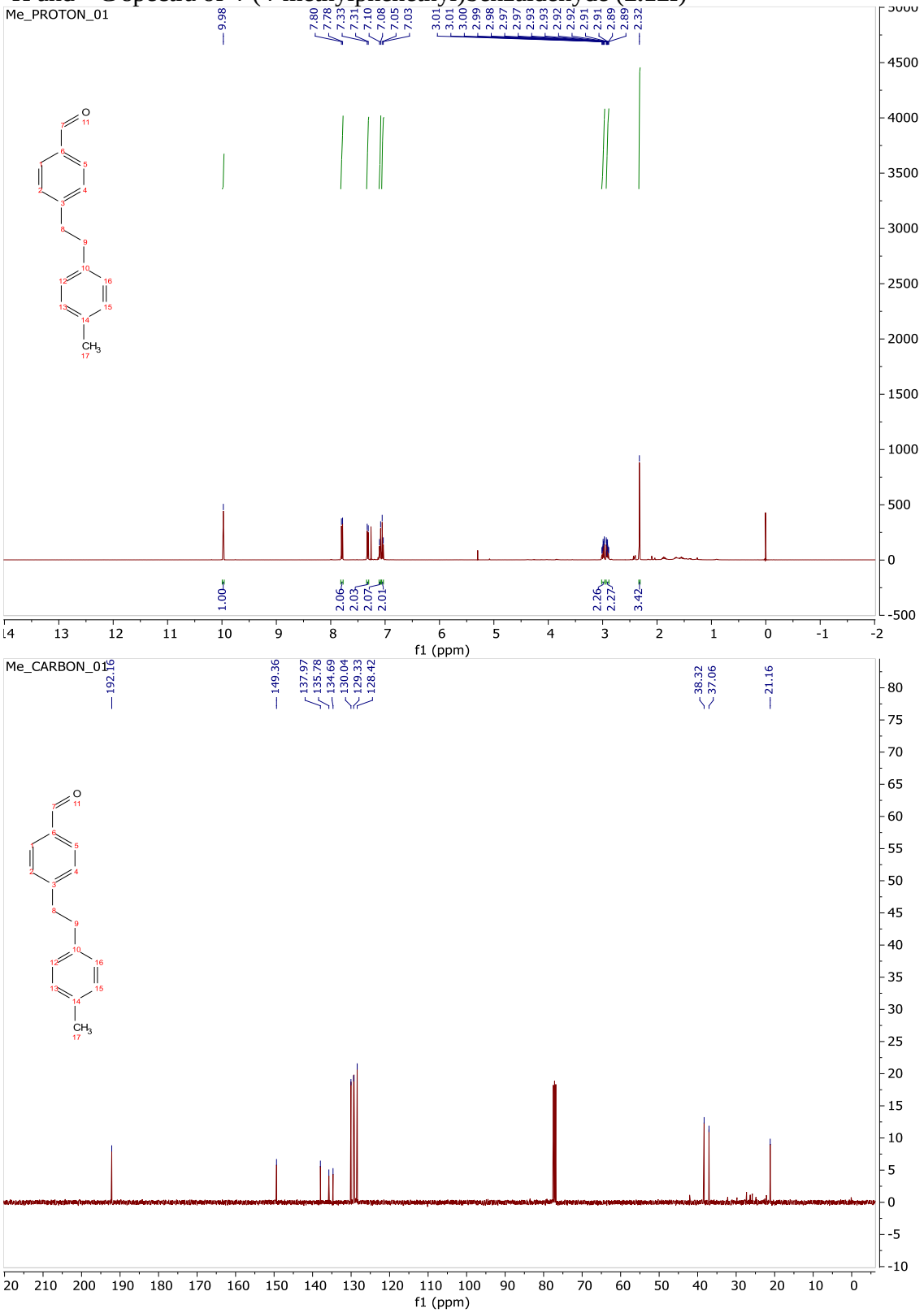

$^{1}H$ and $^{13}C$ spectra of 4-(4-methoxyphenethyl)benzaldehyde (**2.12g**)

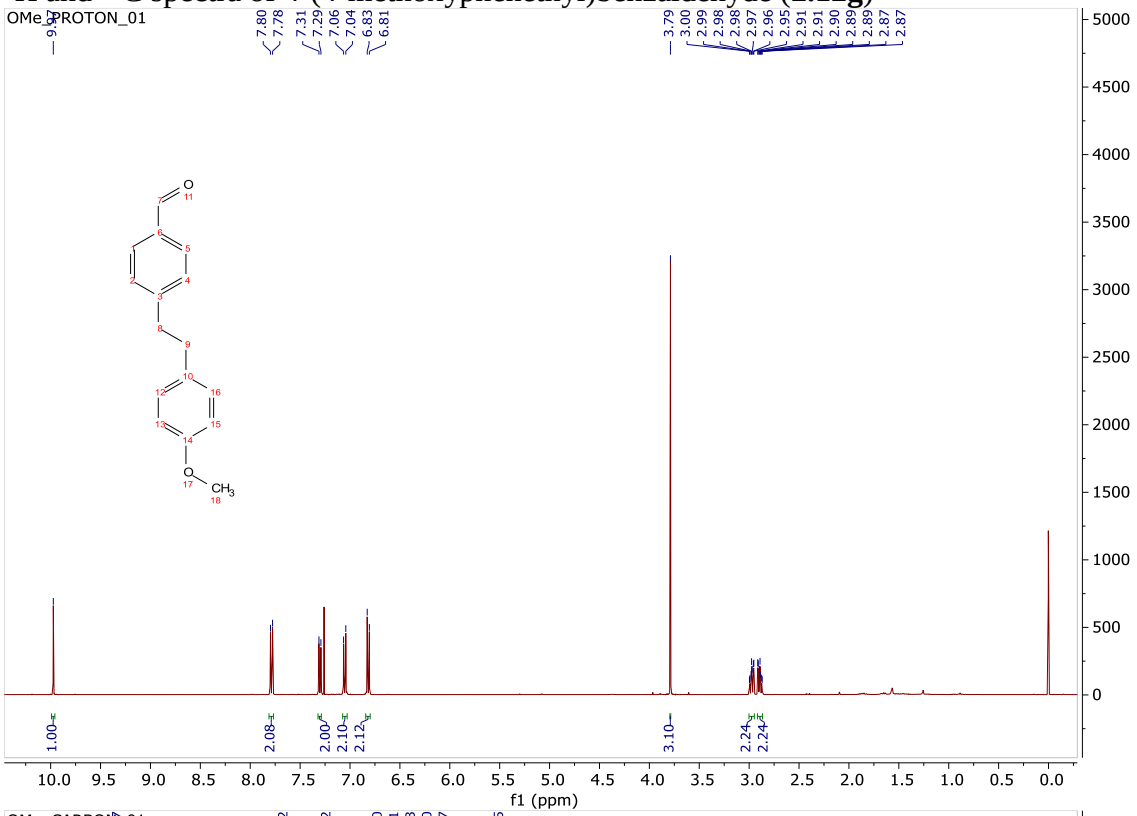


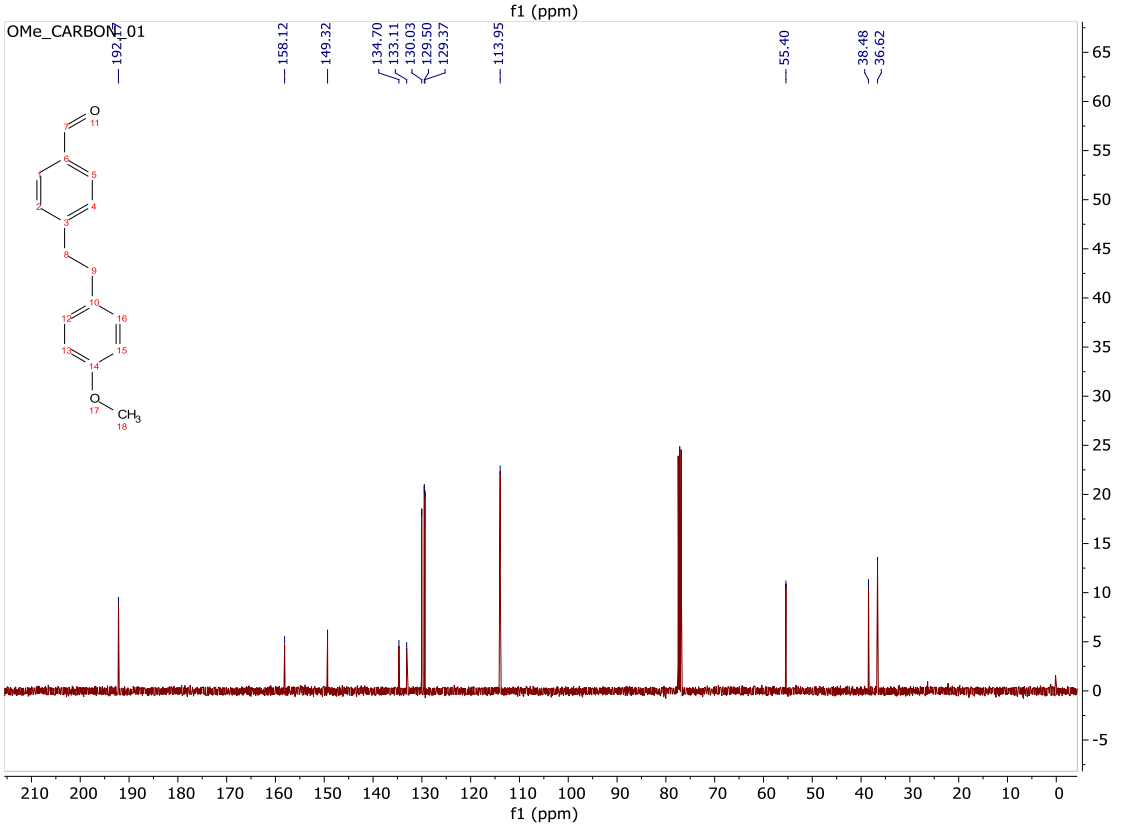

$^{1}$H and $^{13}$C spectra of (*R*)-(1-(4-phenoxybenzyl)pyrrolidin-2-yl)methanol (**2.9a**)

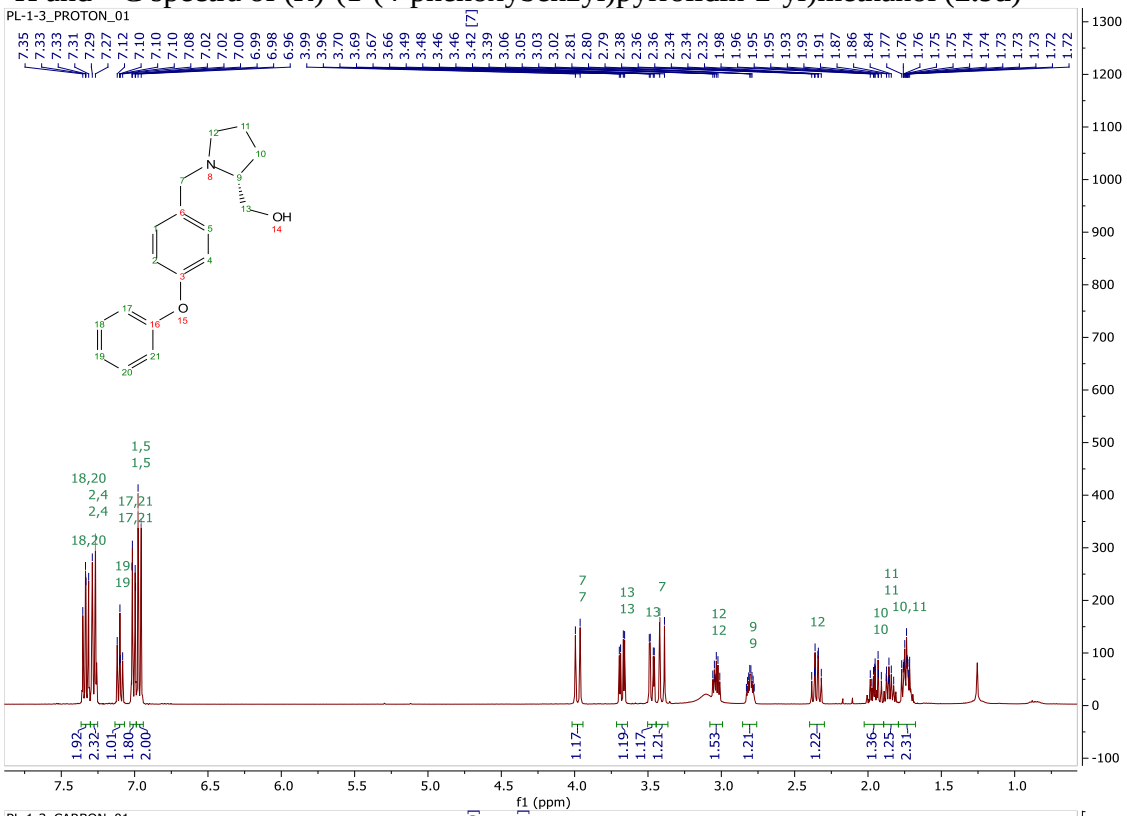


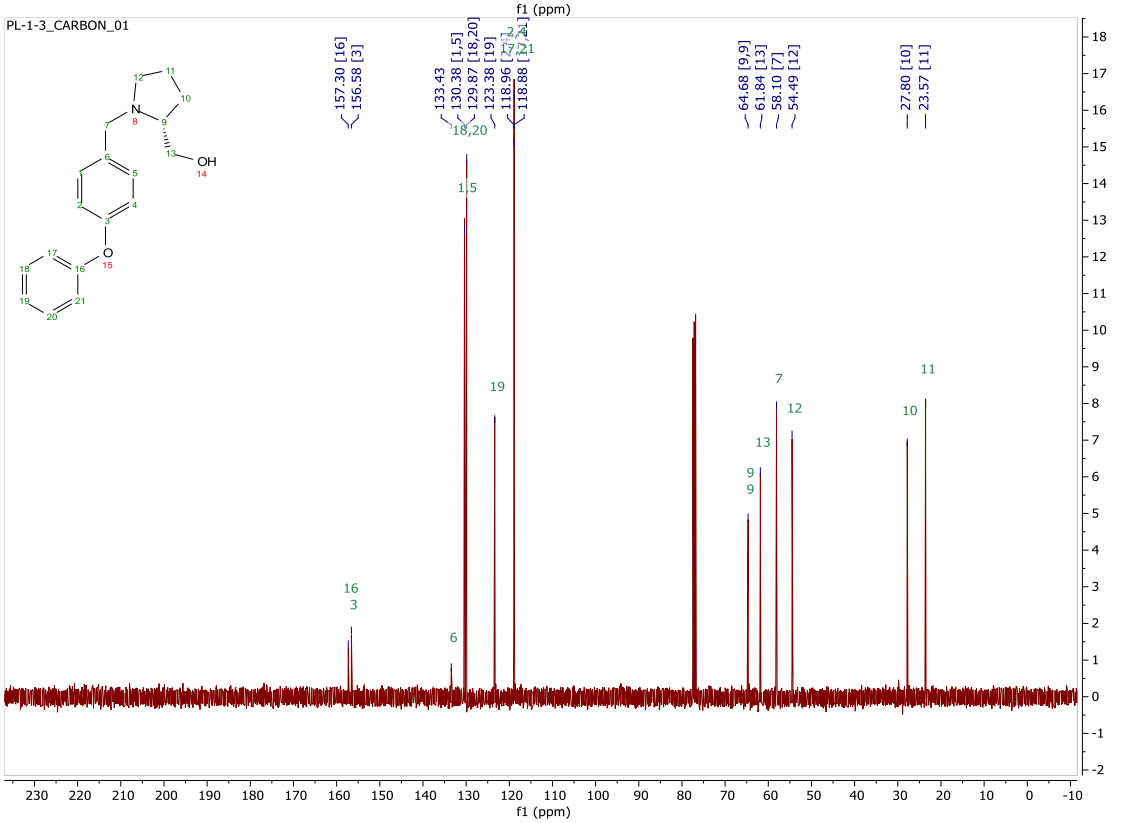

$^{1}H$ and $^{13}C$ spectra of (*R*)-(1-(4-(3-(tert-butyl)phenoxy)benzyl)pyrrolidin-2-yl)methanol (**2.9b**)

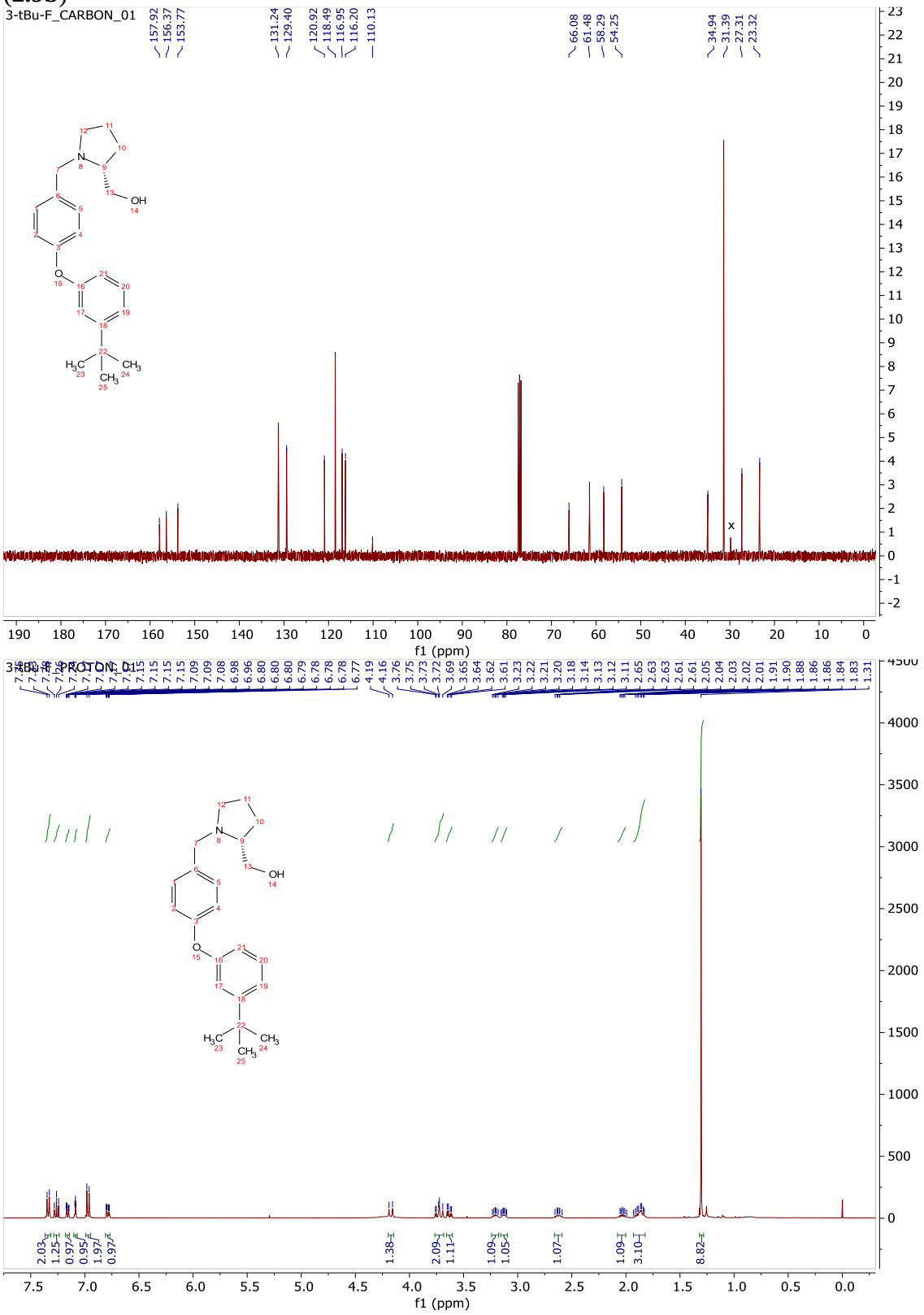

$^{1}$H and $^{13}$C spectra of (*R*)-(1-(4-([1,1'-biphenyl]-3-yloxy)benzyl)pyrrolidin-2-yl)methanol (**2.9c**)

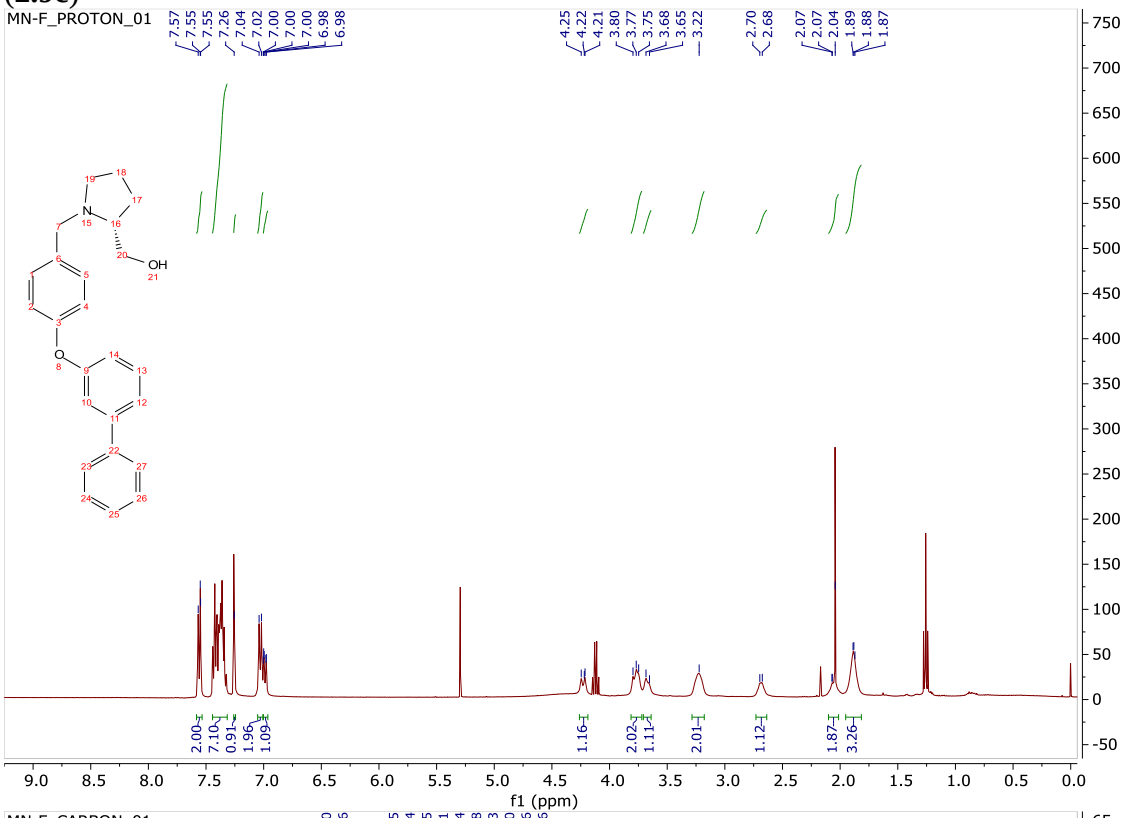


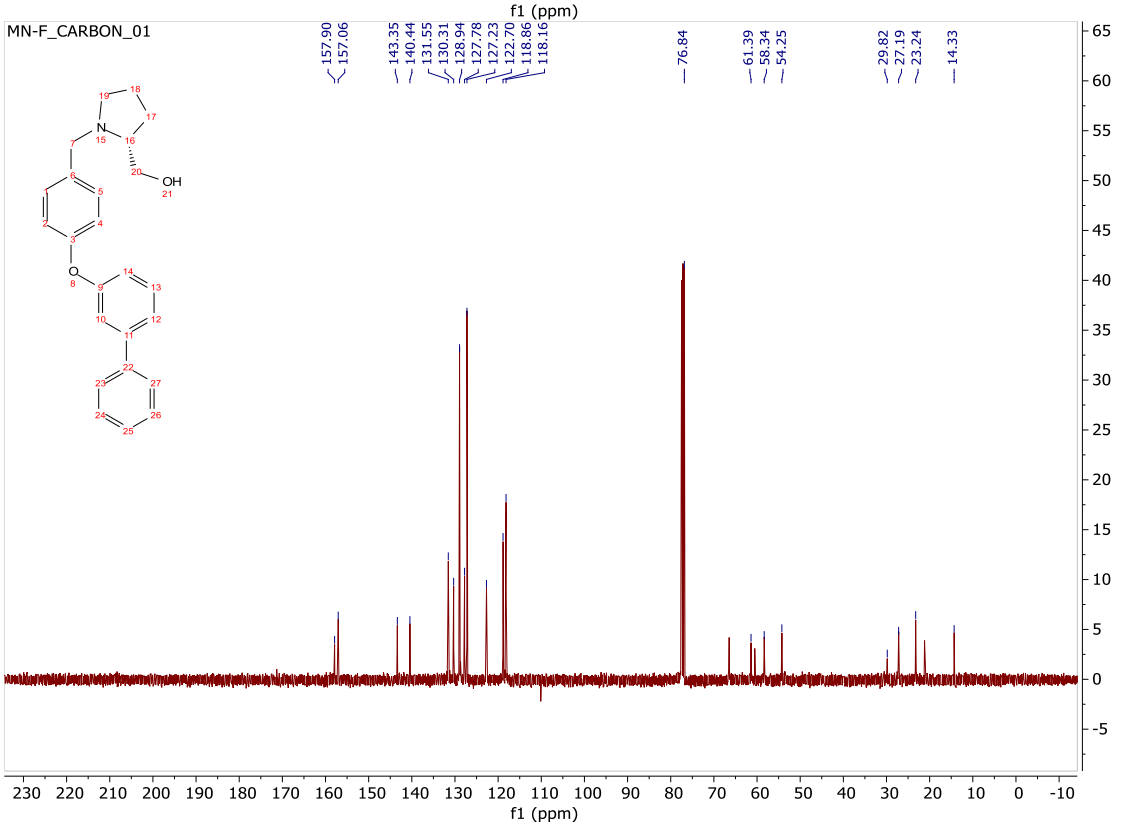

$^{1}H$ and $^{13}C$ spectra of (*R*)-(1-(4-((3'-(trifluoromethyl)-[1,1'-biphenyl]-3-yl)oxy)benzyl)pyrrolidin-2-yl)methanol (**2.9d**)

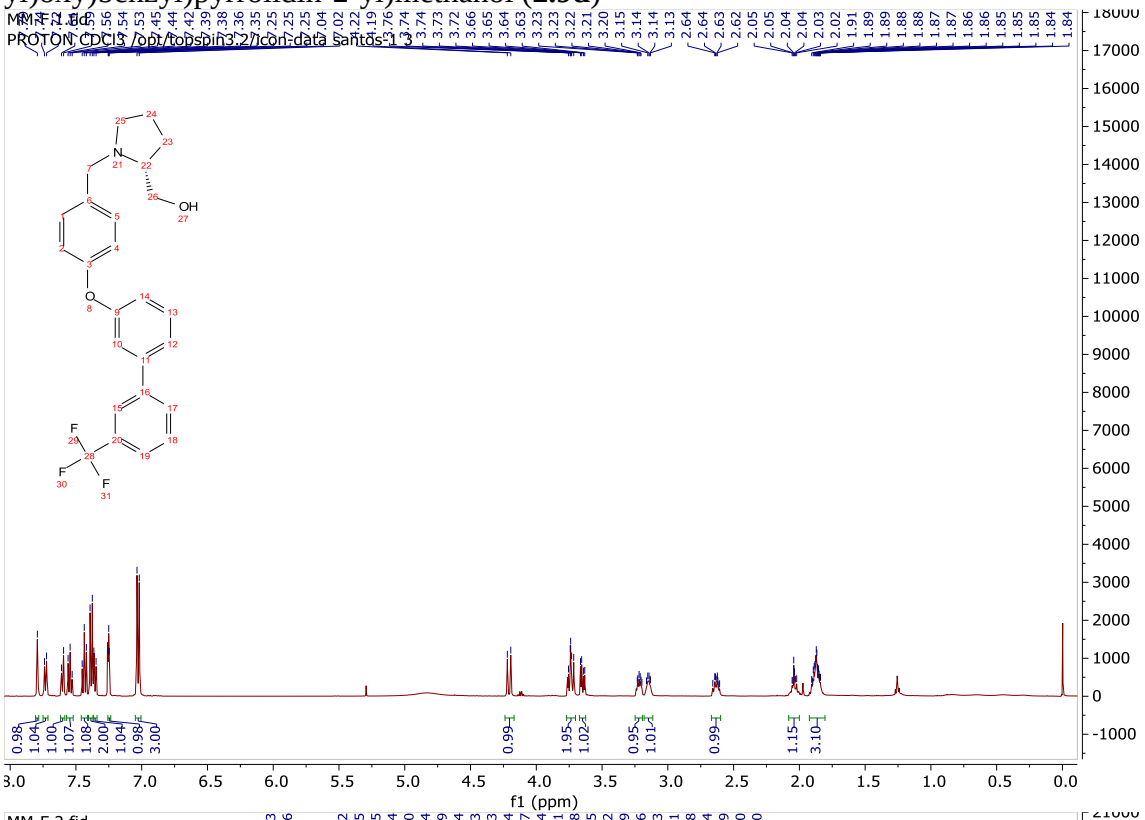


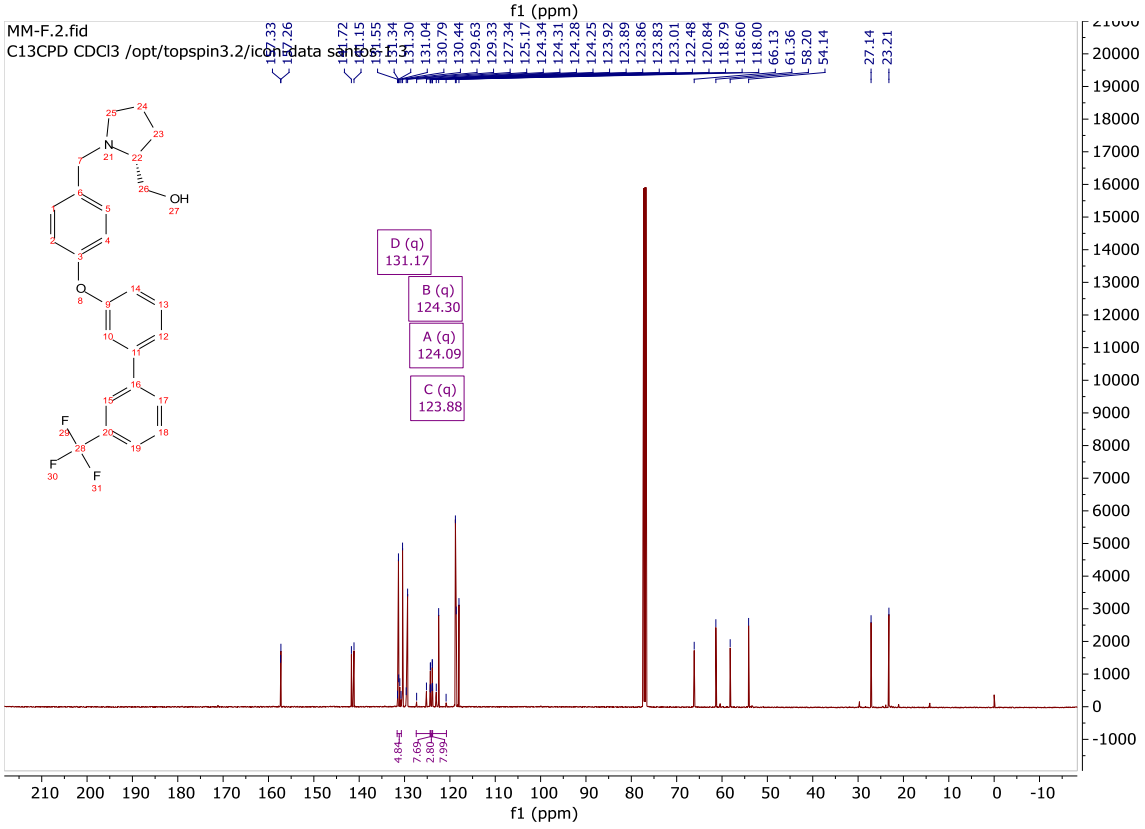

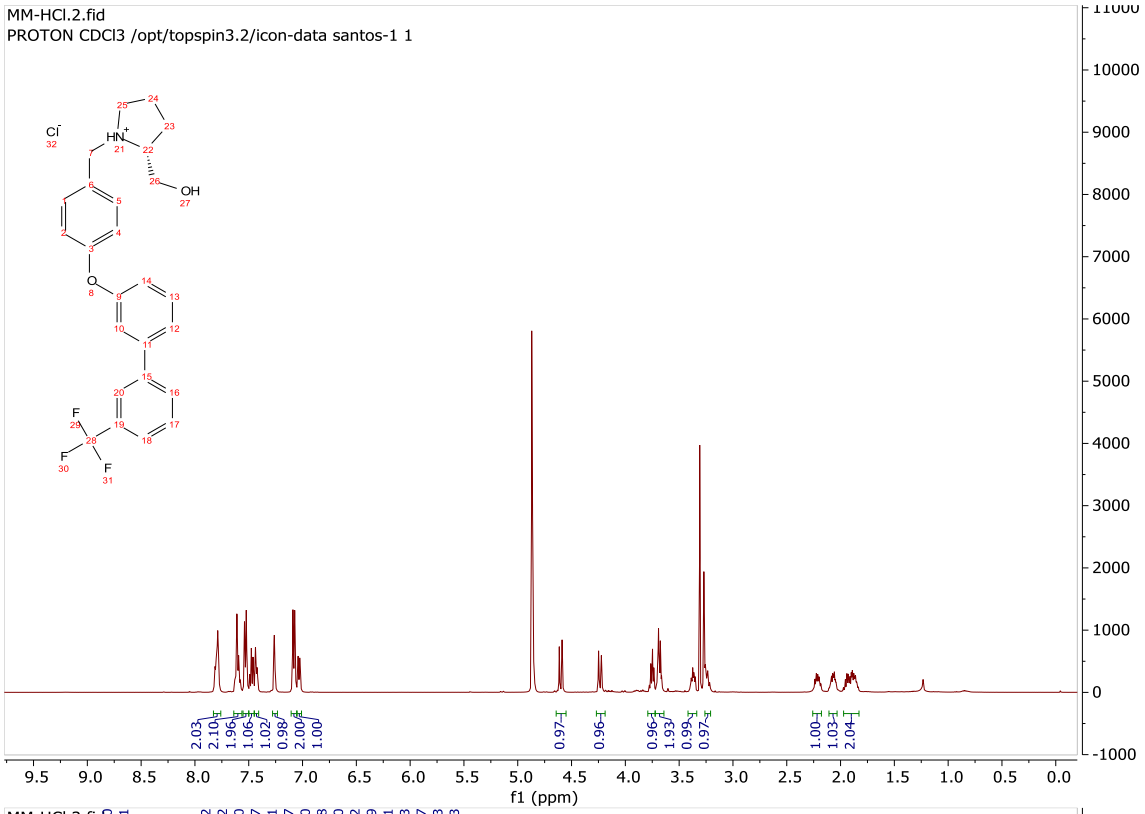
MM-HCl.2.fid
PROTON CDCl3 /opt/topspin3.2/icon-data santos-1 1
2.03
2.10
1.96
1.06
1.02
0.98
2.00
1.00
0.97
0.96
0.96
1.93
0.99
0.97
1.00
1.03
2.04
f1 (ppm)

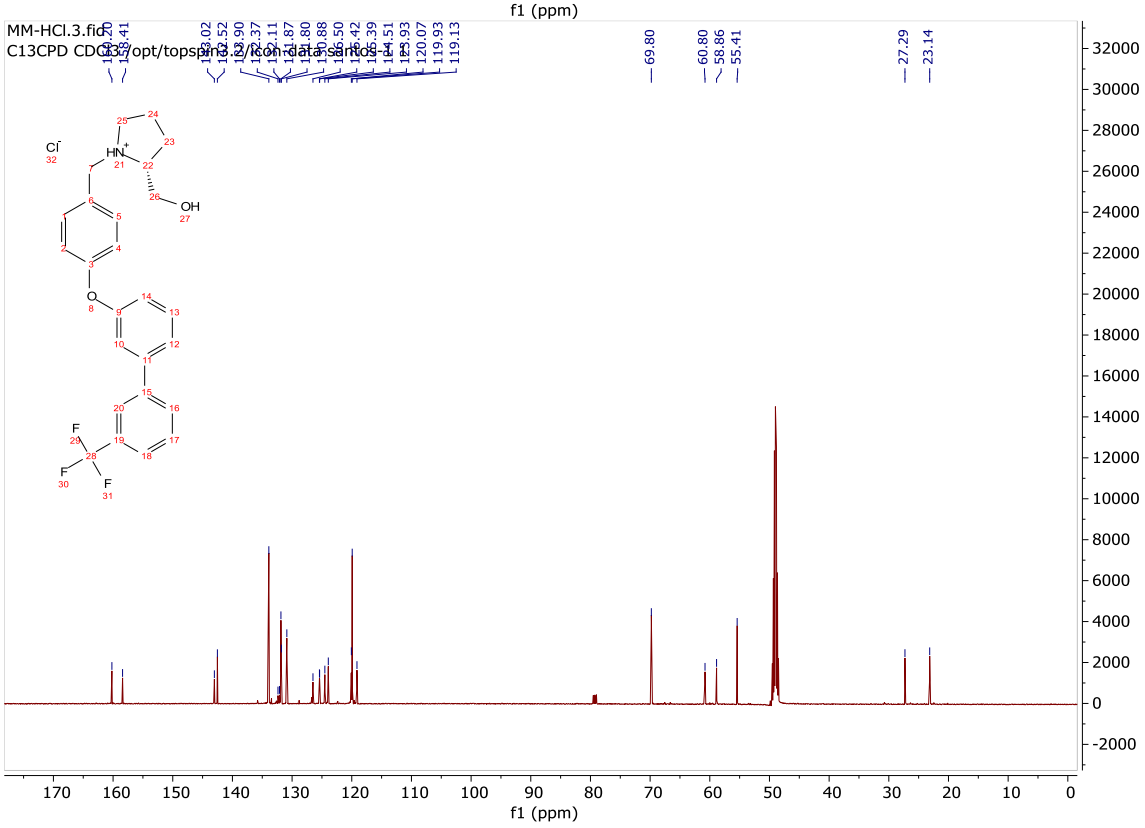
MM-HCl.3.fid
C13CPD CDCl3 /opt/topspin3.2/icon-data santos-1
69.80
60.80
58.86
55.41
27.29
23.14
f1 (ppm)

$^{1}H$ and $^{13}C$ spectra of (*R*)-(1-(4-((4'-(trifluoromethyl)-[1,1'-biphenyl]-3-yl)oxy)benzyl)pyrrolidin-2-yl)methanol (**2.9e**)

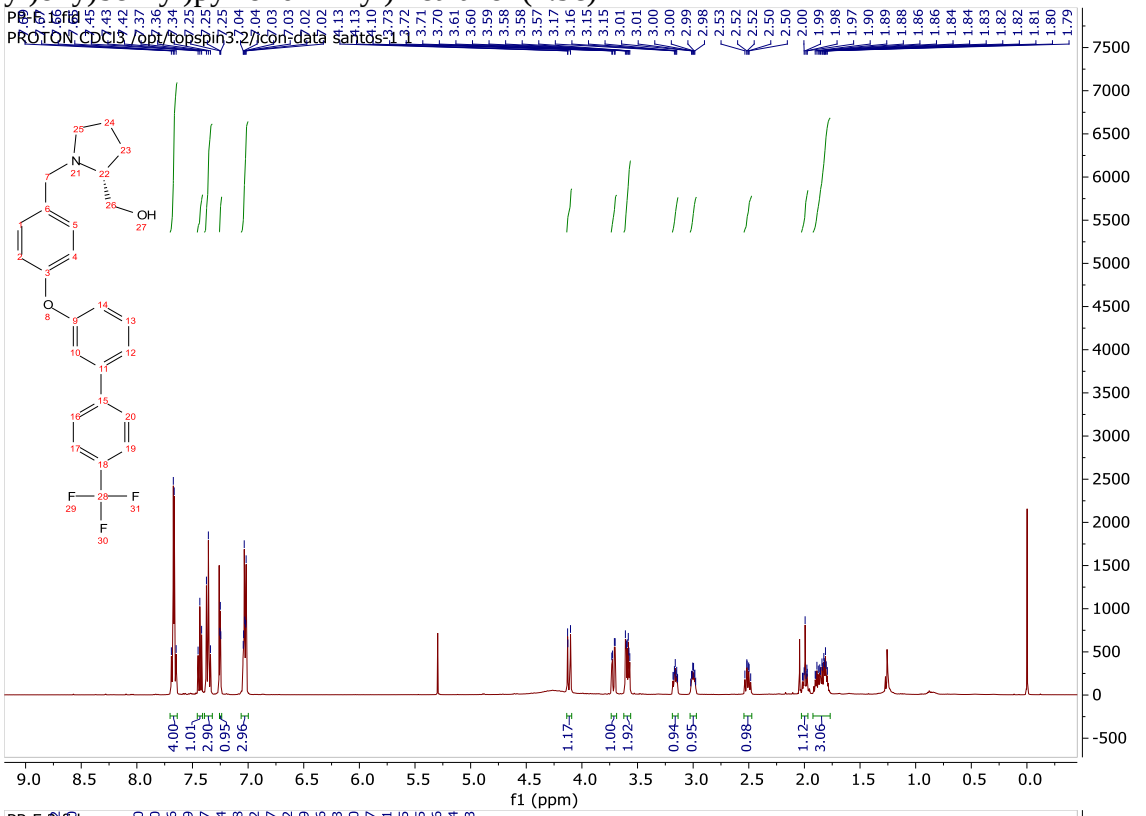


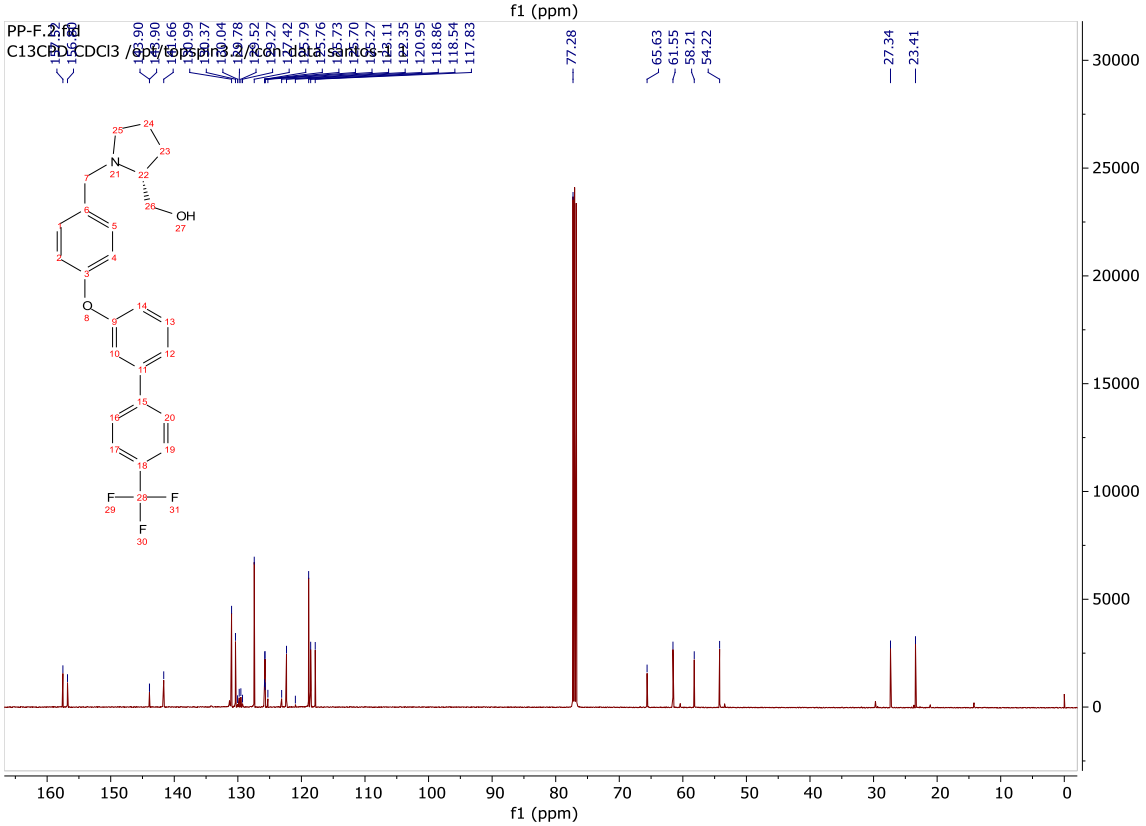

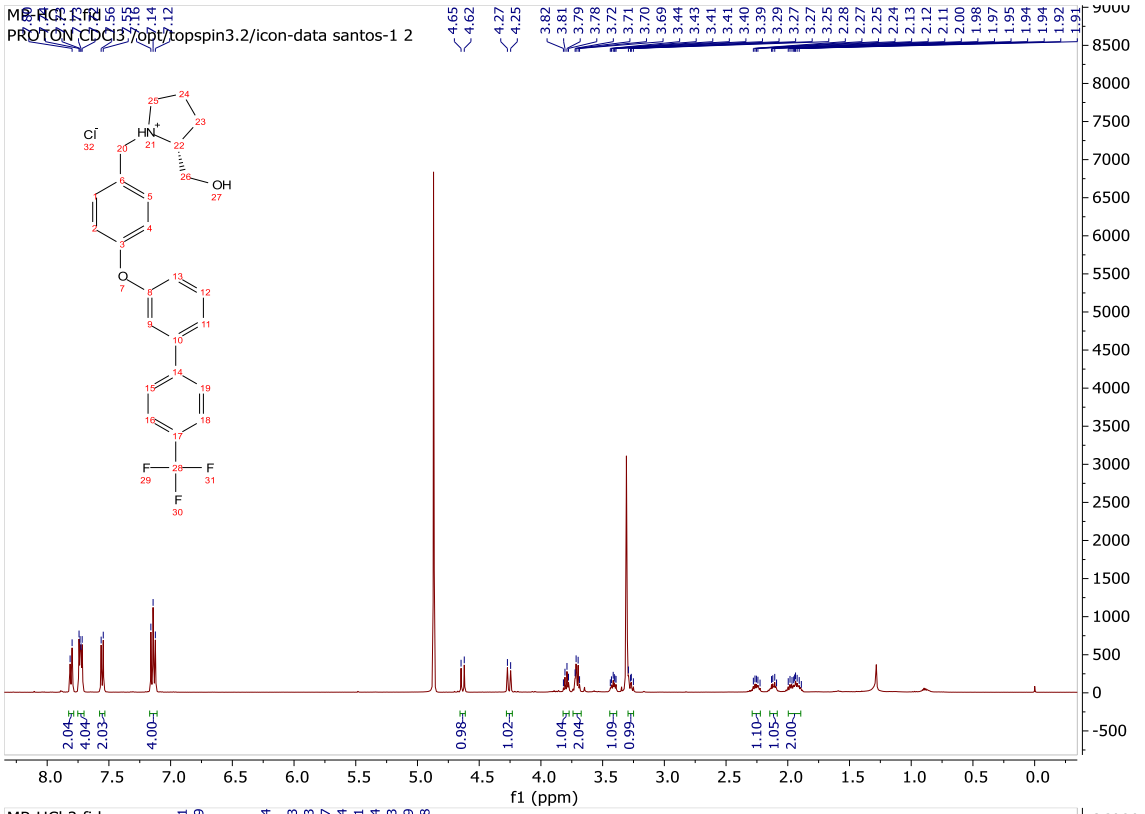
MP-HCl.1.fid
PROTON CDCl3 /opt/topspin3.2/icon-data santos-1 2
f1 (ppm)

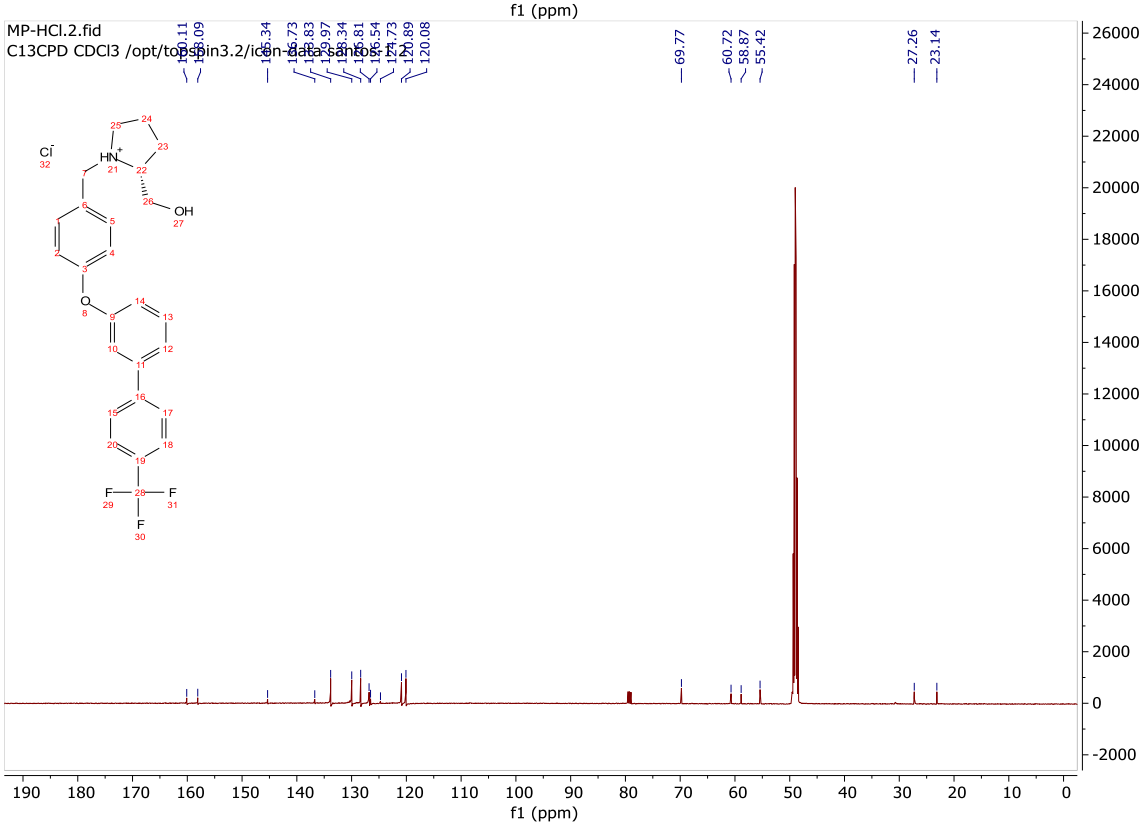
MP-HCl.2.fid
C13CPD CDCl3 /opt/topspin3.2/icon-data santos-1 2
f1 (ppm)

$^{1}H$ and $^{13}C$ spectra of (*R*)-(1-(4-(4-(tert-butyl)phenoxy)benzyl)pyrrolidin-2-yl)methanol (**2.9f**)

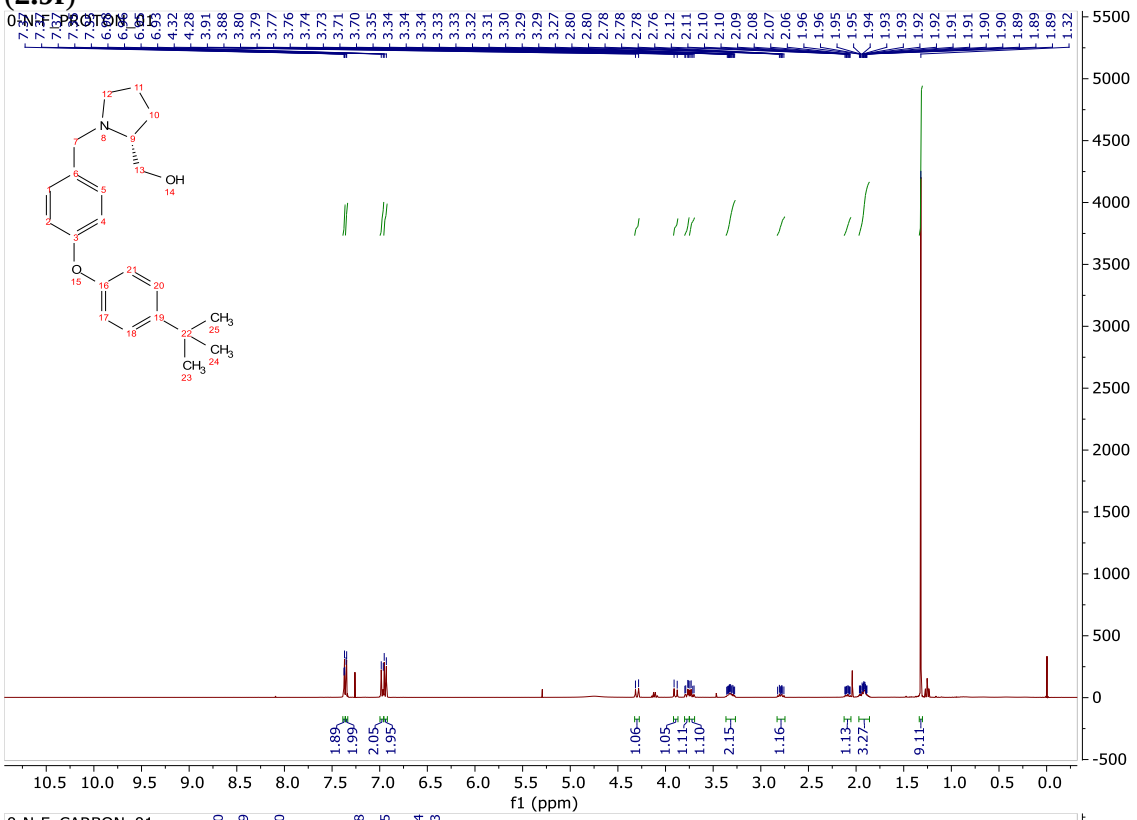


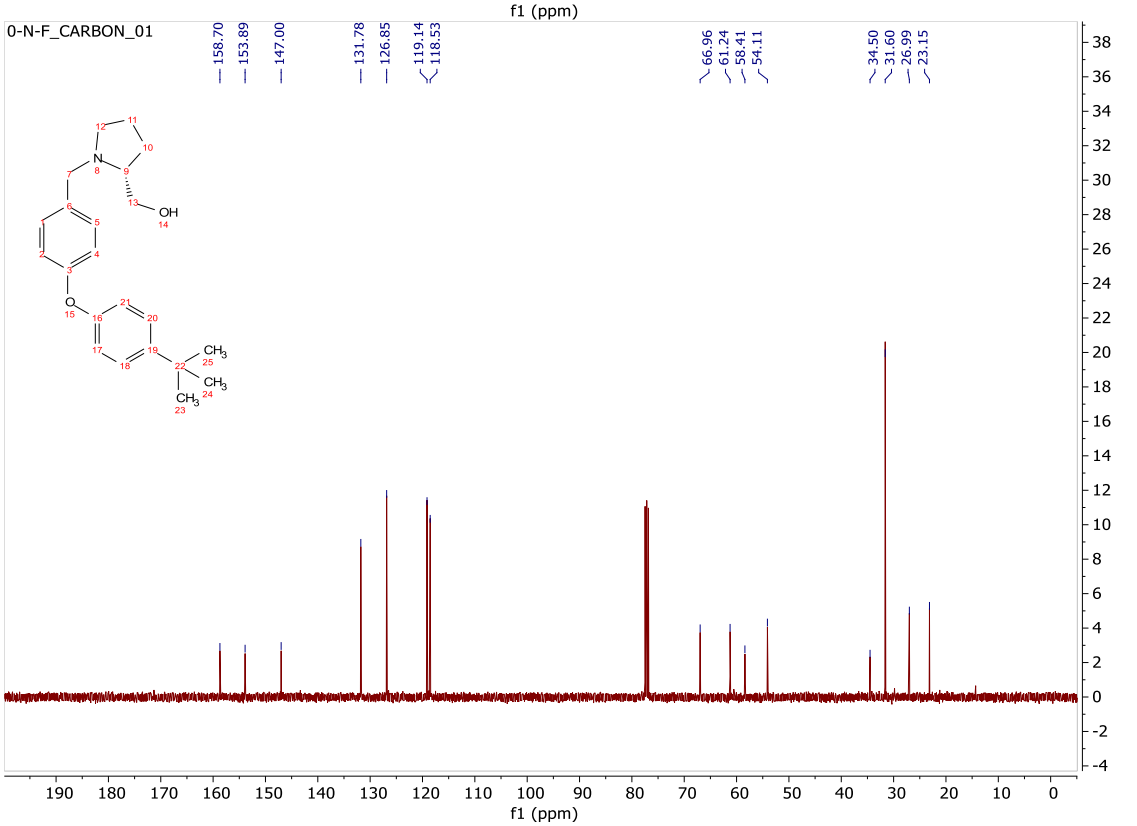

$^{1}H$ and $^{13}C$ spectra of (*R*)-(1-(4-((3'-(trifluoromethyl)-[1,1'-biphenyl]-4-yl)oxy)benzyl)pyrrolidin-2-yl)methanol (**2.9h**)

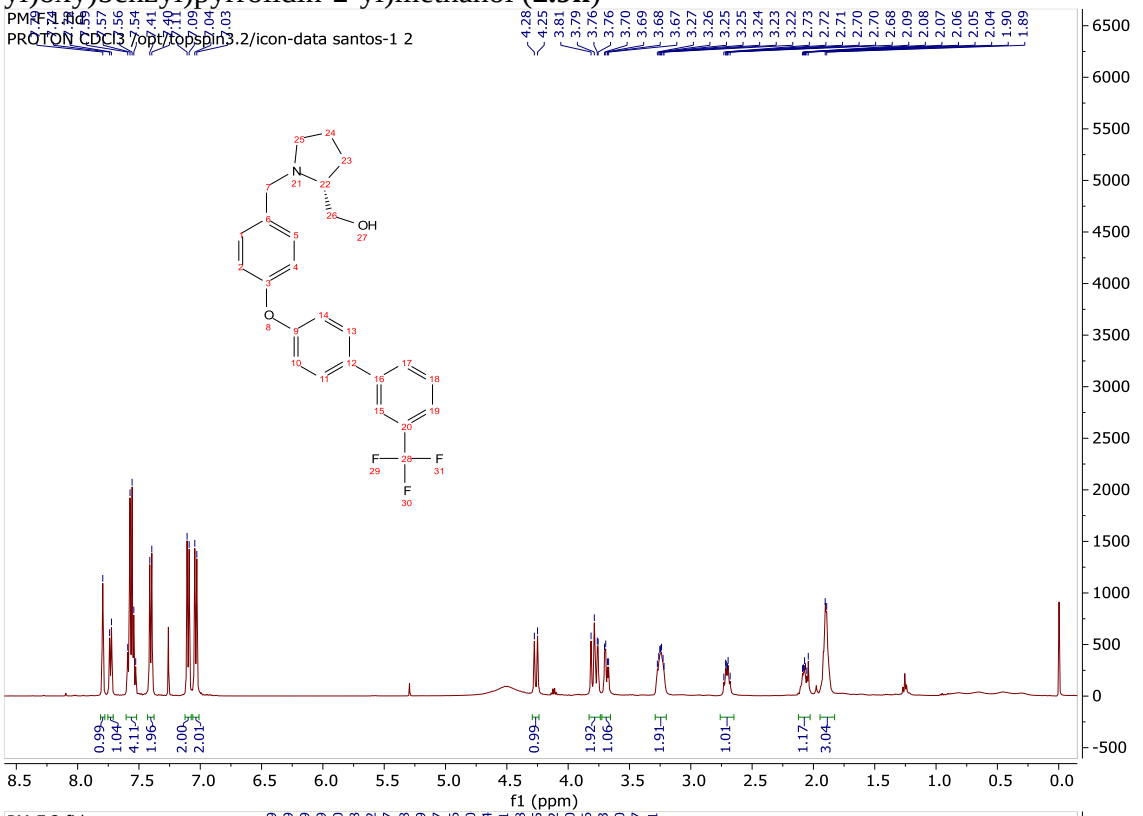


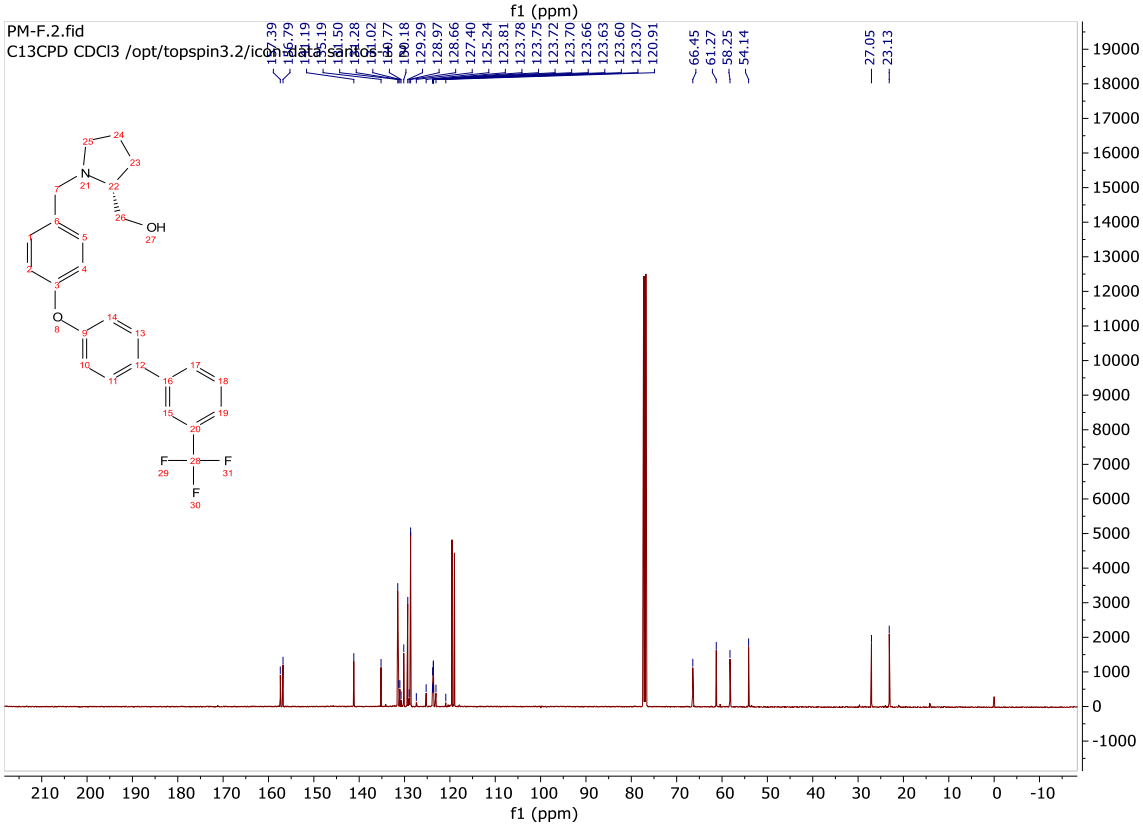

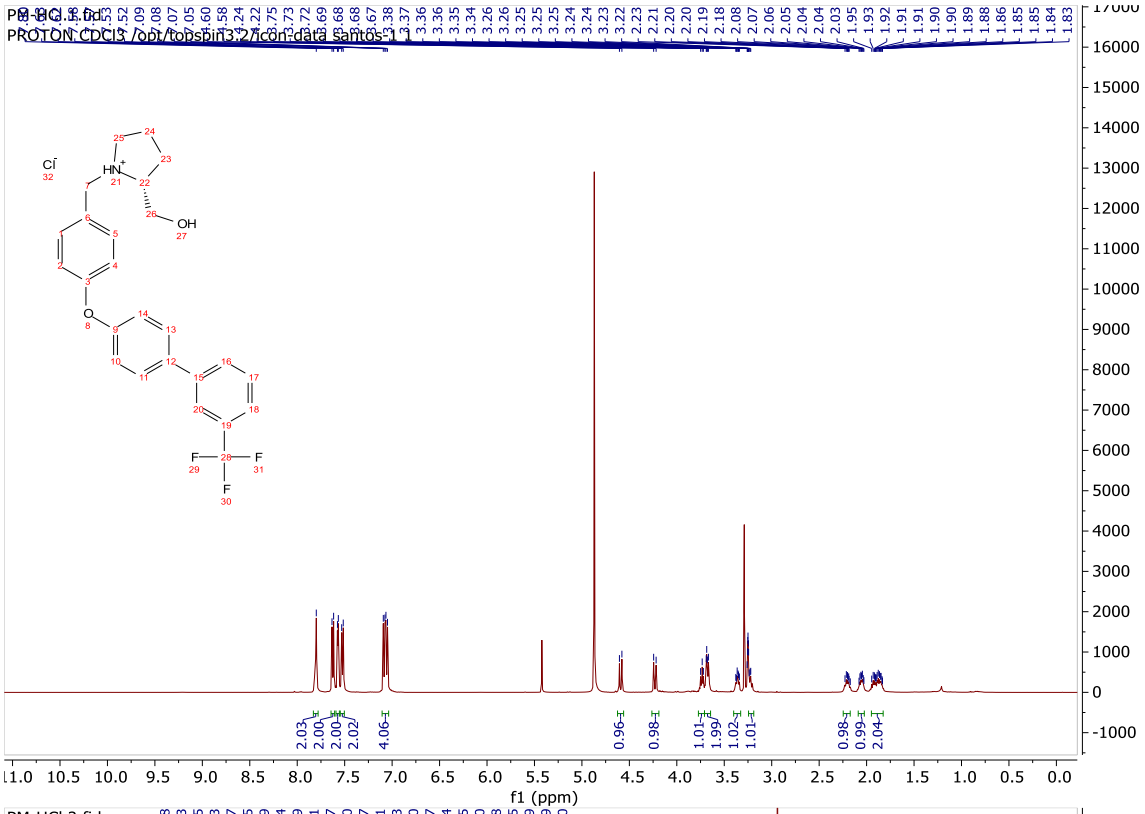
PM-HCl.8.fid
PROTON CDCl3 /opt/topspin3.2/icon-data santos 1
Cl
32
HN
21
OH
27
O
8
F
29
28
31
F
30
2.03
2.00
2.00
2.02
4.06
0.96
0.98
1.01
1.99
1.02
1.01
0.98
0.99
2.04
f1 (ppm)

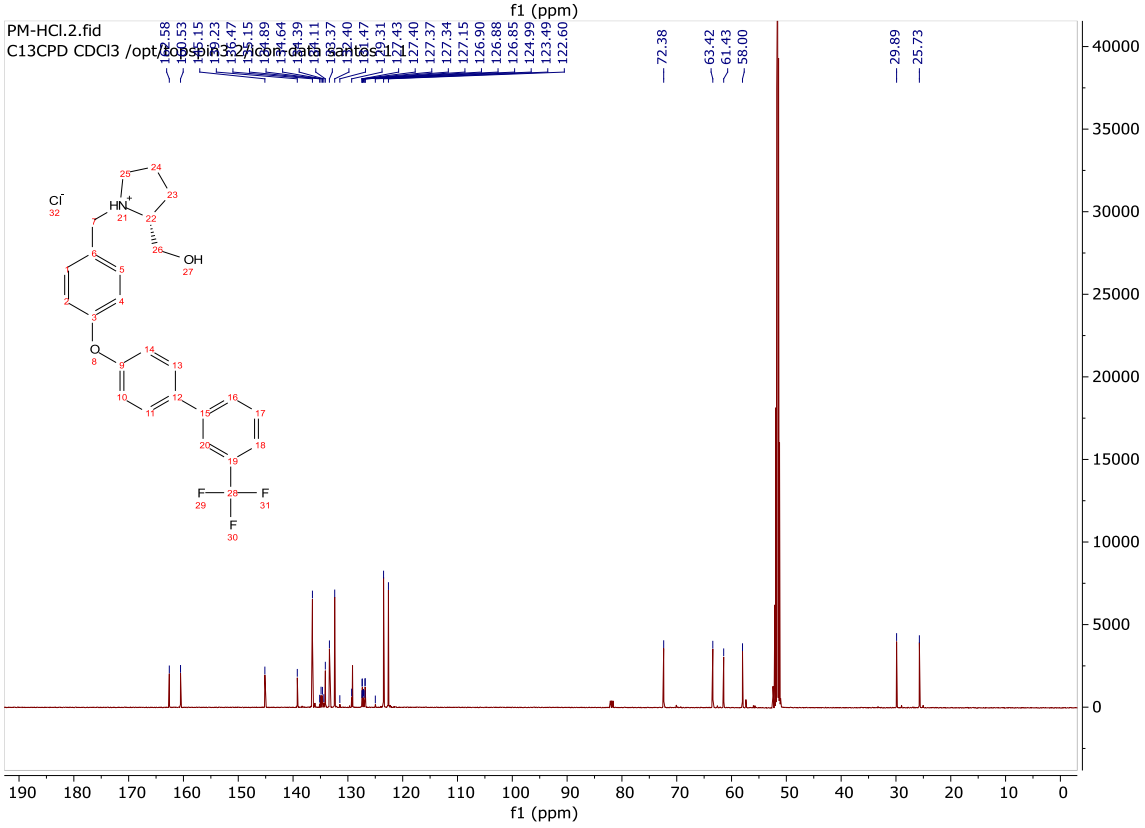
PM-HCl.2.fid
C13CPD CDCl3 /opt/topspin3.2/icon-data santos 1 2
72.38
63.42
61.43
58.00
29.89
25.73
Cl
32
HN
21
OH
27
O
8
F
29
28
31
F
30
f1 (ppm)

$^{1}H$ and $^{13}C$ spectra of (*R*)-(1-(4-((4'-(trifluoromethyl)-[1,1'-biphenyl]-4-yl)oxy)benzyl)pyrrolidin-2-yl)methanol (**2.9i**)

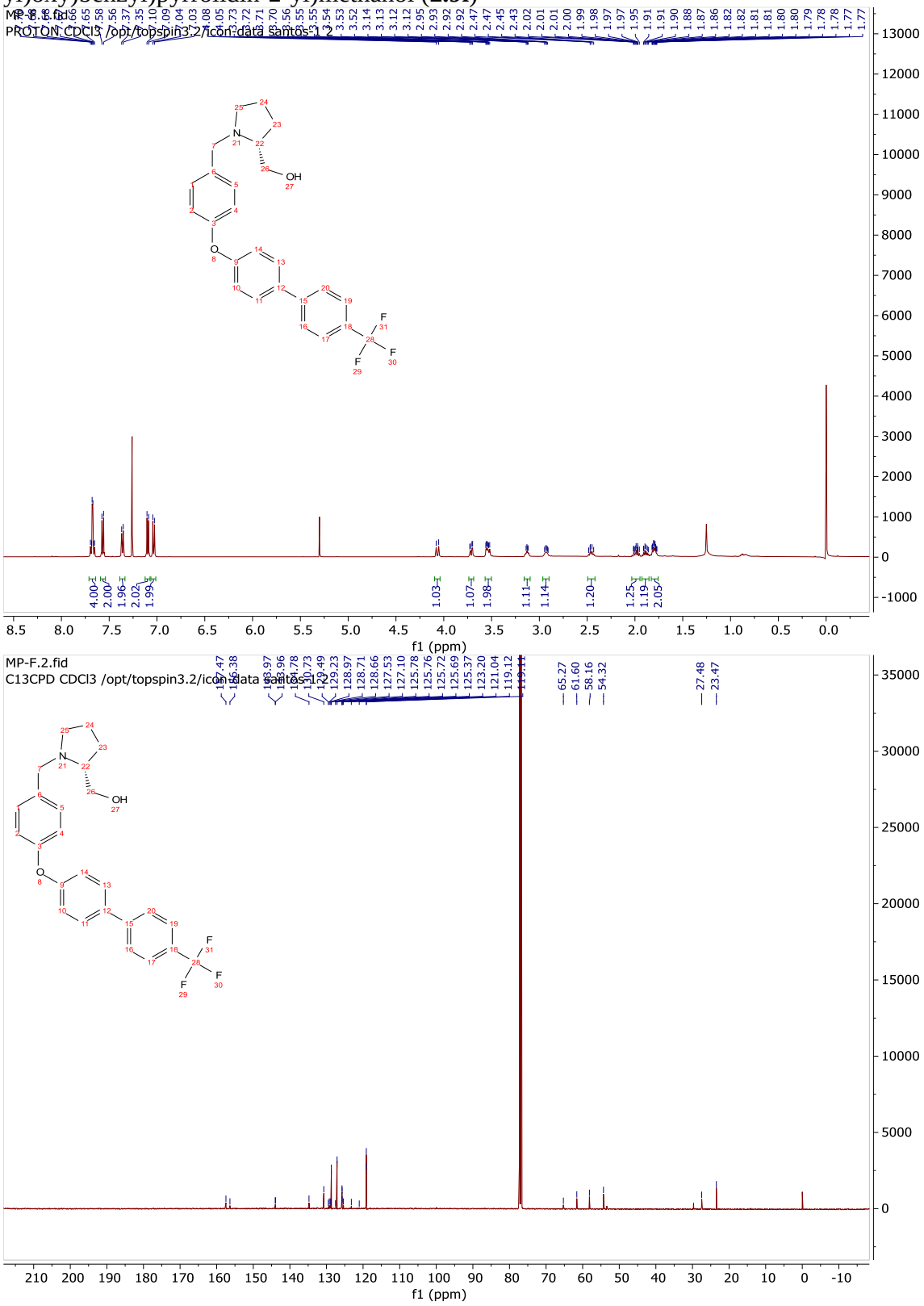

$^{1}H$ and $^{13}C$ spectra of (*R*)-(1-(4-nonylbenzyl)pyrrolidin-2-yl)methanol (**2.13a**)

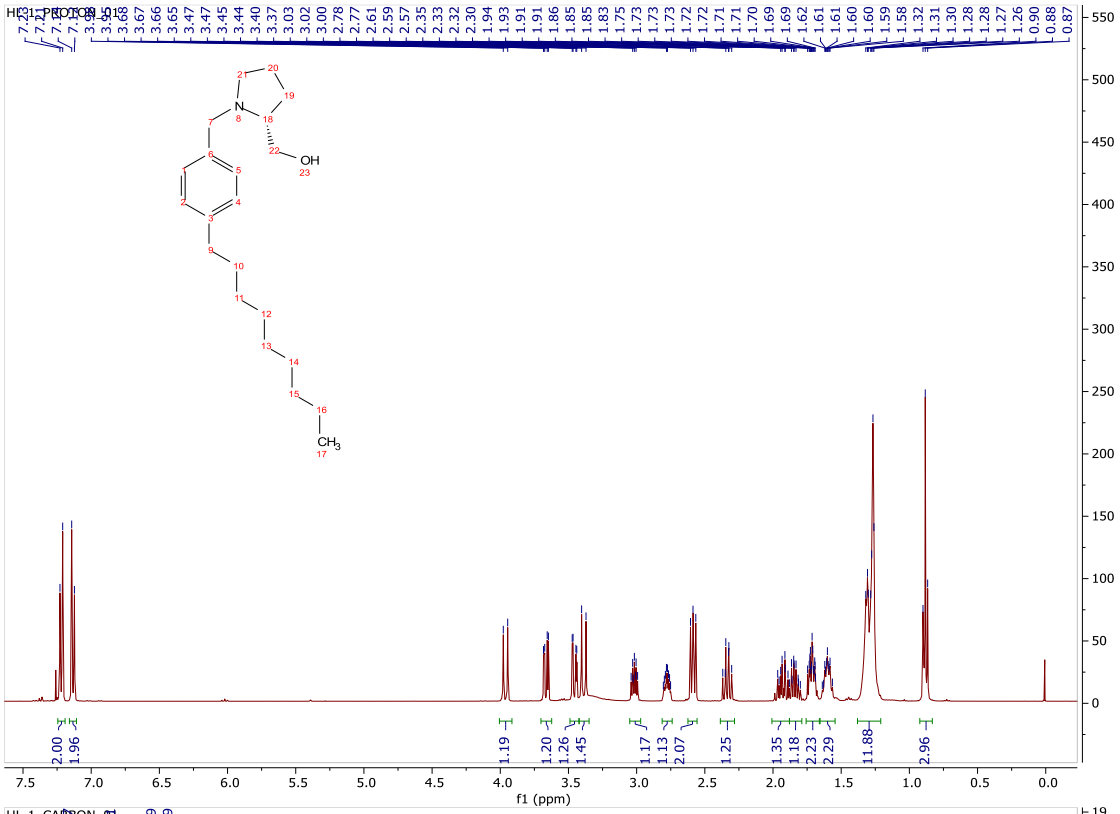


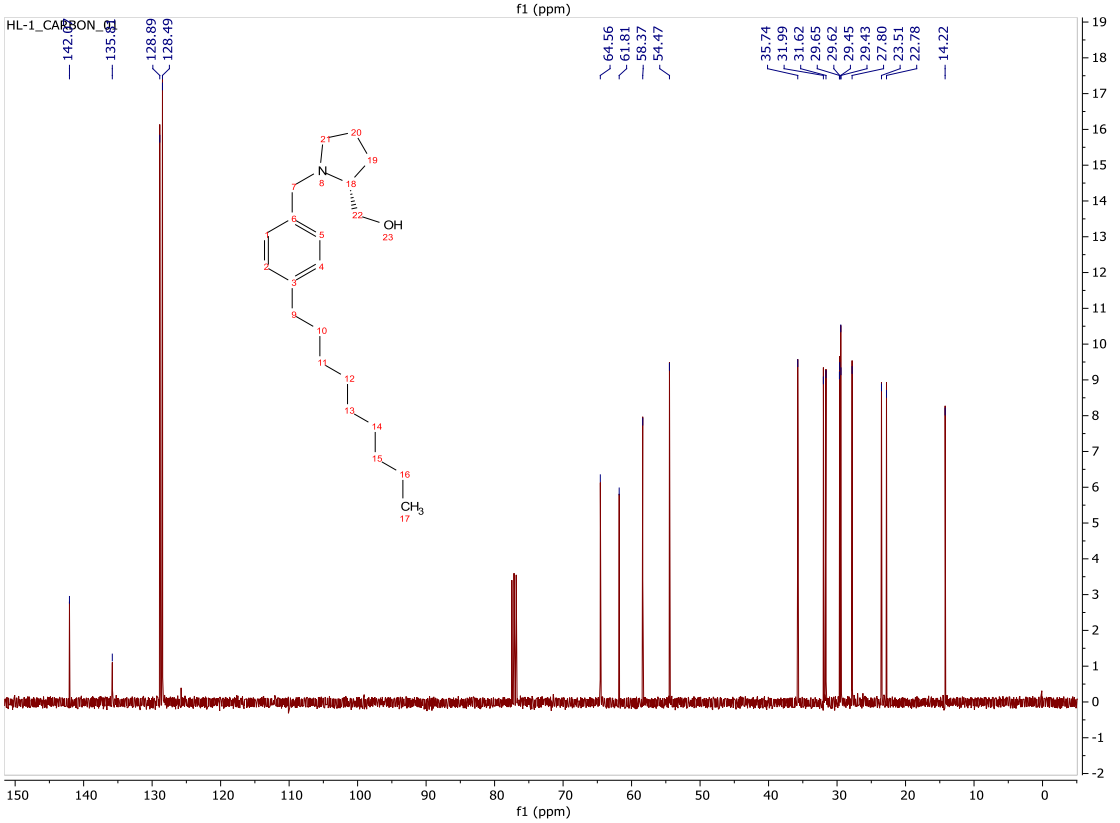

$^{1}$H and $^{13}$C spectra of (*R*)-(1-(4-decylbenzyl)pyrrolidin-2-yl)methanol (**2.13b**)

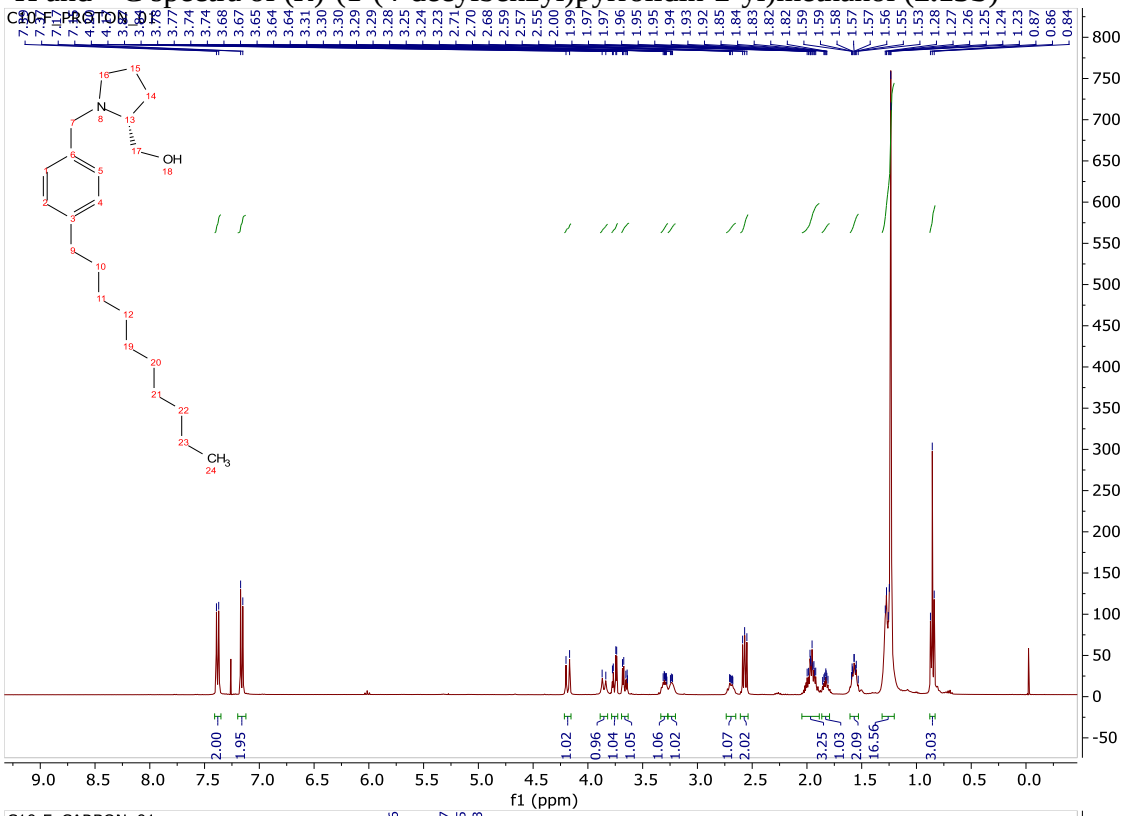


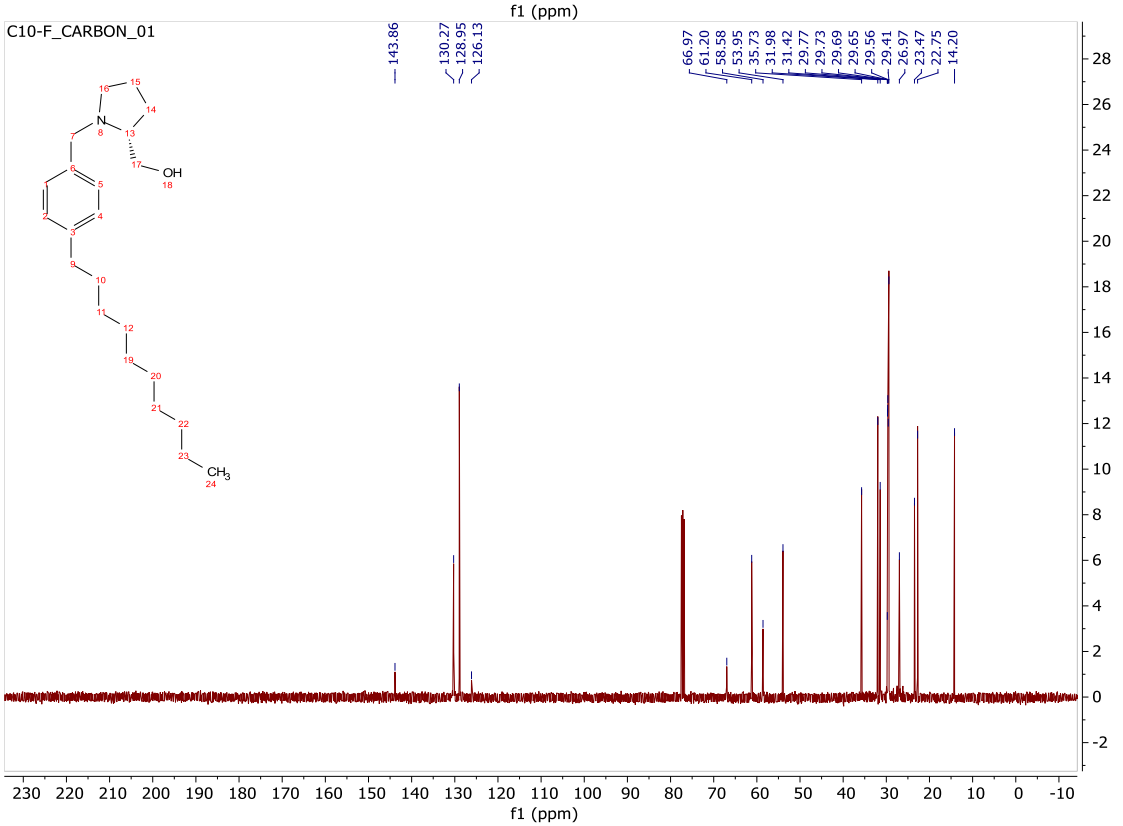

$^{1}H$ and $^{13}C$ spectra of (*R*)-(1-(4-undecylbenzyl)pyrrolidin-2-yl)methanol (**2.13c**)

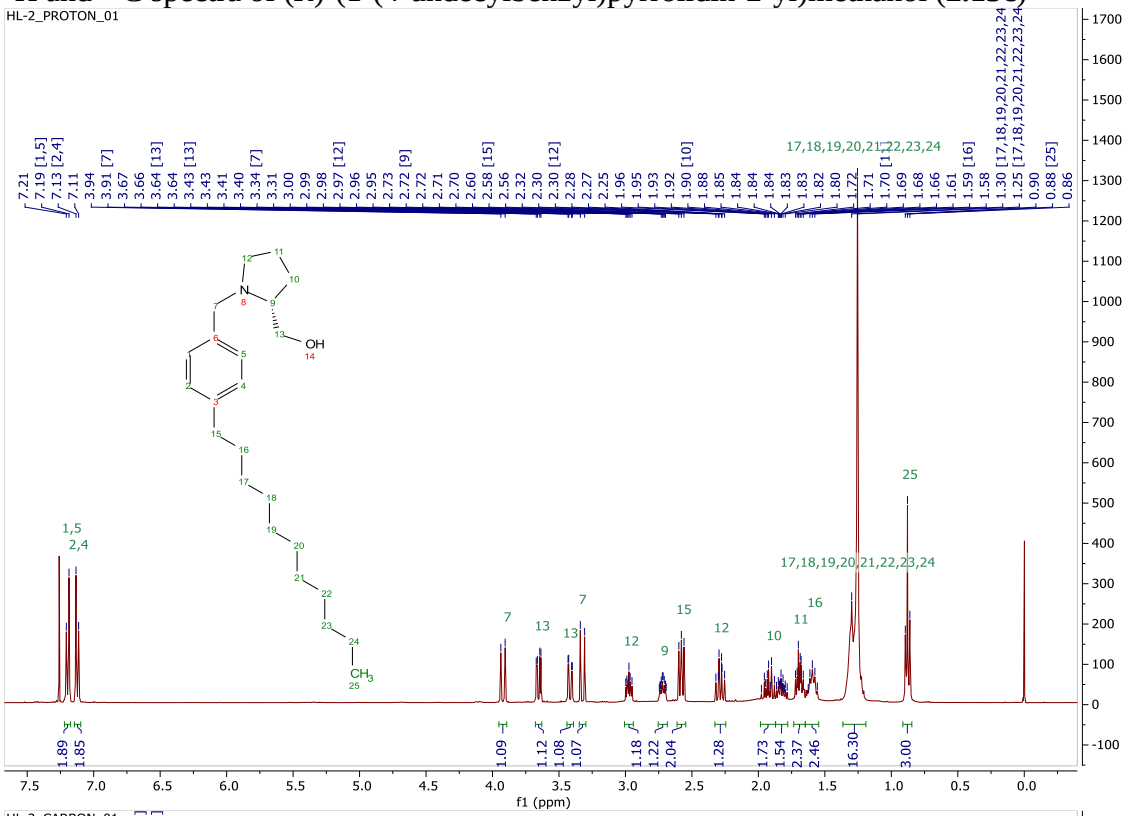


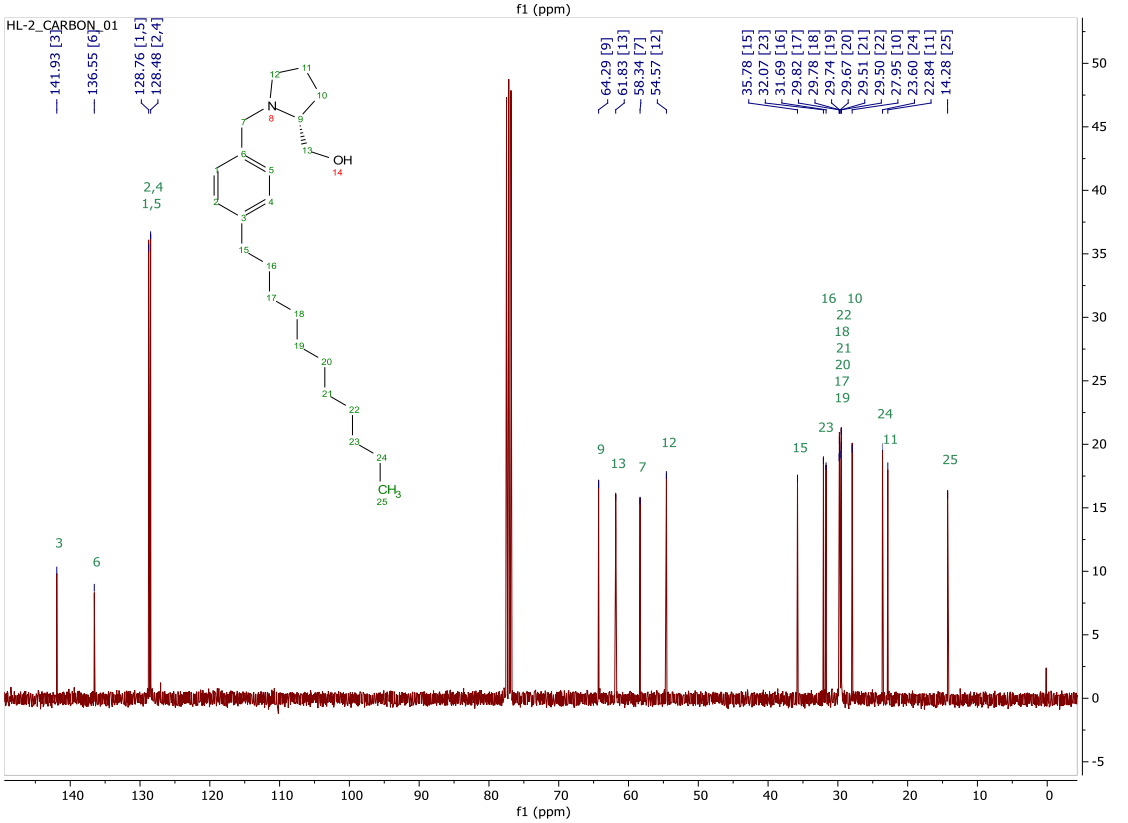

(*R*)-(1-(4-dodecylbenzyl)pyrrolidin-2-yl)methanol (**2.13d**)

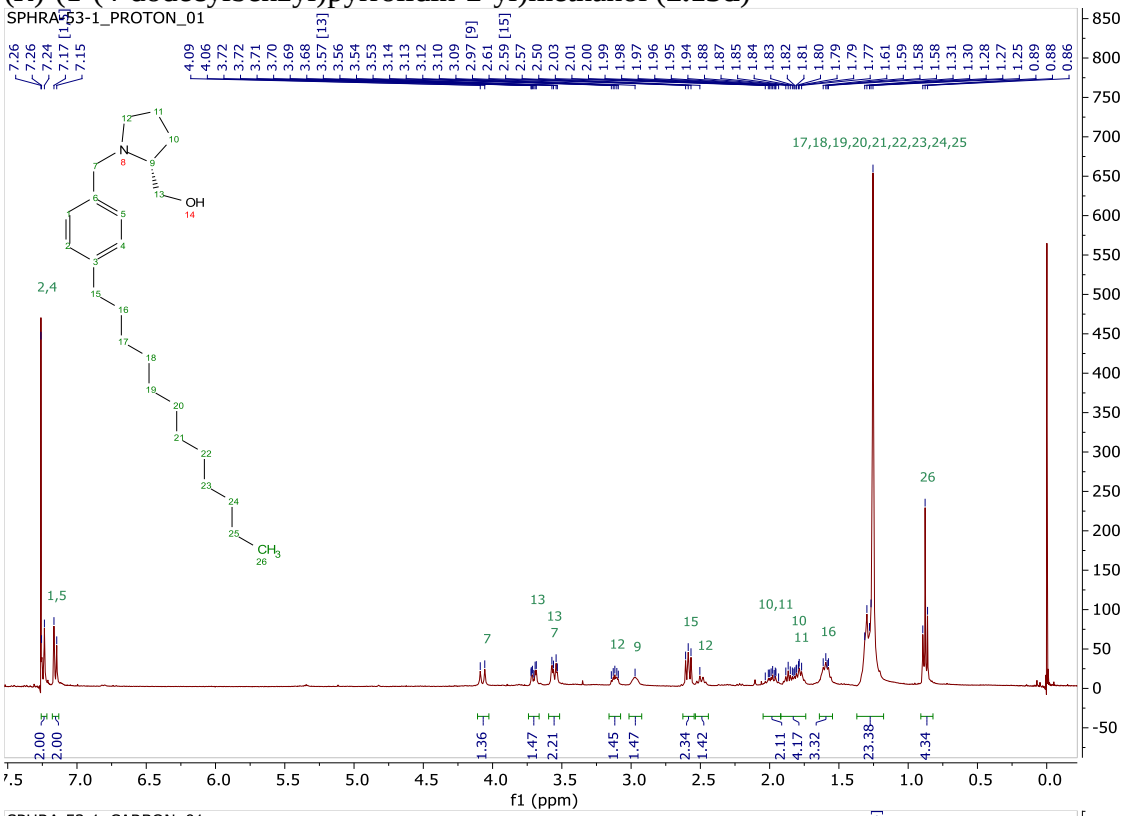


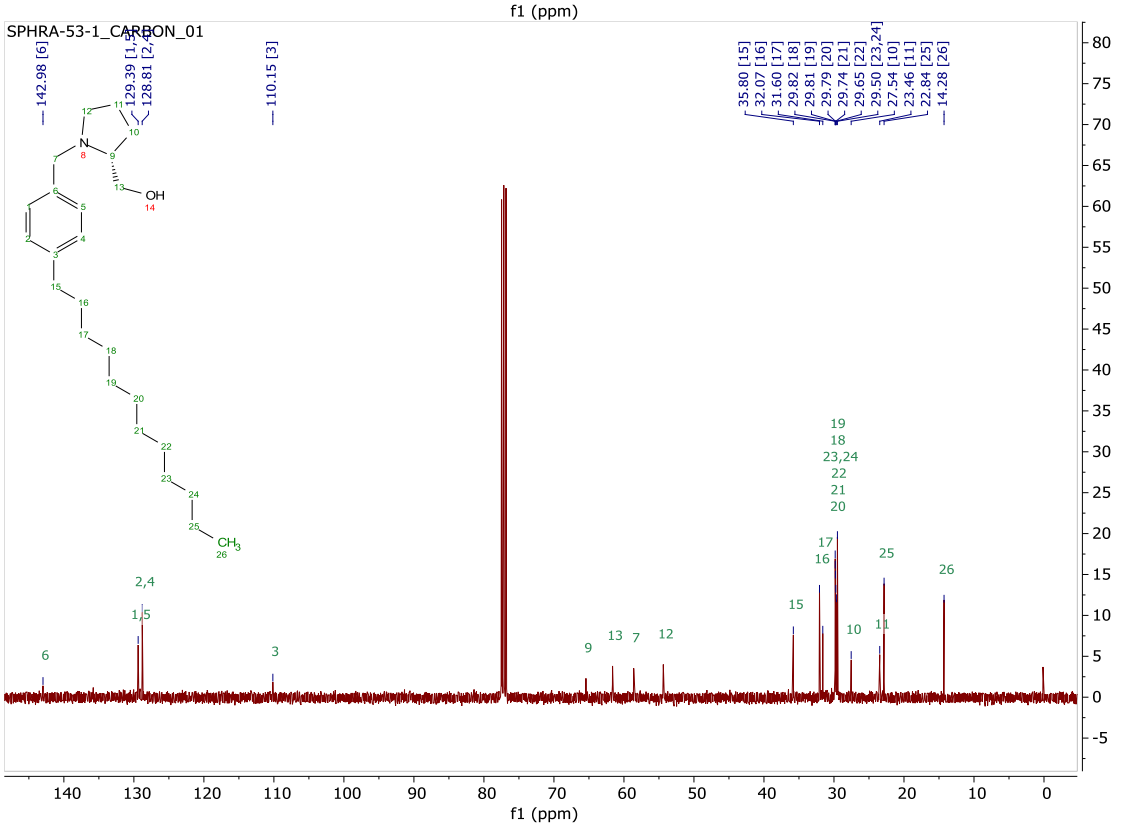

$^{1}H$ and $^{13}C$ spectra of (*R*)-(1-(4-(4-methylphenethyl)benzyl)pyrrolidin-2-yl)methanol (**2.13g**)

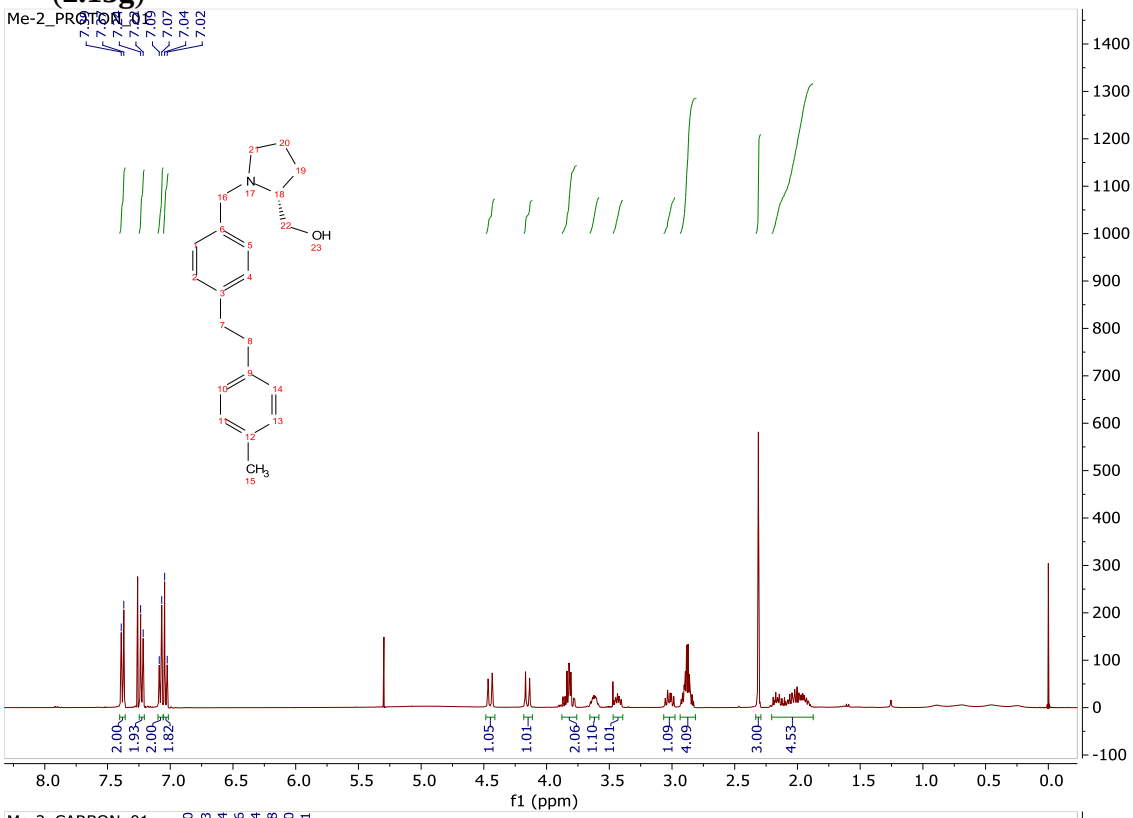


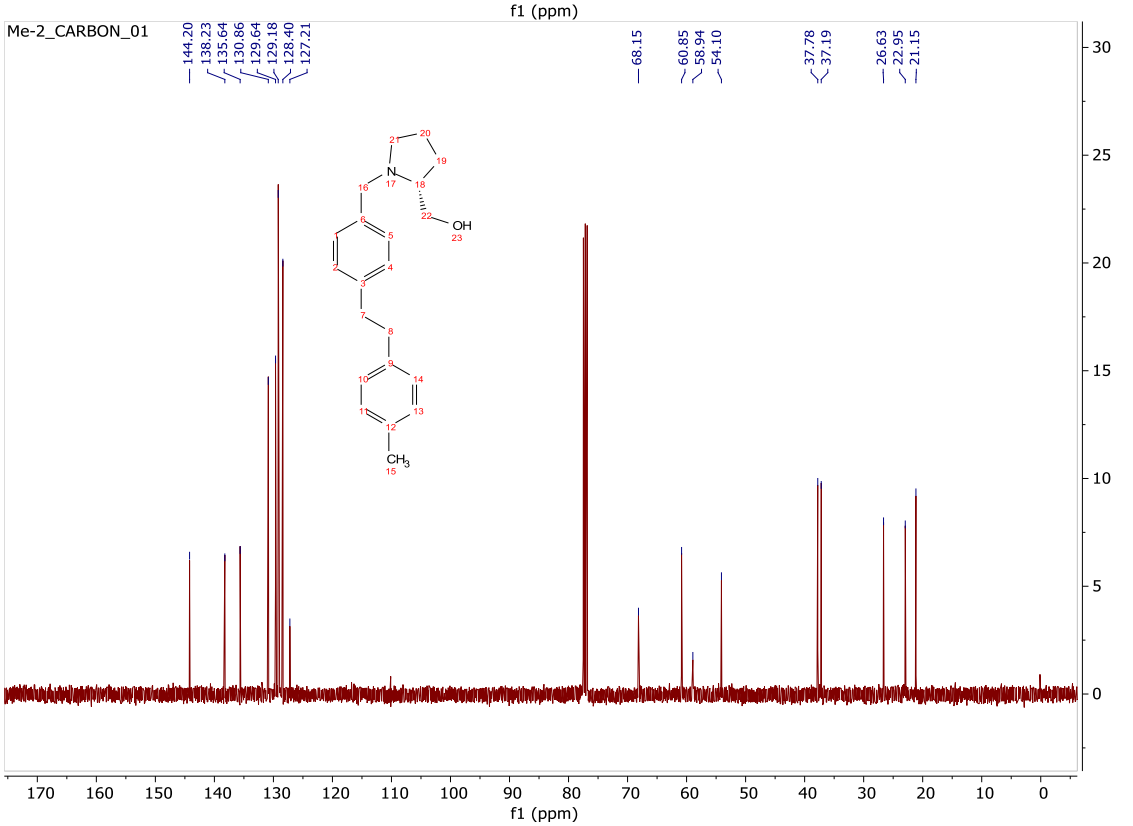

$^{1}H$ and $^{13}C$ spectra of (*R*)-(1-(4-(4-methylphenethyl)benzyl)pyrrolidin-2-yl)methanol (**2.13h**)

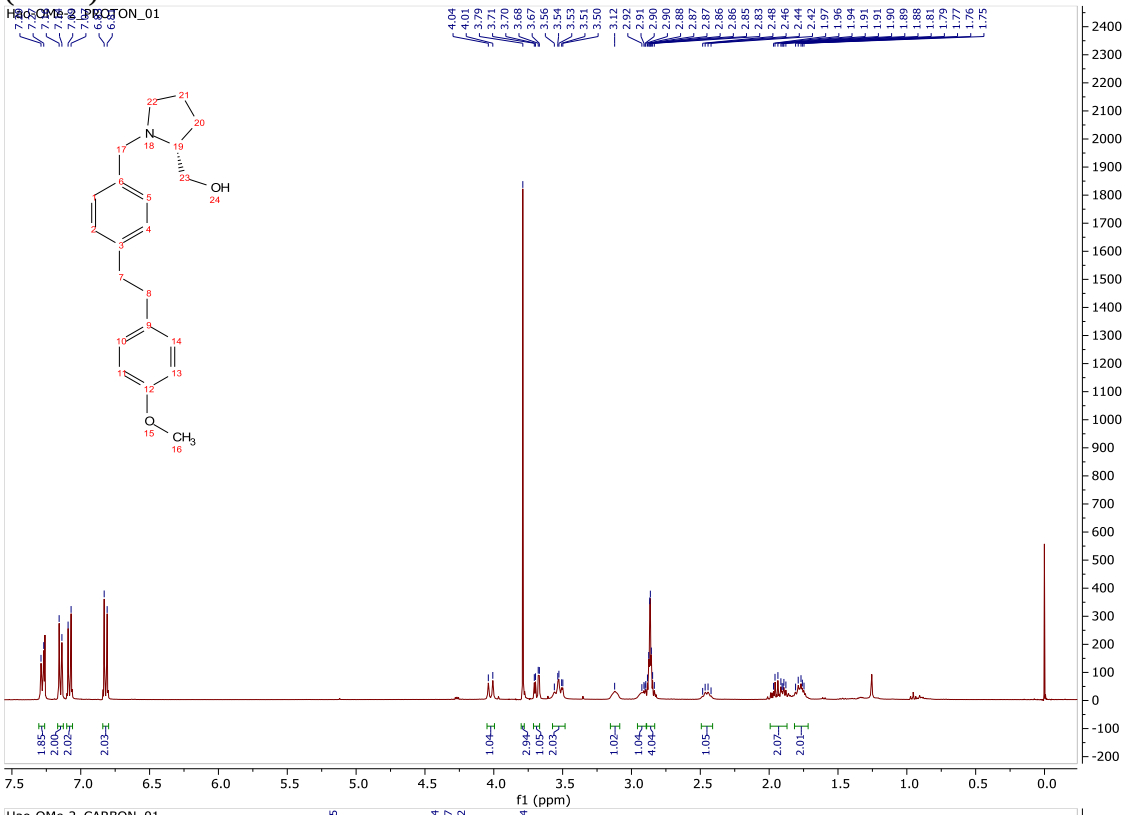


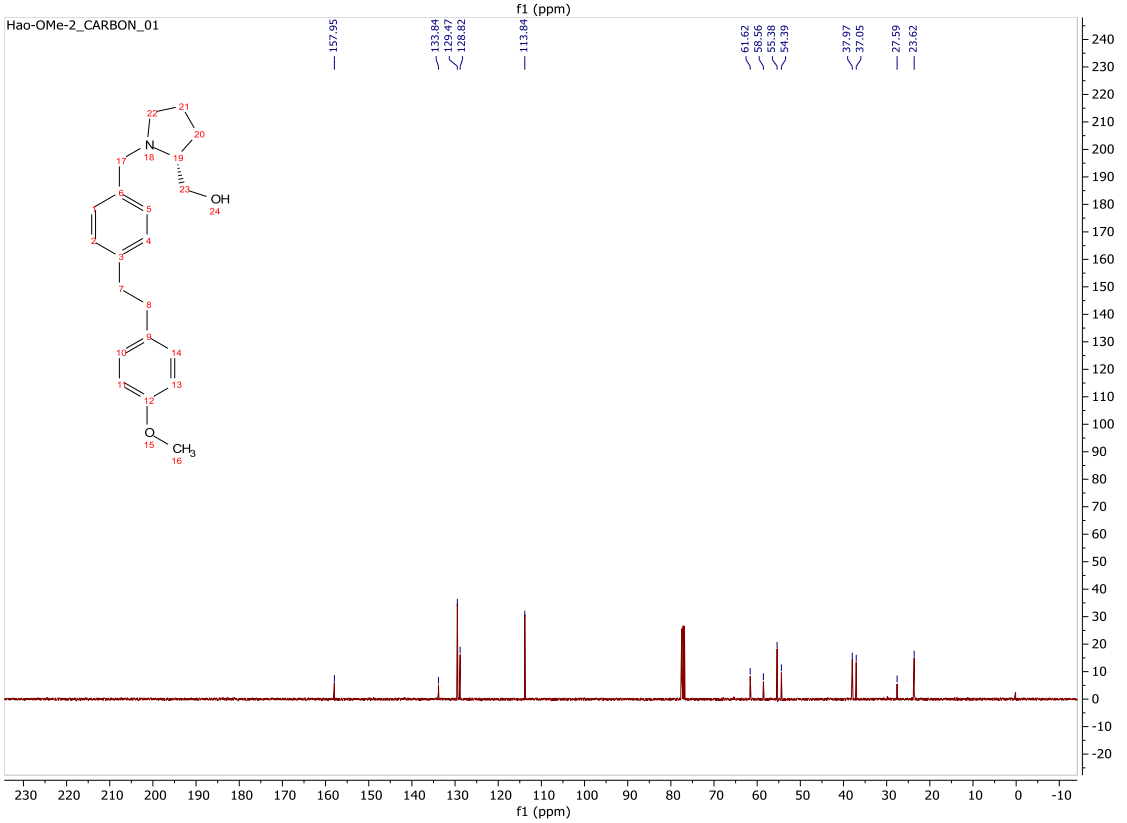

$^{1}H$ and $^{13}C$ spectra of 4-((4-propylphenyl)ethynyl)benzaldehyde(**2.18a**)

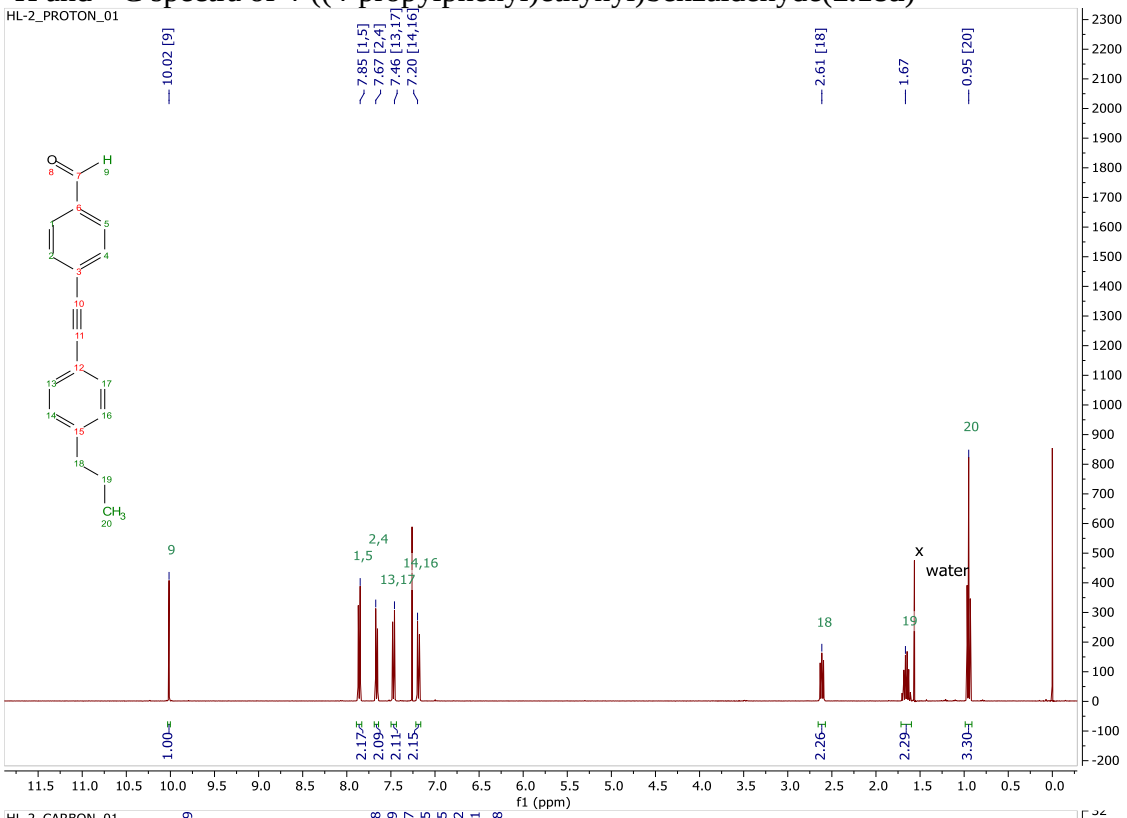


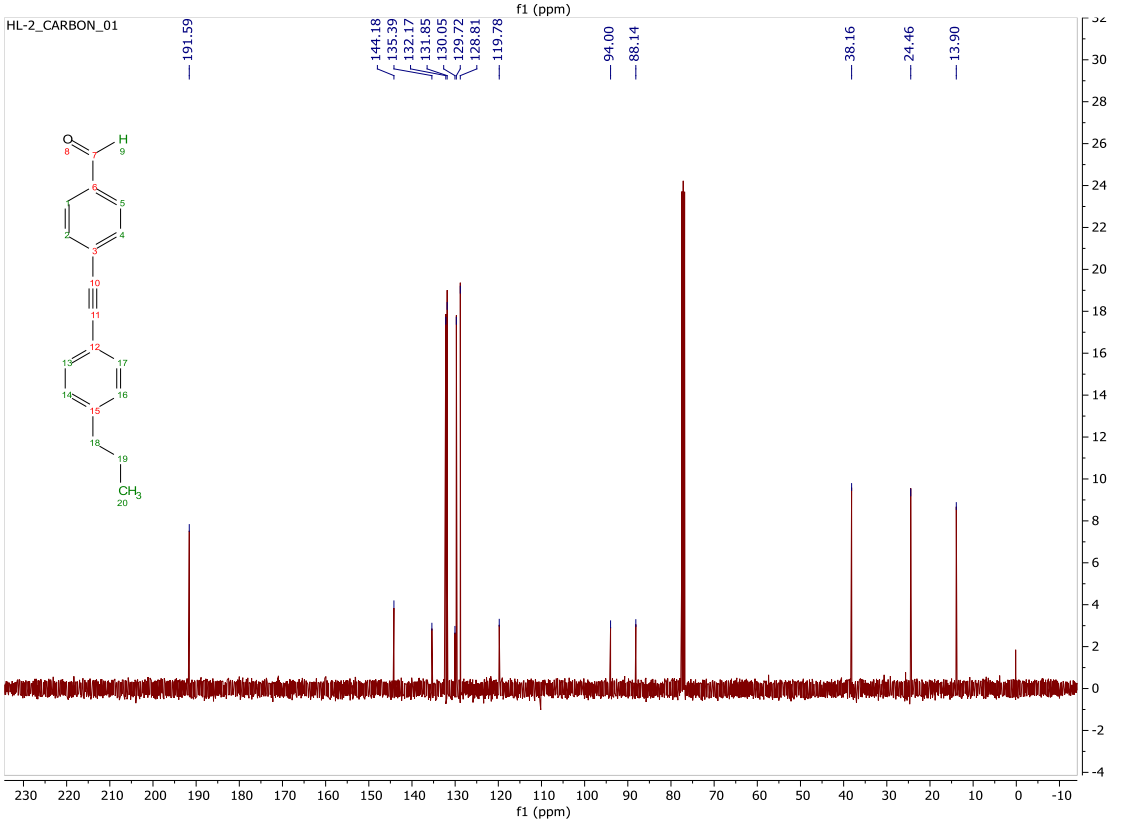

$^{1}H$ and $^{13}C$ spectra of 4-((4-butylphenyl)ethynyl)benzaldehyde(**2.18b**)

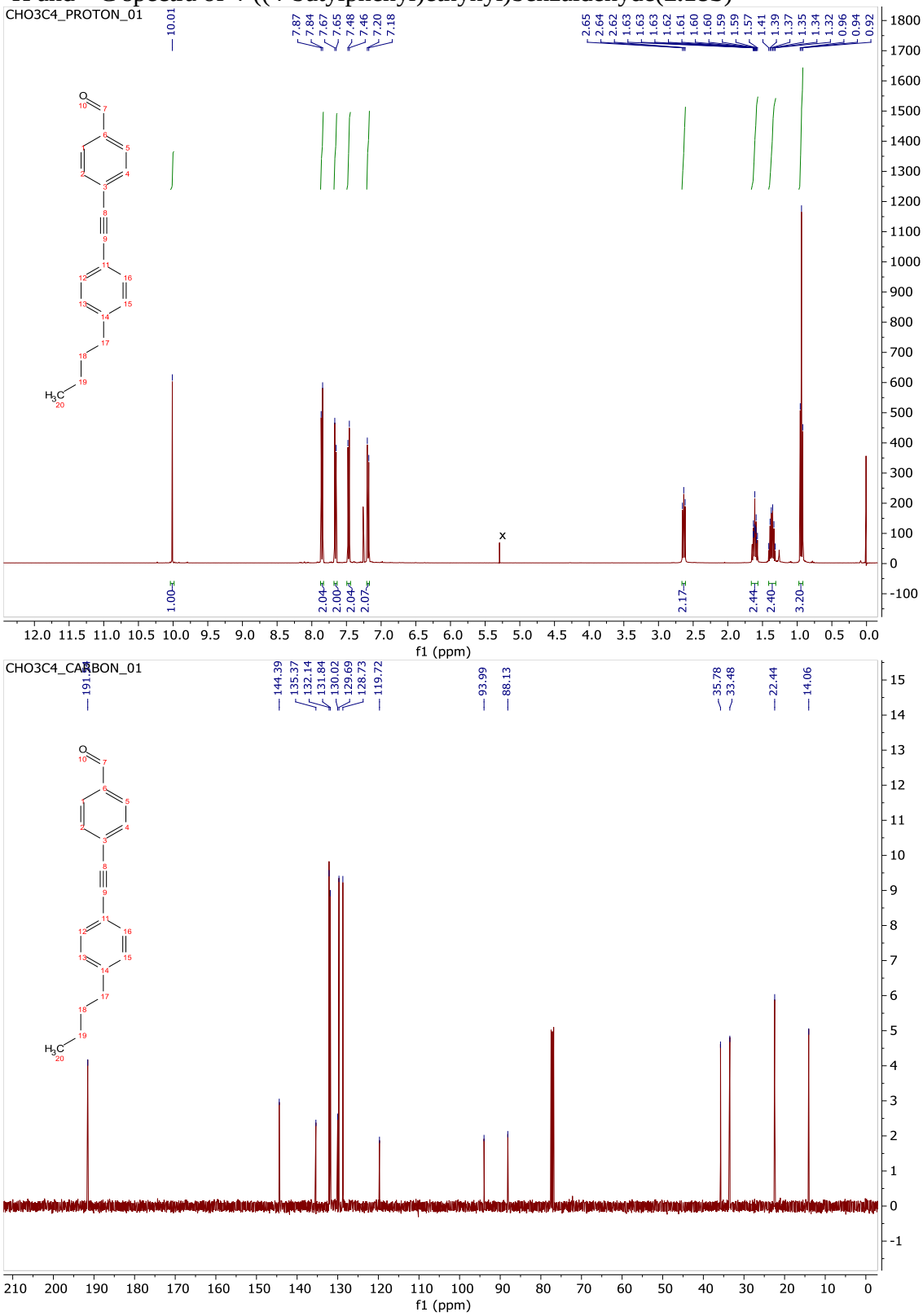

$^{1}H$ and $^{13}C$ spectra of 4-((4-pentylphenyl)ethynyl)benzaldehyde(**2.18c**)

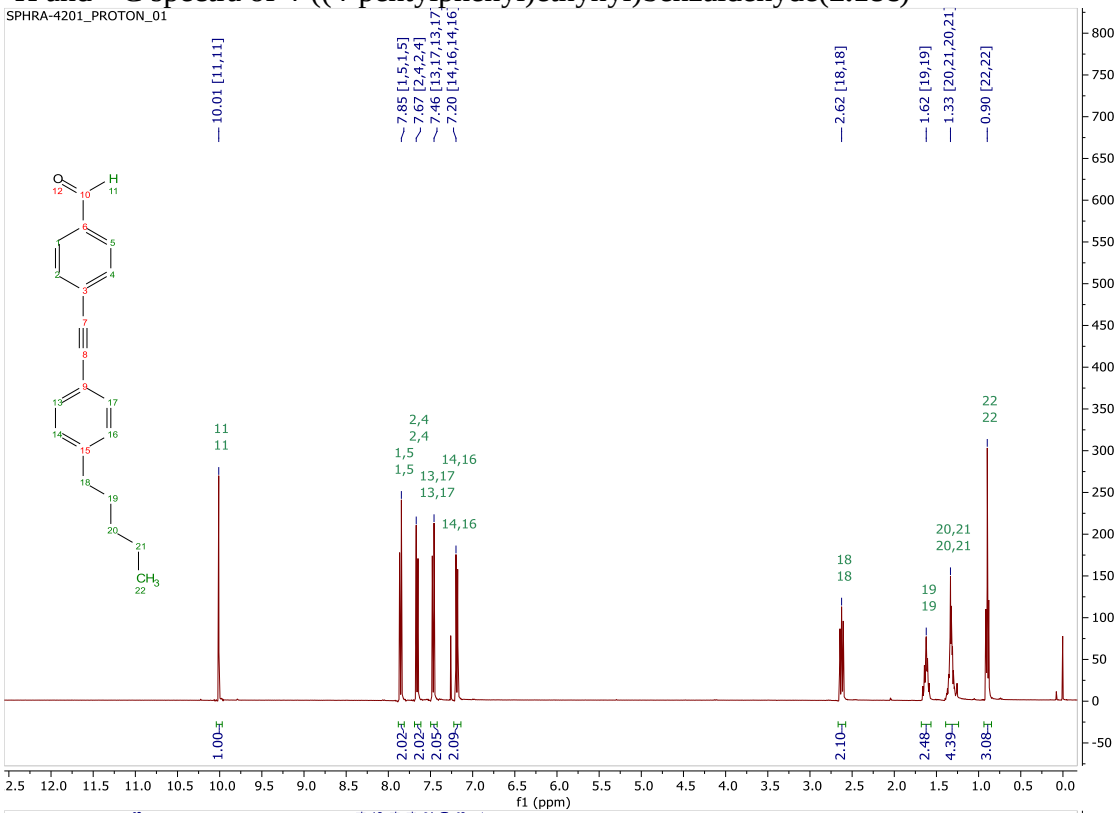


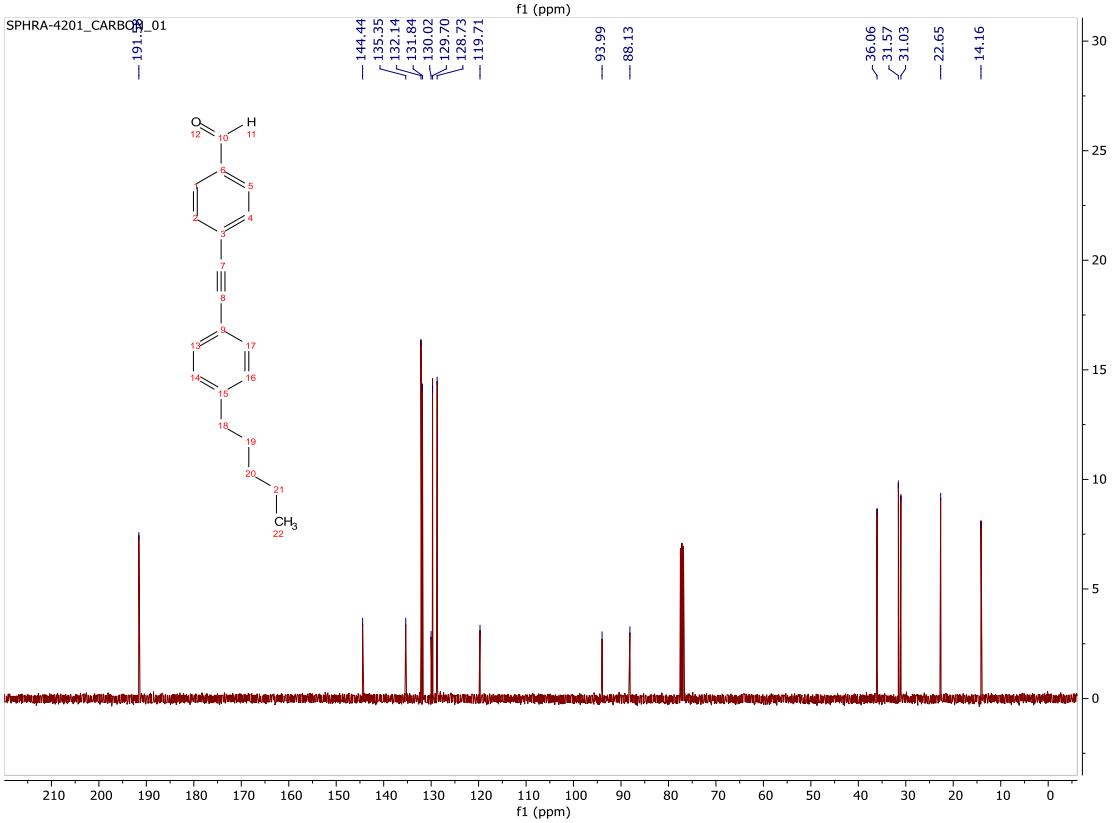

$^{1}H$ and $^{13}C$ spectra of (R)-(1-(4-((4-propylphenyl)ethynyl)benzyl)pyrrolidin-2-yl)methanol (**2.19a**)

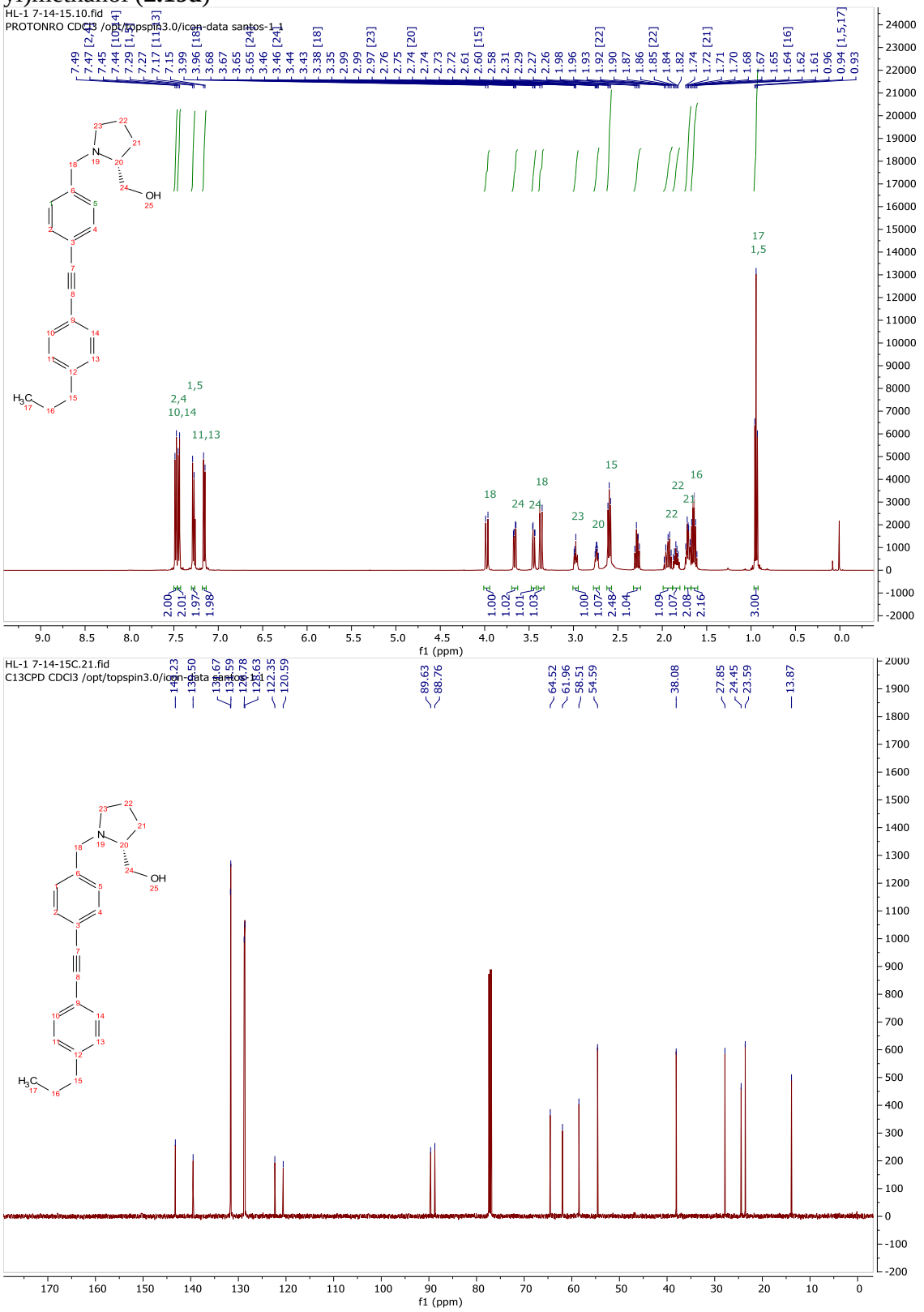

$^{1}H$ and $^{13}C$ spectra of (R)-(1-(4-((4-butylphenyl)ethynyl)benzyl)pyrrolidin-2-yl)methanol (**2.19b**)

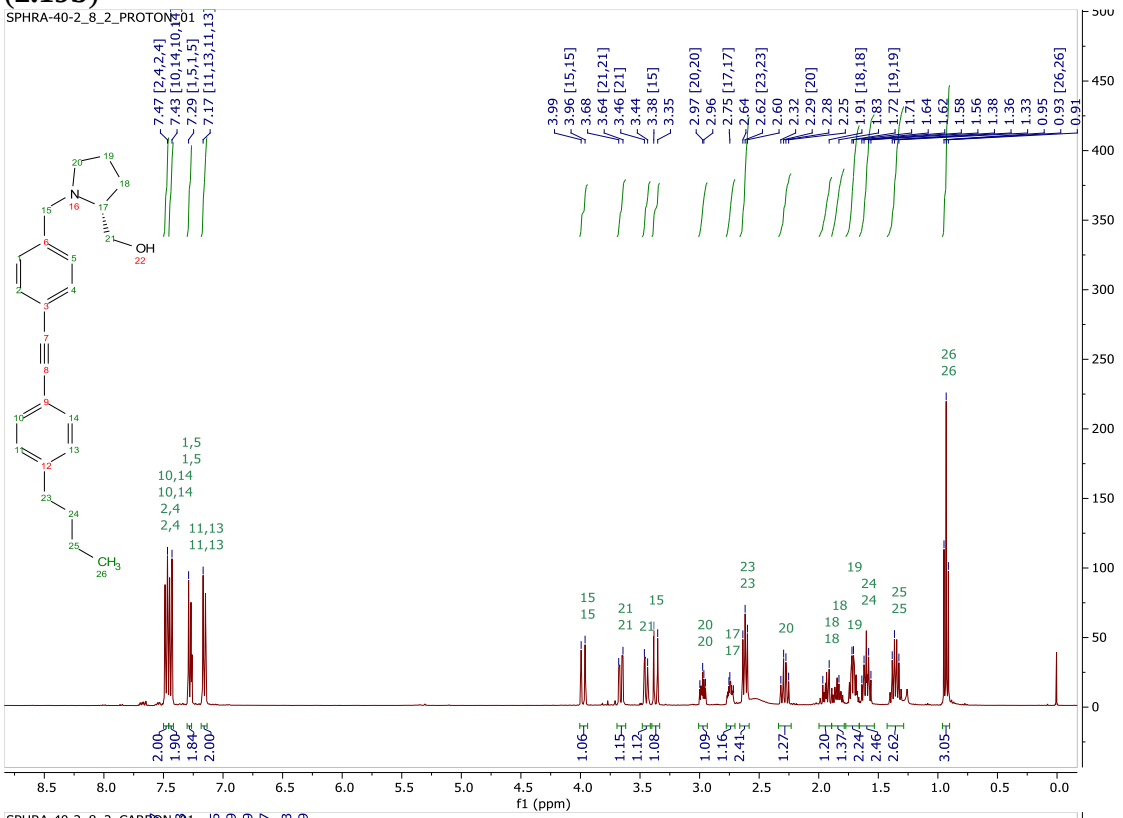


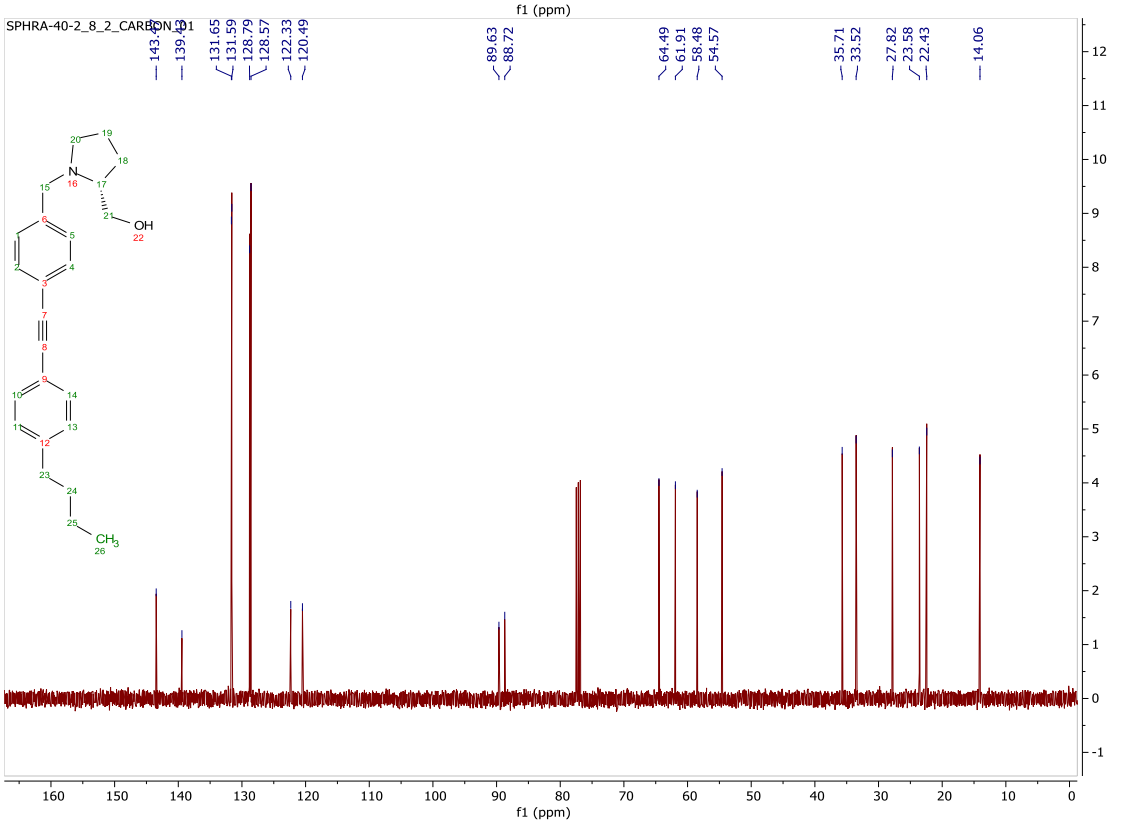

$^{1}H$ and $^{13}C$ spectra of (R)-(1-(4-((4-pentylphenyl)ethynyl)benzyl)pyrrolidin-2-yl)methanol (**2.19c**)

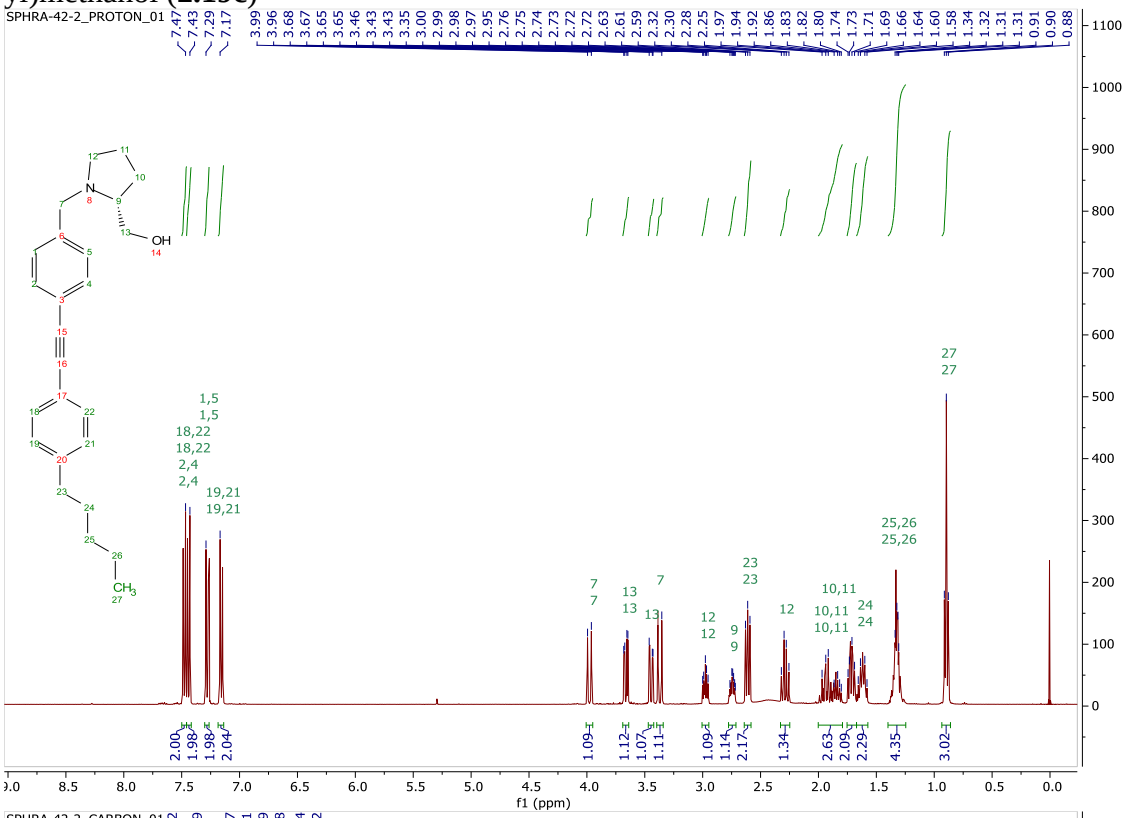


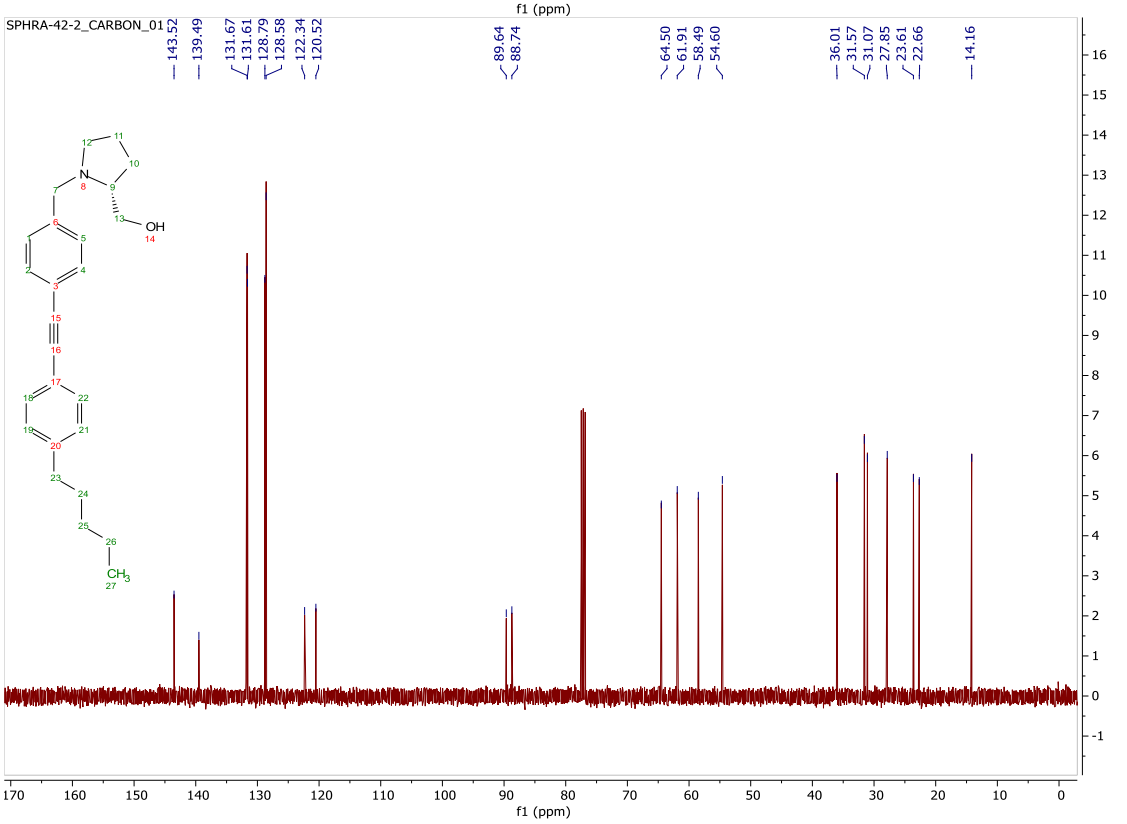

$^{1}H$ and $^{13}C$ spectra of (R)-(1-(4-(4-propylphenethyl)benzyl)pyrrolidin-2-yl)methanol(**2.21a**)

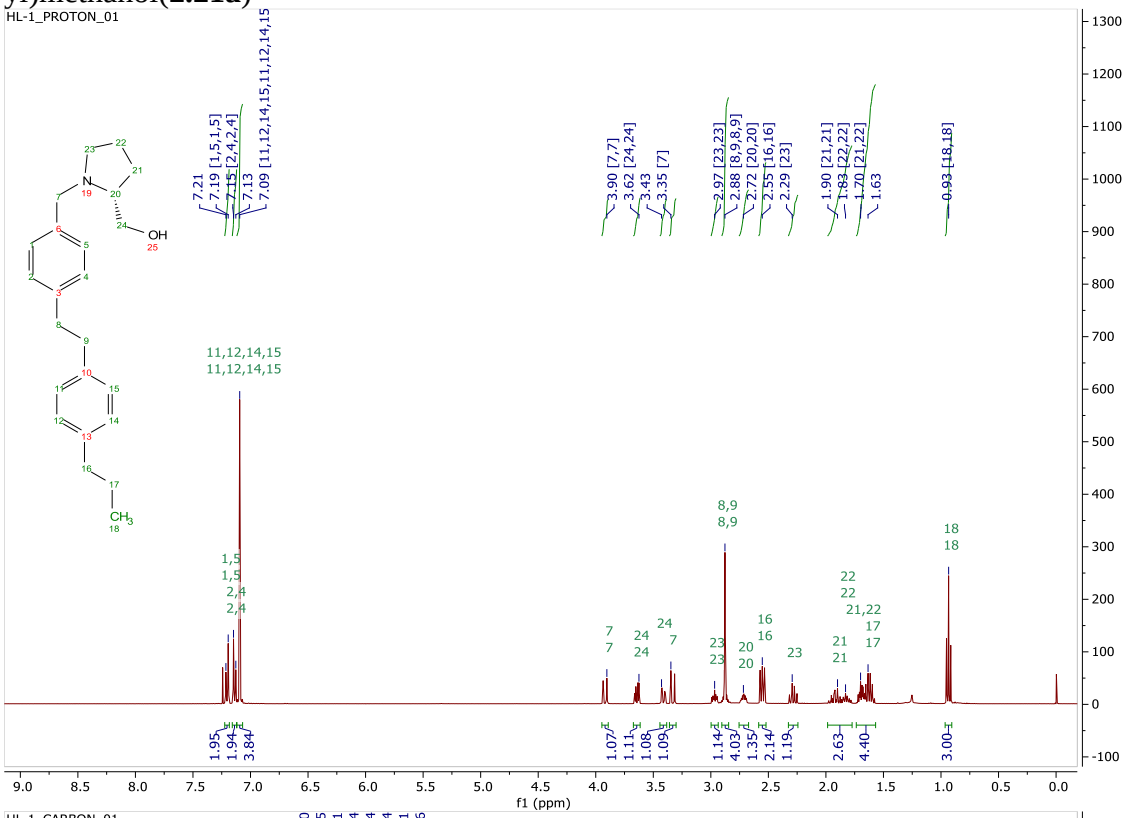


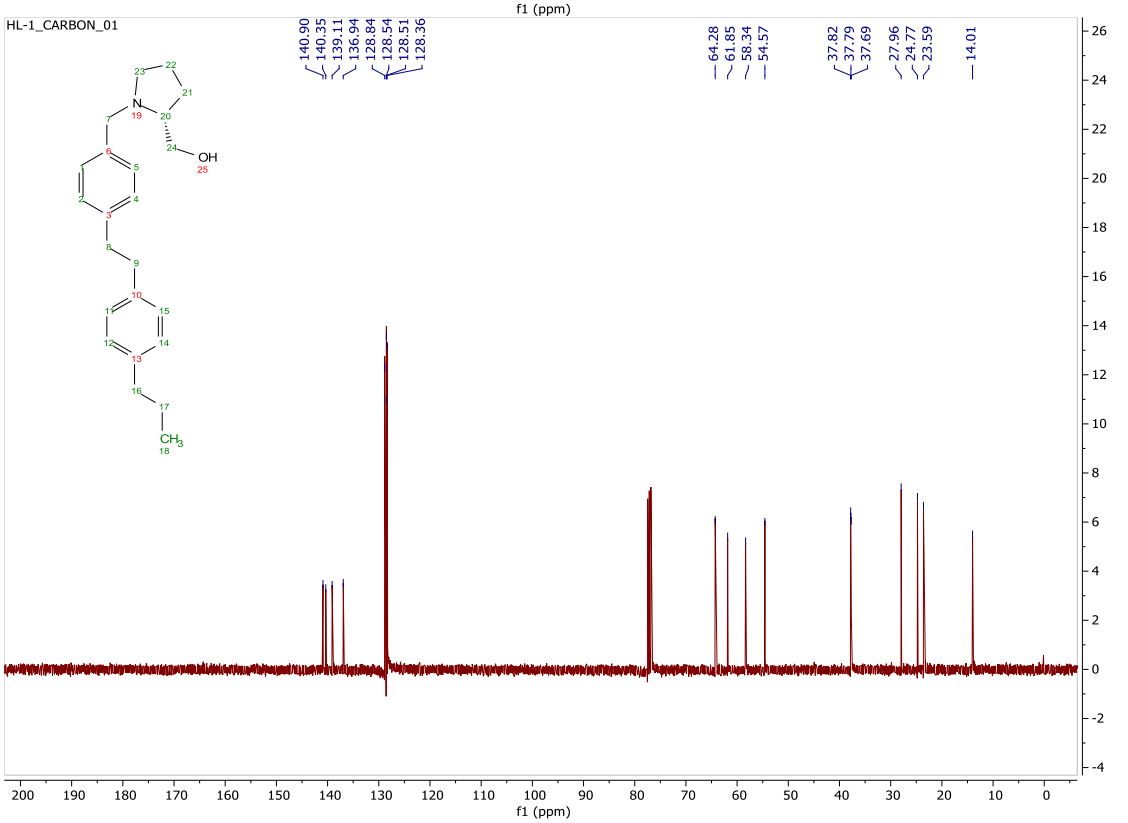

$^{1}H$ and $^{13}C$ spectra of (R)-(1-(4-(4-butylphenethyl)benzyl)pyrrolidin-2-yl)methanol (**2.21b**)

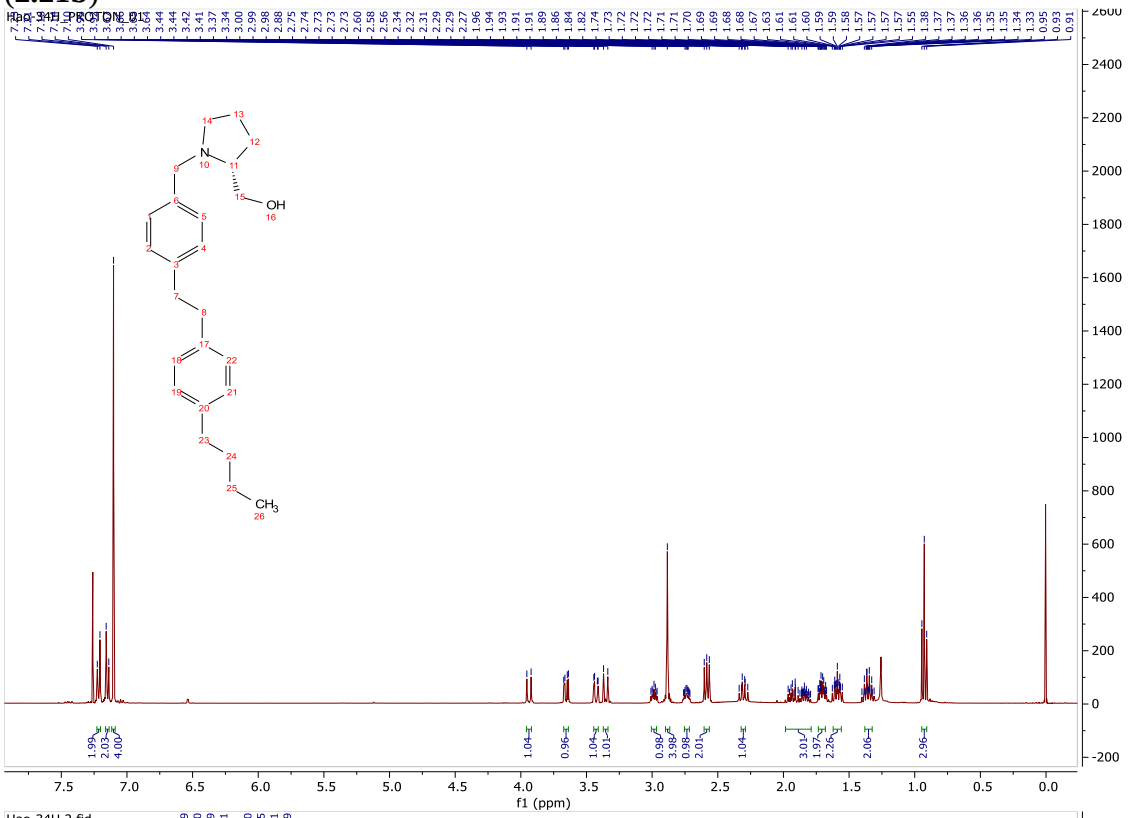


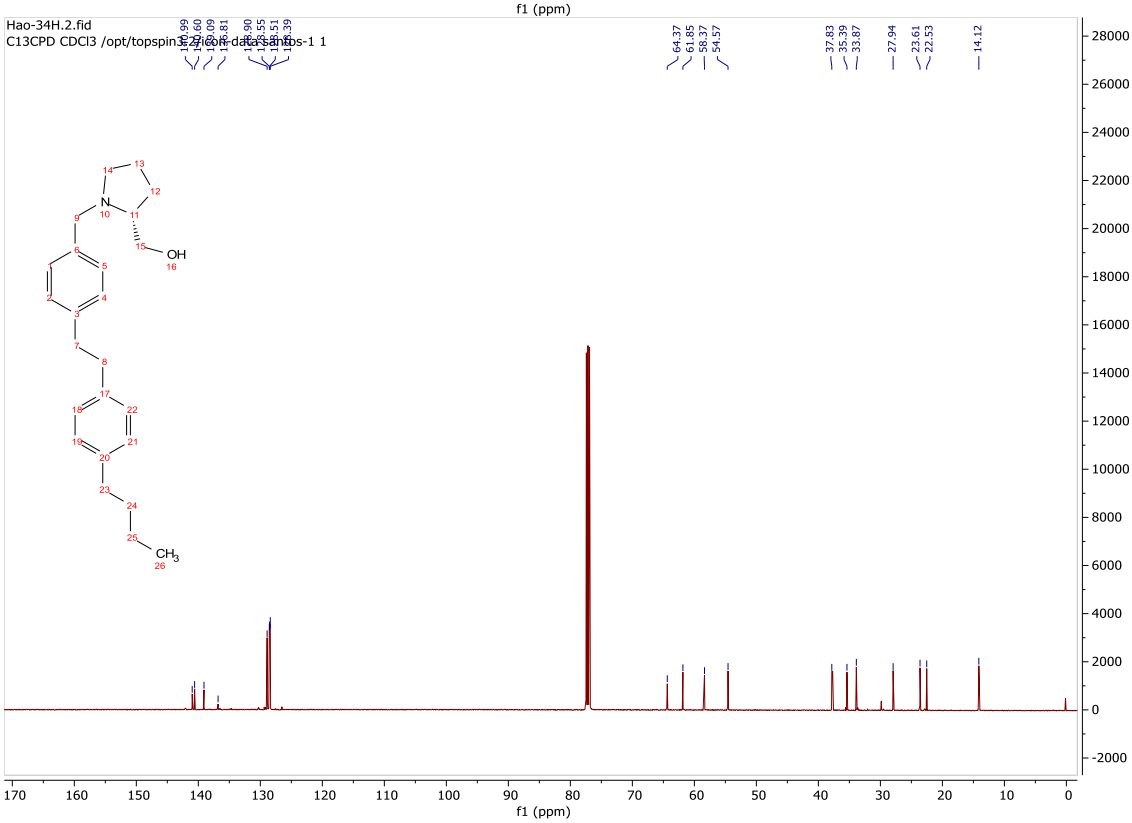

$^{1}H$ and $^{13}C$ spectra of (R)-(1-(4-(4-pentylphenethyl)benzyl)pyrrolidin-2-yl)methanol (**2.21c**)

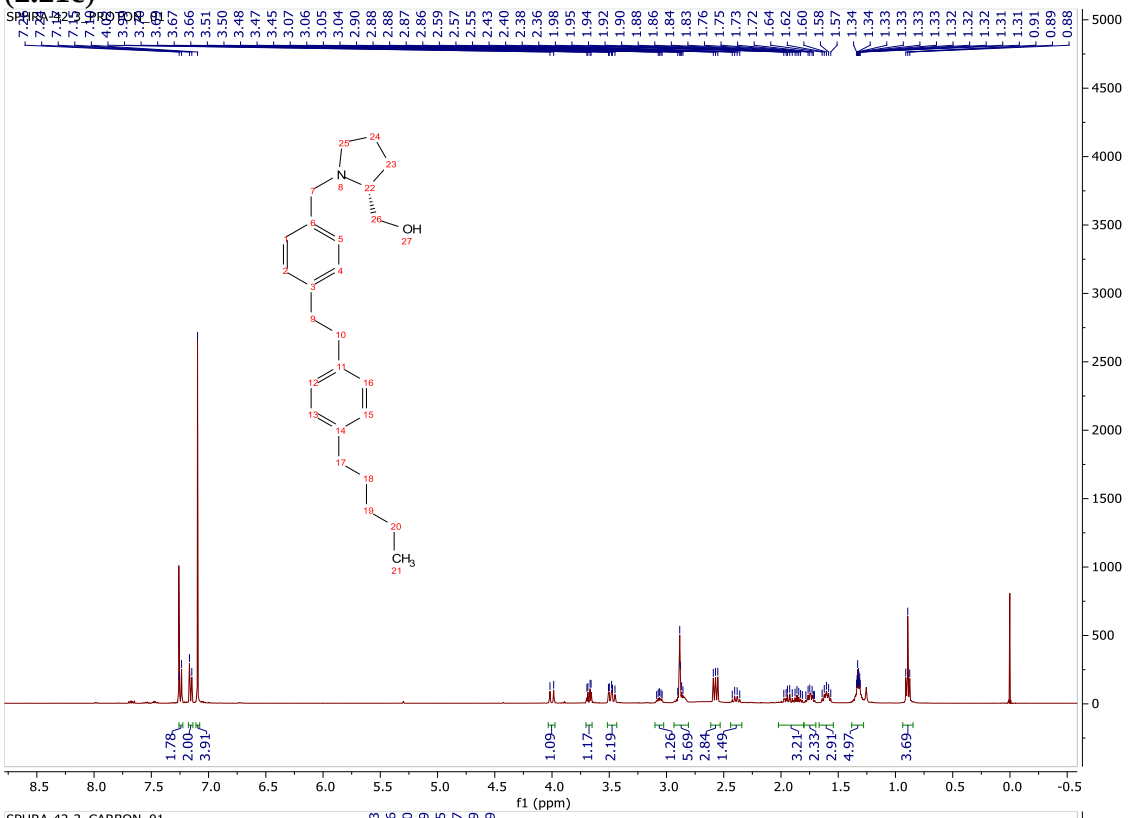


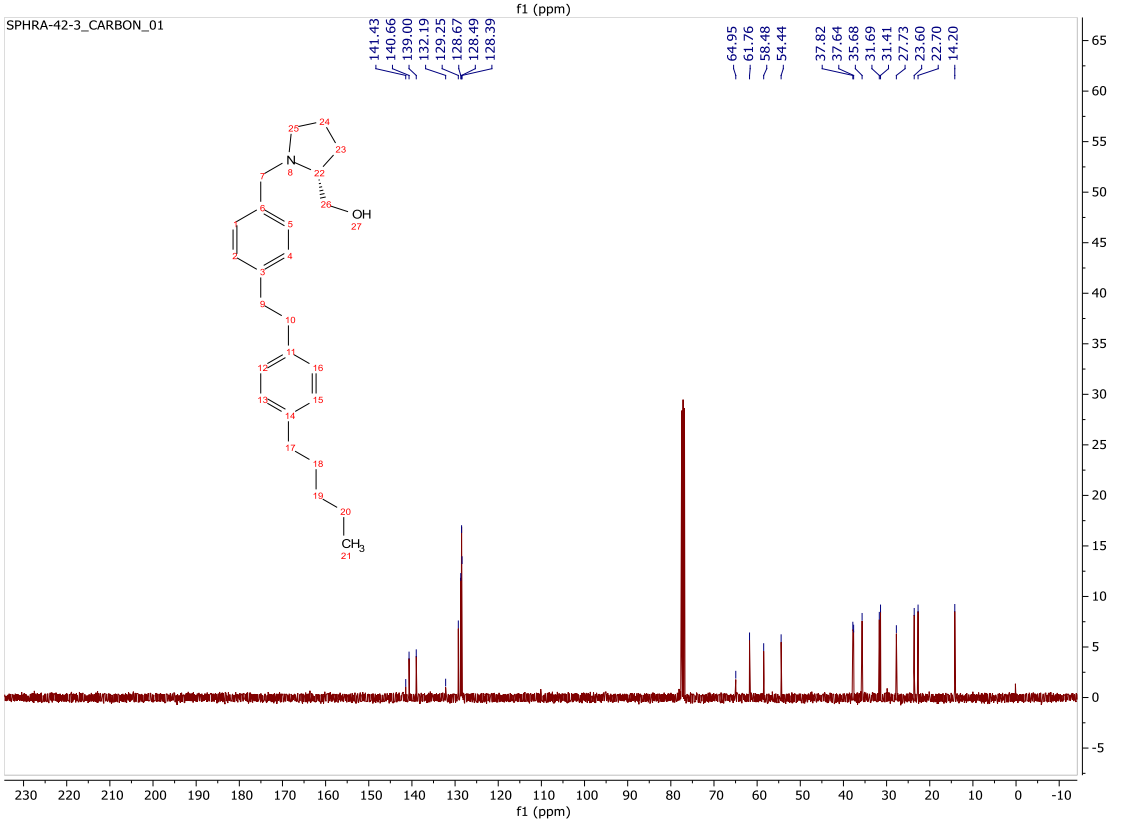

$^{1}H$ and $^{13}C$ spectra of (R)-(1-(4-dodecylbenzyl)pyrrolidin-2-yl)methyl acetate (**2.13f**)

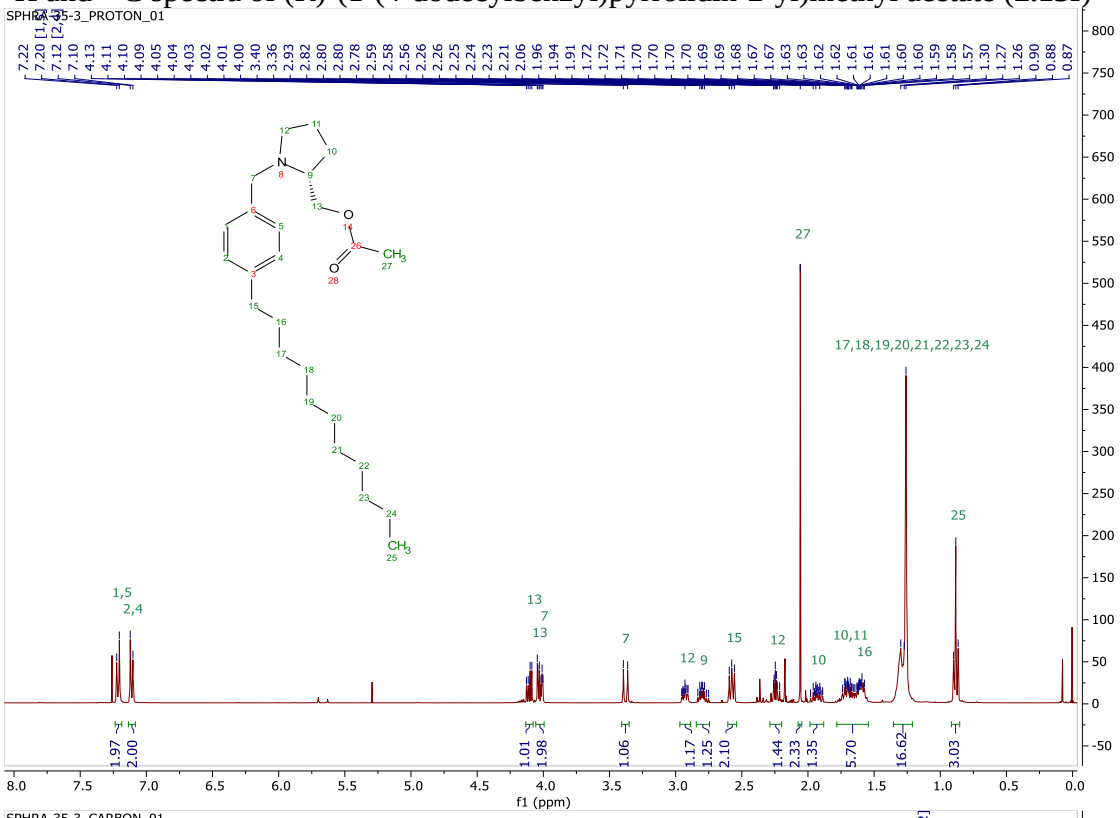


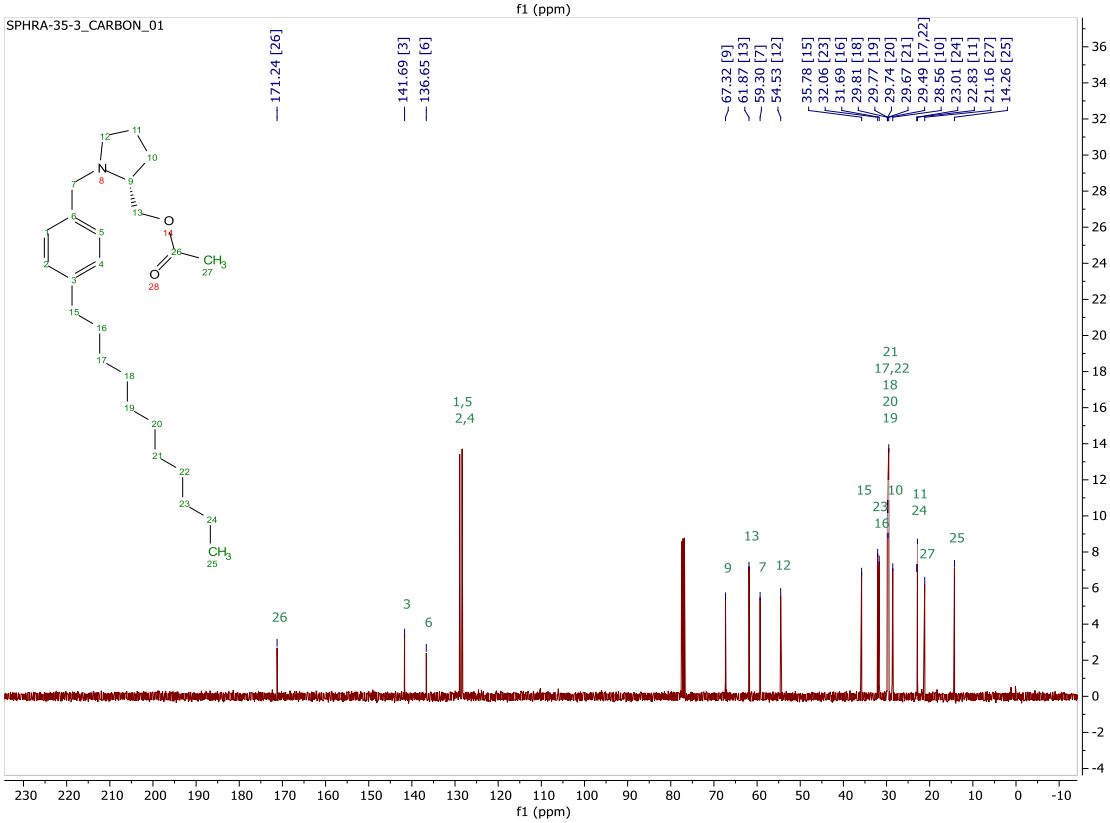

# Appendix A NMR Spectra for Chapter 3

$^{1}$H and $^{13}$C spectra of 1-(4-dodecylphenyl)-3-(piperidin-1-yl)propan-2-ol (**3.5a**)

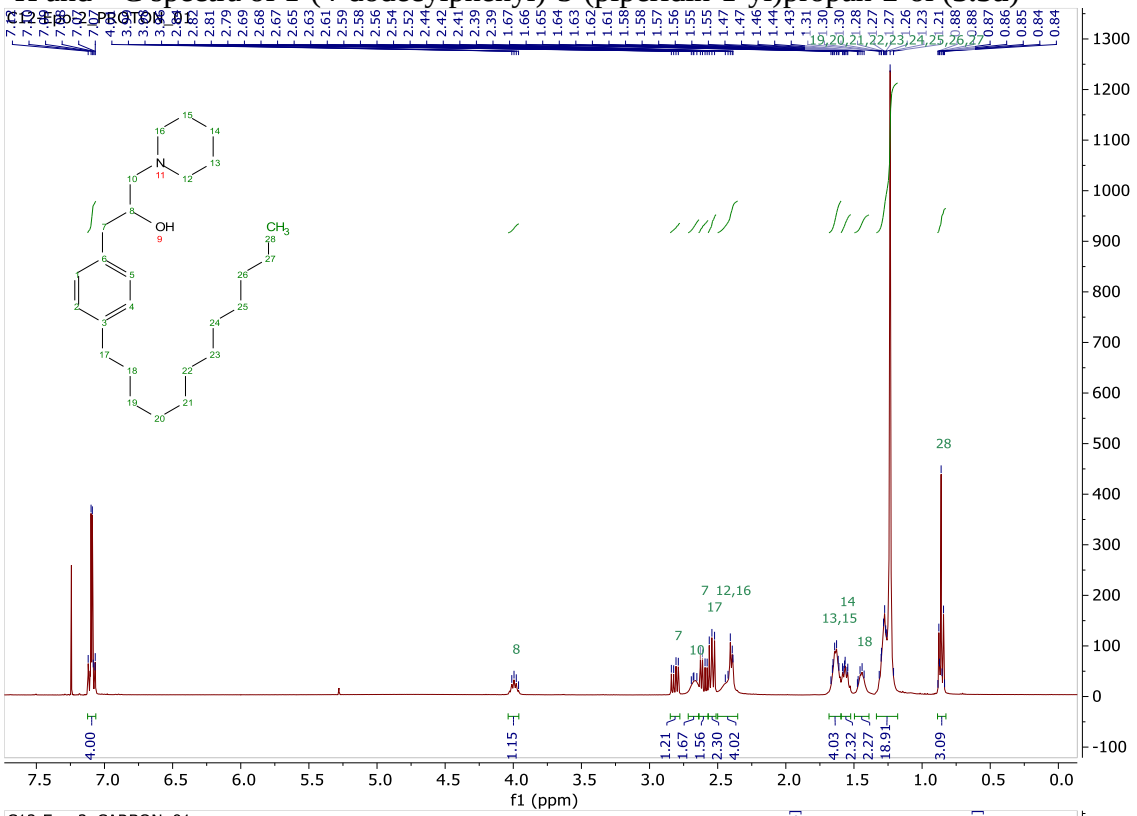


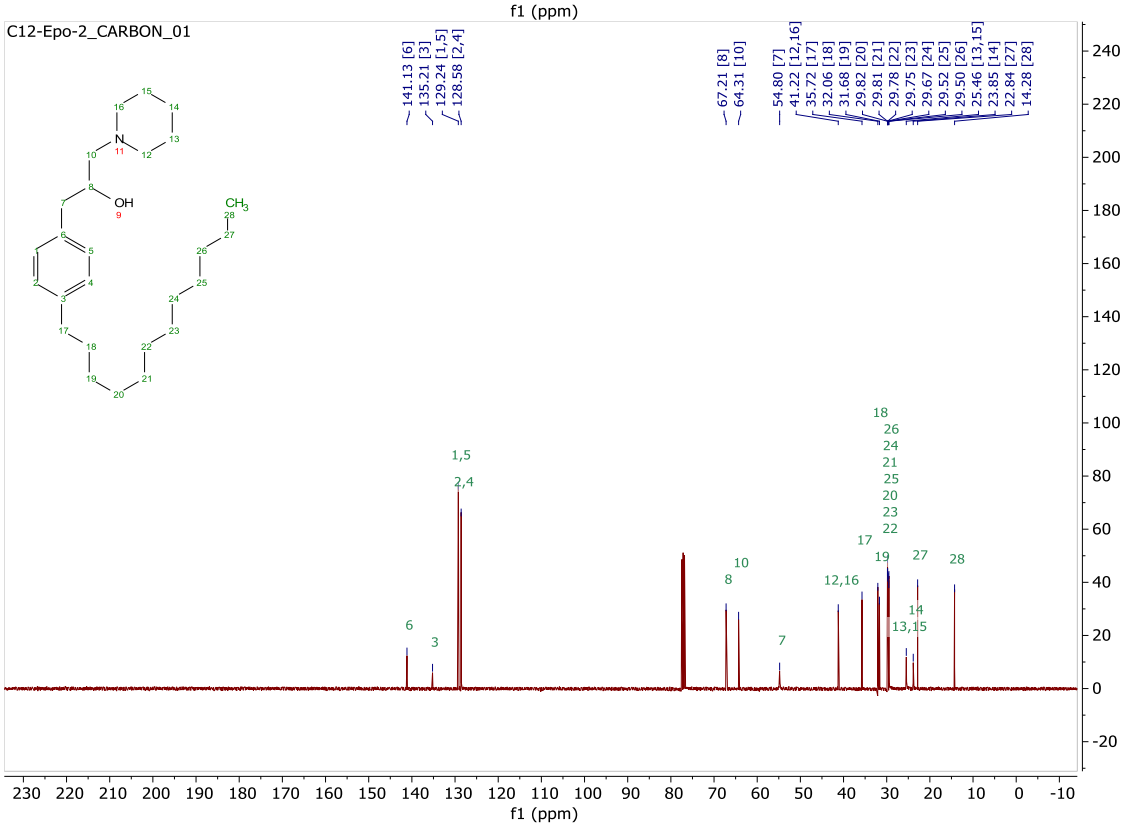

$^{1}H$ and $^{13}C$ spectra of *Tert*-butyl 4-(3-(4-dodecylphenyl)-2-hydroxypropyl)piperazine-1-carboxylate (**3.5b**)

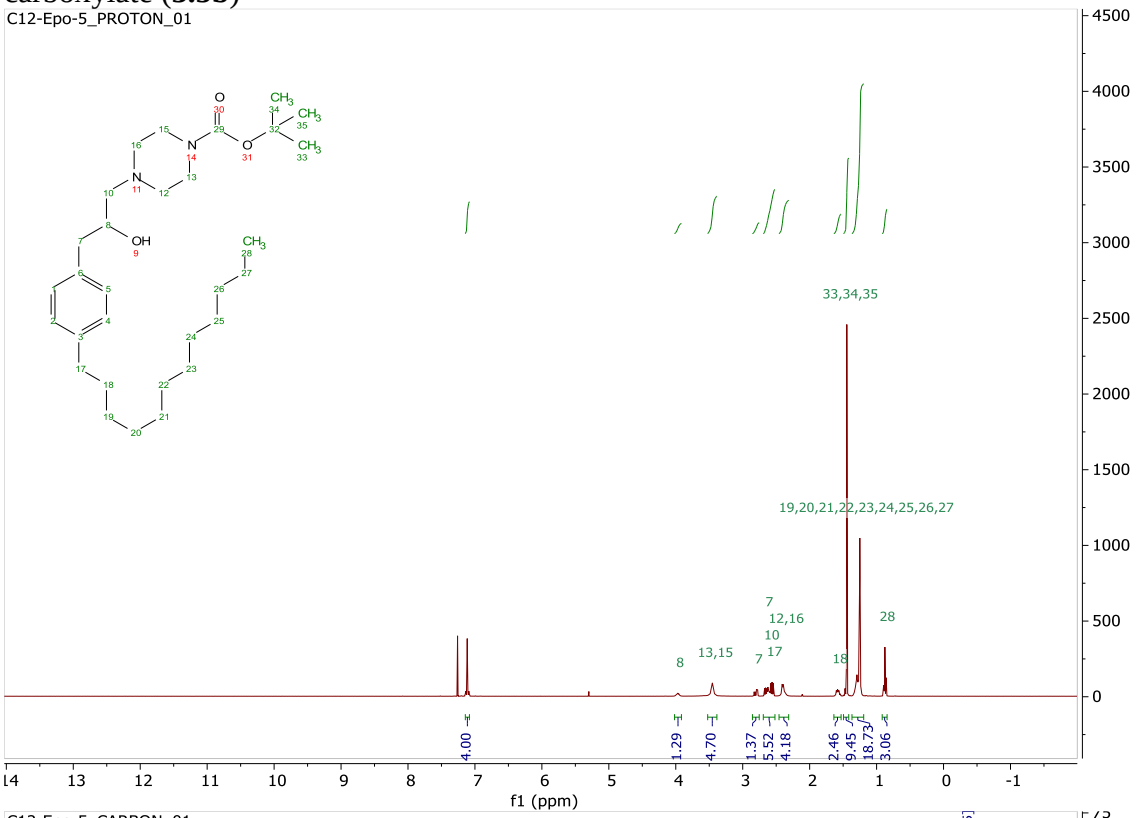


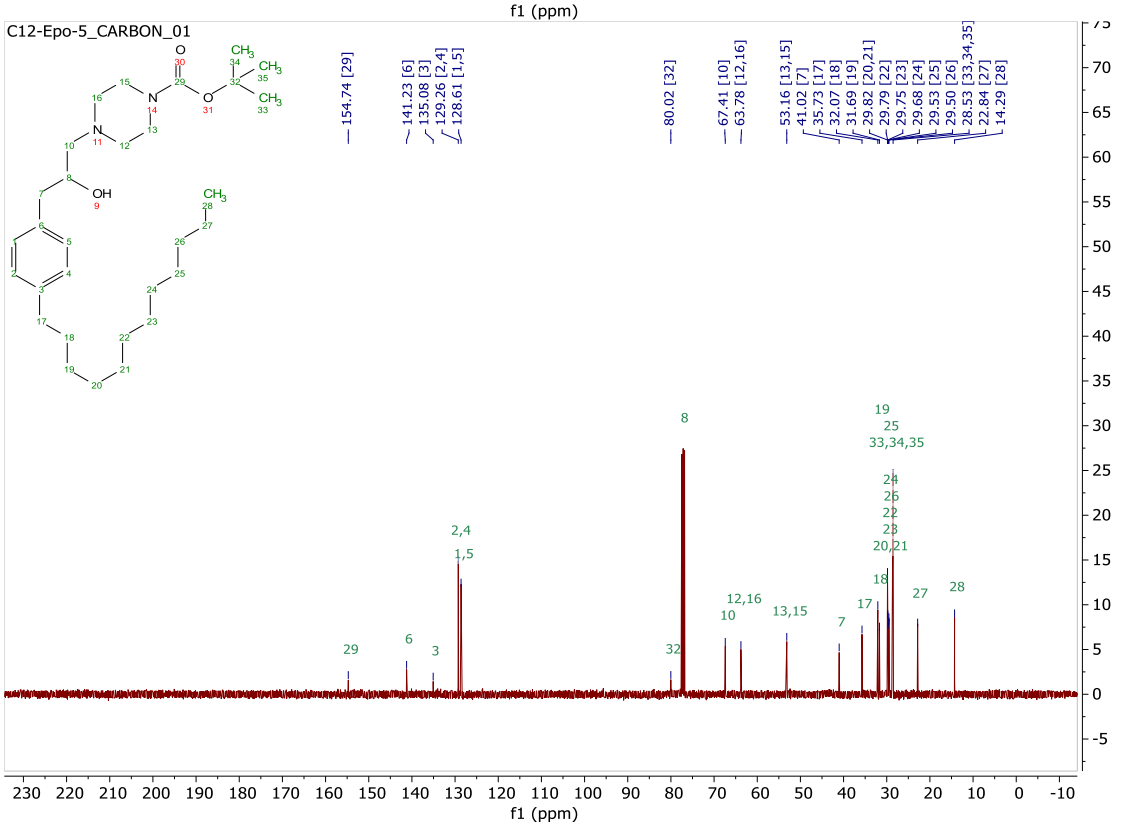

$^{1}H$ and $^{13}C$ spectra of 1-(4-dodecylphenyl)-3-morpholinopropan-2-ol (**3.5c**)

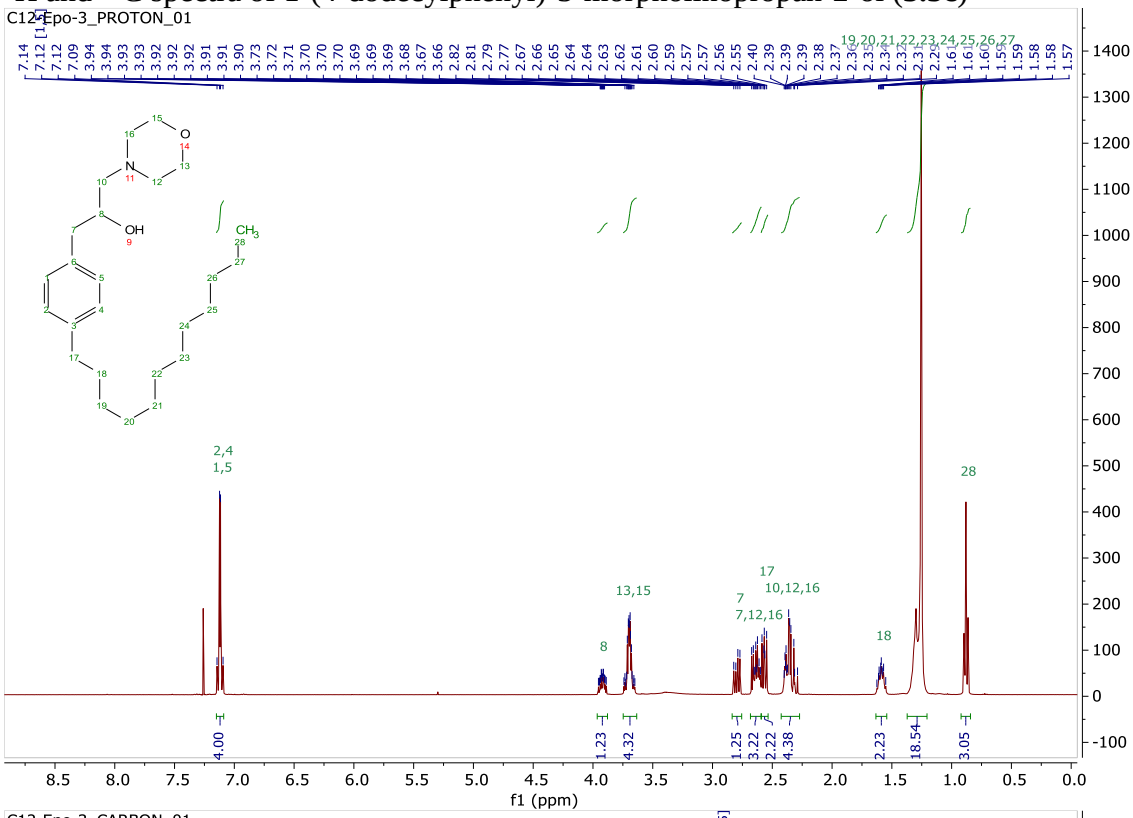


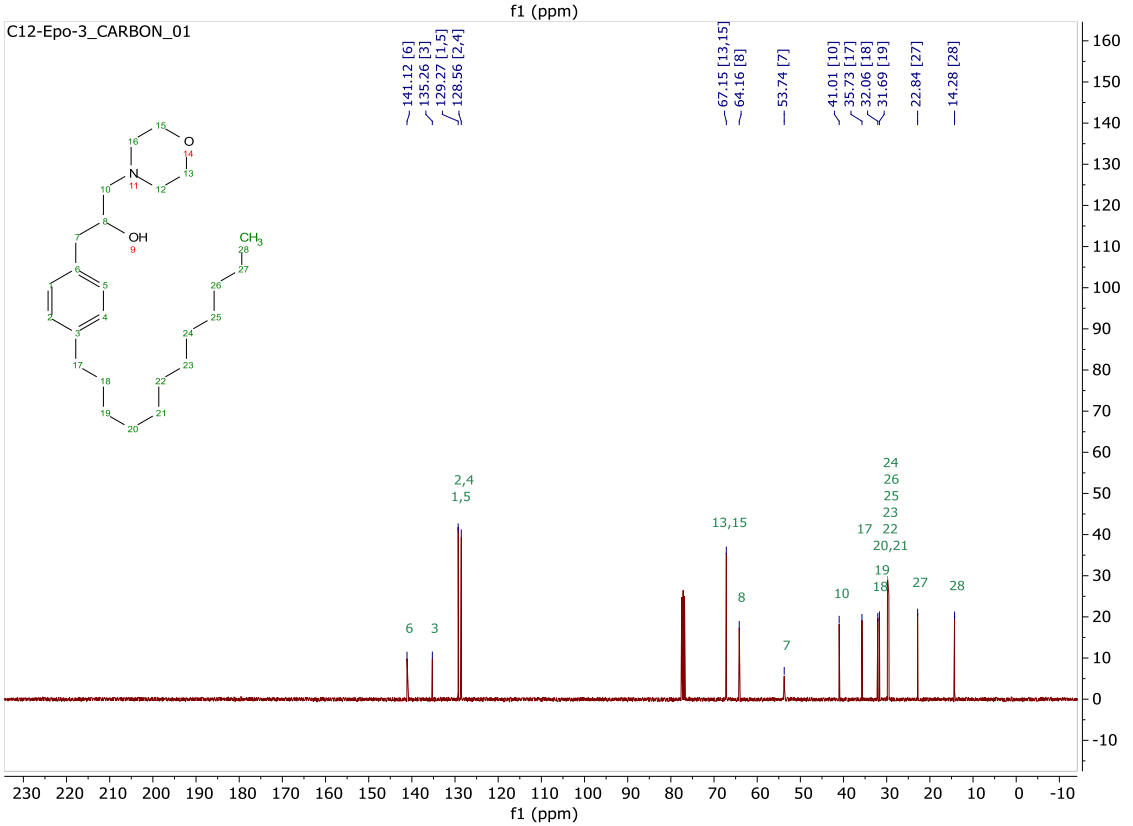

$^{1}H$ and $^{13}C$ spectra of 1-(4-dodecylphenyl)-3-(4-methylpiperazin-1-yl)propan-2-ol (**3.5d**)

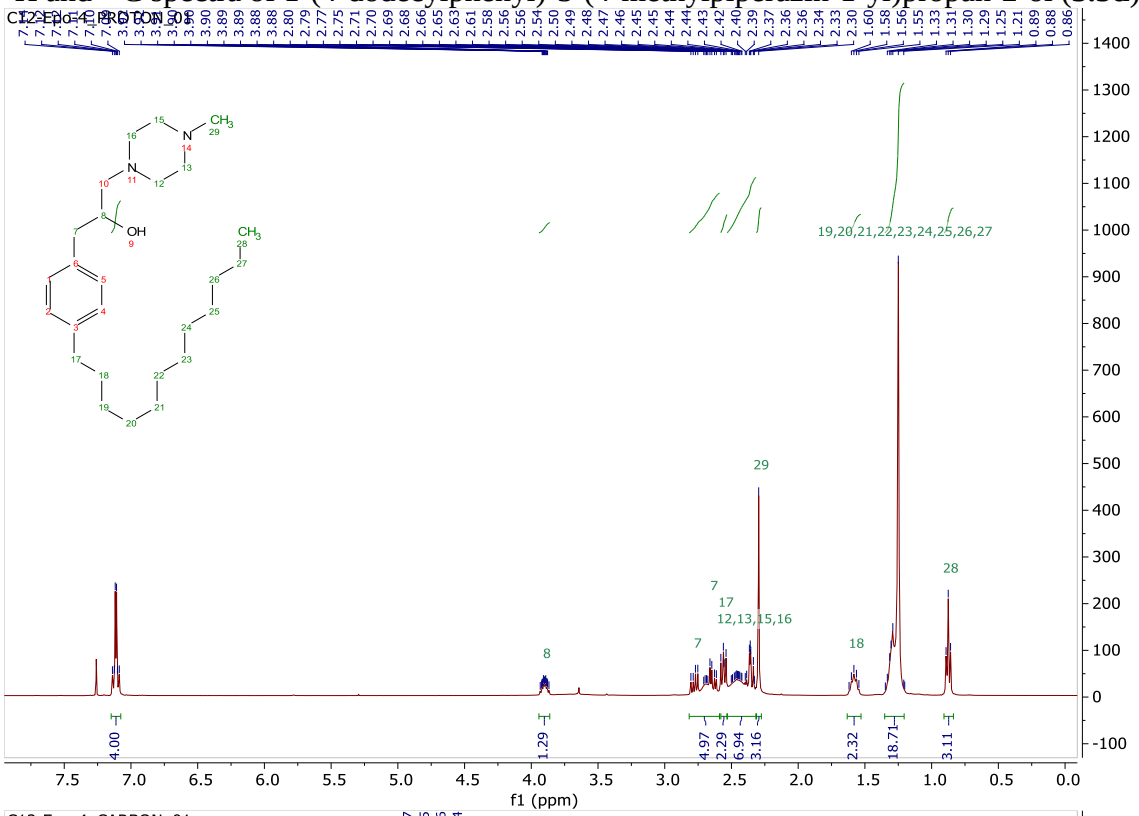


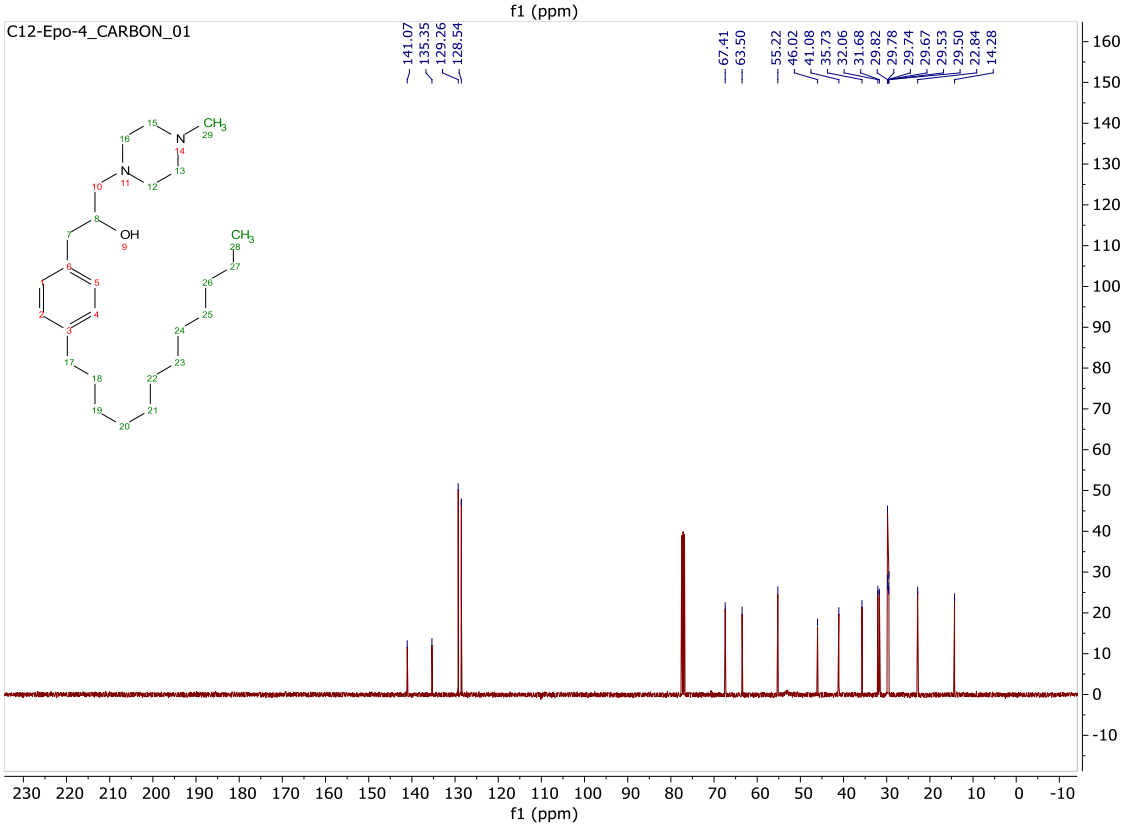

$^{1}H$ and $^{13}C$ spectra of *Tert*-butyl (1-(3-(4-dodecylphenyl)-2-hydroxypropyl)piperidin-4-yl)carbamate (**3.16e**)

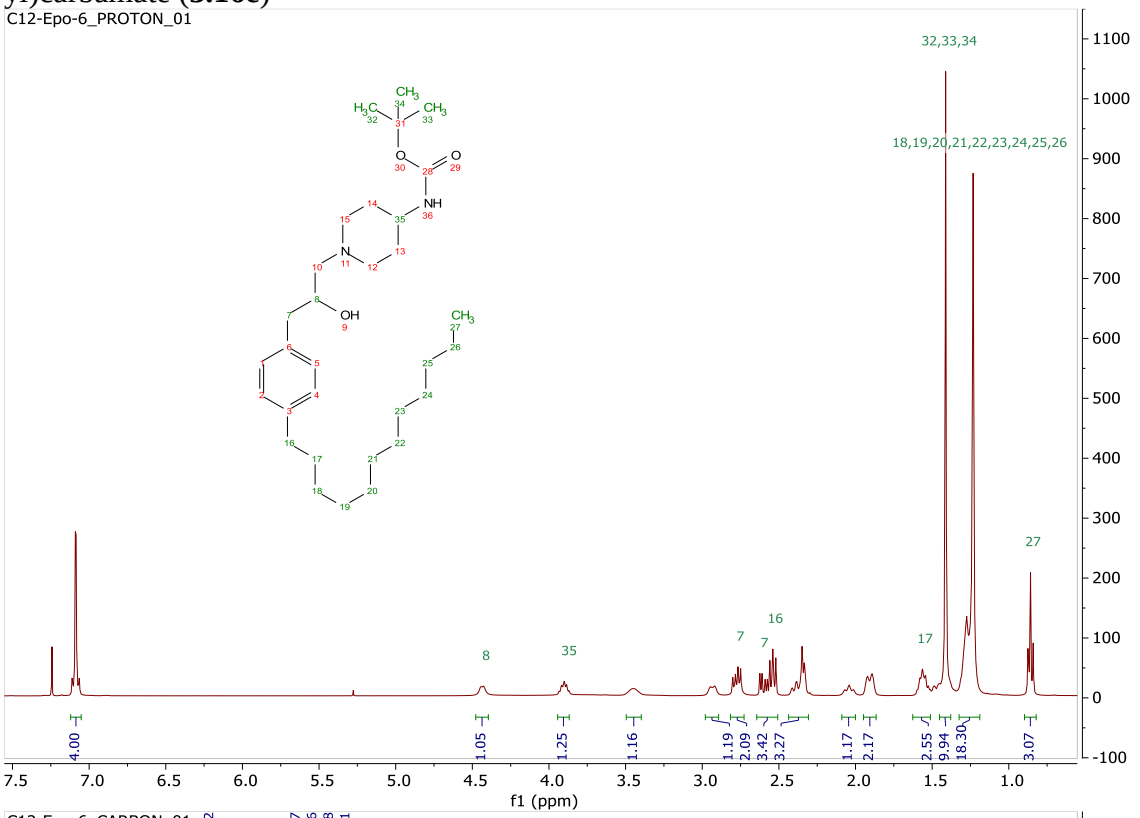


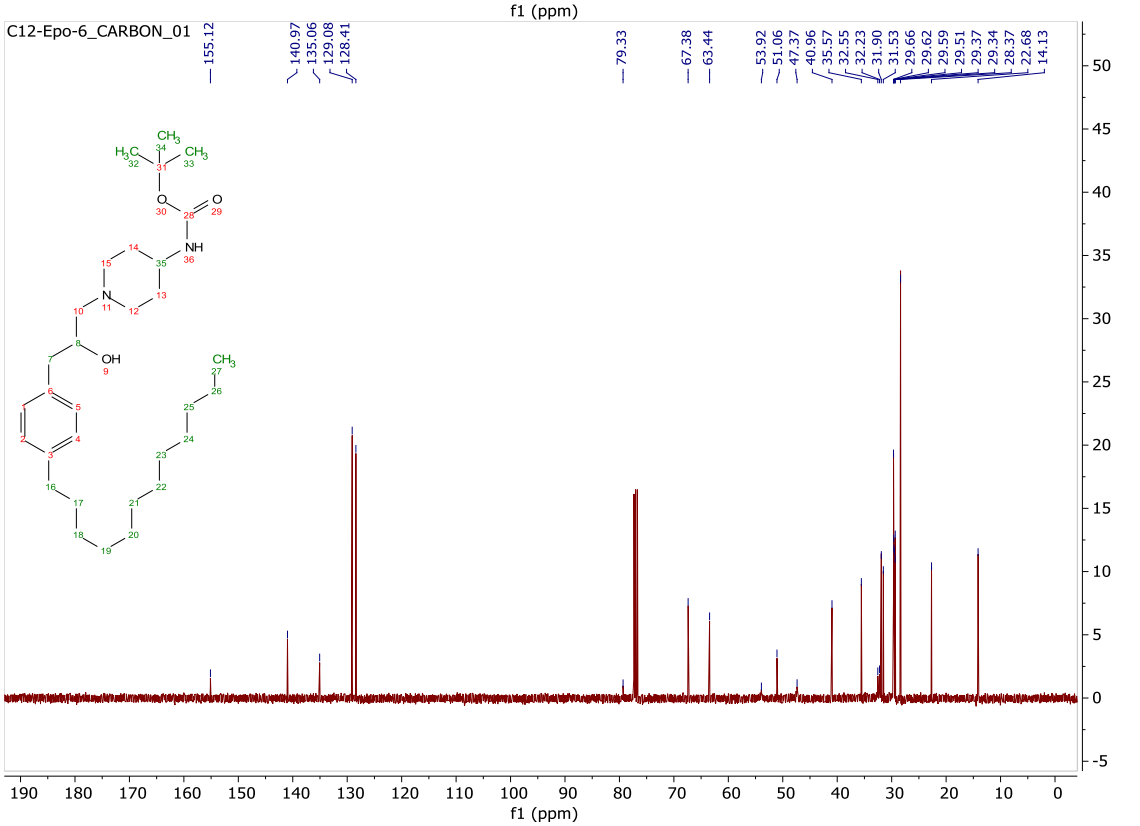

$^{1}H$ and $^{13}C$ spectra of 1-(4-dodecylphenyl)-3-(pyrrolidin-1-yl)propan-2-ol (**3.5h**)

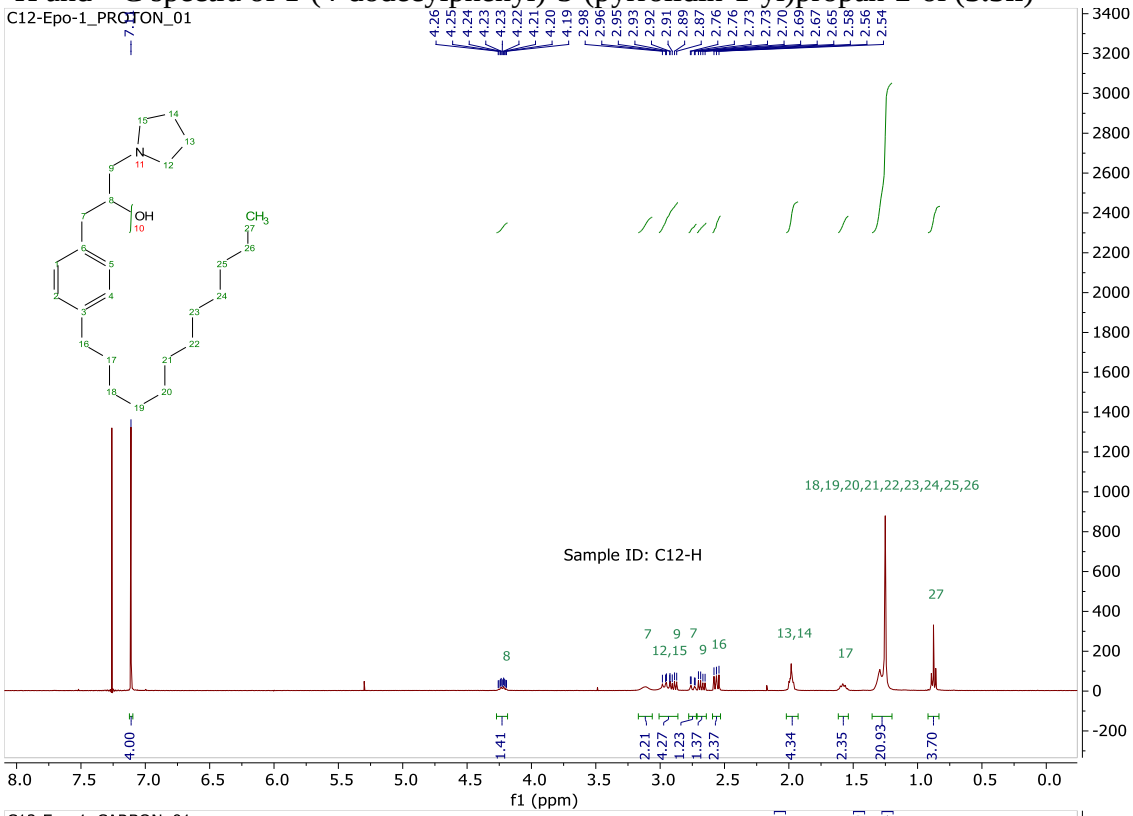


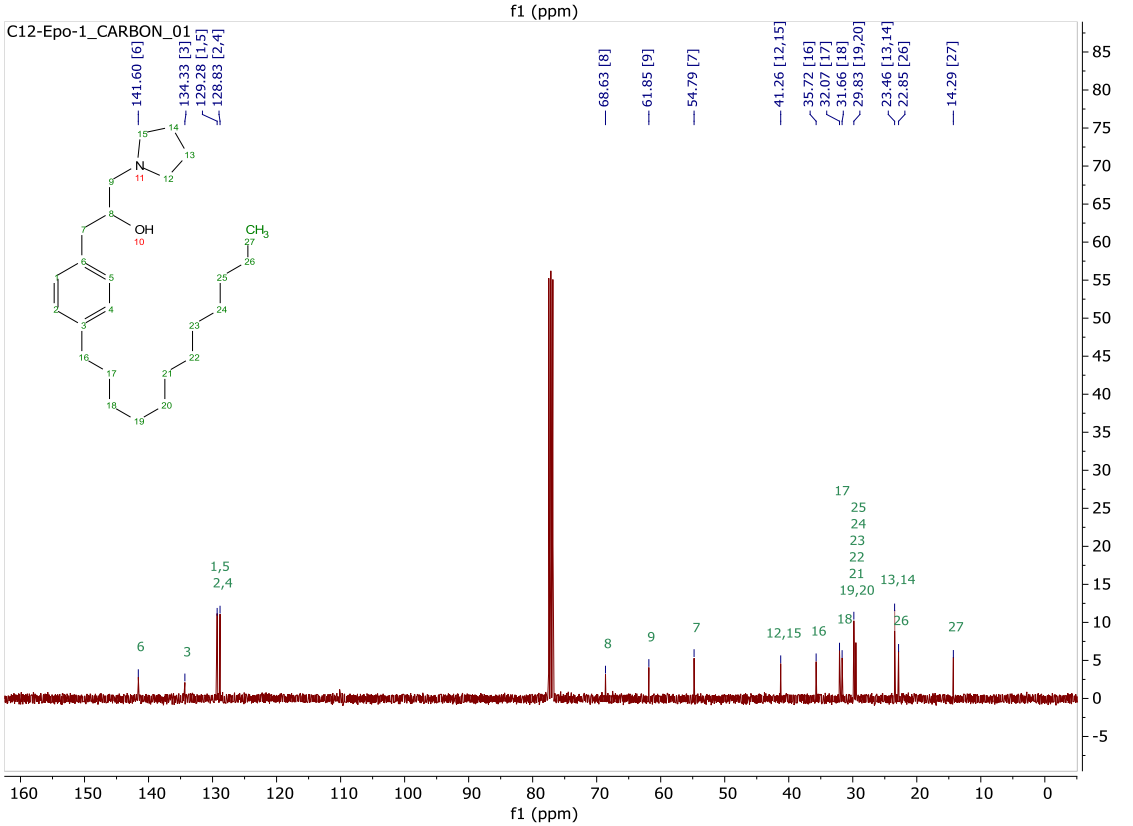

$^{1}H$ and $^{13}C$ spectra of 1-(4-dodecylphenyl)-3-((R)-2-(hydroxymethyl)pyrrolidin-1-yl)propan-2-ol (**3.5j**)

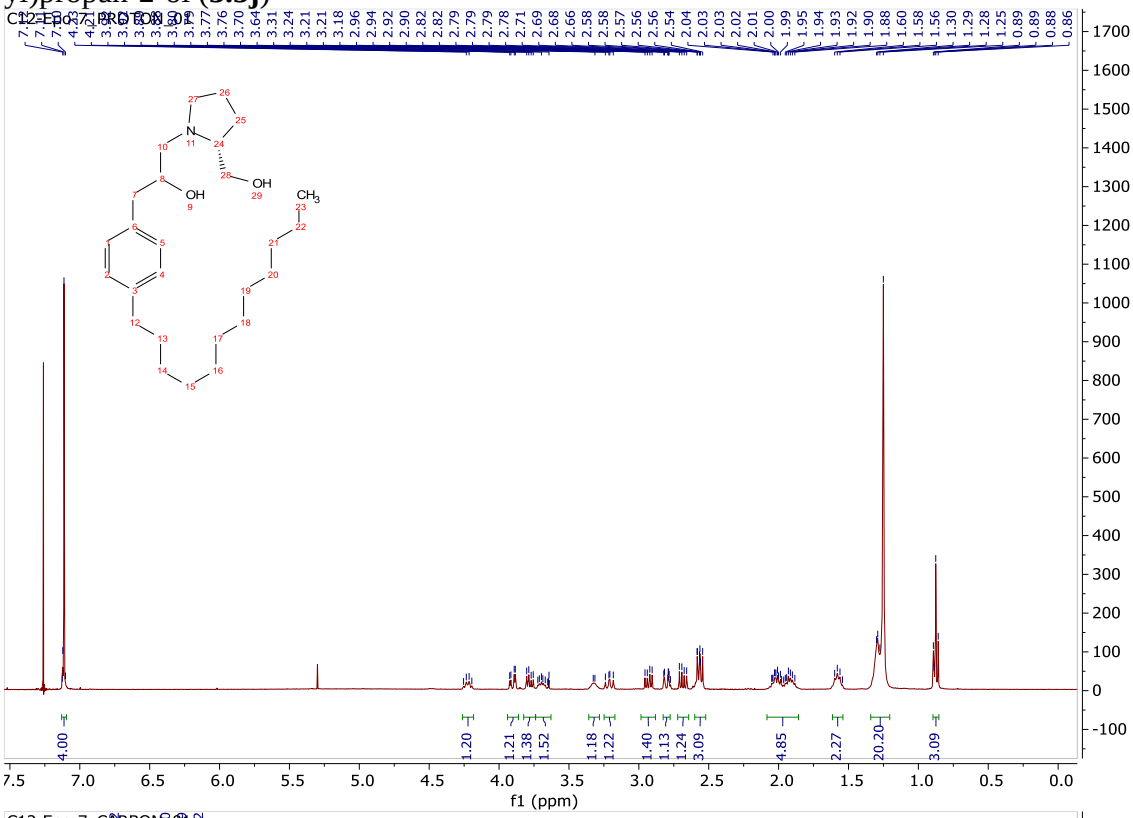


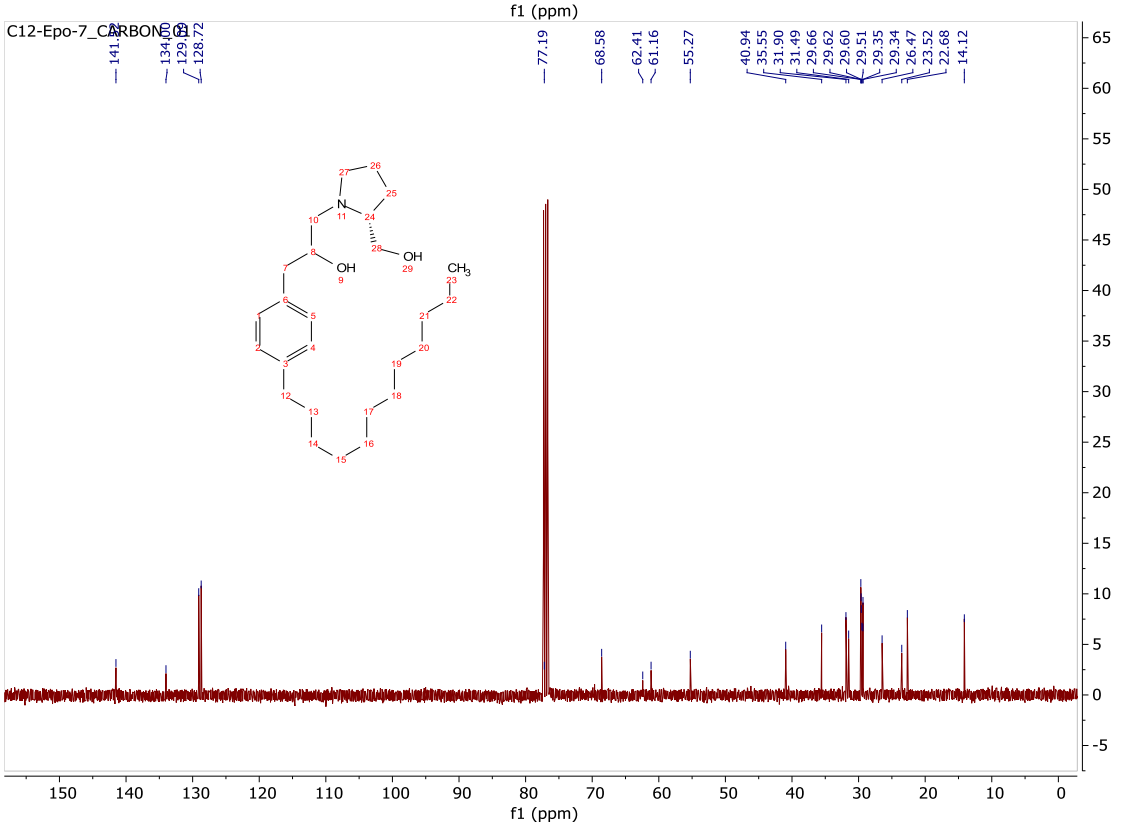

$^{1}H$ and $^{13}C$ spectra of *Rac*-(1R,2R)-2-((4-decylbenzyl)(methyl)amino)cyclopentan-1-ol (**3.9b**)

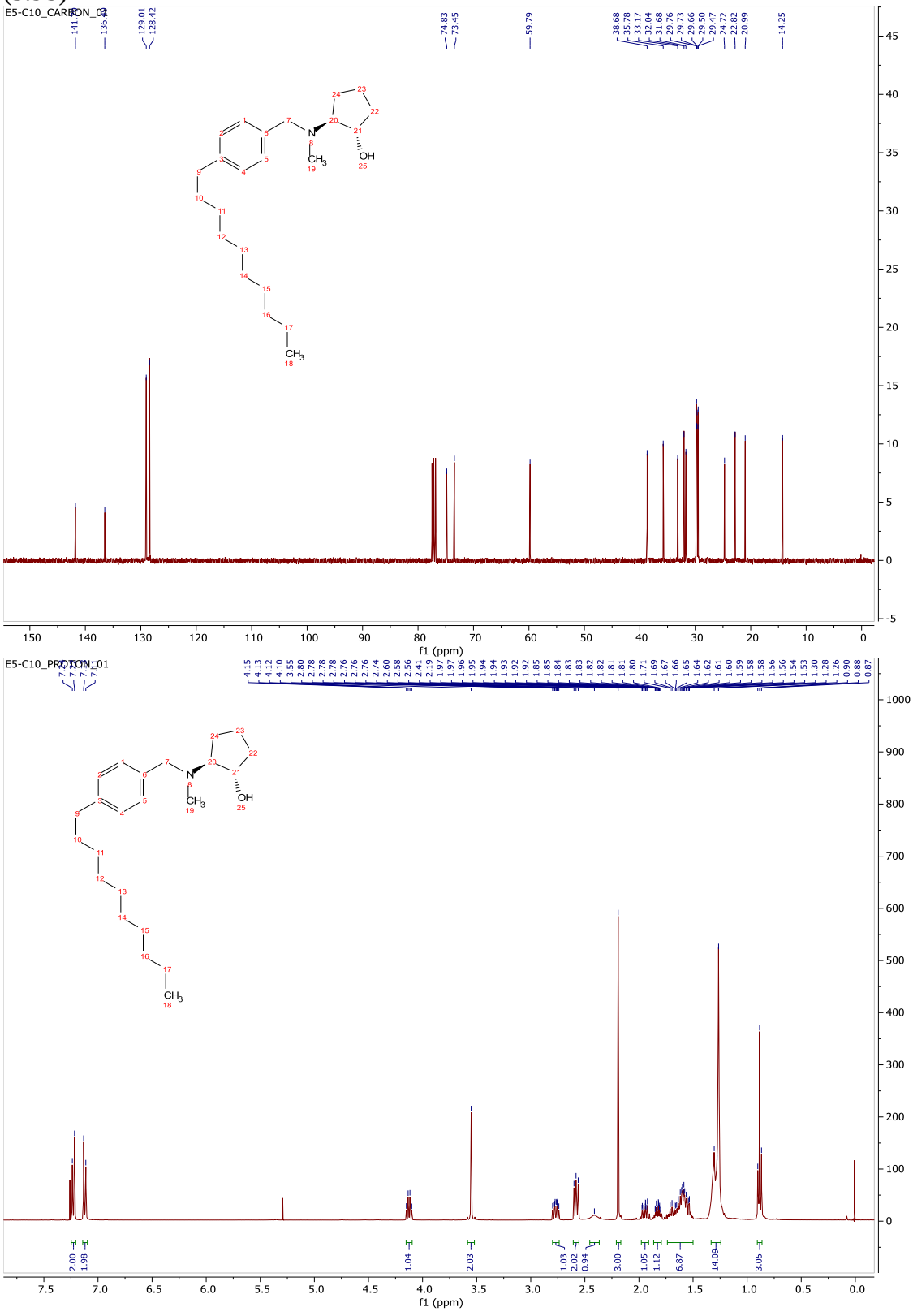

$^{1}H$ and $^{13}C$ spectra of *Rac*-(1S,2S)-2-(methyl(4-undecylbenzyl)amino)cyclopentan-1-ol (**3.9c**)

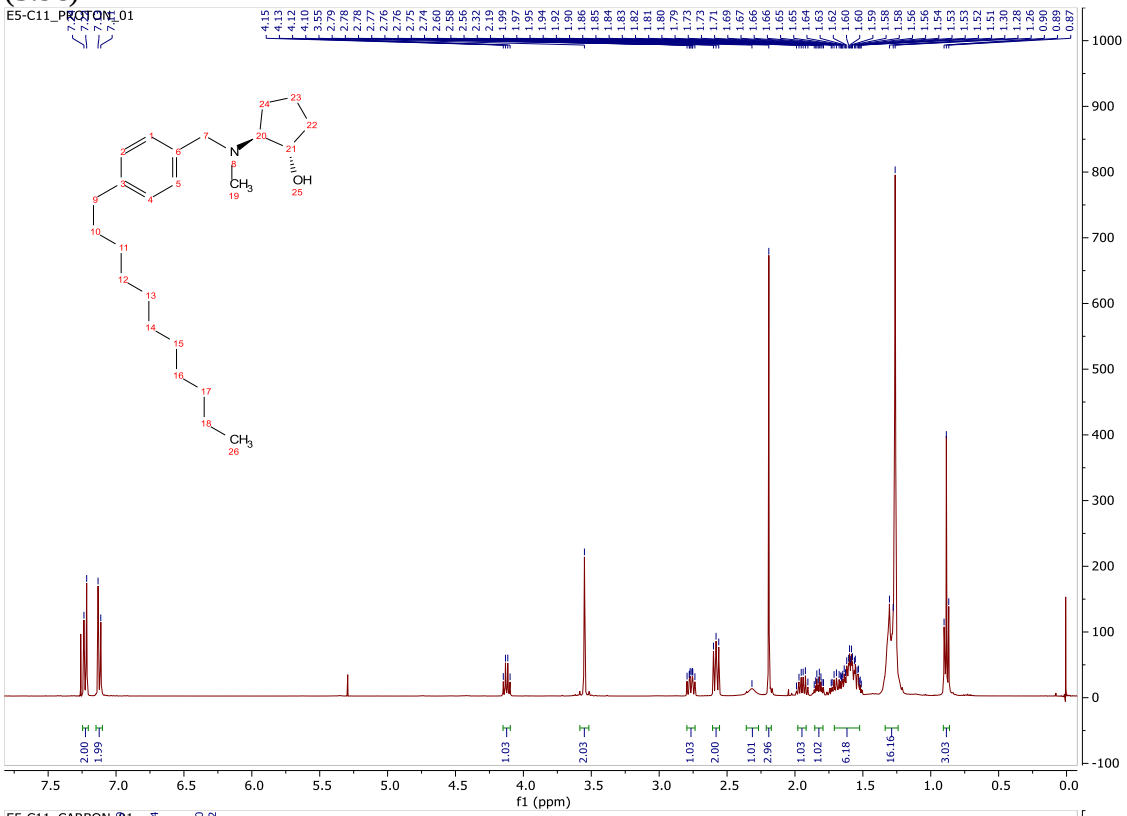


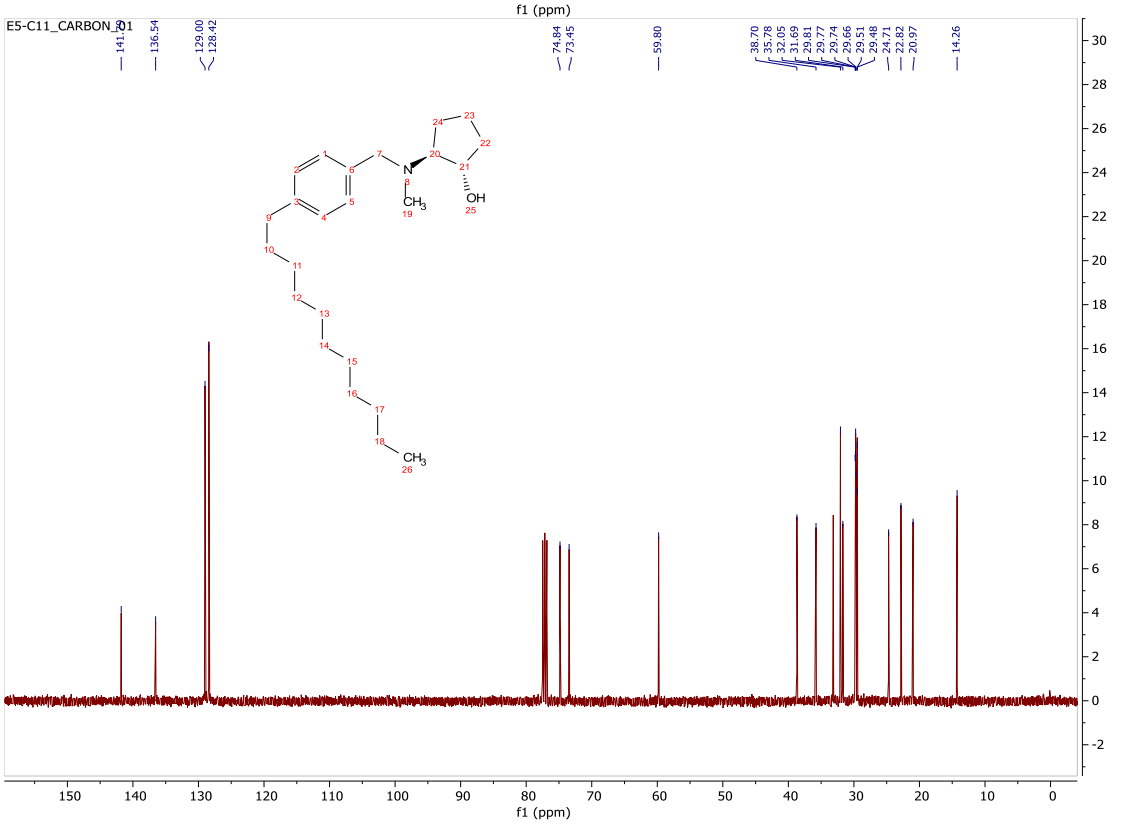

$^{1}$H and $^{13}$C spectra of *Rac*-(1R,2R)-2-((4-undecylbenzyl)amino)cyclopentan-1-ol (**3.10a**)

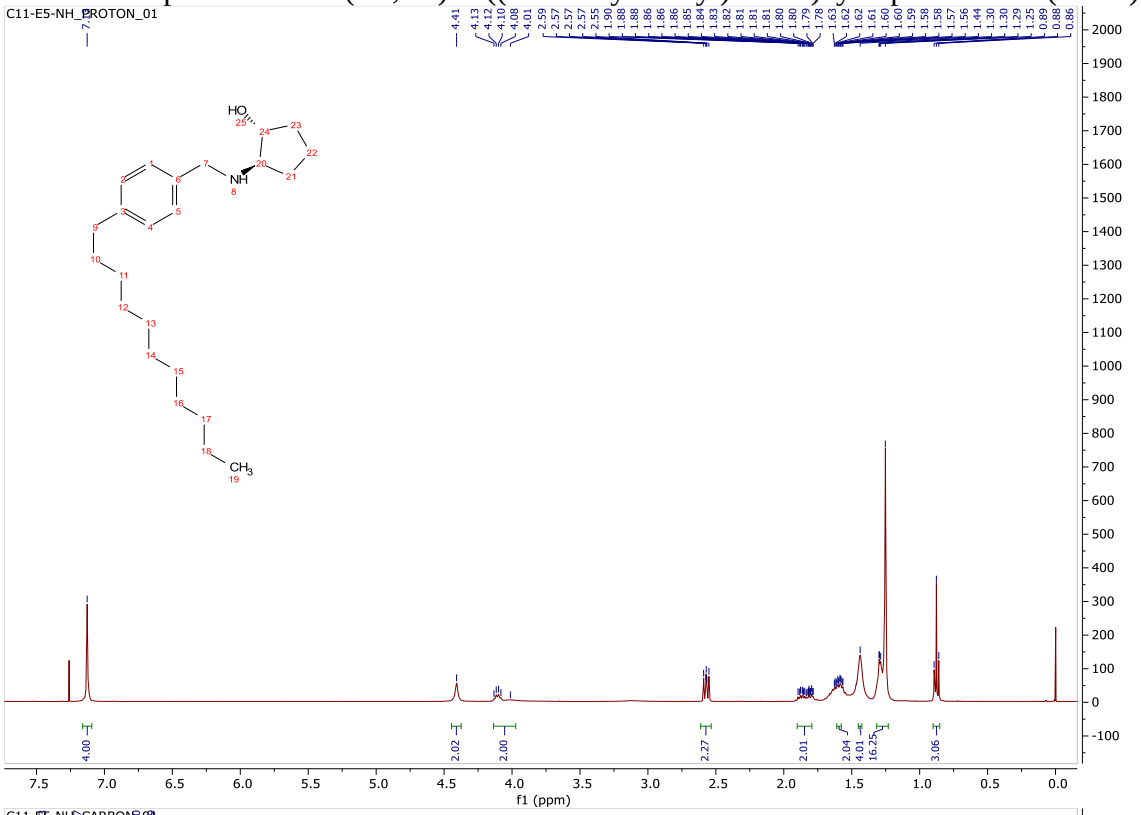


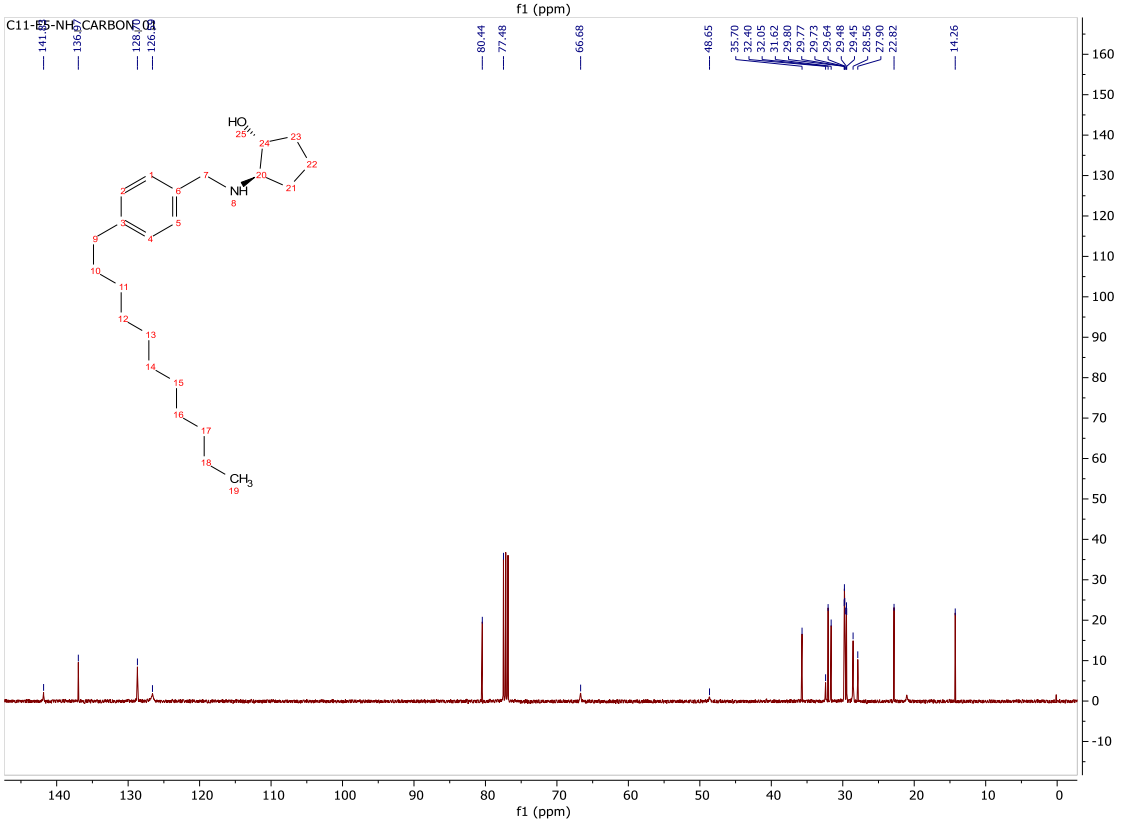

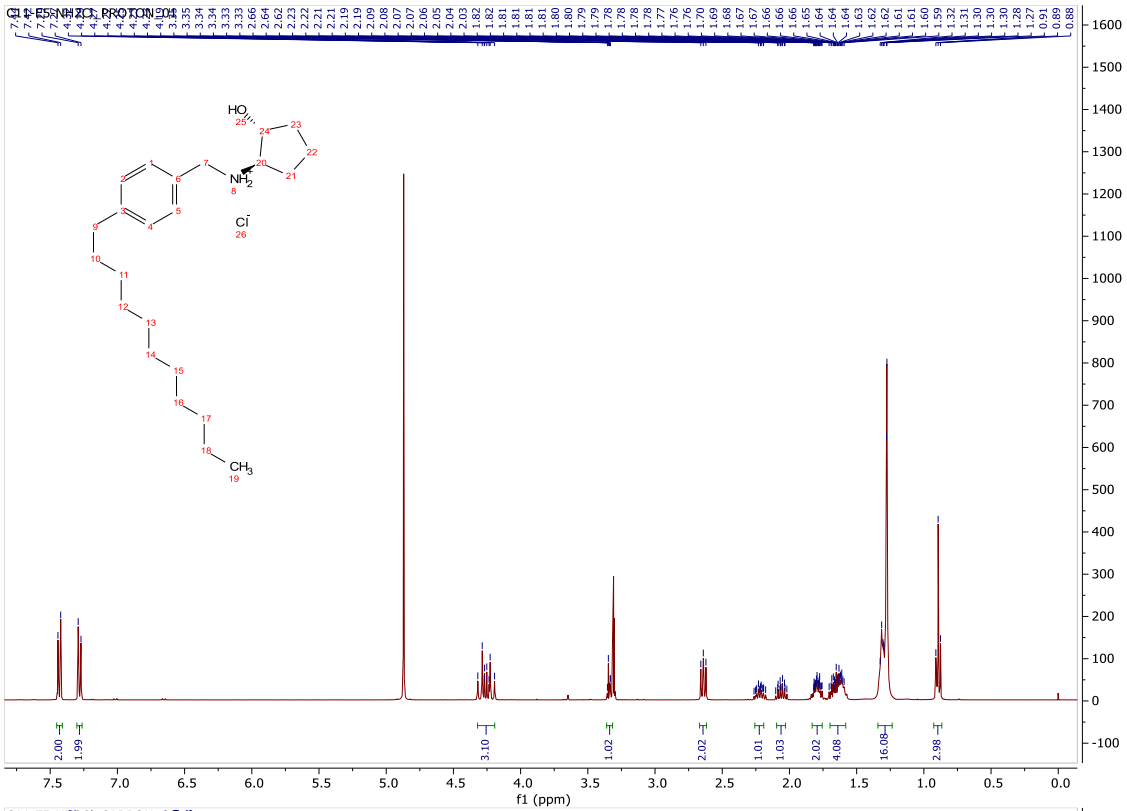
C11-E5-NH2Cl_PROTON_01
HO
NH2
Cl
CH3
f1 (ppm)

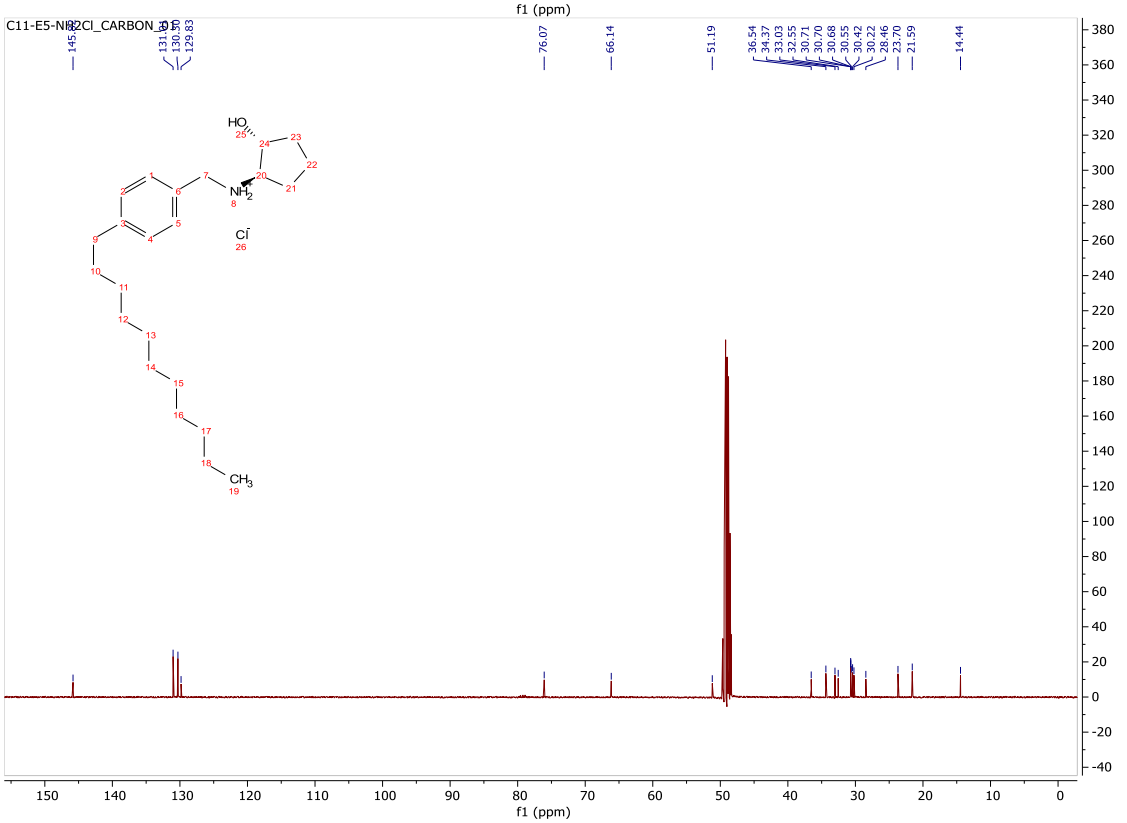
C11-E5-NH2Cl_CARBON_01
HO
NH2
Cl
CH3
f1 (ppm)

$^{1}H$ and $^{13}C$ spectra of *Rac*-(1R,2R)-2-((4-dodecylbenzyl)amino)cyclopentan-1-ol (**3.10b**)